



Copyright Undertaking

This thesis is protected by copyright, with all rights reserved.

By reading and using the thesis, the reader understands and agrees to the following terms:

1. The reader will abide by the rules and legal ordinances governing copyright regarding the use of the thesis.
2. The reader will use the thesis for the purpose of research or private study only and not for distribution or further reproduction or any other purpose.
3. The reader agrees to indemnify and hold the University harmless from and against any loss, damage, cost, liability or expenses arising from copyright infringement or unauthorized usage.

IMPORTANT

If you have reasons to believe that any materials in this thesis are deemed not suitable to be distributed in this form, or a copyright owner having difficulty with the material being included in our database, please contact lbsys@polyu.edu.hk providing details. The Library will look into your claim and consider taking remedial action upon receipt of the written requests.

STUDY OF MULTIFUNCTIONAL ONE-, TWO- AND
THREE-DIMENSIONAL FIBER-BASED TRIBOELECTRIC
NANOGENERATORS AND SELF-POWERED SENSORS

TIAN XIAO

PhD

The Hong Kong Polytechnic University

2023

The Hong Kong Polytechnic University

School of Fashion and Textiles

Study of Multifunctional One-, Two- and Three-Dimensional
Fiber-Based Triboelectric Nanogenerators and Self-Powered
Sensors

Tian Xiao

A thesis submitted in partial fulfilment of the requirements for
the degree of Doctor of Philosophy

December 2022

Certificate of Originality

I hereby declare that this thesis is my own work and that, to the best of my knowledge and belief, it reproduces no material previously published or written, nor material that has been accepted for the award of any other degree or diploma, except where due acknowledgement has been made in the text.

TIAN Xiao (Name of student)

(Signed)

Abstract

With the development of the Internet of Things (IoTs), wearable electronics which can meet the requirements of flexibility and lightweight have attracted long-lasting attentions. However, in order to power wearable electronics, conventional energy storage units such as batteries and capacitors are typically employed, which have limitations such as heavy weight, bulky volume, limited lifetime and requiring recharging by the immobile power plants. The triboelectric nanogenerator (TENG) is a newly developed energy harvesting technology that can effectively convert biomechanical energy into electrical energy. By virtue of its low cost, simple structure and environmental friendliness as well as easy fabrication, integration of TENG with conventional textiles paves a new avenue for wearable electronics. Up to now, a variety of textile-based triboelectric nanogenerators (t-TENGs) with numerous materials, various structures and fabrication techniques have been developed. However, it is still challenging to fabricate high-performance t-TENGs with good electrical properties, wearability and functionality by continuous fabrication technologies. To address these challenges, this thesis focuses on designing and developing flexible and wearable t-TENGs based on the synergistic effect of fiber materials, structures and textile engineering. Four types of t-TENGs, including one-dimensional (1D) PVDF yarn-based textile triboelectric nanogenerator, 1D core-spun yarn structured triboelectric nanogenerator based on chitosan/Tencel fibers, two-dimensional (2D) triboelectric nanogenerator fabric and three-dimensional (3D) woven structured triboelectric nanogenerator fabric, were developed.

Firstly, since 1D fiber/yarn-based t-TENGs are easily extensible, a 1D braiding-

structured triboelectric yarn (BYTENG) fabricated by a polyamide (PA) conductive yarn and wet-spun poly (vinylidene fluoride) (PVDF) yarn has been designed and developed by scalable wet spinning and braiding technologies for energy harvesting and biomechanical sensing. Owing to unique material and structural configuration, the BYTENG possesses the merits of mechanical robustness and flexibility. The BYTENG exhibits good machine washability and sensing performance, with a wide working range from 7 kPa to 127 kPa and a relatively high pressure sensitivity of 0.2V kPa^{-1} . More importantly, compared with PVDF electrospun films, this structure has better integration capability and can be used in sports products for real-time exercise detection. Furthermore, knitted and woven triboelectric fabrics (FTENGs) fabricated by the as-prepared BYTENG not only possess excellent air permeability but also can be applied to the seat cushion, backrest or carpet for human motion monitoring. This work greatly promotes the numerous applications of the t-TENGs and contributes to the further development of wearable electronics.

In order to further improve the functionality, biodegradability and compatibility with textile technology of 1D triboelectric yarn, an extremely durable and eco-friendly 1D core-spun structured triboelectric yarn (CYTENG) as a composite yarn has been developed by a scalable fancy spinning twister technology, which was made of PA conductive yarn (core yarn) and Tencel-chitosan blended yarn (wrapping yarn). The as-prepared CYTENG possesses the characteristics of high softness, small diameter, low weight and cost, high scalability and productivity. A voltage with value of 14.2 V and a current of $0.8\ \mu\text{A}$ can be obtained from the CYTENG with the length of 45 cm under impacting frequency of 3 HZ and force of 100 N. A smart glove with sewed CYTENGs was fabricated, which can be used to monitor various gesture signals.

Subsequently, a novel 2D triboelectric fabric (FTENG) with woven structure was fabricated based on continuously spun CYTENG by automatic weaving machine, which overcame the problems of complicated manufacturing process, high cost, poor comfort and small-scale production. A desirable open-circuit voltage of 31.3 V and a short-circuit current of 1.8 μA as well as instantaneous power density of 15.8 mW/m^2 under a load resistance of 70 $\text{M}\Omega$ are realized by the prepared FTENG with the size of $5 \times 5 \text{ cm}^2$. Besides, the FTENG performs excellent wearability and comfort, such as high flexibility, desirable breathability and good machine washability. Moreover, the FTENG exhibits excellent antibacterial property, wherein the inhibition rates against *Staphylococcus aureus* (*S. aureus*), *Escherichia coli* (*E. coli*) and *Candida albicans* (*C. albicans*) can reach up to 99%. Furthermore, it can be used as a self-powered sensor, wherein the developed FTENG can be attached under the arm and foot to demonstrate the ability to detect different body movements.

At last, based on a rational design of material system and structure, a multifunctional 3D triboelectric nanogenerator fabric (3D SP-FTENG) was designed and developed, which was composed of three layers, including the inner polypropylene (PP)-cotton fabric layer close to skin for moisture transfer and absorption, the middle Ag-cotton fabric layer for conducting electrode and antibacterial agent, and the outer PTFE-cotton fabric layer for tribo-negative layer and repelling water, respectively. The 3D SP-FTENG performs excellent electrical output (27.33 V, 1.76 μA and 61.6 mW/m^2) and wearability (directional water transport and breathability) as well as antibacterial activity. The geometric models of the functional zones of the 3D FTENGs are proposed to explain the electrical output and directional water transport performance. Moreover, in contrast to the previously reported multilayer t-TENGs which were constructed by directly stacking multilayer functional fabrics together, the fabric interface of this new

structure is not easily delaminated through weaving the support area and the functional area together. The 3D SP-FTENG demonstrates outstanding durability such as machine washability and ultrahigh abrasion resistance. In addition, the SP-FTENG is able to drive wearable electronics and be used as a self-powered sensor, such as constantly monitoring the movement signals of human body.

In summary, this thesis carried out a systematic research on developing fully textile-based TENGs including 1D yarn-based TENGs, 2D fabric-based TENG and 3D fabric-based TENG by utilizing the synergistic effect of fiber materials, structures and textile engineering. Various types of flexible t-TENGs have been successfully demonstrated. Such t-TENGs exhibit satisfactory electrical output performance, excellent integration ability and functionality as well as wearability. This study opens a new avenue to combine economically available materials and current textile technologies for fabricating t-TENGs with flexible yarn/fabric structures that are promising to promote the commercialization of smart energy garments. Moreover, fabrication and integration strategies reported in this thesis can not only achieve the desired electrical properties, but also maintain the inherent advantages of the textile, which contribute to the further development of t-TENGs for the self-powered sensor applications.

List of Publications

Related Journal Publications

1. **Tian X**, Hua, T. Antibacterial, scalable manufacturing, skin-attachable, and eco-friendly fabric triboelectric nanogenerators for self-powered sensing. *ACS Sustainable Chemistry & Engineering*, 2021, 9(39), 13356-13366.
2. **Tian X**, Dong S, Yang M, Ng H, Liu Y, Hu H, Hua T. Textile-based triboelectric nanogenerators for smart wearable systems: comfort, integration and application. *Advanced Materials Technologies*, 2022, 2201294.
3. **Tian X**, Hua T, Yang M, Niu B, Yang Y. Multiscale engineering of sustainable and versatile all fiber triboelectric nanogenerator based on multifunctional fibrous materials and 3D woven architecture. *Advanced Materials Technologies*, 2022, 2201105.
4. **Tian X**, Chan K, Hua T, Niu B, Chen S. Wearable strain sensors enabled by integrating one-dimensional polydopamine-enhanced graphene/polyurethane sensing fibers into textile structures. *Journal of Materials Science*, 2020, 55(36), 17266-17283.
5. **Tian X**, Hua T, Poon T, Yang Y, Hu H, Fu J, Li J, Niu B. Study on effects of blending fiber type and ratio on antibacterial properties of chitosan blended yarns and fabrics. *Fibers and Polymers*, 2022, 23(9), 2565-2576.

Other Journal Publications

1. Yang M, **Tian X**, Hua T. Green and recyclable cellulose based TENG for sustainable energy and human-machine interactive system. *Chemical Engineering Journal*, 2022, 136150.
2. Niu B, Yang S, **Tian X**, Hua T. Highly sensitive and stretchable fiber strain sensors empowered by synergetic conductive network of silver nanoparticles and carbon

nanotubes. *Applied Materials Today*, 2021, 25, 101221.

3. Li J, Fu J, **Tian X**, Hua T, Poon T, Koo M, Chan W. Characteristics of chitosan fiber and their effects towards improvement of antibacterial activity. *Carbohydrate Polymers*, 2022, 280, 119031.

4. Niu B, Yang S, Hua T, **Tian X**, Koo M. Facile fabrication of highly conductive, waterproof, and washable e-textiles for wearable applications. *Nano Research*, 2021, 14(4), 1043-1052.

5. Chen S, **Tian X**, Hua T, Chan K, Fu J, Niu B. Exploring the relationship between applied fabric strain and resultant local yarn strain within the elastic fabric based on finite element method. *Journal of Materials Science*, 2020, 55(23), 10258-10270.

6. Li J, **Tian X**, Hua T, Fu J, Koo M, Chan W, Poon T. Chitosan natural polymer material for improving antibacterial properties of textiles. *ACS Applied Bio Materials*, 2021, 4(5), 4014-4038.

Paper in Preparation

Tian X, Niu B, Hua T, Yang M, Yang Y, Dong S. Programmable Textile Triboelectric Nanogenerators Based on Wet-spun PVDF for Diverse Self - Powered Sensing Applications. *ACS Applied Materials & Interfaces*. (Submitted)

Poster Presentation

Tian X, Hua T, Niu B, Dong S, Yang M, Yang Y. Integration of Wet-spinning Polyvinylidene Fluoride Yarns into Programmable Smart Textiles for Biomechanical Energy Harvesting and Sensing. The Fiber Society's Fall 2022 Conference, Raleigh, North Carolina, USA.

Acknowledgements

First of all, I would like to express my sincere gratitude to my respectable supervisor Dr. Tao Hua for giving me such a valuable opportunity to pursue my PhD study. His invaluable guidance and great encouragement during my PhD study enable me to enter the exciting field of wearable electronics from traditional textiles. I would like to thank him for providing the opportunity to participate in different projects, from which I have gained a wealth of research experience, especially the planning of experiments, problem-solving skills, and self-regulation of mentality, all of which will benefit me a lot. I would also like to thank The Hong Kong Polytechnic University and School of Fashion and Textiles for the financial support and research platform.

I would also like to express my great appreciation to technicians of the School of Fashion and Textiles for the instrument operations: Mr. Shui-wing Ng, Mr. Wang-wah Wong, Mr. Cheuk-wai Lau, Dr. Hui Kevin, Mr. Kwan-on Choi. I also want to thank all the members in Dr Hua's group: Dr. Ben Niu, Ms. Mengyan Yang, Ms. Yiyi Yang, who give me great assistance in my research. I would also like to thank my classmates and friends, Ms. Zixin Ju and Ms. Shanshan Dong for their kind help during my research and life.

Finally, I would like to thank my dear family for their love and great support over these years. I also owe my sincere gratitude to my friends who gave me their opinions and helped me solve my problems during the difficult process of my PhD study and life.

Table of Contents

Certificate of Originality.....	I
Abstract.....	II
List of Publications.....	VI
Acknowledgements.....	VIII
List of Figures.....	XIV
List of Tables.....	XXIII
List of Abbreviations.....	XXIV
CHAPTER 1: Introduction.....	27
1.1 Background.....	27
1.2 Research Objectives.....	31
1.3 Methodology.....	32
1.4 Research Significance.....	36
1.5 Outline of the Thesis.....	39
References.....	41
CHAPTER 2: Literature Review.....	43
2.1 Textiles, E-textiles and Textile-Based Triboelectric Nanogenerators.....	43
2.2 Materials for Textile-Based Triboelectric Nanogenerators.....	45
2.2.1 Triboelectric materials.....	45
2.2.2 Electrode materials.....	48
2.3 Basic Working Mechanism and Modes of Textile-Based Triboelectric Nanogenerators.....	50
2.3.1 Vertical contact mode.....	51
2.3.2 Lateral sliding mode.....	53
2.3.3 Single electrode mode.....	54

2.3.4 Freestanding mode.....	55
2.4 Structures and Fabrication Methods of Textile-Based Triboelectric Nanogenerators	56
2.4.1 Fiber/Yarn-based TENGs.....	56
2.4.2 Fabric-based and nanofiber-based TENGs	61
2.4.3 3D structured FTENGs	67
2.5 Desired Performance of Textile-Based Triboelectric Nanogenerators	69
2.5.1 Electrical output performance.....	69
2.5.2 Properties for wearable applications.....	72
2.6 Application.....	87
2.6.1 Harvesting energy	87
2.6.2 Self-powered sensing.....	89
2.7 Summary.....	91
References.....	93
 Chapter 3: One-Dimensional PVDF Yarn-Based Textile Triboelectric Nanogenerator Assisted by Wet Spinning and Braiding Engineering.....	 118
3.1 Introduction.....	118
3.2 Experimental Section	120
3.2.1 Materials	120
3.2.2 Fabrication of the BYTENG.....	120
3.2.3 Fabrication of the woven and knitted FTENGs	122
3.2.4 Characterization and evaluation	122
3.3 Results and Discussion	122
3.3.1 Characterization of the PVDF yarn and BYTENG	122
3.3.2 Working mechanism	125
3.3.3 Electrical output performance of the BYTENG	126

3.3.4	Integration diversity of the BYTENG	130
3.3.5	Application as self-powered wearable sensors	132
3.4	Conclusion	135
References	137
Chapter 4: One-Dimensional Core-Spun Yarn Structured Triboelectric Nanogenerator Based on Chitosan/Tencel Fibers for Improving the Scalability and Functionality .. 141		
4.1	Introduction.....	141
4.2	Experimental Section	143
4.2.1	Materials	143
4.2.2	Fabrication of the CYTENG.....	143
4.2.3	Characterization and evaluation	143
4.3	Results and Discussion	144
4.3.1	Design and fabrication of the CYTENG	144
4.3.2	Morphology, structure and mechanical property of the CYTENG.....	146
4.3.3	Working mechanism	149
4.3.4	Electrical output performance of the CYTENG	150
4.3.5	Self-powered wearable sensors based on the CYTENG	153
4.4	Conclusion	154
References	155
Chapter 5: Two-Dimensional Fabric Triboelectric Nanogenerator by Integrating One- Dimensional Core-Spun Triboelectric Yarn..... 157		
5.1	Introduction.....	157
5.2	Experimental Section	158
5.2.1	Materials	158
5.2.2	Fabrication of the FTENG	159
5.2.3	Characterizations	159

5.3 Results and Discussion	159
5.3.1 Design and fabrication of the FTENG.....	159
5.3.2 Working mechanism	161
5.3.3 Breathability	162
5.3.4 Electrical output performance of the FTENG	163
5.3.5 Antibacterial property of the FTENG	170
5.3.6 Application of the FTENG.....	171
5.4 Conclusion	174
References.....	175
Chapter 6: Three-Dimensional Woven Structured Triboelectric Nanogenerator with Enhanced Wearability and Durability	
6.1 Introduction.....	181
6.2 Experimental Section.....	183
6.2.1 Materials	183
6.2.2 Fabrication of the 3D FTENGs.....	183
6.2.3 Fabrication of the 3D SCP-FTENG.....	184
6.2.4 Characterization and evaluation	184
6.3 Results and Discussion	185
6.3.1 Design and fabrication of the 3D SP-FTENG	185
6.3.2 Working mechanism of the SP-FTENG	190
6.3.3 Geometric models of the functional zones of the 3D FTENGs.....	191
6.3.4 Electrical output performance.....	198
6.3.5 Mechanism, characterization and optimization of directional water transport	206
6.3.6 Antibacterial property of the SP-FTENG	214
6.3.7 Performance comparison of the SP-FTENG	215

6.3.8 Application of the SP-FTENG.....	219
6.4 Conclusion	222
References.....	223
Chapter 7: Conclusions and Suggestions for Future Research	231
7.1 Conclusions.....	231
7.2 Suggestions	233

List of Figures

Figure 2.1 Fabric construction platform and hierarchy.

Figure 2.2 Four basic working modes of t-TENGs.

Figure 2.3 Working principle of t-TENGs based on contact-separation working mode.

Figure 2.4 The sliding mode of energy-harvesting fabric.

Figure 2.5 Working mechanism of fiber-shaped triboelectric nanogenerator at single-electrode mode.

Figure 2.6 Schematic illustration of fabric triboelectric nanogenerator under the free-standing mode.

Figure 2.7 Fiber/yarn-based TENGs under single electrode mode. (a) Schematic illustration of triboelectric yarn developed by a scalable spinning technology. (b) Ultra-stretchable conductive TENG fiber by soluble-core thermal drawing. (c) 3D printed elastic smart fiber with coaxial core-sheath structure realized by a DIW 3D printing technology. (d) Fermat-spiral-based energy yarn fabricated by conjugate electrospinning technique. (e) Tribopositive elastic yarn using interfacial assembly technology. (f) Fiber-shaped triboelectric nanogenerator through a three step coating method. (g) A multifunctional TENG yarn by dip coating method.

Figure 2.8 Fiber/yarn-based TENGs in contact-separation mode. (a) A yarn-shaped TENG with coaxial core-sheath structure. (b) A triboelectric fiber with core-shell structure. (c) A flexible hierarchical helical yarn. (d) A fiber strain sensor with helical structure. (e) A fibrous stretchable TENG-based sensor. (f) A triboelectric fiber with core-sheath structure. (g) A highly stretchable fiber-like TENG.

Figure 2.9 Typical 2D FTENGs. (a) Triboelectric nanogenerator textiles woven or knitted by core-shell yarns. (b) A highly stretchable TENG fabric knitted from an

energy-harvesting yarn. (c) A smart glove sewn with all-textile triboelectric sensor. (d) A woven structured triboelectric nanogenerator by using electrospun nanofibers. (e) A textile-based triboelectric nanogenerator with woven strips of positive and negative triboelectric material. (f) A TENG textile knitted from PNA/PMA fibers and wool threads. (g) A shape-adaptive electronic textile knitted by fiber-shaped coaxial tribo-sensor. (h) A weaved piezoresistive triboelectric nanogenerator. (i) A highly stretchable energy-harvesting textile sewn by energy-harvesting thread. (j) A direct current FTENG.

Figure 2.10 Modified FTENGs. (a) A TENG based self-powered smart textile prepared by wavy-structured PET films sandwiched in two conductive fabrics. (b) A F-TENG constructed by F-silk, nylon fabric and conductive fabric. (c) A grating-structured TENG fabric. (d) An omniphobic (both hydrophobic and oleophobic) triboelectric nanogenerator. (e) A washable electronic textile with screen printing.

Figure 2.11 Nanofiber membrane structured TENGs. (a) A nanofiber film based triboelectric nanogenerator with hierarchical structures. (b) A TENG-based E-skin. (c) A self-powered electronic skin. (d) A ferroelectric-enhanced triboelectric evaporation textile. (e) A tribo-ferroelectric synergistic electronic. (f) A TENG with continuous arch structures based on nanofibrous membrane. (g) A stretchable TENG based e-skin.

Figure 2.12 3D structured FTENGs. (a) A fabric TENG with 3D double-faced interlock structure. (b) A textile TENG with 3D spacer fabric structure. (c) A 3D warp-knitted spacer power fabric. (d) A FTENG with 3D weft-knitted fabric structure. (e) A textile triboelectric generator with double-layer structure. (f) A 3D orthogonal woven TENG. (g) A woven TENG with 3D angle-interlock structure. (h) A 3D braided TENG.

Figure 2.13 Improvement methods of the electrical output of t-TENGs. (a) Modification of surface or interface. (b) Increase of triboelectric textile layer. (c) Surface functionalization. (d) Reduction of inner resistance of triboelectric nanogenerator textiles. (e) Fabric structural design.

Figure 2.14 Wearability of t-TENGs. (a) Energy harvesting textile with silk, PTFE and stainless steel fibers. (b) Highly wearable, breathable, and washable sensing textile constructed with different core-shell yarns. (c) Truly wearable all-textile energy harvester. (d) A knitted textile triboelectric nanogenerator with stretchability. (e) Rib stitch knitted textile triboelectric nanogenerator with stretchability and washability. (f) A coaxial core-sheath fiber based nanogenerator with stretchability. (g) Electronic textile knitted with fermat-spiral-based energy yarns. (h) An all-fiber structured electronic skin with elasticity and breathability. (i) Pressure sensors with machine-washability and breathability based on TENG. (j) A durable and washable triboelectric yarn.

Figure 2.15 t-TENGs with designed aesthetics. (a) Combination of triboelectric all-textile sensor array and clothes. (b) Self-powered triboelectric wearable sensors by sewing PVDF stitch patterns. (c) An energy-management E-Textile with printable smart pattern.

Figure 2.16 t-TENGs with working stability. (a) TENG textile and its steady output performance under typical deformations and wide temperature span. (b) The fabrication process, contaminative-resistance and chemical stability of wearable TENGs.

Figure 2.17 Large-scale industrialized production of t-TENGs. (a) Large-scale industrialized production of textile-based triboelectric nanogenerator by a simple pumping process and weaving technology. (b) Industrial production of triboelectric fabric by using knitting technology. (c) Continuous and scalable fabrication of triboelectric yarns. (d) FTENG production through the thermal drawing and industrial weaving methods.

Figure 2.18 Multifunctionality of t-TENGs. (a) Acid and alkali-resistant textile triboelectric nanogenerator. (b) Flame retardant triboelectric textile. (c) Nanofiber-based triboelectric nanogenerators with UV-protective, self-cleaning, and antibacterial

properties. (d) Flexible and stretchable coaxial triboelectric nanogenerator yarn with force luminescence.

Figure 2.19 Integration of t-TENGs. (a) A seamlessly integrated t-TENG. (b) A 3D spacer structured fabric with integrated triboelectric nanogenerator and zinc-ion battery. (c) A multifunctional energy fiber with coaxial structure for energy collecting, storage, and utilization. (d) A triboelectric nanogenerator and supercapacitor fiber with coaxial structure. (e) A self-powered TENG-SC system.

Figure 2.20 t-TENGs for harvesting energy. (a) Gore-Tex fabric with nanodot-pattern for multiple energy harvesting. (b) A hydrophobic power textile for water droplet energy collecting. (c) Energy harvesting of human motions, raindrops and winds by a textile triboelectric nanogenerator. (d) Energy harvesting of sound, wind and human motion by a full-textile triboelectric nanogenerator. (e) Energy harvesting of tire rotating by a textile-based triboelectric nanogenerator.

Figure 2.21 t-TENGs for self-powered sensing. (a) Human activity monitoring with t-TENGs. (b) Self-powered sensing textile with knitted structure for sitting posture detecting and correction. (c) Wearable triboelectric sensors for detecting footsteps. (d) Self-powered wearable keyboard. (e) 3D triboelectric yarn for smart fitness system. (f) Self-powered sock for detecting healthcare and exercise.

Figure 3.1 Schematic illustration of the fabrication process of the BYTENG.

Figure 3.2 Mechanical property, photographs and potential application scenarios of the BYTENG. (a) Strain-stress curves of wet-spun PVDF yarns using different take-up speeds. (b) Optical microscope images of the wrapping effects of four PVDF yarns wrapping 70D conductive yarn and four PVDF yarns wrapping 360D conductive yarn. (c) Strain-tension curves of the conductive yarn, PVDF yarn and BYTENG. (d) Photograph of the BYTENG. (e) Surface morphology of the BYTENG. (f) SEM image of the cross section of the BYTENG. (g) Photographs of the BYTENG in various

deformable states including knotting, twisting and winding. (h) Schematic diagram of application scenarios of triboelectric yarn/ fabrics for daily motion sensing.

Figure 3.3 Schematic diagram of the BYTENG working mechanism.

Figure 3.4 The electrical performance of the BYTENG. (a) Output voltage and (b) current of the BYTENG under various impacting forces. (c) The linear fit of the voltage and current of the BYTENG with increasing pressure from 7 kPa to 127 kPa. (d) Output voltage and (e) current of the BYTENG at various frequencies. (f) Output voltage and (g) current of the BYTENG with various friction materials. (h) The current and power density of the BYTENG at a series of external loads. (i) Measured voltages of different capacitors charged by the BYTENG. (j) Output voltage of the BYTENG before and after three machine washes.

Figure 3.5 Digital photographs, flexibility, and air permeability of the BYTENG-based knitted and woven FTENGs. (a) Photographic images of the BYTENG-based knitted FTENG. (b) Knitted FTENG under stretched and rolled state. (c) Digital photographs of the BYTENG-based woven FTENG. (d) Woven FTENG under rolled and twisted state. (e) Air permeability of knitted FTENG, woven FTENG and various commercial fabrics.

Figure 3.6 Application of the BYTENG and FTENGs. (a) The photograph of the BYTENG applied into household portable pedal puller. (b) Output current of the BYTENG during the hand pull and foot pull. (c) Output current of the BYTENG during hitting boxing reaction ball. Output current of knitted FTENG and woven FTENG applied into (d) seat cushion, (e) backrest and (f) carpet.

Figure 4.1 (a) Schematic illustration of structure of the CYTENG. (b) Images showing the morphologies of conductive yarn. (c) Images showing the morphologies of Tencel/chitosan yarn. (d) Schematic illustration of the CYTENG fabrication processing. (e) Photograph of fancy yarn machine.

Figure 4.2 FTIR spectra of chitosan fiber, Tencel fiber and Tencel/Chitosan blended yarn.

Figure 4.3 (a) Photograph of the fabricated CYTENG. (b) Visual fineness of the CYTENG. (c) Tensile stress versus strain curve of the conductive yarn, Tencel/chitosan blended yarn and the CYTENG. (d) Cross section of the CYTENG. (e-f) Optical microscope images of the CYTENG. (g) Resistance variation of the CYTENG under bending and straightening.

Figure 4.4 Working principle of the CYTENG, contacting (I), separating (II), separated (III) and approaching (IV).

Figure 4.5 The electrical performance of the CYTENG. (a) The output voltage and (b) current of the CYTENG with various impacting forces (the frequency is fixed at 3 Hz). (c) The relationship between voltage and impacting force. The lines correspond to the linear fitting function. (d) The output voltage and (e) current of the CYTENG with different impacting frequencies (the force is fixed at 100 N and testing length of the CYTENG is 45 cm). (f) The output voltage and (g) current of the CYTENG with different lengths (the impacting force and frequency are fixed at 100 N and 3 HZ, respectively).

Figure 4.6 (a) Image of a smart glove sewn with the CYTENG. (b) Output voltage of the smart glove during the motion of different fingers, index finger (I), middle finger (II), ring finger (III) and making a fist (IV).

Figure 5.1 (a) Weave structure of the FTENG. (b) Schematic illustration of the FTENG. (c) Photograph of the fabricated FTENG. (d) Cross section of the fabricated FTENG. (e) Photographs of the FTENG under different deformations, such as kneaded (I), scrolled (II), and folded (III).

Figure 5.2 Working principle of the FTENG.

Figure 5.3 Air permeability and water vapor permeability of the as-prepared FTENG

and different fabrics.

Figure 5.4 (a) The output voltage and (b) current of the FTENG with various impacting forces (the frequency is fixed at 3 Hz and area is 5 cm*5 cm). (c) The relationship between voltage of the FTENG and pressure. (d) The relationship between current of the FTENG and pressure. The lines correspond to the linear fitting function. (e) Different deformation stages of the FTENG under different pressures.

Figure 5.5 (a) The output voltage and (b) current of the FTENG with different testing areas (the force and frequency are fixed at 100N and 3HZ, respectively).

Figure 5.6 (a) The output voltage and (b) current of the FTENG with different frequencies (the force and area are fixed at 100 N and 5 cm*5 cm, respectively).

Figure 5.7 (a) The output voltage of the FTENG before and after machine washing. (b) The output voltage of the FTENG after suffering various deformations (100 cyclic times of folding and twisting).

Figure 5.8 The current and peak power of the FTENG measured with various external load resistances with frequency of 3 HZ and impacting force of 100 N.

Figure 5.9 (a) A series of LEDs powered by the FTENG. (b) The capacitor charging ability of the FTENG with 5 cm*5 cm area under impacting frequency of 3 Hz and impacting force of 100 N. (c) Circuit diagram for powering electronic watch.

Figure 5.10 (a) Output voltage of the FTENG fixed under the foot, slow motion of heel (I), fast motion of heel (II), forefoot motion (III), heel motion wearing cotton sock (IV) and forefoot motion wearing cotton sock (V). (b) Output voltage of the FTENG fixed under the arm, slow motion of arm swinging (I), fast motion of arm swinging (II), slow motion of arm flapping (III) and fast motion of arm flapping (IV).

Figure 6.1 Structural design, schematic illustration and fabrication process of a 3D SP-FTENG. (a) Design system and weave structure of functional zone of the 3D SP-FTENG, outer layer (I), middle layer (II), inner layer (III), on-machine diagram (IV).

(b) Schematic of weaving yarns. (c) Schematic diagram of fabrication process of the 3D SP-FTENG. (d) Schematic illustration of the 3D SP-FTENG. (e) Schematic diagram of the multifunctional zone structure of the 3D SP-FTENG. (f) Application scenarios of the 3D SP-FTENG. (g) Schematic diagrams of different functional zones of 3D FTENGs: (I) SP-FTENG; (II) LP-FTENG; (III) ST-FTENG; (IV) SCP-FTENG. (h) The photographs of functional zone of the 3D SP-FTENG, outer layer consisting of PTFE yarn and cotton yarn (I), middle layer consisting of Ag yarn and cotton yarn (II), inner layer consisting of PP yarn and cotton yarn (III and IV), SEM images of PTFE yarn, cotton yarn, Ag yarn and PP yarn (V). (i) Photographic images of the fabricated 3D SP-FTENG (I) with different deformations, such as folded (II and III) and scrolled (IV).

Figure 6.2 Schematic illustration of the operation principle of the SP-FTENG.

Figure 6.3 (a) Description of different sides of the functional zones. Characterization of geometry of functional zone in the SP-FTENG, outer layer (b), middle layer (c), inner layer (I5 side: (d), I6 side: (e)). Characterization of geometry of the ST-FTENG outer layer (O1 side: (f), O2 side: (g)). Characterization of geometry of the LP-FTENG inner layer (I5 side: (h), I6 side: (i)). (j) Yarn area percentage on different sides of functional zone in various 3D FTENGs.

Figure 6.4 The output voltage of the 3D FTENGs with different structures and materials.

Figure 6.5 Output voltage of the 3D SP-FTENG (a) and 3D ST-FTENG (b) at different impact forces from 10 N to 200 N. The positive and negative voltage of the SP-FTENG (c) and ST-FTENG (d) at different impact forces from 10 N to 200 N. (e) The linear fit of the peak to peak voltages of the 3D FTENGs with increasing pressure from 4 kPa to 80 kPa.

Figure 6.6 Output voltage (a) and current (b) of the SP-FTENG at different frequencies

from 1 to 3 Hz.

Figure 6.7 Output voltage (a) and current (b) of the SP-FTENG with various friction materials.

Figure 6.8 (a) Digital photograph of martindale abrasion tester. (b) The electrical output performance of the SP-FTENG after 5000 cycles of abrasion. (c) Stability test of the SP-FTENG under ~8000 cycles at a frequency of 3.3 Hz and 200 N mechanical force. Inset: the current waveform of the SP-FTENG at 1000 s and 2000 s, respectively. (d) Output voltage of the SP-FTENG after standard machine wash tests. (e) Current and power density curve of the SP-FTENG at various load resistances. The mechanical force is about 200 N and the frequency is 3 Hz unless otherwise specified.

Figure 6.9 (a) Contact angles of different sides of the SP-FTENG. (b) Schematic illustration explaining directional water transport mechanism of the SP-FTENG, water (I) from skin and (II) from environment. (c) Changes of water droplet behavior when water is dropped on inner layer (I) and outer layer (II) of the SP-FTENG, respectively.

Figure 6.10 MMT results of the top and bottom surfaces of 3D FTENGs when the inner and outer layer are facing up, respectively: (a-b) SP-FTENG, (c-d) LP-FTENG, (e-f) ST-FTENG, (g-h) SCP-FTENG. (i) Contact angles of different 3D FTENGs. (j) Air permeability of the as-prepared 3D FTENGs and different fabrics.

Figure 6.11 Application of the SP-FTENG. (a) Charging performance of the SP-FTENG to different capacitors. (b) Photograph of the SP-FTENG lighting up 36 LEDs. (c) The electrical circuit diagram of powering an electronic watch. (d) A SP-FTENG attached under the arm to detect arm swinging and flapping. (e) Output voltage of the SP-FTENG placed under the foot and cotton sock. (f) Monitoring arm bending by mounting a SP-FTENG on the arm. (g) Detecting sitting behavior of people using a SP-FTENG placed on a chair.

List of Tables

Table 2.1 Triboelectric series of some materials.

Table 3.1 The price of the raw materials of the BYTENG.

Table 4.1 The price of raw materials.

Table 5.1 Antibacterial efficiency after inoculation with *S. aureus*, *E. coli* and *C. albicans* suspensions incubated with the FTENG for 18 h.

Table 6.1 Wetting time, absorption rate, max wetted radius and spreading speed of functional zones of four 3D FTENGs when water is dropped on inner layer.

Table 6.2 Antibacterial activity results of the SP-FTENG against *S. aureus*, *E. coli* and *C. albicans*.

Table 6.3 Performance comparison to fabric-based t-TENGs in previous reports.

List of Abbreviations

IoTs	Internet of Things
TENG	triboelectric nanogenerator
t-TENGs	textile-based triboelectric nanogenerators
1D	one-dimensional
2D	two-dimensional
3D	three-dimensional
BYTENG	braided structured triboelectric yarn
PA	polyamide
PVDF	poly(vinylidene fluoride)
FTENG	triboelectric fabric
CYTENG	core-spun structured triboelectric yarn
<i>S. aureus</i>	<i>Staphylococcus aureus</i>
<i>E. coli</i>	<i>Escherichia coli</i>
<i>C. albicans</i>	<i>Candida albicans</i>
3D SP-FTENG	3D triboelectric nanogenerator fabric
PP	polypropylene
SEM	scanning electron microscope
PVC	polyvinyl chloride
PDMS	polydimethylsiloxane
PTFE	polytetrafluoroethylene
PLA	Polylactic acid
ITOs	indium-doped tin oxides
CNT	carbon nanotubes
PEDOT: PSS	Poly(3,4-ethylenedioxythiophene) polystyrene sulfonate
PZT	lead zirconate titanate
FRTY	flame-retardant single-electrode triboelectric yarn
SEBS	styrene-ethylene-butylene-styrene
DIW	Direct-Ink-Writing
FSBEY	fermat-spiral based energy yarn

P(VDF-TrFE)	poly(vinylidene fluoride-trifluoroethylene)
PEI/MWCNTs/PA	polyethyleneimine/multiwalled carbon nanotubes/phytic acid
PEO/ WPU/alliin	polyethylene oxide/waterborne polyurethane/alliin
AgNPs	Ag nanoparticles
PU	polyurethane
AgNWs	silver nanowires
rGO	Reduced Graphene Oxide
SSY	stainless steel yarn
PMA	poly (methyl acrylate)
PNA	poly (NAGA-co-AAm)
Ag	silver
ELD	electroless deposition
RF-TENGs	omniphobic triboelectric nanogenerators
PLGA	polylactic-coglycolic acid
PVA	polyvinyl alcohol
TPU	thermoplastic polyurethane
3DFIF-TENG	3D double-faced interlocking fabric TENG
PAN	polyacrylonitrile
PE	polyethylene
PET	poly (ethylene terephthalate)
GO	graphene oxide
SE-PDMS	surface-assembled polydimethylsiloxane
NW	nanowire
NF	nanoflake
TET	triboelectric textile
STET	single-layer TET
DTET	double-layer-stacked TET
PEI	poly(ethylenimine)
EHT	energy harvesting textile
SSF	stainless steel fiber
PTFEF	polytetrafluoroethylene fiber
A-TEH	all-textile energy harvester

FNG	fiber nanogenerator
WVT	water vapor transmission
TATSA	triboelectric all-textile sensor array
SF	silk fibroin
LCFs	liquid metal/polymer core/shell fibers
SETY	single-electrode triboelectric yarn
SC	supercapacitor
Si ₃ N ₄	silicon nitride

CHAPTER 1: Introduction

1.1 Background

With the fast progress of innovative electronics technology, an increasing number of people are pursuing portable sensors, actuators and transmitters which aim to improve work efficiency and quality of life. Wearable electronics which can meet the requirements of flexibility as well as lightweight have attracted long-lasting attentions.¹ However, in order to power wearable electronics, conventional energy storage units such as batteries and capacitors are typically employed, which have limitations such as heavy weight, bulky volume, limited lifetime cycles, frequent replacement, potential safety risks and even environmental hazards.^{2,3} These drawbacks greatly hinder the practical applications of the wearable electronics. Thus, the advancement of sustainable power supply is of vital importance.

Among various methods, triboelectric nanogenerator (TENG), on the basis of triboelectrification effect and electrostatic induction, is a newly developed energy-harvesting technology which can convert almost all forms of mechanical energy in a sustainable way. Considering its inherent characteristics such as low cost, extensive material source, high efficiency and versatility, TENG has promising applications in harvesting energy. As one of common and sustainable energy, human motion energy can be harvested when the TENG is placed on the human body. In view of this, textiles can be chosen as the ideal medium for TENG owing to its lightness, breathability and flexibility, which can be integrated with electrical functions without additional burden and aesthetic sacrifice.⁴ Integration of TENG technology with traditional textiles paves

CHAPTER 1

a new way for wearable electronics.

Up to now, as next-generation wearable energy harvesters, a variety of textile-based TENGs (t-TENGs) with numerous materials, various structures and fabrication techniques have been reported. However, a gap between research and practical commercialization still exists, and the research frontier in the field of energy harvesting is mainly focused on improving electrical performance. Only a few studies have aimed at the scalable processability, functionality, wearability and durability of t-TENGs.

In practical wearable scenarios, available planar or strip structured TENGs exhibit some limitations, such as difficulty in adapting to irregular human motion in multiple directions and complicated implementation. Therefore, the TENGs with 1D fiber/yarn shape are highly promising with the merits of good shape-adaptability, breathability and integration capability, which can be fabricated into smart textiles by mature textile forming technology.^{5,6} Although 1D fiber/yarn shaped TENGs have been developed by several methods, there are still some challenges with the current production method, such as hand-based, lab-scale, centimeter-length fabrication, which greatly limit large-scale production of t-TENGs.⁷ Moreover, harmful conductive materials (such as carbon fillers and harmful metals) and some chemicals are involved during the manufacturing process of fiber/yarn shaped TENGs.^{8,9} In addition, most existing 1D fiber/yarn-based TENGs are either too hard or too soft to some extent, which are difficult to withstand the pulling stress and beating force exerted on them during the process of textile weaving. Therefore, in practical and efficient long-term applications, it is important to explore easily extensible 1D fiber/yarn shaped TENG by simple, cost-effective and scalable manufacturing method, which not only withstands mechanical deformations but also exhibits high triboelectrification for desirable output performance.

CHAPTER 1

Most of tribomaterials utilized in TENGs were synthetic polymers or metallic materials, which are generally non-renewable and non-biodegradable, thus limiting the potential development of cost-effective and eco-friendly TENGs and causing severe electronic waste. Despite some studies have realized the fabrication of biodegradable and environmentally friendly TENG by using suitable natural materials, such as wood,¹⁰ paper,¹¹ feather,¹² etc., the preparation approaches are relatively complicated, time-consuming and expensive. Also, the fabricated eco-friendly TENGs are usually planar structured, which greatly restrict the wearability, comfort and compatibility with textile technology. Therefore, there is a great need for fabricating eco-friendly 1D fiber/yarn-based TENG with small diameter, good mechanical strength, excellent wearability using green materials by an efficient and sustainable fabrication method.

For the purpose of enhancing the output and broadening applications, fabric-based TENGs have been extensively reported. A majority of fabric-based TENGs were fabricated by coating, electrospinning, electrospraying and other techniques, which have the limitations of long fabrication time, complex equipment, high cost, or poor replicability. Meanwhile, these methods attached some conductive and frictional materials to the yarn and fabric. Due to the variable bending structure and uneven surface characteristics of textiles, the coating on t-TENG was prone to cracking/delamination, leading to low abrasion resistance and durability. A promising strategy is to prepare FTENGs by various mature textile forming techniques, such as braiding, weaving, knitting, etc. Among these structures, woven structure is attractive owing to its stability of the structure. However, the majority of woven-structured t-TENGs are fabricated by one kind of fiber system, which greatly limits the functionality and comfort of t-TENGs. Therefore, it is significant to explore fabric-based TENGs with optimized textile structures by the textile engineering strategy without involving

CHAPTER 1

the chemical processing.

To address the challenges that are mentioned above, this study focuses on developing high performance t-TENGs with good flexibility, functionality and wearability based on synergistic effect of fiber materials, structures and textile engineering. In terms of structural characteristics, this work systematically studies various t-TENGs with 1D braided yarn structure, 1D core-spun yarn structure, 2D woven fabric structure and 3D woven fabric structure. From the perspective of fabrication techniques, textile processing techniques such as wet spinning, braiding, fancy yarn spinning, weaving, and knitting were used, which basically cover most textile processing techniques.

Firstly, a 1D PVDF-based triboelectric yarn (BYTENG) with braided core-shell structure by scalable wet spinning and braiding technologies was developed. The fabricated BYTEBG exhibits a mechanical robustness, flexibility, excellent pressure sensing and machine washability, which has better integration capability and can be fabricated into knitted and woven TENGs for real-time motion detection. Subsequently, an extremely durable and sustainable 1D core-spun structured triboelectric yarn (CYTENG) based on chitosan/Tencel fibers was prepared by a scalable and eco-friendly fancy spinning twister technology, realizing the yarn shaped TENG with high flexibility, small diameter and light weight, great scalability and productivity as well as low cost. Moreover, an antibacterial, skin-attachable and eco-friendly 2D FTENG based on woven structure was fabricated by the continuously spun CYTENG, which overcomes the complex manufacturing process, high cost, poor comfort and small-scale production of previous functional FTENGs. The fabricated FTENG exhibits excellent wearability, functionality and comfort, such as high flexibility, desirable breathability, good machine washability and excellent antibacterial property. Furthermore, a 3D

CHAPTER 1

triboelectric nanogenerator fabric (SP-FTENG) with support zone and functional zone was designed, which was composed of three layers, including the inner polypropylene (PP)-cotton fabric layer close to skin for moisture transfer and absorption, the middle Ag-cotton fabric layer for conducting electrode and antibacterial agent, and the outer PTFE-cotton fabric layer for tribo-negative layer and repelling water, respectively. Benefiting from structural design and rational materials configuration, multifunctionality of woven-structured t-TENG is realized, including excellent electrical performance, wearability and antibacterial property.

1.2 Research Objectives

This study aims at developing t-TENGs with excellent performance, including good electrical output and great wearability as well as multifunctionality based on synergistic effect of fiber materials, structures and textile engineering in a facile and scalable manner. The specific objectives in this study are listed as follow:

- (1) To explore and prepare a 1D PVDF yarn-based triboelectric textile by scalable wet spinning and braiding technologies with good integration capability and flexibility.
- (2) To design and fabricate 1D sustainable and eco-friendly triboelectric yarn based on chitosan/Tencel fibers by scalable fancy spinning twister technology which not only has excellent electrical performance and wearability but also is compatible with current automated textile technology.
- (3) To develop 2D triboelectric fabric for energy harvesting and self-powered sensing by a commercial weaving method which qualifies high power output, functionality

CHAPTER 1

and good wearability, including washability, breathability, and excellent antibacterial property.

- (4) To construct a multifunctional 3D FTENG based on synergistic effect of fiber materials, structures and textile engineering with excellent electrical output, wearability, and durability as well as antibacterial activity.

1.3 Methodology

To solve the above potential research issues, the study is investigated through using the following methodologies:

M1. Design and fabrication of one-dimensional PVDF yarn-based textile triboelectric nanogenerator assisted by wet spinning and braiding engineering for diverse self-powered sensing applications

A 1D novel triboelectric yarn with braided core-shell structure (BYTENG) based on wet-spun PVDF will be designed. Commercial silver-coated nylon yarn will be selected as the core conductive electrode, due to its low cost and maturity in industrial production. PVDF will be used as triboelectric material, which serves as shell layer considering its high electron affinity, excellent stability and desirable flexibility. The PVDF yarn will be prepared by wet spinning, which is facile for scaled-up and continuous production. Then four PVDF yarns will be interwoven on the conductive yarn by using the braiding machine to fabricate the BYTENG. The mechanical property and electrical performance will be investigated. With the merits of mechanical robustness, flexibility, good electrical output performance and integration ability, the

CHAPTER 1

as-prepared BYTENGs will be fabricated into knitted and woven FTENGs. Also, the BYTENG and FTENGs will be applied to sports products, seat cushion, backrest and carpet to testify the ability of human motion detecting.

M2. Design and fabrication of one-dimensional core-spun yarn structured triboelectric nanogenerator based on chitosan/Tencel fibers for improving the scalability and functionality

The property of energy harvesting yarn depends on the conductive electrode, dielectric materials and structure. Polyamide yarn is a common textile material in the market, with high production and excellent properties, such as high breaking strength and elongation as well as abrasion resistance. Due to its high conductivity and excellent antibacterial property of Ag, polyamide (PA) yarn coated with Ag will be selected as the conductive electrode for fabricating core-spun yarn structured triboelectric nanogenerator. Moreover, eco-friendly Tencel/chitosan blended yarns will be selected as dielectric materials due to its excellent antibacterial property, biocompatibility, biodegradability and non-toxic. The use of natural fiber as the outer shell fiber is conducive for improving the comfort of the human body. There is no chemical fiber that directly contacts the skin which may cause discomfort. An extremely durable and eco-friendly 1D core-spun triboelectric yarn (CYTENG) as a composite yarn will be made of PA conductive yarn (core yarn) and Tencel-chitosan blended yarn (wrapping yarn) by a scalable spinning fancy twister technology. The commercial machine will be used to wind the shell fiber at high speed for producing this CYTENG, making the preparation of the TENG simple and high production efficiency, and providing a strong basis for industrial large-scale production line manufacturing. Also, the CYTENG exhibits high softness, small diameter and low cost, which promotes the wide

CHAPTER 1

application of t-TENG. A smart glove with the CYTENG will be fabricated to detect finger motion.

M3. Design and fabrication of two-dimensional triboelectric nanogenerator fabric by integrating one-dimensional core-spun triboelectric yarn

Various textile manufacturing approaches have been suggested for integrating modified yarns or wires into fabric. Compared with the method of embedding yarns in textiles, weaving and knitting using one-dimensional functional yarn have the advantage of manufacturing relatively diverse and sophisticated textile structures. With the merits of its stable structure, woven structure is a good choice for fabricating triboelectric fabric. By using available weaving technologies, the above obtained CYTENGs as weft yarns and the cotton yarns as warp yarns will be introduced into the woven structure. Owing to excellent air permeability and softness, a sateen structure will be utilized to fabricate the FTENG. The contact area between two dielectric layers affects the number of friction charges generated which contributes to a better electrical output for the FTENG. To analyze the effects of contact area on the electrical output, FTENGs will be fabricated with three sizes. Since different magnitudes of impact force and frequency can be exerted to the FTENG in practical application scenarios, the impact of force and frequency on the electrical performance of the FTENG will be studied. The machine washability, breathability and antibacterial properties of the FTENG will be further evaluated to demonstrate its excellent wearability. The FTENG with the desirable performance will be utilized to investigate the energy-harvesting, charging and sensing capabilities.

CHAPTER 1

M4. Design and fabrication of three-dimensional woven structured triboelectric nanogenerator fabric with enhanced wearability and durability

A 3D triboelectric nanogenerator fabric (SP-FTENG) with support zone and functional zone will be designed by traditional weaving technology, which is composed of three layers, including the inner polypropylene (PP)-cotton fabric layer close to skin for moisture transfer and absorption, the middle Ag-cotton fabric layer for conducting electrode and antibacterial agent, and the outer polytetrafluoroethylene (PTFE)-cotton fabric layer for tribo-negative layer and repelling water, respectively. Fabric geometric models will be proposed to calculate the effective area of each yarn on each side for investigating electrical output performance and wearability of various 3D FTENGs. The effects of impacting force, frequency and materials on output performance of as-prepared 3D FTENGs will be systematically studied. Meanwhile, the antibacterial property and wearability, including durability, directional water transport and breathability will be evaluated. Then, the applications of the 3D SP-FTENG in driving wearable electronics and self-powered sensing will be demonstrated.

M5. Characterization of materials and yarn- and fabric-based triboelectric nanogenerators

The surface morphologies, yarn blending ratio, molecular information and tensile properties will be evaluated. The electrometer (Keithley 6514) and oscilloscope (DS1054Z) can be used for measuring the electrical output performance, in which Keyboard Life Tester (ZX-A03) can provide the compressing motions. In terms of wearability, the air permeability, water vapor transmission and machine washability as well as abrasion resistance will be investigated. For the functionality, the water contact

CHAPTER 1

angle, moisture management behavior and antibacterial activities will be characterized.

1.4 Research Significance

In the era of rapid advancement of Internet of Things (IoT), energy-autonomous wearable electronics which can get rid of traditional batteries with limited lifetime cycles, frequent replacement, potential safety risks and even environmental hazards are particularly in demand. As an emerging mechanical energy harvesting technology, triboelectric nanogenerator (TENG), which is based on the coupling effect of contact electrification/triboelectrification and electrostatic induction, can convert ubiquitous and irregular low-frequency mechanical energy into electricity for achieving the self-sufficient characteristic of wearable electronics. With the virtues of low cost, environmentally friendly, and easy availability, along with the wide range of material options, TENG has huge application prospects, including wearable powering, multifunctional self-powered sensing, personal healthcare monitoring and human-machine interactions. However, the development of available TENGs with planar or strip structures has limitations due to the difficulty of adapting to irregular human motion in multiple directions, clothing aesthetics and implementation complexity in real wearable scenarios. In comparison to other existing forms of carrying, attaching, embedding, etc., textiles can be an ideal for seamlessly integrating with electrical functions without additional burden and aesthetic sacrifice, thus providing a diverse design carrier for TENGs. Therefore, a new type of smart textiles, namely textile-based TENG (t-TENG) with mechanical energy harvesting ability and satisfactory wearing comfort, are emerging rapidly, thus opening up a new research direction for the development of TENGs. This thesis designs and fabricates new-type t-TENGs with good electrical performance, multifunctionality and wearability by combining

CHAPTER 1

advanced material science, structure and textile engineering.

Firstly, the design strategy of t-TENG from 1D yarn to 2D fabric structure provides great flexibility for the development of multifunctional t-TENGs. A 1D core-shell braiding-structured triboelectric yarn with a wide working range from 7 kPa to 127 kPa and a relatively high pressure sensitivity of 0.2V kPa^{-1} has been designed and fabricated through scalable wet spinning and braiding technologies using conductive yarn as the core and wet-spun PVDF yarn as the shell. The fabricated YTENG exhibits a mechanical robustness, flexibility and good machine washability. Compared with PVDF electrospun films, this 1D structure has better integration capability, which can be fabricated into 2D FTENGs. The resultant triboelectric yarn and fabrics can be used as multifunctional pressure sensors for diverse self-powered sensing applications.

Then, on the basis of the above design strategy, the advanced spinning technology has been effectively applied to fabricate 1D core-spun-structured t-TENG with chitosan and Tencel blended yarn as the wrapping and conductive yarn as the core electrode. The fabricated 1D yarn TENG possesses good weavability, such as good mechanical properties, unlimited length and small diameter. At the same time, it has the softness and flexibility of textiles. The functionality, biodegradability, and textile technology compatibility of 1D triboelectric yarn are greatly improved.

Subsequently, owing to the good weavability of 1D core-spun-structured Tencel/chitosan/conductive yarn-assembled TENGs, a 2D sateen-architected FTENG with good antibacterial, skin-attachable, and eco-friendly properties has been successfully developed through automatic weaving technique. The output, current and power density of fabricated FTENG operating at a single-electrode mode can reach

CHAPTER 1

31.3V, 1.8 μ A, 15.8 mW/m² by applying a 3 Hz mechanical drive of 100 N with the size of 5 \times 5 cm². The inhibition rates against *S. aureus*, *E. coli*, and *C. albicans* can reach up to 99%. This facile and environmentally friendly technique also contributes to the realization of large-scale production, facilitating the future low-cost and extensive use of t-TENGs.

Next, compared with 1D yarn and 2D fabric, 3D fabric structure has advantages in improving wearability and multifunctionality of textile TENGs. To enhance the wearability and durability, a 3D triboelectric nanogenerator fabric (3D SP-FTENG) has been proposed, which performs excellent electrical output (27.33 V, 1.76 μ A and 61.6 mW/m²) and wearability (directional water transport and breathability) as well as antibacterial activity. The 3D SP-FTENG demonstrates outstanding machine washability, durability and ultrahigh abrasion resistance. In addition, the SP-FTENG is able to drive wearable electronics and be used as a self-powered sensor, such as constantly monitoring the movement signals of human body.

Finally, due to the porous structure of the fabric with different structures and material configurations, the different yarn configuration on each side determines the different area percentage of the yarn on each side, which further affects the electrical output and wearability of the FTENG. In this study, the fabric geometric models are put forward to theoretically calculate the material area percentage, which is of significance to deeply explain the electrical output and directional water transport performance.

t-TENGs show unique advantages and great potential as energy sources for wearable electronics or sensors. This work has presented a series of novel fiber/fabric-based TENGs by combining advanced material system, structures and textile processing

CHAPTER 1

technologies, which addresses issues of wearing comfort, multifunctionality and scalable manufacturing of the t-TENG with low-cost and eco-friendly materials, while providing new insights into human motion monitoring, resulting in a promising research direction for sustainable and functional textiles.

1.5 Outline of the Thesis

This thesis is organized as follows:

Chapter 1 briefly introduces the research background of wearable t-TENGs and the current research issues towards this field. In light of the challenges, the research objectives, methodologies and significance of this study are described in details.

Chapter 2 reviews the recent research progress of t-TENGs, including materials, working mechanism, structures and fabrication methods, properties, applications of textile-based triboelectric nanogenerators.

Chapter 3 exploits a 1D PVDF-based triboelectric yarn (BYTENG) with braided core-shell structure by scalable wet spinning and braiding technologies. The BYTENG exhibits good integration capability and can be used in sports products for real-time exercise detection. The FTENGs knitted/woven by the BYTENG have good softness and breathability, which can be applied into seat cushions, backrest and carpet for human motion monitoring.

Chapter 4 designs and fabricates a 1D core-spun yarn structured triboelectric nanogenerator (CYTENG) based on chitosan/Tencel fibers by a scalable fancy spinning

CHAPTER 1

twister technology. The output performance of the CYTENG is systematically evaluated. The CYTENG not only has excellent electrical performance but also is compatible with current textile technology.

Chapter 5 develops a 2D triboelectric fabric based on woven structure which is fabricated by the continuously spun CYTENG. The FTENG exhibits good electrical output performance and wearability, including breathability, antibacterial property and machine washability.

Chapter 6 proposes a novel 3D FTENG with support zone and functional zone via a scalable weaving process. Based on structural design and rational materials configuration, multifunctionality of 3D woven-structured t-TENG is realized, including excellent electrical performance, wearability and antibacterial property.

Chapter 7 summarizes the whole research projects and states the existing limitations, further discusses the future work of t-TENGs.

CHAPTER 1

References

- (1) Zeng, W.; Shu, L.; Li, Q.; Chen, S.; Wang, F.; Tao, X. M. Fiber-based wearable electronics: a review of materials, fabrication, devices, and applications. *Adv. Mater.* **2014**, *26*, 5310-5336.
- (2) Chen, Y.; Chen, E.; Wang, Z.; Ling, Y.; Fisher, R.; Li, M.; Hart, J.; Mu, W.; Gao, W.; Tao, X.; Yang, B.; Yin, R. Flexible, durable, and washable triboelectric yarn and embroidery for self-powered sensing and human-machine interaction. *Nano Energy* **2022**, *104*, 107929.
- (3) Tan, D.; Xu, B.; Gao, Y.; Tang, Y.; Liu, Y.; Yang, Y.; Li, Z. Breathable fabric-based triboelectric nanogenerators with open-porous architected polydimethylsiloxane coating for wearable applications. *Nano Energy* **2022**, *104*, 107873.
- (4) Zhou, M.; Xu, F.; Ma, L.; Luo, Q.; Ma, W.; Wang, R.; Lan, C.; Pu, X.; Qin, X. Continuously fabricated nano/micro aligned fiber based waterproof and breathable fabric triboelectric nanogenerators for self-powered sensing systems. *Nano Energy* **2022**, *104*, 107885.
- (5) Niu, L.; Wang, J.; Wang, K.; Pan, H.; Jiang, G.; Chen, C.; Ma, P. High-Speed Sirospun Conductive Yarn for Stretchable Embedded Knitted Circuit and Self-Powered Wearable Device. *Adv. Fiber Mater.* **2022**, 1-14.
- (6) Ning, C., Wei, C., Sheng, F., Cheng, R., Li, Y., Zheng, G., Dong K., Wang, Z. L. Scalable one-step wet-spinning of triboelectric fibers for large-area power and sensing textiles. *Nano Res.* **2022**.
- (7) Xie, L.; Chen, X.; Wen, Z.; Yang, Y.; Shi, J.; Chen, C.; Peng, M.; Liu, Y.; Sun, X. Spiral Steel Wire Based Fiber-Shaped Stretchable and Tailorable Triboelectric Nanogenerator for Wearable Power Source and Active Gesture Sensor. *Nano-Micro Lett.* **2019**, *11*, 1-10.

CHAPTER 1

- (8) He, E.; Sun, Y.; Wang, X.; Chen, H.; Sun, B.; Gu, B.; Zhang, W. 3D angle-interlock woven structural wearable triboelectric nanogenerator fabricated with silicone rubber coated graphene oxide/cotton composite yarn. *Composites, Part B* **2020**, *200*, 108244.
- (9) Ning, C.; Dong, K.; Cheng, R.; Yi, J.; Ye, C.; Peng, X.; Sheng, F.; Jiang, Y.; Wang, Z. L. Flexible and Stretchable Fiber-Shaped Triboelectric Nanogenerators for Biomechanical Monitoring and Human-Interactive Sensing. *Adv. Funct. Mater.* **2020**, *31*, 2006679.
- (10) Luo, J.; Wang, Z.; Xu, L.; Wang, A. C.; Han, K.; Jiang, T.; Lai, Q.; Bai, Y.; Tang, W.; Fan, F. R.; Wang, Z. L. Flexible and Durable Wood-Based Triboelectric Nanogenerators for Self-Powered Sensing in Athletic Big Data Analytics. *Nat. Commun.* **2019**, *10*, 5147.
- (11) Zhang, Z.; Jie, Y.; Zhu, J.; Zhu, Z.; Chen, H.; Lu, Q.; Zeng, Y.; Cao, X.; Wang, Z. L. Paper triboelectric nanogenerator designed for continuous reuse and quick construction. *Nano Research* **2022**, *15*, 1109-1114.
- (12) Zhu, J., Cheng, Y., Hao, S., Wang, Z. L., Wang, N., Cao, X. A self-healing triboelectric nanogenerator based on feathers for sensing and energy harvesting. *Adv. Funct. Mater.* **2021**, *31*, 2100039.

CHAPTER 2

CHAPTER 2: Literature Review

2.1 Textiles, E-textiles and Textile-Based Triboelectric Nanogenerators

Textiles are generally divided into three categories: fibers, yarns, and fabrics. Figure 2.1 shows fabric construction platform and hierarchy. Fibers with much shorter diameter than its length are the first level of integration in textiles. Fiber materials can be classified into natural fiber and synthetic fiber. Natural fibers are fibers existing in nature, which can be directly obtained and divided into three types: plant fiber (cotton, linen, ramie), animal fiber (silk, wool) and mineral fiber (asbestos). Synthetic fibers are made of synthetic polymer compounds by means of chemical synthesis and mechanical processing such as polyester, nylon, and acrylic. For the natural fibers, they are usually breathable and soft as well as easily degradable, but their mechanical strength is not as high as synthetic fibers. Synthetic fibers are generally durable, cheap and fast-drying, but lack air permeability and degradability.

By means of twisting, twining, or blending, fibers can form threads or yarns which is considered a secondary integration. Yarn is a strand made of fibers, filaments (extremely long single fibers) or other natural or man-made materials, suitable for constructing interwoven fabrics, such as woven or knitted fabric. Fiber is made into yarn, which needs to go through the processes of opening and blowing, carding, drawing, combing, roving, spinning and winding.

Fabrics are manufactured from yarns by weaving, knitting, stitching, braiding, and felting techniques. They are characterized as hierarchically structured fibrous materials

CHAPTER 2

which are the third level of integration. Fabrics are generally classified into woven, knitted and non-woven fabrics. Woven fabric is a fabric in which two system yarns of warp and weft are interwoven perpendicularly to each other according to a certain rule. Knitted fabric is constructed by forming loops of yarn with knitting needles, then stringing the yarn loops into each other. Instead of spinning and weaving, non-woven fabric is constructed by arranging short textile fibers or filaments to form a web structure and then reinforced by some methods, such as mechanical, thermal bonding or chemical methods.

Compared to conventional fabrics, a new type of fabric, called composite fabric, is further evolved by adding extra oriented yarns. They are the fourth level.¹

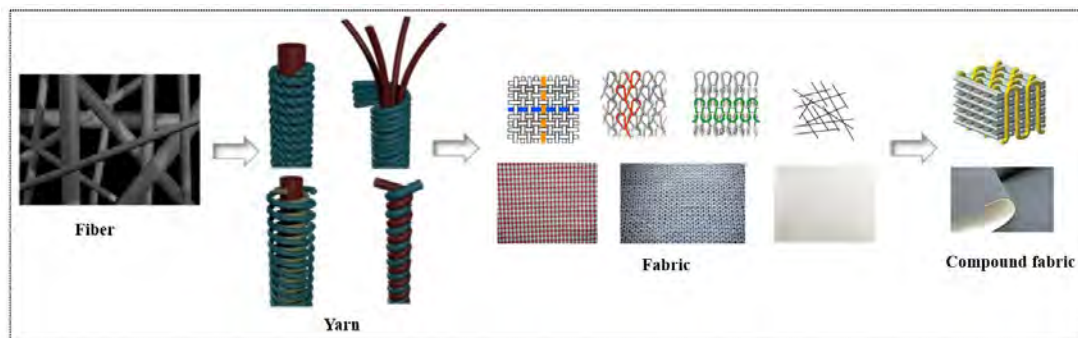


Figure 2.1 Fabric construction platform and hierarchy.^{1,2}

E-textiles indicate textile materials and products which can perform advanced electronic functions but still retain textile characteristics. With the advancement of the Internet of Things (IoT), people are focusing on the electronic textile field.³ By integrating various electronic components in yarns, fabrics, or garments, e-textiles can perceive and respond to external stimuli. Meanwhile, this structure can endow the electronic devices with good wearability and portability. Therefore, textiles can be the ideal substrates and platforms to monitor, process information and interact with

CHAPTER 2

environment.

In order to perform electronic functions, e-textiles need energy supply devices that have the advantages of flexibility, stability, wearability, and excellent energy and power performance. The triboelectric nanogenerator (TENG) couples triboelectricity and electrostatic induction together which can convert mechanical energy into electrical energy, and collect electrical energy from surrounding mechanical movements to drive electronic devices and realize self-powered wearable systems.⁴ Consequently, integrating TENGs into textiles by the employment of textile materials, structure and manufacturing technology is a promising strategy for the above implement of E-textiles.⁵⁻⁸ In particular, the utilization of traditional textile technology to construct TENG provides a versatile solution for the portable, flexible and green energy supply in wearable systems.⁹ With the mature development of the textile technology, textile-based TENG (t-TENG) will enable high design flexibility and mass production for practical applications.¹⁰⁻¹⁸

2.2 Materials for Textile-Based Triboelectric Nanogenerators

The materials used in t-TENGs can be divided into two categories, namely triboelectric materials and electrode materials.

2.2.1 Triboelectric materials

As we all know, from wood, polymer, metal to silk, almost all materials have triboelectric effects. Consequently, the TENGs can be fabricated by using all kinds of materials.¹⁹ However, it is not every pair of materials that can achieve high electrical


CHAPTER 2

output.²⁰ The material choices are of great significance for the electrical output performance of TENGs.²¹ It largely depends on the polarity difference of the material pair.²² A guiding principle of material selection is the triboelectric series, which is a list of various materials sorted according to their ability to lose or gain electrons. The position of the material determines the efficiency of charge exchange. Table 2.1 summarizes the triboelectric sequence of a series of common materials. The arrow pointing upward represents the stronger ability to lose electrons, such as polyamide, or common metal materials such as aluminum and copper. The arrow pointing downward denotes the stronger ability to gain electrons, such as polyvinyl chloride (PVC), polydimethylsiloxane (PDMS), polytetrafluoroethylene (PTFE), etc. Ideally, in the triboelectric sequence, the use of two materials with a large difference in gain and loss of electron abilities can enhance the triboelectric effect and obtain a higher charge transfer rate. Therefore, the selection of a suitable pair of triboelectric materials with opposite triboelectric polarity is vital to enhance the electrical output performance of the TENG. The triboelectrification between two materials is not only based on their charge affinity, but also depends on other physical characteristics, such as elasticity, friction, and surface structure.²¹ Most textile materials are ideal choices for generating tribo-electrostatic charges. As shown in Table 2.1, nylon, silk, wool, leather, cellulose and cotton tend to provide electrons to obtain a positive electrostatic surface charge while other man-made fiber materials are likely to acquire electrons to achieve a negative electrostatic surface charge, namely polyester, acrylic, and polyurethane fibers. Liu et al. investigated the electron charge density of different textile fabrics fabricated by polymeric fibers.²³ The results show that PTFE fabric exhibits the highest negative value of -2.75 nC/cm^2 , among these fabrics. Polylactic acid (PLA) fabric possesses the highest positive charge density of $+0.81 \text{ nC/cm}^2$. The lowest value, about $+0.01 \text{ nC/cm}^2$, is observed in fabrics fabricated from cotton fibers. Regardless of the material used, t-



CHAPTER 2

TENG should possess the properties of good electrical output, flexibility and high mechanical strength as well as excellent breathability.

Table 2.1 Triboelectric series of some materials.²⁴

	Polyformaldehyde 1.3-1.4	(continued)	
	Etylcellulose	Polyester (Dacron)	
	Polyamide 11	Polyisobutylene	
	Polyamide 6-6	Polyurethane flexible sponge	
	Melanime formol	Polyethylene Terephthalate	
	Wool, knitted	Polyvinyl butyral	
	Silk, woven	Polychlorobutadiene	
	Aluminum	Natural rubber	
	paper	Polyacrilonitrile	
	Cotton, woven	Acrylonitrile-vinyl chloride	
	Steel	Polybisphenol carbonate	
	Wood	Polychloroether	
	Hard rubber	Polyvinylidene chloride (Saran)	
	Nickel, copper	Polystyrene	
	Sulfur	Polyethylene	
	Brass, silver	Polypropylene	
	Acetate, Rayon	Polyimide (Kapton)	
	Polymethyl methacrylate (Lucite)	Polyvinyl Chloride (PVC)	
	Polyvinyl alcohol	Polydimethylsiloxane (PDMS)	
	(continued)	Polytetrafluoroethylene (Teflon)	

CHAPTER 2

	Aniline-formol resin	Polyvinyl alcohol	
	Polyformaldehyde 1,3-1,4	Polyester (Dacron) (PET)	
	Etylcellulose	Polyisobutylene	
	Polyamide 11	Polyurethane flexible sponge	
	Polyamide 6-6	Polyethylene terephthalate	
	Melanime formol	Polyvinyl butyral	
	Wool, knitted	Formo-phenolique, hardened	
	Silk, woven	Polychlorobutadiene	
	Polyethylene glycol succinate	Butadiene-acrylonitrile copolymer	
	Cellulose	Nature rubber	
	Cellulose acetate	Polyacrilonitrile	
	Polyethylene glycol adipate	Acrylonitrile-vinyl chloride	
	Polydiallyl phthalate	Polybisphenol carbonate	
	Cellulose (regenerated) sponge	Polychloroether	
	Cotton, woven	Polyvinylidene chloride (Saran)	
	Polyurethane elastomer	Poly(2,6-dimethyl polyphenyleneoxide)	
	Styrene-acrylonitrile copolymer	Polystyrene	
	Styrene-butadiene copolymer	Polyethylene	
	Wood	Polypropylene	
	Hard rubber	Polydiphenyl propane carbonate	
	Acetate, Rayon	Polyimide (Kapton)	
	Polymethyl methacrylate (Lucite)	Polyethylene terephthalate	
	Polyvinyl alcohol	Polyvinyl Chloride (PVC)	
	(continued)	Polytrifluorochloroethylene	
		Polytetrafluoroethylene (Teflon)	

2.2.2 Electrode materials

As important part of TENGs, electrodes are electrical conductors that undergo electrostatic induction. Poor electrical properties may result in a large amount of energy loss in the material, which decreases TENG efficiency.²⁵ In this regard, various electrode materials have been applied in TENGs such as metal and carbonaceous materials, conductive polymers, indium-doped tin oxides (ITOs) and hydrogels.

Owing to high electrical conductivity, the widely used electrode in fabricating t-TENGs is metal film, which can be attached to the textile material using adhesive or double-

CHAPTER 2

sided tape. However, metal thin films exhibit poor behavior because of their inappropriate elastic behavior when they are used for non-conformal surfaces. Besides, the coating or bonding process may affect the durability and service life of the device due to poor bonding between the metal electrode and the soft polymer contact layer.²⁶ Some researchers also use metal-based conductive fabrics. Li et al. developed a cloth-based power shirt which used magnetron sputtering method to deposit Ag onto fabric substrate.²⁷ Pu et al. adopted electroless deposition of Ni coating on polyester yarns.²⁸ For fiber/yarn-based TENG, metal fibers are commonly employed as electrodes, such as conductive silver filament, stainless steel/polyester fiber.²⁹ They can be simply spun or woven with other commercial yarns through using textile manufacturing techniques.³⁰ This technology brings opportunities for large scale production and commercialization of t-TENGs.

Because of good electrical properties and excellent flexibility, carbonaceous materials are considered as electrodes. Carbon nanoparticles, carbon nanotubes (CNT), carbon fibers and graphene are expected to be used as electrodes of t-TENGs. Among these, CNT is the most extensively used for t-TENGs owing to the simple manufacturing process and low cost.^{31,32} Cao et al. investigated the electrode formed by printing CNT, which showed great performance under severe mechanical deformation.¹⁶ According to Zhu et al., they selected graphene ink to coat the surface of nylon fabric.³³ Although it has advantages, carbon-based t-TENG has not yet been commercialized on a large scale due to the difficulty of scaling up production and the high cost of materials.

Conductive polymers have aroused widespread scientific interest owing to their special electrical, optical and mechanical properties.³⁴ Poly(3,4-ethylenedioxythiophene) polystyrene sulfonate (PEDOT: PSS), as a commercial conductive polymer, is

CHAPTER 2

commonly used as a coating or printable electrode with high conductivity and good stability. Zhu et al. fabricated a self-powered and self-functional sock which utilized PEDOT: PSS to coat TENG textile integrated lead zirconate titanate (PZT) piezoelectric sensor.³⁵

2.3 Basic Working Mechanism and Modes of Textile-Based Triboelectric Nanogenerators

The triboelectric effect is one of the common phenomena in nature, which is easy to see in daily life and can be found in nearly all materials, for instance metals, ceramics and polymers.³⁶ However, the mechanism of frictional electrification is not yet clear. The two main phenomena of TENG are contact electrification (triboelectrification) and induced charge transfer.¹⁹ In metal-metal, metal-semiconductor and metal-insulator contact friction, triboelectrification through electron transfer has been accepted. Some researchers have also proposed ion transfer to explain the contact electrification. The ions containing functional groups have an important effect on contact electrification.^{37, 38} Based on atomic or molecular orbital models, an electron cloud potential well model was presented to clarify the contact electrification mechanism of all two interacting material systems.³⁹ A curvature dependent charge transfer model was developed to illustrate the contact electrification between two identical materials.⁴⁰ A variety of structures and operating modes of TENGs have been developed to realize mechanical energy collection under different conditions. According to circuit connection method and load applied direction, the basic operating modes of TENGs include four types: vertical contact-separation mode, lateral-sliding mode, single-electrode mode and freestanding triboelectric-layer mode.⁴¹ Figure 2.2 illustrates the four basic operation modes of t-TENGs. The yellow fabrics represent conductive fabrics, while the gray,

crimson, and blue fabrics represent dielectric fabrics.

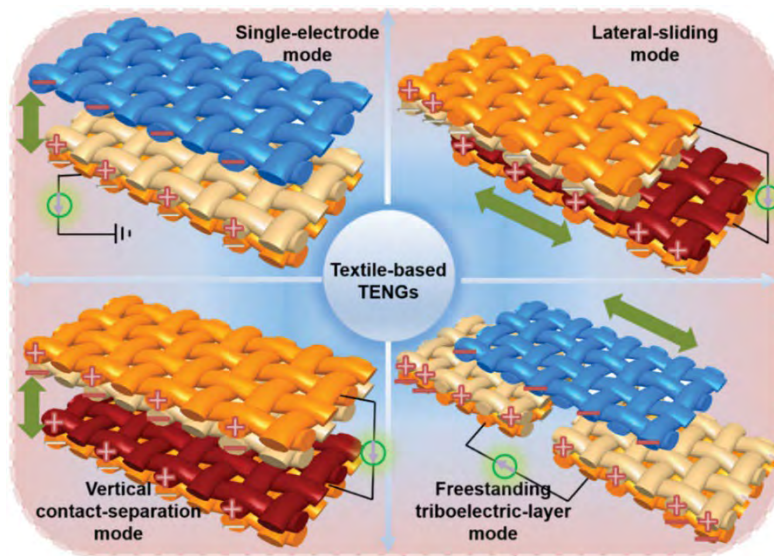


Figure 2.2 Four basic working modes of t-TEGs. ⁴¹

2.3.1 Vertical contact mode

The operating mechanisms of t-TEGs under four working modes are all based on the combination of electrification effect and electrostatic induction. Figure 2.3 shows the working principle of the t-TEG under vertical contact-separation mode. The upper and lower fabrics contain a conductive fabric and a dielectric fabric respectively. In the beginning, no electrical charge is generated. Under the action of external force, when upper and lower fabrics come into contact, electrification occurs on the interfaces of the fabrics, creating the same amount of opposite charges. The upper fabric with strong electron-acquiring ability will get electrons from the lower fabric with strong electron-losing ability. As a result, the inner surface of the upper fabric is negatively charged and the inner surface of the lower fabric is positively charged. When the external force is removed, the upper and lower fabrics gradually separate. Due to the presence of electrodes on the back of the fabric, positive and negative charges are induced at the

CHAPTER 2

top and bottom electrodes of the fabrics because of electrostatic induction effect. The fabric electrode on the back forms a loop through an external wire, so that the generated potential difference will drive the charge of the electrode to move in the external circuit, and then generate an electrical signal. When the layers of two fabrics are fully separated, the positive and negative charges are completely balanced by electrostatic induced charges. In this case, there is no electrical signal between the two fabric layers, which reflects the neutralization of the charge during this period. It is worth noting that the accumulated charges will not be completely wiped out. Owing to the inherent characteristics of insulators, the charges will be maintained for a certain period of time. In the opposite case, if the two fabric layers are close to each other, the accumulated induced electrical charge of fabric layer will flow back via the external load to compensate for the potential differences. Therefore, instantaneous alternating potential and current will be generated.

Most t-TENGs work under this mode owing to the characteristics of human movement and easy fabrication. For instance, they could be designed on socks to collect energy from human motion, or embedded in the fabric to generate energy by pressing or stretching the fabric.⁴² This motion causes contact and separation motion. The t-TENG can be fabricated in a variety of forms, such as yarns or multilayer fabrics.^{33, 43-47}

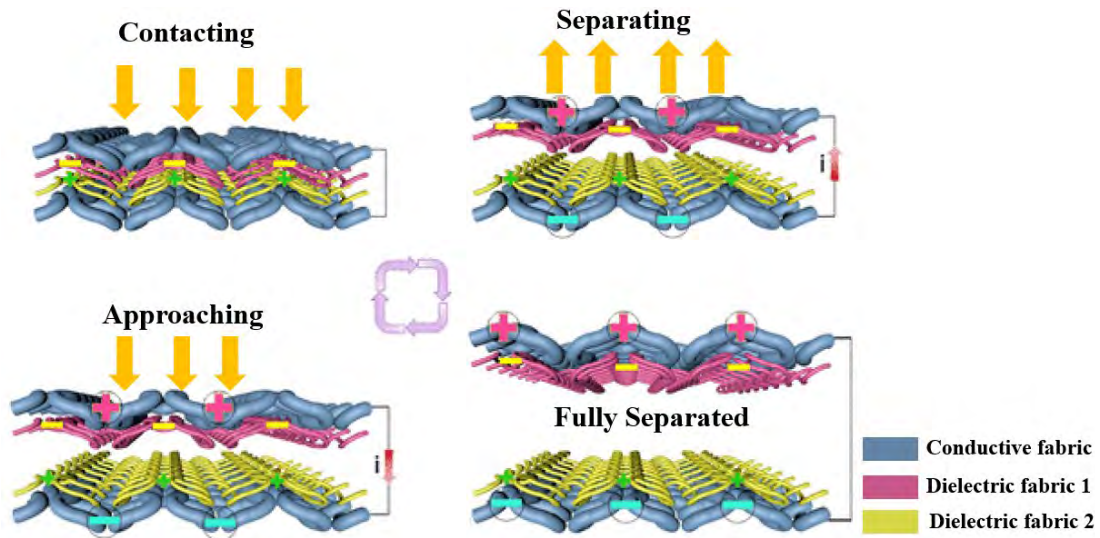


Figure 2.3 Working principle of t-TENGs under contact-separation working mode.⁴⁸

2.3.2 Lateral sliding mode

Under the lateral sliding mode, the fundamental structure comprises two various dielectric layers with two back electrodes, which is similar to that of the vertical contact mode. However, the gap in the vertical direction does not exist. As there is an external force exerted in the lateral direction, sequential contact is made on the surfaces of the two dielectric materials. After triboelectric charging is generated on the surfaces of the two different dielectric materials, an electric field is formed on the back electrode during the continuous approach and separation. Then, an electron flow is generated between the two electrodes to achieve the neutralization of potential difference. This mode is often utilized in plane motion, or the rotation of disks or cylinders.

An example of t-TENGs under the lateral sliding mode was demonstrated by Dong et al., as shown in Figure 2.4. They fabricated an energy-harvesting fabric by using the energy-harvesting yarns, acrylic yarns and polyester yarns.⁴⁹ The back-and-forth sliding between the upper copper electrode and bottom fabric caused periodic changes in the

CHAPTER 2

potential difference, which drove the alternating flow of free electrons through the electrodes.

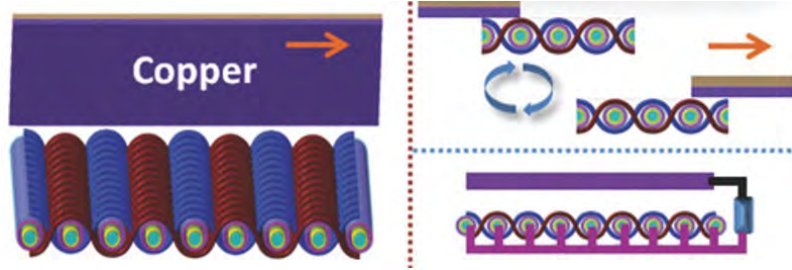


Figure 2.4 The sliding mode of energy-harvesting fabric.⁴⁹

2.3.3 Single electrode mode

The TENG using single electrode mode consists of a dielectric material and an electrode. The reference electrode is usually connected to the main electrode in practical applications so that it can serve as an electron source. Continuous approach and separation of the dielectric layers cause the flow of electron between the main electrode and the ground because of the changes in the induced potential on the main electrode. This working mode is widely employed in t-TENGs. In this working mode, external materials can be utilized as dielectrics, for instance conventional fabrics or human skin, because the electrical connection or electrode is not required for the freely moving dielectric. This working mode is also suitable for vertical and lateral movement. The dielectric layer under this mode can move easily, making it applicable in a variety of situations. An example was reported by Xie et al. who designed a single electrode stretchable and tailorable triboelectric nanogenerator with fiber structure (Figure 2.5). The t-TENG was fabricated by coating silicone rubber onto a steel wire conductive core. The results show that the device can generate the voltage of 59.7 V, charge of 23.7 nC and current of 2.67 μA as well as average power of 2.13 μW at under 2.5 Hz.⁵⁰

CHAPTER 2

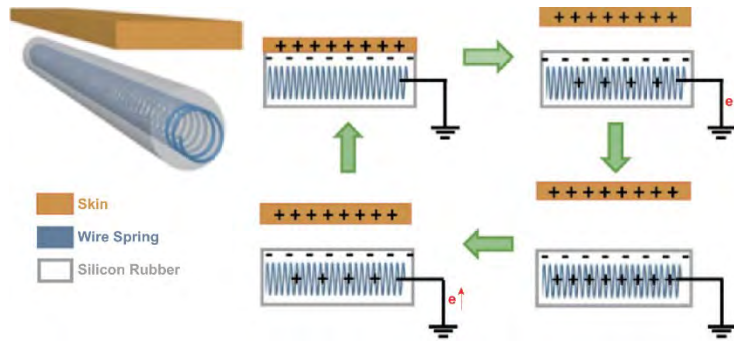


Figure 2.5 Working mechanism of fiber-shaped triboelectric nanogenerator at single-electrode mode.⁵⁰

2.3.4 Freestanding mode

The structure of the freestanding mode comprises of two electrodes underneath a dielectric material and moving object. With approaching or moving away of object, asymmetrical charge distribution will occur on each electrode. As a result, electrons move across the external circuit that connects the two electrodes to achieve the balance. Some t-TENGs operating in this mode have been designed.⁵¹⁻⁵³ For instance, Chen et al. developed the FTENG at free-standing mode by designing horizontal motion of PTFE grating textile and interdigital carbon textile electrode, as shown in Figure 2.6.⁵¹ The approach and departure between the dielectric textile and the electrodes created a charge distribution, which led to the electrons flowing between the two electrodes.

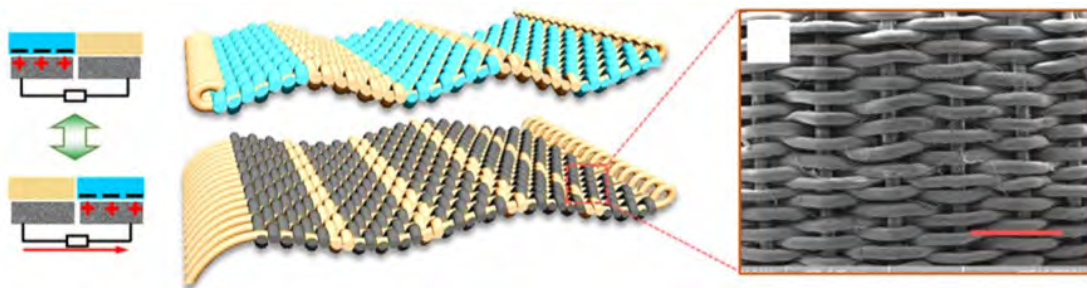


Figure 2.6 Schematic illustration of fabric triboelectric nanogenerator under the free-

CHAPTER 2

standing mode.⁵¹

2.4 Structures and Fabrication Methods of Textile-Based Triboelectric Nanogenerators

Since the main component of t-TENG is two friction surfaces with distinct properties, the basic idea behind t-TENG design is to properly assemble these two surfaces to the textile. In this way, not only the function of the TENG can be achieved, but also the characteristics of the textile such as flexibility, lightweight and wearability can be maintained. In order to achieve this goal, some structures and fabrication methods have been developed. The structures can be briefly classified into four categories. In this section, these structures design and corresponding fabrication methods are introduced.

2.4.1 Fiber/Yarn-based TENGs

One structure of t-TENG adopts a fiber/yarn form. The remarkable merits of fiber/yarn-based structure are that they have great design feasibility for integration, allowing the energy harvesting fiber/yarn to be easily woven, knitted, stitched or embroidered into any existing textile substrates. Typically, coaxial and core-shell architectures are used to create fiber- and yarn-based TENGs. In terms of working modes, it is common practice to use fiber/yarn-based TENGs in the single electrode and vertical contact separation modes.

Fiber/yarn-based TENG in single electrode mode

Considering the benefits of simple structure, easy fabrication and good performance,

CHAPTER 2

the fiber/yarn-based TENGs operating in single electrode mode have been widely reported. The fiber/yarn-based TENG under single electrode mode is composed of inner fiber electrode and an outer dielectric layer. In this regard, different approaches have been adopted to obtain this structure, such as yarn spinning technology,^{54, 55} electrospinning,^{56, 57} thermal drawing,⁵⁸ 3D printing,⁵⁹ coating techniques,^{32, 60-63} etc. Among them, wrapping dielectric materials around the core fiber electrodes is the simplest configuration for fiber/yarn-based TENGs. As shown in Figure 2.7a, a flame-retardant single-electrode triboelectric yarn (FRTY) was fabricated through wrapping the polyimide yarn over the conductive core yarn using a scalable spinning fancy twister technology.⁵⁴ It exhibited high power density of 73.55 $\mu\text{W}/\text{m}$. The obtained FRTY had unlimited length and good flexibility, which could meet various mechanical requirements and processing conditions of weaving. Besides, Chen et al. proposed a soluble-core method to fabricate ultra-stretchable styrene-ethylene-butylene-styrene (SEBS) hollow fibers, then the TENG fibers were developed through incorporating liquid metal into the hollow SEBS fibers (Figure 2.7b).⁵⁸ The eight TENG fibers could be stretched to a strain of 1000% with an output of ~ 7.5 V. Moreover, a Direct-Ink-Writing (DIW) 3D printing technology was used to develop PDMS based coaxial stretchable fibers for self-powered tactile sensing. A 3D printed elastic fiber with coaxial core-sheath structure was developed, which was composed of PDMS/graphene as conductive core and PDMS/ PTFE as insulative sheath (Figure 2.7c).⁵⁹ As exhibited in Figure 2.7d, a fermat-spiral based energy yarn (FSBEY) was constructed by twisting poly(vinylidene fluoride-trifluoroethylene) (P(VDF-TrFE)) nanofibers on the stretchable conductive yarn using conjugate electrospinning.⁵⁷ With the merits of outstanding structural dynamic stability, the FSBEY obtained excellent electrical output (105 V, ≈ 1.2 μA at 2 Hz), ultrahigh abrasion resistance and stable reversible strain (100%). Figure 2.7e presents a highly tribopositive elastic yarn, which was assembled

CHAPTER 2

using polyethyleneimine/multiwalled carbon nanotubes/phytic acid (PEI/MWCNTs/PA) nanomaterial as electrode and polyethylene oxide/waterborne polyurethane/alliin (PEO/WPU/alliin) composite as stretchable triboelectrode onto the yarn substrate.⁶⁴ The yarn TENG working in single-electrode mode could reach high voltage of 137 V and power density of 2.25 mW/m. In addition, the most commonly used method for fabricating single electrode TENG yarn is to coat PDMS or silicone rubber on the conductive fiber surface. As presented in Figure 2.7f, a highly stretchable fiber-shaped triboelectric nanogenerator was created through coating silver nanowires/carbon nanotubes and PDMS onto the stretchable spandex fiber.⁶¹ Similarly, as shown in Figure 2.7g, a conductive fiber was constructed by coating an elastic fibre with MXene ink, then growing Ag nanoparticles (AgNPs) on MXene nanosheets. PDMS was used to coat the conductive fiber to form a single-electrode mode TENG yarn. The resulting TENG yarn exhibited extraordinary output performance (a voltage of 7.7 V under the testing length of 3cm).⁶⁰

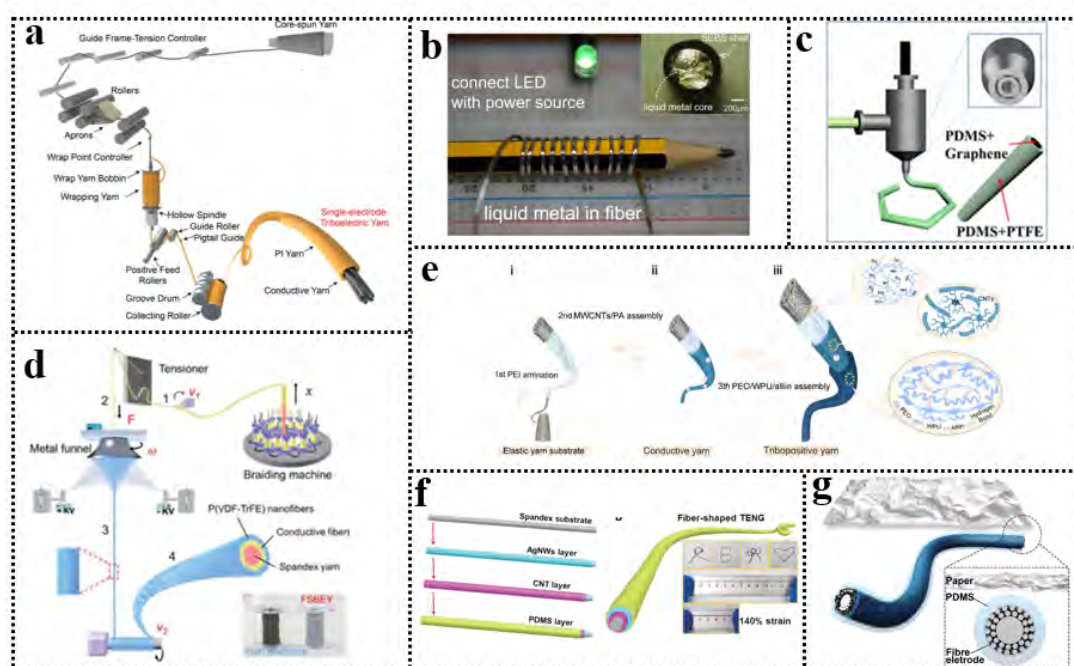


Figure 2.7 Fiber/yarn-based TENGs under single electrode mode. (a) Schematic

CHAPTER 2

illustration of triboelectric yarn developed by a scalable spinning technology.⁵⁴ (b) Ultra-stretchable conductive TENG fiber by soluble-core thermal drawing.⁵⁸ (c) 3D printed elastic smart fiber with coaxial core-sheath structure realized by a DIW 3D printing technology.⁵⁹ (d) Fermat-spiral-based energy yarn fabricated by conjugate electrospinning technique.⁵⁷ (e) Tribopositive elastic yarn using interfacial assembly technology.⁶⁴ (f) Fiber-shaped triboelectric nanogenerator through a three step coating method.⁶¹ (g) A multifunctional TENG yarn by dip coating method.⁶⁰

Fiber/yarn-based TENG in contact-separation mode

Compared to fiber/yarn-based TENG in single electrode mode, fiber/yarn-based TENG under vertical contact-separation mode provides higher electrical output performance. The TENG fiber/yarn in contact-separation mode is designed with a coaxial structure in which a gap occurs between inner core and outer shell. The main principle of tribomaterial selection is that the materials of the core layer and the shell layer possess opposite triboelectric polarities. For example, a yarn-based TENG with core-sheath structure was designed (Figure 2.8a).⁴⁹ The internal core was constructed by winding a conductive nylon yarn (inner electrode) onto a silicone rubber fiber (as a support). Meanwhile, the external sheath tube was formed by twisting another conductive nylon yarn (outer electrode) on a commercial elastic silicone rubber (framework), then encapsulated by silicone rubber solution (encapsulating layer). The yarn-based TENG was fabricated after inserting the internal core into the external sheath, which showed an output voltage of 13.5 V under a strain of 100%. As shown in Figure 2.8b, a stretchable triboelectric fiber (STEF) was fabricated with multilayered core-shell and wrinkle structure by wrapping silver-coated nylon yarn, electrospun P(VDF-TrFE) mat and CNT sheets around polyurethane (PU) fiber. The STEF could generate 24 mV under

CHAPTER 2

a strain of 50%.⁶⁵ Chen et al. reported a highly stretchable yarn-based triboelectric nanogenerator, which was made of highly stretchable PU and ultra-flexible silicone rubber with multi-gradient hierarchical structure (Figure 2.8c).⁴⁴ First, the conductive electrode was wrapped around highly stretchable PU, then the first helical layer was formed and served as the inner electrode. Ultra-flexible silicone rubber was encapsulated on the first helical layer, which was used for electrification and generating the charges. Finally, copper wires as the outer electrode and the other triboelectrification layer were wound around the silicone rubber. The hierarchical helical yarn demonstrated excellent flexibility which could work in the strain range of 60%-120%. By using a multiaxial fiber winding machine, a helical fiber strain sensor was developed by winding nylon/Ag braided fibers and PTFE/Ag braided fibers alternately, and the output voltage could reach 0.5 V even at a stretch strain of 1% (Figure 2.8d).⁶⁶ As exhibited in Figure 2.8e, a stretchable TENG-based sensor was constructed with a core-sheath structure by utilizing a PU/CNTs/Dragon Skin multilaminate fiber as the core and a silver nanowires (AgNWs)-coated Reduced Graphene Oxide (rGO)/PDMS film as the sheath, which exhibited the output voltage and current of 10 V and 0.6 μ A, respectively.⁶⁷ Similarly, as presented in Figure 2.8f, a stretchable triboelectric fiber with sheath-core structure was reported.⁶⁸ Nylon fiber wound conductive fiber was used as the core, and AgNWs coated bamboo fiber sandwiched between silicon rubber tube and PDMS film was served as the shell. An output voltage of 3.22 V under high working strain (100%) was obtained owing to unique built-in wavy of the core fiber. As shown in Figure 2.8g, a TENG with fiber shape was designed by using silicone rubber wrapped carbon nanotubes as the core and convolved Cu wire as the shell, which could achieve high strains up to 70% with good electrical output.⁴³

CHAPTER 2

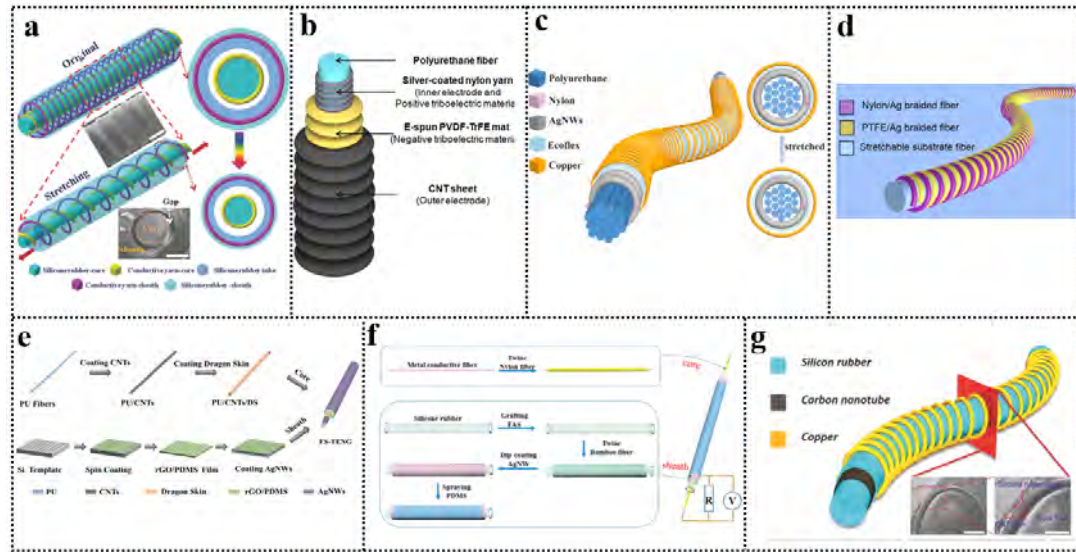


Figure 2.8 Fiber/yarn-based TENGs in contact-separation mode. (a) A yarn-shaped TENG with coaxial core-sheath structure.⁴⁹ (b) A stretchable fiber with core-shell structure.⁶⁵ (c) A flexible hierarchical helical yarn.⁴⁴ (d) A fiber strain sensor with helical structure.⁶⁶ (e) A fibrous stretchable TENG-based sensor.⁶⁷ (f) A triboelectric fiber with core-sheath structure.⁶⁸ (g) A highly stretchable fiber-like TENG.⁴³

2.4.2 Fabric-based and nanofiber-based TENGs

In order to enhance electrical performance, t-TENGs are typically fabricated in terms of fabrics. Since the quantity of charge generated at the interface determines the output of TENG, the fabric can provide more surface area for the electrification process, leading to improved performance. Up till now, various types of FTENGs have been proposed such as 2D FTENGs, modified FTENGs and nanofiber-based TENGs.

2D FTENGs

One kind of 2D FTENGs structures is fabricated by the utilization of energy harvesting fiber/yarn described above.^{4, 36, 69} As shown in Figure 2.9a, Yu et al. reported a

CHAPTER 2

comfortable and flexible TENG textile by weaving or knitting from core-shell yarns, which were made of conductive fiber as the core and common textile fiber as the covering sheath.³⁰ The fabricated TENG textiles demonstrated the advantages of apparel fabrics: lightweight, flexible and universally applicable in fiber material selection. Similarly, Figure 2.9b presents a stretchable TENG fabric, which was knitted from energy-harvesting yarns (silicone rubber coated stainless steel/polyester fiber blended yarn). An all-textile triboelectric sensor was designed by sewing the sensing yarn into the glove, as shown in Figure 2.9c.⁷⁰

Another type of 2D FTENGs is made by narrow thin film or strips of cloth.⁵² As exhibited in Figure 2.9d, PA66 or P(VDF-TrFE) nanofiber strips were wrapped onto stainless steel yarn (SSY), thus forming core-sheath yarns. A woven-structured TENG was fabricated by weaving PA66-SSY as weft and P(VDF-TrFE)-SSY as warp with a handloom.⁷¹ A woven-TENG consisted of woven strips of PTFE coated fiberfill fabric and nylon fabric, which constructed a checker-like pattern over the electrodes woven by Ag coated PVC fabrics strips (Figure 2.9e).⁵² Moreover, a stretchable TENG textile knitted by black wool threads and poly (methyl acrylate) (PMA) coated poly (NAGA-co-AAm) (PNA) hydrogel fibers showed an output open-circuit voltage (V_{oc}) of -36 V (Figure 2.9f).⁷² As shown in Figure 2.9g, a self-powered textile was knitted by fiber-shaped coaxial tribo-sensor with silver (Ag) filaments as electrodes and PTFE yarn as frictional layer, which delivered the output voltage and current of 8 V and 90 nA, respectively.⁷³ Furthermore, a weaved piezoresistive TENG was reported by using the Ag NWs coated nylon thread as core electrode, CNTs/Parafilm as the sensing element and PDMS/CNTs coating as the triboelectric layer, as shown in Figure 2.9h.⁷⁴ Besides, a highly stretchable energy-harvesting textile was constructed by sewing the energy-harvesting thread (silicone rubber coated stainless-steel thread) into a serpentine shape

CHAPTER 2

on an elastic textile (Figure 2.9i).⁷⁵ By utilizing electrostatic breakdown phenomenon of clothes, a direct current FTENG with plain structure was realized through using polyamide (PA, nylon-66) nonconductive yarn as warp yarns, PA nonconductive yarns and PA conductive yarns as weft yarns, as shown in Figure 2.9j.⁷⁶

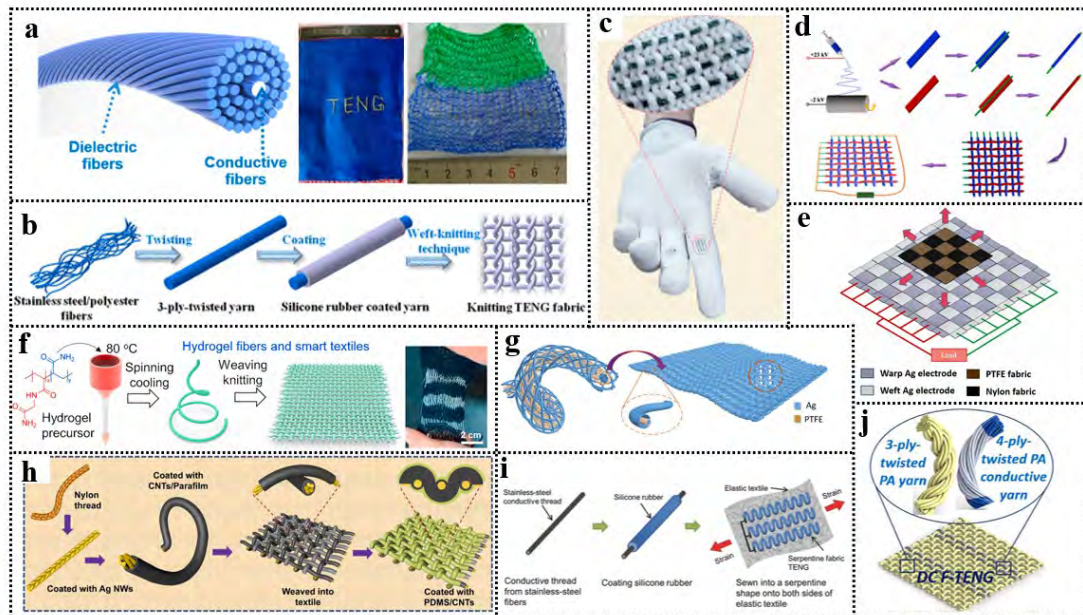


Figure 2.9 Typical 2D FTENGs. (a) Triboelectric nanogenerator textiles woven or knitted by core-shell yarns.³⁰ (b) A highly stretchable TENG fabric knitted from an energy-harvesting yarn.⁷⁷ (c) A smart glove sewn with all-textile triboelectric sensor.⁷⁰ (d) A woven structured triboelectric nanogenerator by using electrospun nanofibers.⁷¹ (e) A textile-based triboelectric nanogenerator with woven strips of positive and negative triboelectric material.⁵² (f) A TENG textile knitted from PNA/PMA fibers and wool threads.⁷² (g) A shape-adaptive electronic textile knitted by fiber-shaped coaxial tribo-sensor.⁷³ (h) A weaved piezoresistive triboelectric nanogenerator.⁷⁴ (i) A highly stretchable energy-harvesting textile sewn by energy-harvesting thread.⁷⁵ (j) A direct current FTENG.⁷⁶

CHAPTER 2

Modified FTENGs

Fabric surface modification is considered to be another efficient methodology to construct FTENGs.⁷⁸ Surface coating method has been widely used to develop t-TENG.^{25, 79} As shown in Figure 2.10a, a large-scale and washable smart textile as self-powered sleeping monitoring was obtained from conductive fibers and elastomeric materials, which composed of three layers, including top and bottom fabrics laminated by arrays of conductive fibers, and a wavy-shaped PET film sandwiched by the top and bottom fabrics.⁸⁰ In order to improve incessant friction and washing ability of wearable FTENGs, functionalized FTENGs were reported via using F-silk (urethane perfluorooctyl silane (NHCOO-PFOTS) coated silk fabric) and nylon fabric as friction pairs. The conductive fabric was served as the electrode, which was stuck on the F-silk and nylon fabric, respectively (Figure 2.10b).⁸¹ In addition, laser-scribing masking and electroless deposition (ELD) were proposed to fabricate the synthetic conductive circuits/patterns on textiles. For example, an interdigitated grating-structured FTENG was designed with slider and stator fabrics.¹² The slider fabric was composed of interdigitated metal electrodes. The stator fabric containing interdigitated Ni electrodes was coated by parylene using chemical vapor deposition, which was served as an electrification layer (Figure 2.10c). Omniphobic triboelectric nanogenerators (RF-TENGs) with stretchability, breathability, waterproof and antibacterial properties were fabricated through combining embroidery technology with the spray-based deposition of fluoroalkylated organosilanes, AgNFs and PTFE (Figure 2.10d).⁸² Taking advantage of the feasibility of screen-printing technology, a tribo-sensor was assembled from three layers, including silk fabric served as one frictional material (top layer), CNT electrode array (middle layer) and nylon fabric (bottom layer). CNT ink served as electrode array was printed on the nylon fabric, as shown in Figure 2.10e.¹⁶

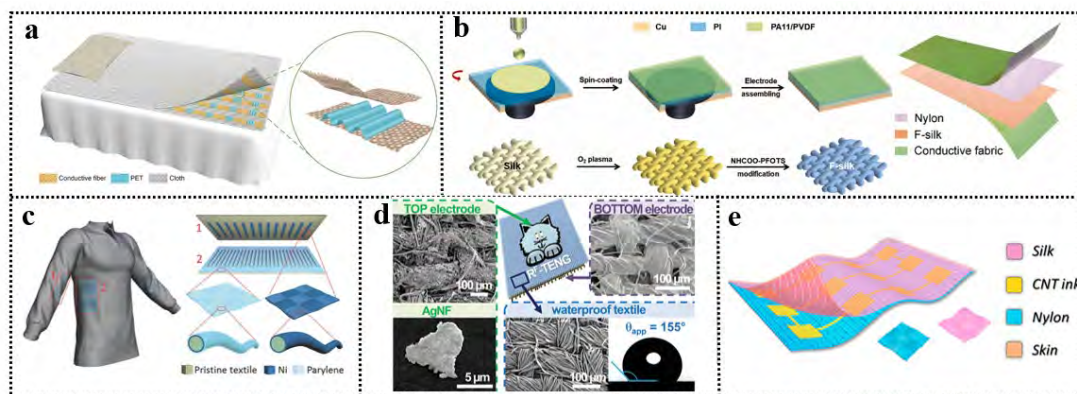


Figure 2.10 Modified FTENGs. (a) A TENG based self-powered smart textile prepared by wavy-structured PET films sandwiched in two conductive fabrics.⁸⁰ (b) A F-TENG constructed by F-silk, nylon fabric and conductive fabric.⁸¹ (c) A grating-structured TENG fabric.¹² (d) An omniphobic (both hydrophobic and oleophobic) triboelectric nanogenerator.⁸² (e) A washable electronic textile with screen printing.¹⁶

Nanofiber membrane structured TENGs

Alternatively, another way to construct TENG is to use nanofiber films. Due to its unique characteristics, especially large surface area and high porosity as well as inherent rough structure, electrospinning film is an ideal material for TENG.⁸³ For instance, as shown in Figure 2.11a, a nanofiber structured TENG was fabricated, which consisted of PA66/MWCNTs (tribo-positive layer) and PVDF (tribo-negative layer) nanofiber films for contact electrification, two conductive fabrics for electrode and waterproof breathable cotton fabric for protecting, respectively.⁸⁴ Moreover, TENG-based E-skin was constructed by electrospinning and spraying alternately using multilayered structure (Figure 2.11b).⁸⁵ The fabricated E-skin possessed excellent pressure sensitivity and outstanding thermal-moisture comfort as well as remarkable antibacterial activity. Similarly, Peng et al. developed an all-nanofiber electronic skin, which was composed of AgNW nanofiber film, polylactic-coglycolic acid (PLGA)

CHAPTER 2

nanofiber film and polyvinyl alcohol (PVA) nanofiber film by a facile electrospinning strategy (Figure 2.11c).⁸⁶ In order to enhance moisture evaporation rate and achieve higher output performance, as shown in Figure 2.11d, a ferroelectric-enhanced triboelectric evaporation textile was developed, which was composed of a TENG with ferroelectric-enhancement and a fabric with directional moisture-wicking property.⁸⁷ In addition, an all-fiber triboferroelectric e-textile was fabricated by four functional layers, namely, P(VDF-TrFE) and PA6 nanofiber nonwovens with opposite tribo-polarity, nickel-copper (Ni-Cu) fabric electrode and the moisture-wicking fabric, which showed excellent thermal-moisture comfortability (Figure 2.11e).⁸⁸ Additionally, nanofiber-based TENGs could also be designed into other structures. As presented in Figure 2.11f, a TENG with continuous arch structure was prepared via electrospinning and ultrasonic welding method.⁸⁹ Besides, a highly stretchable TENG was constructed by spraying rGO and AgNWs conductive network on the TPU mats layer by layer, in which TPU prepared by electrospinning was used as the triboelectric and protection layers (Figure 2.11g).⁹⁰ These structures contributed to high stability of the TENG.

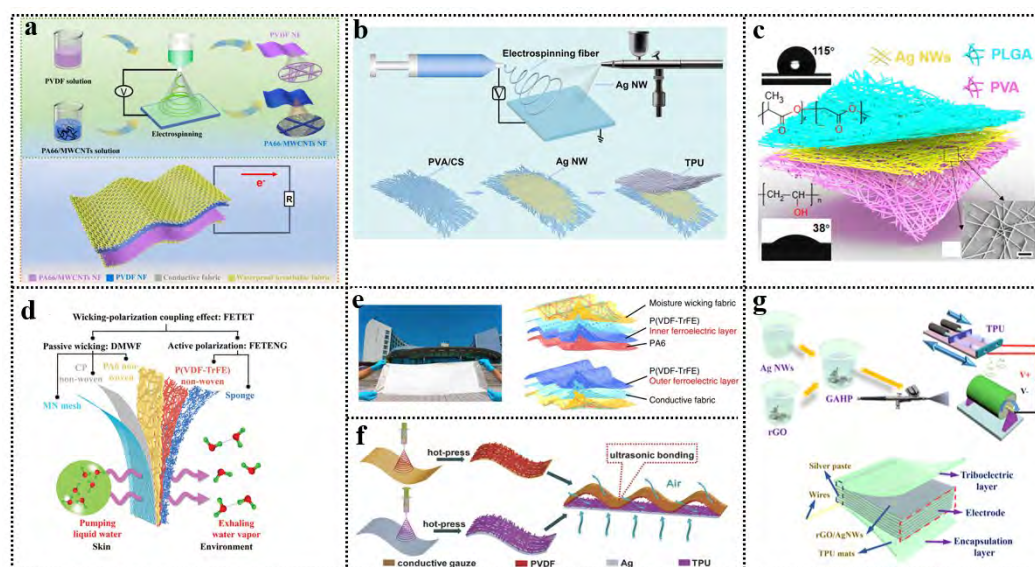


Figure 2.11 Nanofiber membrane structured TENGs. (a) A nanofiber film based triboelectric nanogenerator with hierarchical structures.⁸⁴ (b) A TENG-based E-skin.⁸⁵

CHAPTER 2

(c) A self-powered electronic skin.⁸⁶ (d) A ferroelectric-enhanced triboelectric evaporation textile.⁸⁷ (e) A tribo-ferroelectric synergistic electronic.⁸⁸ (f) A TENG with continuous arch structures based on nanofibrous membrane.⁸⁹ (g) A stretchable TENG based e-skin.⁹⁰

2.4.3 3D structured FTENGs

Currently, 2D textile structures have been widely used in developing FTENGs due to its easy preparation and compatibility with textile technology. However, the power output of 2D FTENG is relatively low. FTENGs with 3D structures have increasingly been used to further improve the output performance.⁹¹ In terms of textile manufacturing techniques, 3D fabric structures consist of 3D weaving, knitting and braiding. In order to increase the stretchability, elasticity and spaces of contact and separation, FTENGs with 3D knitted structures have been prepared. For instance, a 3D double-faced interlocking fabric TENG (3DFIF-TENG) was knitted using two sets of yarns including cotton and modified PA composite yarns, as shown in Figure 2.12a.⁹² By improving the 3D structure of TENG, the 3DFIF-TENG could be used as energy harvesting devices and multifunctional sensors. Moreover, the 3D spacer knitting structure have been widely employed to fabricate t-TENGs, which exhibited enough internal spaces and high compression resilience to contact and separate. In order to improve electrical output, comfort and scalability, a 3D spacer fabric TENG was prepared by continuous coating and knitting technologies, as shown in Figure 2.12b.⁹³ Two different core-spun yarns, namely TPU coated Ag-cotton and PDMS coated Ag-cotton, were employed as triboelectric materials to knit the upper and lower surfaces. Polyacrylonitrile (PAN) yarns were adopted to connect the two layers. Similarly, as shown in Figure 2.12c, a 3D warp-knitted power fabric was designed and fabricated,

CHAPTER 2

which was composed of polyethylene (PE) braided layer (top layer), poly (ethylene terephthalate) (PET) layer (spacer layer) and poly(tetrafluoroethylene) (PTFE) braided layer (bottom layer).⁹⁴ With the advantages of 3D warp-knitted power fabric TENG, the enhanced power output and improved pressure sensitivity could be obtained. A 3D weft-knitted fabric generally consists of three layers, namely two outer layers with the opposite tribo-polarity and a spacer yarn layer. For example, as exhibited in Figure 2.12d, the nylon of the upper layer and PTFE coated nylon electrode of lower layer were served as friction layers.³³ The spacer yarn layer fabricated by the polyester monofilament could provide the good resilience. The prepared TENG with 3D weft-knitted structure possessed excellent force sensitivity. 3D woven FTENGs with the benefits of mechanical robustness and stability have been widely reported. For example, as shown in Figure 2.12e, a textile triboelectric generator with double-layer structure was fabricated by weaving technique, using polyurethane (PU) nanofiber wrapped copper core-spun yarn and Si₃N₄-doped PVDF nanofiber wrapped copper core-spun yarn.⁹⁵ A nylon filament was used to bind the two plain fabrics produced by two different nanofiber core-spun yarns. As presented in Figure 2.12f, a woven TENG with 3D orthogonal structure was designed, which was fabricated by three kinds of yarns, namely, stainless steel/polyester fiber blended yarns used as warp yarns, PDMS-coated energy-harvesting yarns served as weft yarns and nonconductive cotton yarns used as the bonding Z-yarns.²⁹ Particularly, the Z-binding yarns interconnecting warp and weft yarns were used to solidify the fabric. In addition, a 3D angle-interlock FTENG was prepared by using two system yarns including silicone rubber coated graphene oxide (GO)/cotton composite yarns and z-binding yarns to improve output performance (Figure 2.12g).⁹⁶ 3D braided fabric is made of multiplied braided yarn interwoven with each other in various directions. Due to excellent flexibility, mechanical stability and structural integrity, TENG with 3D braided structure has been developed. For instance,

CHAPTER 2

a 3D braided TENG was fabricated by a four-step rectangular braiding technology, in which PDMS-coated energy yarn and eight-axial winding yarn were used as the braided yarn and the axial yarn, respectively (Figure 2.12h).⁹⁷ The improved output performance and high compression resilience could be obtained by the fabricated 3D braided TENG.

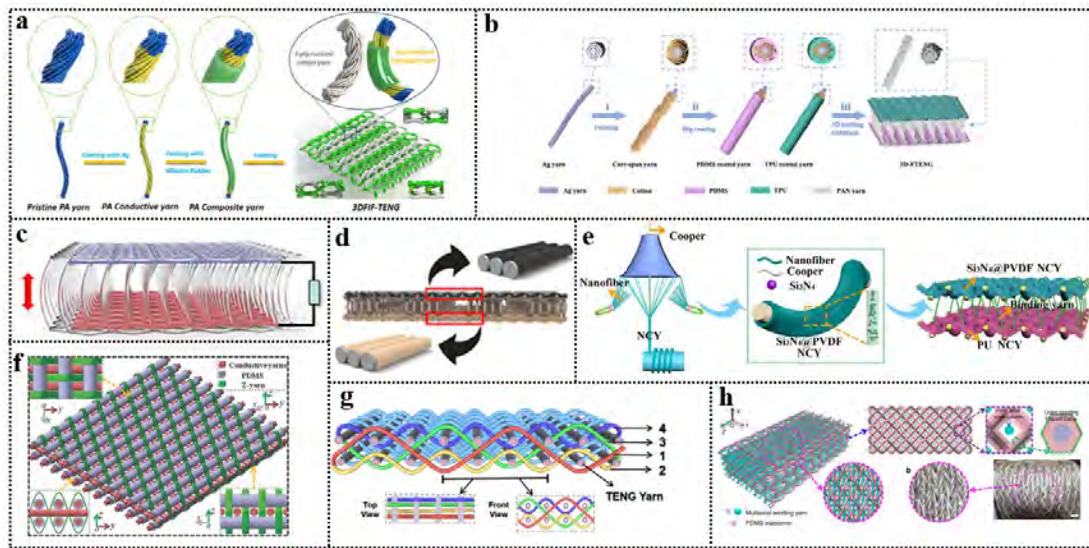


Figure 2.12 3D structured FTENGs. (a) A fabric TENG with 3D double-faced interlock structure.⁹² (b) A textile TENG with 3D spacer fabric structure.⁹³ (c) A 3D warp-knitted spacer power fabric.⁹⁴ (d) A FTENG with 3D weft-knitted fabric structure.³³ (e) A textile triboelectric generator with double-layer structure.⁹⁵ (f) A 3D orthogonal woven TENG.²⁹ (g) A woven TENG with 3D angle-interlock structure.⁹⁶ (h) A 3D braided TENG.⁹⁷

2.5 Desired Performance of Textile-Based Triboelectric Nanogenerators

2.5.1 Electrical output performance

Considering the continuous work of t-TENGs, a high and efficient power output is

CHAPTER 2

needed. To date, various approaches have been proposed to improve the output performance of t-TENGs, such as surface modifications,⁹⁸⁻¹⁰⁵ material optimization,¹⁰⁶⁻¹¹¹ device structure improvement,^{96, 112-115} circuit management,¹¹⁶ and environmental improvement.^{117, 118} Surface/interface modification has been utilized to enhance the effective contact area by introducing nanostructures, such as nanoparticles, nanorods, nanowires and nanopatterns, which could increase the surface charge densities of the interfaces. By using the hydrothermal method, Choi et al. constructed nanostructured surface-assembled polydimethylsiloxane (SE-PDMS) by depositing ZnO nanowire (NW) and nanoflake (NF) frames on bare fabrics (Figure 2.13a).¹⁰⁰ The output voltage and current density of the TENGs with SE-PDMS on NM or NF were higher than those with bare flat PDMS. Meanwhile, a slight enhancement could be observed in the electrical output of the Al layer-coated top fabric compared with the bare Cu-Ni fabric. This may be due to the relatively high electrical conductivity of the Al layer, which resulted in nanoscale roughness. Some methods have been adopted to improve the device structure by increasing the effective contact area, and thus increasing the triboelectric surface charge. For example, as shown in Figure 2.13b, Tian et al. developed a triboelectric textile (TET) composed of a Ni-coated polyester conductive yarn as the warp and silicone rubber as the weft.¹¹⁵ The output voltage and current of the single-layer TET (STET) reached 500 V and 60 μ A, respectively. To boost the output performance, a double-layer-stacked TET (DTET) was fabricated. A thin layer of silicone rubber film was added between the two STETs, which could increase the effective contact area, thereby improving the output performance of the DTET. The results showed that the DTET delivered a higher electrical output (540 V and 140 μ A) than the STET. Although the triboelectric sequence of various materials has been quantified to reveal the abilities of materials to gain or lose electrons, it was demonstrated that the triboelectric charge density could be altered by introducing

CHAPTER 2

functional groups on the material surface. Feng et al. developed an efficient approach by enriching hierarchical structures and tribo-positive amide bonds on the fabric by a polyamidation reaction (Figure 2.13c).¹⁰⁶ By introducing optimized concentrations of CNTs and amide bonds on commercial velvet fabric, a more than 10-fold improvement in output performance could be realized by the fabric-based TENG. This may be because the roughness of the fibers could be increased and hierarchical structures were introduced by the grafting of CNTs and poly(ethylenimine) (PEI) on the fiber surface, resulting in an increase in the friction and electrification area. Jing et al. prepared a parallel multifiber TENG (parallel-teng) using stretchable gel electrode-based fibers. As shown in Figure 2.13d, the fabricated continuous triboelectric fiber was cut into individual fibers of the same length, and then the individual triboelectric fibers were arranged as warp fibers.¹¹⁶ A silicone hollow fiber was used as the weft to weave the parallel-teng. Another type of TENG fabric (GS-teng) was knitted by a single long continuous triboelectric fiber. The voltage generated by the parallel-teng was more than twice that of the GS-teng. This improvement was due to the lower electrode resistance of parallel-teng (megohms) compared with that of GS-teng (hundreds of megohm). Huang et al. demonstrated that the output performance could be improved via the design of the knit fabric texture. Five different fabric textures (types 1, 2, 3, 4 and 5) were knitted, and their outputs were compared, as shown in Figure 2.13e.¹¹² Owing to the larger contact area, the voltage and current of the face sides (with more loop legs) of types 1 and 2 were almost twice those of the back sides (with more loop sinkers). Although type 3 had a face side structure similar to those of types 1 and 2, its output performance was slightly lower than those of types 1 and 2. The reason could be attributed to the difference in the stitch density. The results demonstrated that TENG textiles with higher stitch density possessed great output performance due to the large effective contact area.

CHAPTER 2

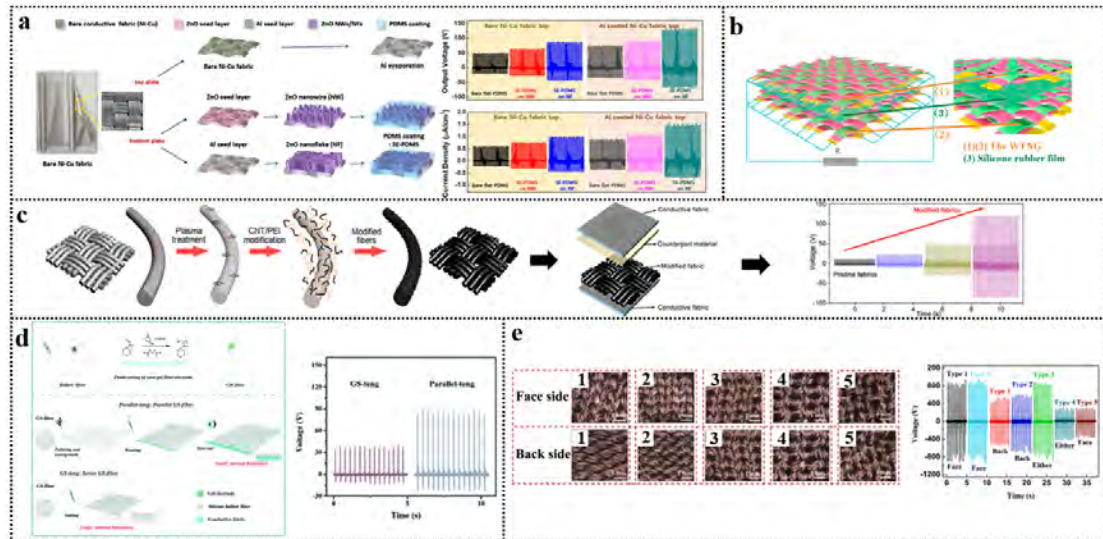


Figure 2.13 Improvement methods of the electrical output of t-TENGs. (a) Modification of surface or interface.¹⁰⁰ (b) Increase of triboelectric textile layer.¹¹⁵ (c) Surface functionalization.¹⁰⁶ (d) Reduction of inner resistance of triboelectric nanogenerator textiles.¹¹⁶ (e) Fabric structural design.¹¹²

2.5.2 Properties for wearable applications

Wearability

As t-TENGs are mainly used in wearable applications, they should possess various comfort properties, including tactile comfort, stretchability, washability and breathability.¹¹⁹

Since t-TENGs are frequently in contact with human skin in wearable applications, tactile comfort, such as skin irritation, static electricity, and cold stimulation, is of great significance. The materials utilized to fabricate t-TENGs must be nontoxic, safe, and biocompatible in order to achieve tactile comfort. Therefore, the use of some hazardous conductive materials should be minimized throughout the manufacturing procedure. In

CHAPTER 2

addition, the majority of fibrous conductive materials now in use are either too stiff or too soft. For instance, some flexible polymers have a tendency to break when subjected to high mechanical stresses. In contrast, metal wires are too stiff to be used in t-TENGs. Due to the complicated mechanical deformations induced by human movement, flexibility and mechanical strength requirements are necessary for t-TENGs. Some ordinary fibers, are good choices, including artificial polymer fibers (e.g., polyurethane, polyester, nylon, polytetrafluoroethylene) and natural fiber materials (e.g., cotton, silk, wool), which can be used for the electrification layer of t-TENGs. Due to the excellent conductivity and softness, commercial conductive yarn is selected as the electrode. For example, some researchers constructed t-TENGs with core-shell yarns that were made of commercial and conductive yarns and then integrated them into fabrics through weaving, knitting and sewing technologies, which could provide greater tactile comfort.^{30, 120, 121} As shown in Figure 2.14a, Ye et al. developed an energy harvesting textile (EHT) by weaving or embroidering a TENG yarn, which was fabricated by using a stainless steel fiber (SSF) as the core layer and natural silk fiber and polytetrafluoroethylene fiber (PTFEF) as the shell layers.¹²² By taking advantage of rational material screening and structural design, the overall performance of the EHT could be improved, including the flexibility, wearability, triboelectric output and mechanical strength. Similarly, Lou et al. described a woven TENG textile constructed with core-shell yarns, which showed the advantages of apparel fabrics, such as lightweight and flexible (Figure 2.14b).¹²¹ The core-shell yarn was made of stainless steel yarn core and nylon filament or polytetrafluoroethylene filament sheath covering. As shown in Figure 2.14c, Gong et al. developed an all-textile energy harvester (A-TEH) with three sets of fibers (commercial silver-plated nylon, polyacrylonitrile fibers and cotton fibers) by using a computerized knitting strategy.¹²³ The fabricated A-TEH was ultrathin, lightweight and flexible for scrolling, folding and kneading. These

CHAPTER 2

examples indicate that constructing a t-TENG with commercial fibers and common textile processing technology can endow the t-TENG with flexibility, softness and tactile comfort.

Good stretchability is a basic requirement for wearable t-TENGs to ensure that the deformation is consistent with the human body. To achieve the stretchability of t-TENGs, various strategies have been employed. One means is to utilize a special structure that can realize stretchability due to the structural design rather than the elasticity of the constituent materials.^{42, 46, 89, 124-127} This method can expand the scope of inelastic materials with good triboelectric properties to be used for stretchable t-TENGs. Knitted structures seem to be ideal structures for this purpose. Because many interdependent loops of knitted fabrics can be elongated in multiple directions by an external force, it has higher stretchability than woven or nonwoven fabrics. As shown in Figure 2.14d, Kwak et al. designed a stretchable knitted TENG with rib-knitted structure by using PTFE and Ag yarns.⁴⁶ The rib-knitted TENG exhibited superior stretchability, which significantly improved the triboelectric performance. By stretching the TENG with a rib structure up to 30%, the maximum voltage and current (23.50 V and 1.05 μ A) could be obtained. Similarly, Javid Rezaei et al. fabricated a knitted t-TENG with double twisted thread by using a rib stitch technique (Figure 2.14e).¹²⁶ The maximum stretchability of the t-TENG was approximately 80%. An alternative is to employ inherently stretchable materials. Recently, some common elastomers, such as polyurethane (PU) substrates,^{44, 45, 67} styrene-ethylene-butylene-styrene (SEBS, a typical elastomer),^{58, 128} polydimethylsiloxane (PDMS),^{59, 129} silicone rubber^{49, 63, 68, 77, 130, 131} and elastomeric poly(methyl acrylate) (PMA) have been widely used to create stretchable energy devices. Cheng et al. introduced a stretchable fiber nanogenerator (FNG) that could capture multiple mechanical energies, such as a strain

CHAPTER 2

of 0-50%, bending, twisting and pressing.⁴⁵ In this coaxial fiber configuration, the FNG consisted of the core fiber with the PU-silver nanowire (AgNW)-polytetrafluoroethylene (PTFE) layer and the sheath with the PDMS-AgNW layer (Figure 2.14f). The as-prepared FNG was highly stretchable, making it able to conform to arbitrarily curved surfaces.

In the true application scenario of t-TENGs, breathability is one of the key factors of wearing comfort, and mainly includes air permeability, moisture permeability, and heat permeability.¹³² It plays a great role in managing and adjusting the temperature and humidity balance in the human microenvironment. To endow t-TENGs with good breathability, the void between fibers serves as a flow channel between the human skin and the external environment. A widely used method is to employ commercial yarns, modified yarns or energy harvesting yarn to fabricate t-TENGs by using weaving/knitting technology.^{57, 71, 133, 134} For example, as shown in Figure 2.14g, an energy harvesting yarn was fabricated by twisting P(VDF-TrFE) nanofibers around stretchable conductive yarn, which was knitted into fabric by a hand-cranked flat machine.⁵⁷ The water vapor and heat produced could be effectively exchanged between the skin and the environment through the fabric. The resultant knitted/woven e-textiles exhibited a higher water vapor transmission rate ($\approx 0.024 \text{ g cm}^{-2} \text{ h}^{-1}$) than some commercial nonwovens. Additionally, the knitted e-textile presented a higher air permeability (ranging from 1035 to 1430 mm s^{-1} at a differential pressure of 100 Pa) due to the larger pore size. Alternatively, another method to realize this is to use electrospinning, which has some unique characteristics, including a large surface area and high porosity, as well as an inherently rough structure.^{84-88, 135} These notable properties of high output and excellent breathability make electrospun films ideal materials for t-TENGs. Figure 2.14h shows another similar electronic skin with a

CHAPTER 2

multilayered structure.¹³⁵ The prepared electronic skin was fabricated with PVDF nanofibers (NFs), conductive carbon NFs and highly elastic PU NFs, which were selected as the triboelectric (sensing) layer, effective electrode and substrate layer, respectively. The TENG exhibited excellent water vapor permeability, with a water vapor transmittance rate of $10.26 \text{ kg m}^{-2} \text{ d}^{-1}$. Although the value was lower than that of the pure PU membrane, it remained at a high level.

Washability is one of the essential characteristics that determines the feasibility of using t-TENGs in real-life practical applications. Recently, some t-TENGs have demonstrated the ability to be washed directly.^{15, 52, 81, 136-138} Zhao et al. fabricated TENG-based textile pressure sensors composed of Cu-PAN and parylene-Cu-PAN yarns.¹³⁷ By using stitching, weaving, and knitting technologies, TENG-based textile pressure sensors were fabricated (Figure 2.14i). The washabilities of the textile pressure sensors were investigated by AATCC Test Method 135, which includes washing, rinsing and spinning processes. It also showed that the output signals of textile pressure sensors with sewing and weaving structures presented some degradation, while the signal of knitted fabric structures remained at a similar level. As shown in Figure 2.14j, Busolo et al. prepared a triboelectric yarn using the electrospinning method, which was made of CNT yarn coated with PVDF fibers.¹³⁶ After washing, the power output did not significantly change.

CHAPTER 2

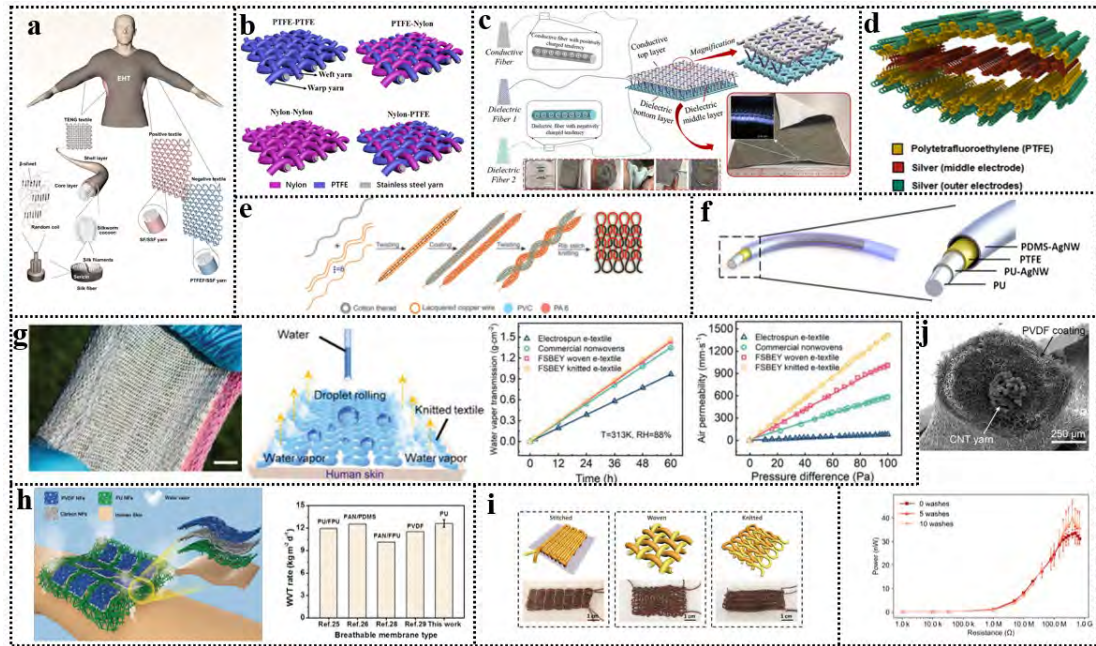


Figure 2.14 Wearability of t-TENGs. (a) Energy harvesting textile with silk, PTFE and stainless steel fibers.¹²² (b) Highly wearable, breathable, and washable sensing textile constructed with different core-shell yarns.¹²¹ (c) Truly wearable all-textile energy harvester.¹²³ (d) A knitted textile triboelectric nanogenerator with stretchability.⁴⁶ (e) Rib stitch knitted textile triboelectric nanogenerator with stretchability and washability.¹²⁶ (f) A coaxial core-sheath fiber based nanogenerator with stretchability.⁴⁵ (g) Electronic textile knitted with feramat-spiral-based energy yarns.⁵⁷ (h) An all-fiber structured electronic skin with elasticity and breathability.¹³⁵ (i) Pressure sensors with machine-washability and breathability based on TENG.¹³⁷ (j) A durable and washable triboelectric yarn.¹³⁶

Aesthetic

The aesthetic of the design is an important factor to promote the commercialization of t-TENGs, however, it has not received enough attention thus far. Most t-TENGs work by attaching to the human body or clothing through an additional process, resulting in

CHAPTER 2

a loss of continuous and unobtrusive aesthetics. Another challenge is that the coating changes the appearance of the t-TENGs. Some recent studies have focused on aesthetics of t-TENGs.^{133, 139-141} A triboelectric all-textile sensor array (TATSA) was knitted in a full cardigan stitch by using conductive yarns and nylon yarns as well as ordinary threads (Figure 2.15a).¹³³ TATSAs might be produced in a range of colors to satisfy the demands of fashion and aesthetics thanks to the variety of commercial nylon yarns. The developed TATSA could be integrated into different parts of clothing to achieve aesthetics and then employed for the realization of pulse and respiratory detecting. As shown in Figure 2.15b, Shin et al. introduced triboelectric wearable sensors with programmable patterns, which were fabricated by using PVDF fibers via the sewing method.¹³⁹ In the fabrication process, PVDF thread as the bottom thread and PET thread as the upper thread were used to achieve stable sewing and support the PVDF sewn on the knitted conductive fabric, respectively. For the triboelectric sensor, PVDF and conductive fabric were used as the main triboelectric material and conductive electrode, respectively. Owing to the excellent mechanical properties of PVDF fibers, they could be sewn into different textile patterns. The prepared triboelectric sensors could meet the aesthetic and functional requirements. Zhang et al. developed a smart pattern for energy harvesting, which was composed of carbon nanotubes (CNTs) @ silk fibroin (SF) core sheath fiber.¹⁴⁰ As shown in Figure 2.15c, by simultaneously injecting CNT ink and SF ink into the inner spinneret and outer spinneret respectively, the CNTs@SF fiber with core sheath structure was formed. By regulating the movement of the coaxial spinneret, various core-sheath fiber designs created by customers could be printed into fabrics. The as-prepared patterns, including Chinese characters of “PRINTING”, English letters spelling “SILK” and a silhouette of a pigeon, were presented. The results demonstrated that this method could be employed to create smart patterns to achieve aesthetic requirements and integrate the TENG into the fabric. Additionally, the printed patterns

CHAPTER 2

presented excellent flexibility against twisting and folding.

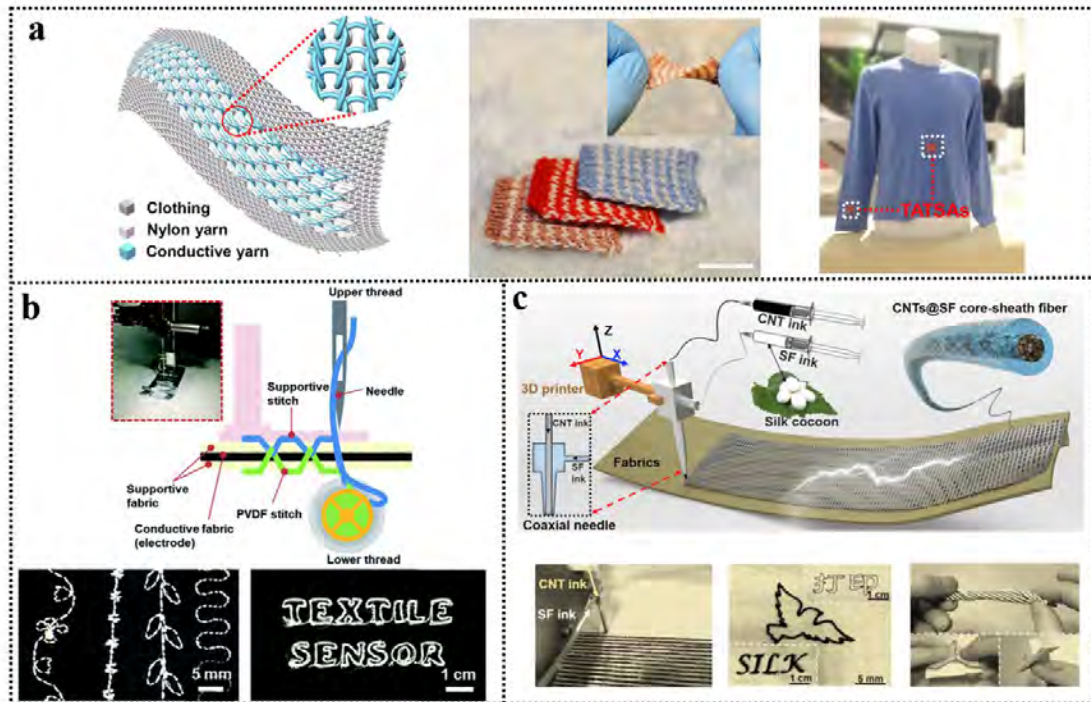


Figure 2.15 t-TEG sensors with designed aesthetics. (a) Combination of triboelectric all-textile sensor array and clothes.¹³³ (b) Self-powered triboelectric wearable sensors by sewing PVDF stitch patterns.¹³⁹ (c) An energy-management E-Textile with printable smart pattern.¹⁴⁰

Working stability

In the case of wearing, bending, stretching and shearing movements will often occur, therefore, the flexibility of the t-TEG is very critical. Mechanical flexibility is preserved for the majority of the t-TEG mentioned above. Some t-TEG have been reported to stretch. In order to make textiles capable of generating electricity, physical, chemical or even biological coatings are often used to add functional modifications to traditional yarns and textiles. These yarns and fabrics are often constructed of organic, chemically inert, and electrically insulating materials. Smart textiles are frequently

CHAPTER 2

damaged in daily wearing scenarios by a variety of ongoing mechanical forces, leading to the cracking of the adhesive's conductive layer or even peeling off of textile substrate. Consequently, in order to gain strong mechanical strength and durability, it is essential to develop adequate adhesion between functional coatings and soft textile materials. The interfacial adhesion between the fiber/fabric electrode and triboelectric material is the key to achieve long-term mechanical durability. Suitable choice of conductive materials and interface design is required to make sure that the TENG can withstand the accompanying deformation. In most cases, the energy collected from the human motion and its surroundings results in unpredictable electrical output variations. In practical use, many factors such as temperature, humidity and PH have a great influence on their stability. Therefore, it is essential to overcome the influence of instabilities caused by environmental changes on the electrical output performance of t-TENG. As shown in Figure 2.16a, a TENG fabric was knitted by triboelectric fibers with a gel electrode as the core and silicone as the shell.¹⁴² The TENG fabric exhibited steady output performance when it was folded, twisted and stretched to 200%. Meanwhile, it possessed excellent robustness against hot and cold environments. Figure 2.16b shows the wearable TENG woven by the liquid-metal/silicone rubber fibers with core/shell structure.¹⁴³ The wearable TENG presented outstanding stability and reliability, including the mechanical robustness, contaminative-resistant, chemical and high-temperature stability. There was no obvious change in the output performance of the TENG under harsh environments, for example soaking in acid solution, alkaline solution and hot water.

CHAPTER 2

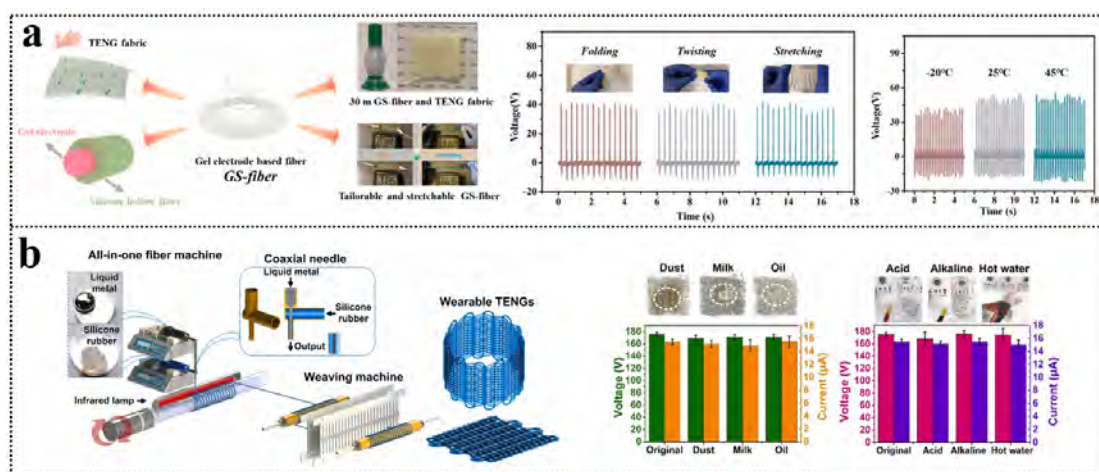


Figure 2.16 t-TENGs with working stability. (a) TENG textile and its steady output performance under typical deformations and wide temperature span.¹⁴² (b) The fabrication process, contaminative-resistance and chemical stability of wearable TENGs.¹⁴³

Large-scale industrialized production

Regarding the mass production of t-TENGs, there are still some challenges with the current production methods, such as hand-based, lab-scale, centimeter-length fabrication. Many t-TENGs are manually fabricated and restricted to small dimensions due to their complexity. Various techniques have been proposed to realize large-scale fabrication of t-TENGs, such as spinning,⁵⁴ braiding,^{94, 144} weaving,^{51, 145} knitting,^{146, 147} sewing, thermal drawing process,^{148, 149} wet-spinning,¹⁵⁰ continuous coating technology,^{151, 152} melt-spinning¹⁵³ and electrospinning technology.^{56, 154, 155} Weaving and knitting technologies are the basis of realizing the commercial production of t-TENGs. To address the above-mentioned issues, researchers designed functional fibers with small diameters and good mechanical strength, which are able to meet the requirements of the modern textile industry. Then, the functional fiber woven into fabric can provide a possible solution for mass production, which includes utilizing a

CHAPTER 2

modern machine. For instance, Wang et al. proposed a large-scale t-TENG fabricated by liquid metal/polymer core/shell fibers (LCFs) (Figure 2.17a).¹⁴⁵ The liquid metal electrode was pumped into polymer hollow fibers, such as PTFE hollow fibers. Hollow commercial polymer fibers and the fluid properties of liquid metal made mass manufacturing of LCFs possible. Taking advantage of the prepared LCFs, large pieces of TENG textiles with various colors could be fabricated by weaving. A commercially feasible t-TENG was introduced by Niu et al., who used industrial fully formed knitting technology for industrial production of knitting triboelectric generators (Figure 2.17b).¹⁴⁶ Based on the designed knitting structure, three types of commercial yarns, including PTFE yarn, nylon yarn and Ag-plated nylon yarn, were employed to knit the TENG. Another study described a method for large-scale fabrication by employing electrospinning technology, which was a continuous and automated process. Ma et al. proposed a single-electrode triboelectric yarn (SETY) with a core-shell structure, which was composed of PVDF and PAN hybrid nanofibers, as well as conductive silver yarn (Figure 2.17c).⁵⁶ The electrification nanofibers were wrapped around the silver yarn. Ultralight (0.33 mg cm^{-1}), excellent flexibility, and fineness ($350.66 \text{ }\mu\text{m}$ in diameter) could be realized by the prepared SETY. As shown in Figure 2.17d, Feng et al. developed a fiber-based triboelectric nanogenerator with a core-cladding structure by employing the thermal drawing process.¹⁴⁸ Due to the small diameter ($\sim 350 \text{ }\mu\text{m}$) and high drawing speed (up to 4 m/min), as well as the long length ($\sim 100 \text{ m}$) of the prepared fiber-shaped triboelectric nanogenerator, the weaveability of the fiber-based triboelectric nanogenerator was improved. Thin metal (tungsten) wire as the core and polymer cladding as the outside were used as the electrode and triboelectric material, respectively. By using such fibers, a variety of patterns could be woven manually or by industrial looms.

CHAPTER 2

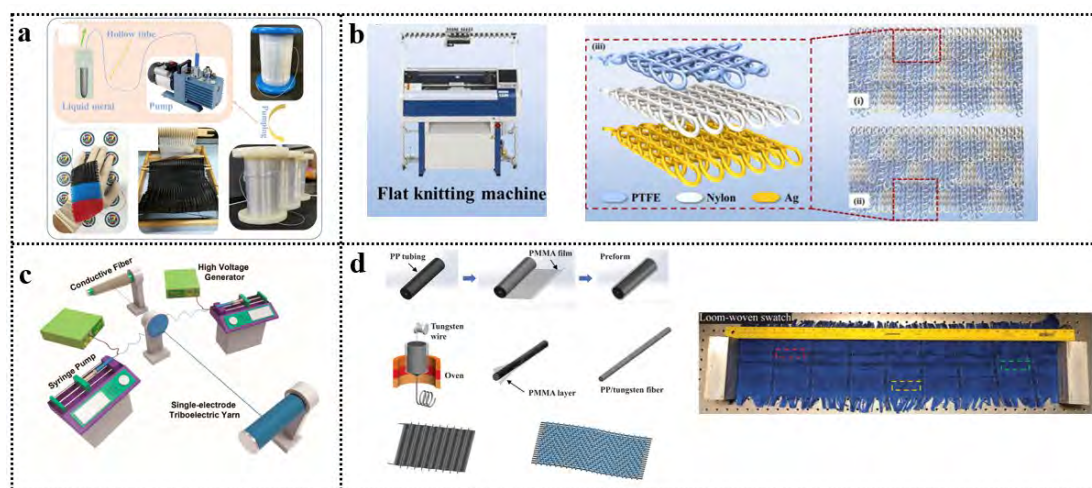


Figure 2.17 Large-scale industrialized production of t-TENGs. (a) Large-scale industrialized production of textile-based triboelectric nanogenerator by a simple pumping process and weaving technology.¹⁴⁵ (b) Industrial production of triboelectric fabric by using knitting technology.¹⁴⁶ (c) Continuous and scalable fabrication of triboelectric yarns.⁵⁶ (d) FTENG production through the thermal drawing and industrial weaving methods.¹⁴⁸

Multifunctionality

To enhance the overall performance of t-TENGs, special functionalities such as antibacterial,^{86, 156} flame-retardant,^{17, 54, 157} UV-Protective,¹⁵⁸ self-cleaning, waterproof,¹⁵⁹⁻¹⁶¹ mechanical luminescence capability,¹⁶² self-luminescent,¹⁶³ acid and alkali-resistant¹⁶⁴ and thermal management¹⁶⁵ have been proposed in recent years. As shown in Figure 2.18a, Ma et al. developed a triboelectric nanogenerator yarn (SETY) with excellent acid and alkali resistance by using a fancy twisting machine to produce a core-sheath yarn with a conductive yarn as the core yarn and PTFE as the sheath yarn.¹⁶⁴ The PTFE yarn was well wrapped around the conductive yarn, and the fabric TENG was successfully woven. After being washed and immersed in acid and alkali

CHAPTER 2

solution, the sheath and core yarns were not damaged. The electrical output of the SETY showed a slight decline after washing. However, an increase could be observed in the output of the SETY after soaking in acid and alkali solutions. Similarly, Ma et al. also proposed flame-retardant single-electrode triboelectric yarn (FRTY) with a core-shell structure, which was fabricated by wrapping polyimide yarn (PI) around a conductive core yarn (Figure 2.18b).⁵⁴ It indicated that the T/C-32s (polyester/cotton with a count of 32 s) TENG burned quickly, while the appearance of PI-60s FRTY (5-20 yarns) remained unaffected after testing. The electrical output performance of the TENG yarn decreased slightly after the flame retardancy testing. The 3D FTENG woven from the FRTY exhibited excellent noise-reduction ability and flame retardancy. Focusing on the special functions of t-TENGs, as shown in Figure 2.18c, Jiang et al. developed an ultraviolet (UV)-protective, self-cleaning, antibacterial, and self-powered all-nanofiber-based TENG by electrospinning.¹⁵⁸ Another multifunctional TENG fabric was fabricated by mix-weaving coaxial TENG yarns and other yarns.¹⁶² The coaxial TENG yarns consisted of a coil spring and mechanoluminescent ZnS:Cu/PDMS composite, which could be used as a self-powered body motion detector (Figure 2.18d). The proposed TENG fabric was adaptable to the skin, reusable, and had mechanical luminescence capability.

CHAPTER 2

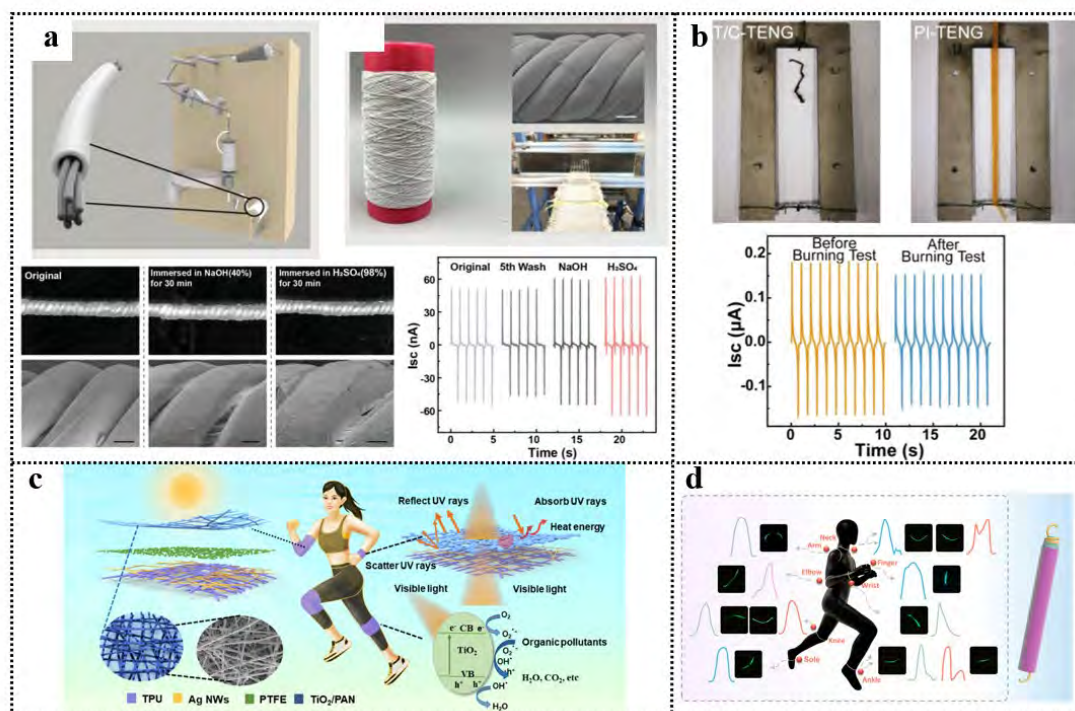


Figure 2.18 Multifunctionality of t-TENGs. (a) Acid and alkali-resistant textile triboelectric nanogenerator.¹⁶⁴ (b) Flame retardant triboelectric textile.⁵⁴ (c) Nanofiber-based triboelectric nanogenerator with UV-protective, self-cleaning, and antibacterial properties.¹⁵⁸ (d) Flexible and stretchable coaxial triboelectric nanogenerator yarn with force luminescence.¹⁶²

Integration

Structural and functional integration of t-TENGs is indispensable for further application including the integration of TENG and cloth,^{42, 166} batteries,^{14, 167} supercapacitors,^{13, 168-171} and back-end functional devices due to the alternating current pulse output characteristic of TENG.¹⁷²⁻¹⁷⁴ The intarsia technique seems to be a promising strategy for the integration of knitted t-TENGs. For example, as shown in Figure 2.19a, a comfortable t-TENG fabricated by using PTFE wrapped Ag conductive yarns and PA66 wrapped Ag conductive yarns was developed by advanced knitting technology, which

CHAPTER 2

could be integrated into knitted pants seamlessly to realize energy harvesting.⁴² For purpose of realizing continuous and stable electrical output, it is necessary to integrate the t-TENG with battery. A 3D spacer fabric composed of separate upper and lower layers is an ideal choice to fabricate TENG due to the special structure. As exhibited in Figure 2.19b, a 3D spacer fabric was designed to embed the TENG and Zn-ion battery.¹⁶⁷ The TENG worked with the movement of the upper and lower layer, which could convert mechanical energy into electrical energy. The flexible battery with three-layer configuration was prepared by filling the gel electrolyte into the intermediate layer, and further the electricity could be stored in flexible batteries to supply power for other electronic devices. In order to achieve sustainable and continuous utilization in various application scenarios, TENG and energy storage device as well as sensors are preferred to be combined in one unit. For example, as shown in Figure 2.19c, an energy fiber with coaxial geometry consisted of TENG for energy harvesting, supercapacitor (SC) for energy storage, and pressure sensor for energy utilization.¹⁶⁸ Similarly, a flexible coaxial fiber with a TENG outside and a SC inside was fabricated, which could harvest mechanical energy and store energy (Figure 2.19d).¹⁷¹ As shown in Figure 2.19e, the TENG-SC bio-motion harvesting/storage system was fabricated by stitching TENG textile and asymmetric supercapacitor into the cloth, which could convert biomechanical energy into electricity and store it.¹⁶⁹

CHAPTER 2

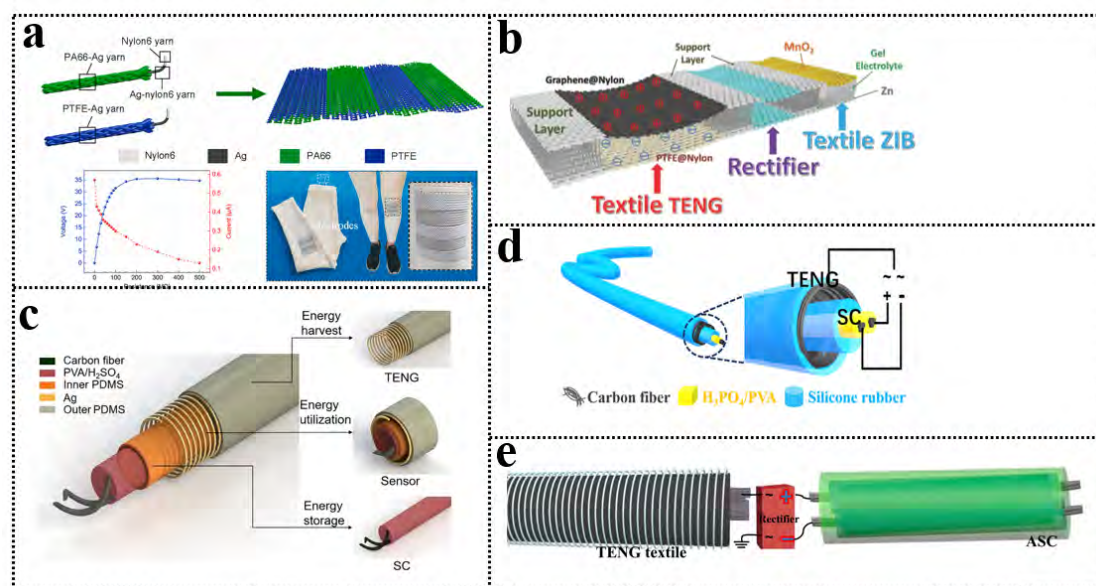


Figure 2.19 Integration of t-TENGs. (a) A seamlessly integrated t-TENG.⁴² (b) A 3D spacer structured fabric with integrated triboelectric nanogenerator and zinc-ion battery.¹⁶⁷ (c) A multifunctional energy fiber with coaxial structure for energy collecting, storage, and utilization.¹⁶⁸ (d) A triboelectric nanogenerator and supercapacitor fiber with coaxial structure.¹⁷¹ (e) A self-powered TENG-SC system.¹⁶⁹

2.6 Application

2.6.1 Harvesting energy

Due to the softness and flexibility of textiles, textile-based energy harvesters are appropriate for wearing, which can be integrated into clothing for collecting mechanical energy from movements.¹⁷⁵ For example, as shown in Figure 2.20a, a waterproof and breathable t-TENG which consisted of polyurethane-based bottom lining, PTFE membrane as center layer and woven nylon fabric as an outer layer was fabricated.¹⁷⁶ It was demonstrated that the t-TENG could be attached to the cloth to collect mechanical energy through the friction of human motion. On the basis of this structure,

CHAPTER 2

nanodot-patterned textile was applied as air flow driven flutter-membrane to harvest renewable wind energy. In addition, t-TENG has also been shown to harvest clean, renewable, widely distributed raindrop energy. Figure 2.20b presents an all-fabric triboelectric nanogenerator with good air permeability, hydrophobicity, and self-repairing performance, which consisted of a top electrode and three fabric layers (top hydrophobic fabric, middle conductive fabric and bottom PET fabric).¹⁷⁷ This TENG could be used as water droplet power generation with the output of 22 V. As shown in Figure 2.20c, a waterproof dual-mode t-TENG has been designed for scavenging multiple energies, including human motions, raindrops, and winds.¹⁷⁸ In order to harvest energy from various sources, a fabric TENG was fabricated, which was composed of silicone-coated fabric, silk conductive fabric, and Ag-coated nylon fabric. The prepared fabric TENG could be applied for collecting energy from sound, wind and human motion (Figure 2.20d).¹⁷⁹ Moreover, t-TENG has been applied to tires of the vehicle to efficiently harvest mechanical energy by rolling the tire through the inner space. As exhibited in Figure 2.20e, polydimethylsiloxane-coated silver textile and woven nylon textile were served as the tire tread material and internal tire cord material, respectively.¹⁸⁰ By the dual friction of the road, the tire tread and tire cord, the power was generated and harvested as the tire rotated.

CHAPTER 2

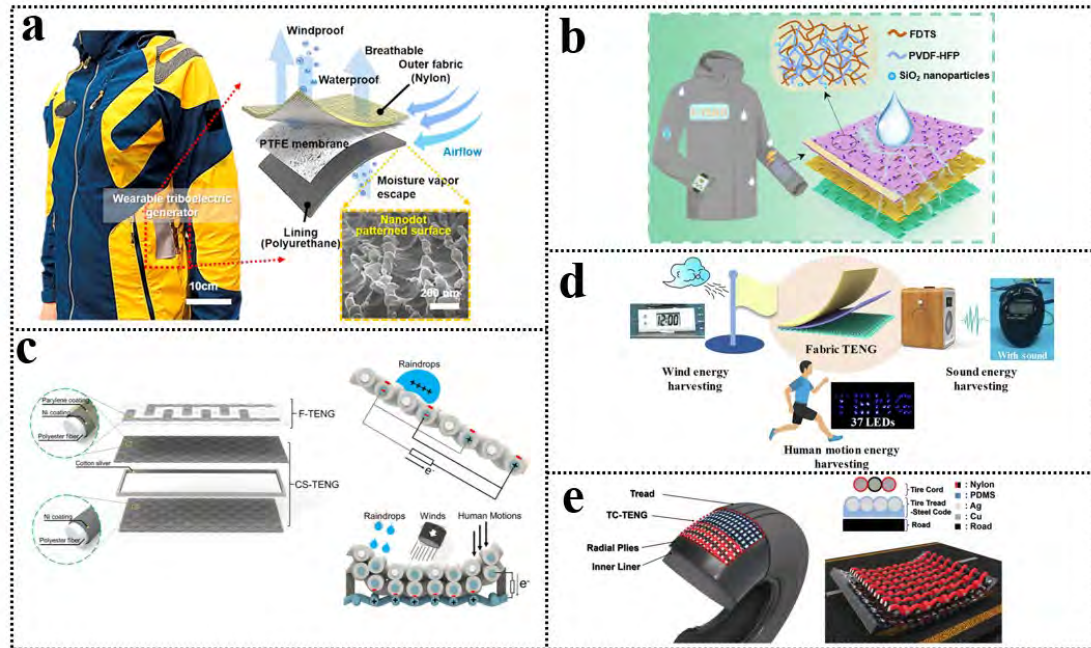


Figure 2.20 t-TEGs for harvesting energy. (a) Gore-Tex fabric with nanodot-pattern for multiple energy harvesting.¹⁷⁶ (b) A hydrophobic power textile for water droplet energy collecting.¹⁷⁷ (c) Energy harvesting of human motions, raindrops and winds by a textile triboelectric nanogenerator.¹⁷⁸ (d) Energy harvesting of sound, wind and human motion by a full-textile triboelectric nanogenerator.¹⁷⁹ (e) Energy harvesting of tire rotating by a textile-based triboelectric nanogenerator.¹⁸⁰

2.6.2 Self-powered sensing

In addition to energy harvesting, t-TEG can also be used as a sensor with the merits of simple structure and common material, etc. On the basis of t-TEG technology, self-powered sensing has been widely applied in different fields, for example, pressure sensing,^{92, 181, 182} cardiovascular monitoring,^{183, 184} motion monitoring,^{130, 185-192} sitting posture monitoring,¹⁹³ respiratory monitoring¹⁹⁴ and further extend to human-machine interaction^{125, 195-198} and Internet of Things fields.¹⁹⁹ As shown in Figure 2.21a, smart textile-based self-powered sensors were fabricated, which could be attached to different

CHAPTER 2

parts of human body to monitor human activities, such as standing up, walking, sudden fall and sitting, ect.²⁰⁰ Recently, sitting disease caused by prolonged sedentary lifestyle is becoming prevalent worldwide. Figure 2.21b shows a self-powered vest knitted by conductive fiber and nylon yarn. The vest stitched into various parts of the clothing could be used as sitting position monitoring to realize real-time posture recognition, provide feedback and warn users¹⁹³. Moreover, a smart textiles shoe sensor based on single electrode triboelectric mode was developed by common embroidery technique (Figure 2.21c).²⁰¹ Specially, the self-powered shoe sensor could be applied for sensing and detecting footsteps. A self-powered wearable keyboard was proposed by employing an all-fabric-based TENG.¹⁸ As illustrated in Figure 2.21d, when external touch was applied to the wearable fabric keyboard composed of 12 units sensor cells, electrical signals were generated and delivered to computer or phone. In addition, a 3D fancy yarn TENG was designed for self-powered biomechanical sensing.¹⁸⁹ A smart fitness system was constructed by integrating the yarn TENG into a smart belt, which could be applied for real-time exercise detection, exercise frequency statistical analysis as well as posture correction alarming (Figure 2.21e). Figure 2.21f presents a self-powered and self-functional sock using PEDOT:PSS-coated cotton textile and lead zirconate titanate (PZT) piezoelectric sensor.³⁵ The sock demonstrated various functions such as walking pattern recognition, gait sensing and motion tracking, which could contribute to sports and healthcare monitoring.

CHAPTER 2

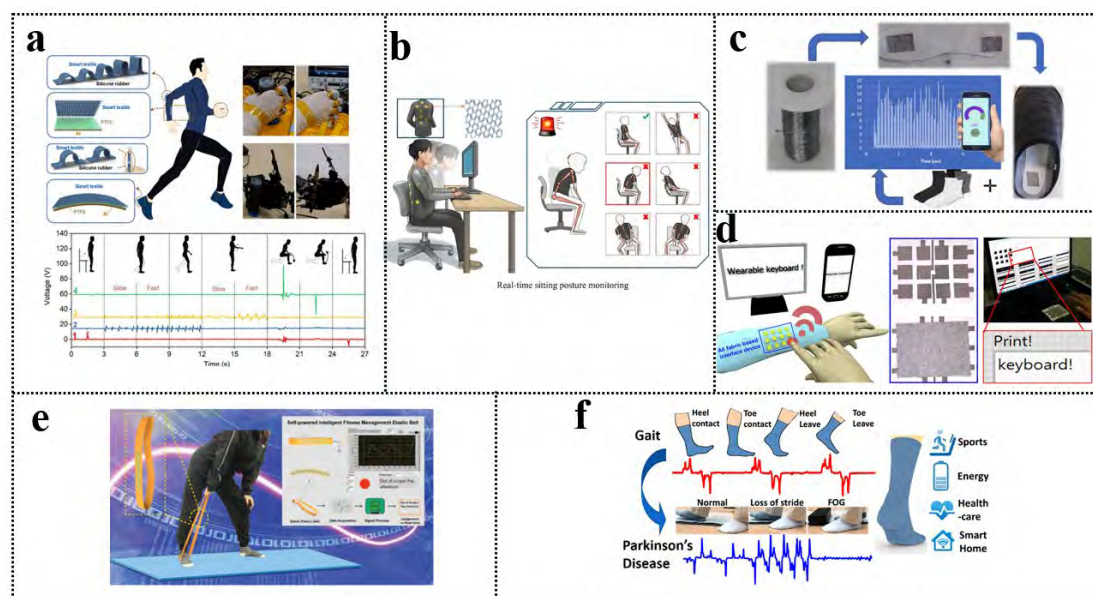


Figure 2.21 t-TENGs for self-powered sensing. (a) Human activity monitoring with t-TENGs.²⁰⁰ (b) Self-powered sensing textile with knitted structure for sitting posture detecting and correction.¹⁹³ (c) Wearable triboelectric sensors for detecting footsteps.²⁰¹ (d) Self-powered wearable keyboard.¹⁸ (e) 3D triboelectric yarn for smart fitness system.¹⁸⁹ (f) Self-powered sock for detecting healthcare and exercise.³⁵

2.7 Summary

In this chapter, materials, working mechanism and modes, structures and fabrication methods of t-TENGs are introduced. Desired performance and applications are also discussed. In conclusion, t-TENGs including fiber/yarn-based and fabric-based TENGs have broad prospects as sustainable power sources and self-powered sensors. Various types of t-TENGs have been proposed by combining different triboelectric materials with electrode materials utilizing textile fabrication techniques. Although great achievements have been realized in t-TENG development, the gap between research and practical commercialization is still widening. Lots of researchers have reported some wearable t-TENGs by using conventional materials such as PDMS, silicone

CHAPTER 2

polymer and PTFE sheets as triboelectric active surfaces. These materials and structures could provide good electrical output, but they still have some limitations, such as difficulty in adapting to irregular human motion in multiple directions, complicated implementation, low breathability and washability. Despite integrating 1D fiber/yarn shaped TENGs into fabric have been proposed, most 1D fiber/yarn shaped TENGs exhibit large diameter, short length, low softness and mechanical strength, which are not suitable for textile processing technology, such as not being able to withstand the pulling and beating forces during the weaving. Besides, existing t-TENGs were usually fabricated by employing various types of expensive or harmful materials and involved complicated structure and processing conditions. Such production methods are not optimal for mass-production.

CHAPTER 2

References

- (1) Wang, J.; Lu, C.; Zhang, K. Textile-Based Strain Sensor for Human Motion Detection. *Energy Environ. Mater.* **2020**, *3*, 80-100.
- (2) Chatterjee, K.; Tabor, J.; Ghosh, T. K. Electrically Conductive Coatings for Fiber-Based E-Textiles. *Fibers* **2019**, *7*, 51.
- (3) Ismar, E.; Bahadir, S. K.; Kalaoglu, F.; Koncar, V. Futuristic Clothes: Electronic textiles and Wearable Technologies. *Glob. Chall.* **2020**, *4*, 1900092.
- (4) Hu, Y.; Zheng, Z. Progress in textile-based triboelectric nanogenerators for smart fabrics. *Nano Energy* **2019**, *56*, 16-24.
- (5) Wang, H.; Han, M.; Song, Y.; Zhang, H. Design, manufacturing and applications of wearable triboelectric nanogenerators. *Nano Energy* **2021**, *81*, 105627.
- (6) Song, Y.; Wang, N.; Hu, C.; Wang, Z. L.; Yang, Y. Soft triboelectric nanogenerators for mechanical energy scavenging and self-powered sensors. *Nano Energy* **2021**, *84*, 105919.
- (7) Shen, S.; Xiao, X.; Chen, J. Wearable Triboelectric Nanogenerators for Heart Rate Monitoring. *Chem. Commun.* **2021**, *57*, 5871-5879.
- (8) Cheng, R.; Ning, C.; Chen, P.; Sheng, F.; Wei, C.; Zhang, Y.; Peng, X.; Dong, K.; Wang, Z. L. Enhanced Output of On-Body Direct-Current Power Textiles by Efficient Energy Management for Sustainable Working of Mobile Electronics. *Adv. Energy Mater.* **2022**, *12*, 2201532.
- (9) Dong, K.; Hu, Y.; Yang, J.; Kim, S.-W.; Hu, W.; Wang, Z. L. Smart Textile Triboelectric Nanogenerators: Current Status and Perspectives. *MRS Bull.* **2021**, *46*, 512-521.
- (10) Huang, P.; Wen, D. L.; Qiu, Y.; Yang, M. H.; Tu, C.; Zhong, H. S.; Zhang, X. S. Textile-Based Triboelectric Nanogenerators for Wearable Self-Powered Microsystems.

CHAPTER 2

Micromachines **2021**, *12*, No. 158.

(11) Zhang, Z.; Chen, Y.; Debeli, D. K.; Guo, J. S. Facile Method and Novel Dielectric Material Using a Nanoparticle-Doped Thermoplastic Elastomer Composite Fabric for Triboelectric Nanogenerator Applications. *ACS Appl. Mater. Interfaces* **2018**, *10*, 13082-13091.

(12) Pu, X.; Song, W.; Liu, M.; Sun, C.; Du, C.; Jiang, C.; Huang, X.; Zou, D.; Hu, W.; Wang, Z. L. Wearable Power-Textiles by Integrating Fabric Triboelectric Nanogenerators and Fiber-Shaped Dye-Sensitized Solar Cells. *Adv. Energy Mater.* **2016**, *6*, 1601048.

(13) Liu, M.; Cong, Z.; Pu, X.; Guo, W.; Liu, T.; Li, M.; Zhang, Y.; Hu, W.; Wang, Z. L. High-Energy Asymmetric Supercapacitor Yarns for Self-Charging Power Textiles. *Adv. Funct. Mater.* **2019**, *29*, 1806298.

(14) Pu, X.; Li, L.; Song, H.; Du, C.; Zhao, Z.; Jiang, C.; Cao, G.; Hu, W.; Wang, Z. L. A self-charging power unit by integration of a textile triboelectric nanogenerator and a flexible lithium-ion battery for wearable electronics. *Adv. Mater.* **2015**, *27*, 2472-2478.

(15) Qiu, Q.; Zhu, M.; Li, Z.; Qiu, K.; Liu, X.; Yu, J.; Ding, B. Highly flexible, breathable, tailorable and washable power generation fabrics for wearable electronics. *Nano Energy* **2019**, *58*, 750-758.

(16) Cao, R.; Pu, X.; Du, X.; Yang, W.; Wang, J.; Guo, H.; Zhao, S.; Yuan, Z.; Zhang, C.; Li, C.; Wang, Z. L. Screen-Printed Washable Electronic Textiles as Self-Powered Touch/Gesture Tribo-Sensors for Intelligent Human-Machine Interaction. *ACS Nano* **2018**, *12*, 5190-5196.

(17) Cheng, R.; Dong, K.; Liu, L.; Ning, C.; Chen, P.; Peng, X.; Liu, D.; Wang, Z. L. Flame-Retardant Textile-Based Triboelectric Nanogenerators for Fire Protection Applications. *ACS Nano* **2020**, *14*, 15853-15863.

CHAPTER 2

- (18) Jeon, S.-B.; Park, S.-J.; Kim, W.-G.; Tcho, I.-W.; Jin, I.-K.; Han, J.-K.; Kim, D.; Choi, Y.-K. Self-powered wearable keyboard with fabric based triboelectric nanogenerator. *Nano Energy* **2018**, *53*, 596-603.
- (19) Yang, B.; Xiong, Y.; Ma, K.; Liu, S.; Tao, X. Recent advances in wearable textile-based triboelectric generator systems for energy harvesting from human motion. *EcoMat* **2020**, *2*, e12054.
- (20) Chen, A.; Zhang, C.; Zhu, G.; Wang, Z. L. Polymer Materials for High-Performance Triboelectric Nanogenerators. *Adv. Sci.* **2020**, *7*, 2000186.
- (21) Zhang, R.; Olin, H. Material choices for triboelectric nanogenerators: A critical review. *EcoMat* **2020**, *2*, e12062.
- (22) Yu, A.; Zhu, Y.; Wang, W.; Zhai, J., Progress in Triboelectric Materials: Toward High Performance and Widespread Applications. *Adv. Funct. Mater.* **2019**, *29*, 1900098.
- (23) Liu, S.; Zheng, W.; Yang, B.; Tao, X. Triboelectric charge density of porous and deformable fabrics made from polymer fibers. *Nano Energy* **2018**, *53*, 383-390.
- (24) Wang, Z. L. Triboelectric Nanogenerators as New Energy Technology for Self-Powered Systems and as Active Mechanical and Chemical Sensors. *ACS Nano* **2013**, *7*, 9533-9557.
- (25) Paosangthong, W.; Torah, R.; Beeby, S. Recent progress on textile-based triboelectric nanogenerators. *Nano Energy* **2019**, *55*, 401-423.
- (26) Zhao, P.; Bhattacharya, G.; Fishlock, S. J.; Guy, J. G. M.; Kumar, A.; Tsonos, C.; Yu, Z.; Raj, S.; McLaughlin, J. A.; Luo, J.; Soin, N. Replacing the metal electrodes in triboelectric nanogenerators: High-performance laser-induced graphene electrodes. *Nano Energy* **2020**, *75*, 104958.
- (27) Li, S.; Zhong, Q.; Zhong, J.; Cheng, X.; Wang, B.; Hu, B.; Zhou, J. Cloth-Based Power Shirt for Wearable Energy Harvesting and Clothes Ornamentation. *ACS Appl. Mater. Interfaces* **2015**, *7*, 14912-6.

CHAPTER 2

- (28) Pu, X.; Li, L.; Liu, M.; Jiang, C.; Du, C.; Zhao, Z.; Hu, W.; Wang, Z. L. Wearable Self-Charging Power Textile Based on Flexible Yarn Supercapacitors and Fabric Nanogenerators. *Adv. Mater.* **2016**, *28*, 98-105.
- (29) Dong, K.; Deng, J.; Zi, Y.; Wang, Y. C.; Xu, C.; Zou, H.; Ding, W.; Dai, Y.; Gu, B.; Sun, B.; Wang, Z. L. 3D Orthogonal Woven Triboelectric Nanogenerator for Effective Biomechanical Energy Harvesting and as Self-Powered Active Motion Sensors. *Adv. Mater.* **2017**, *29*, 1702648.
- (30) Yu, A.; Pu, X.; Wen, R.; Liu, M.; Zhou, T.; Zhang, K.; Zhang, Y.; Zhai, J.; Hu, W.; Wang, Z. L. Core-Shell-Yarn-Based Triboelectric Nanogenerator Textiles as Power Cloths. *ACS Nano* **2017**, *11*, 12764-12771.
- (31) Liu, L.; Pan, J.; Chen, P.; Zhang, J.; Yu, X.; Ding, X.; Wang, B.; Sun, X.; Peng, H. A triboelectric textile templated by a three-dimensionally penetrated fabric. *J. Mater. Chem. A* **2016**, *4*, 6077-6083.
- (32) Kim, W. J.; Cho, S.; Hong, J.; Hong, J. P. Geometrically versatile triboelectric yarn-based harvesters via carbon nanotubes-elastomer composites. *Compos. Sci. Technol.* **2022**, *219*, 109247.
- (33) Zhu, M.; Huang, Y.; Ng, W. S.; Liu, J.; Wang, Z.; Wang, Z.; Hu, H.; Zhi, C. 3D spacer fabric based multifunctional triboelectric nanogenerator with great feasibility for mechanized large-scale production. *Nano Energy* **2016**, *27*, 439-446.
- (34) Kaushik, V.; Lee, J.; Hong, J.; Lee, S.; Lee, S.; Seo, J.; Mahata, C.; Lee, T. Textile-Based Electronic Components for Energy Applications: Principles, Problems, and Perspective. *Nanomaterials* **2015**, *5*, 1493-1531.
- (35) Zhu, M.; Shi, Q.; He, T.; Yi, Z.; Ma, Y.; Yang, B.; Chen, T.; Lee, C. Self-Powered and Self-Functional Cotton Sock Using Piezoelectric and Triboelectric Hybrid Mechanism for Healthcare and Sports Monitoring. *ACS Nano* **2019**, *13*, 1940-1952.
- (36) Kwak, S. S.; Yoon, H.-J.; Kim, S.-W. Textile-Based Triboelectric Nanogenerators

CHAPTER 2

- for Self-Powered Wearable Electronics. *Adv. Funct. Mater.* **2019**, *29*, 1804533.
- (37) Lacks, D. J.; Sankaran, R. M. Contact Electrification of Insulating Materials. *J. Phys. D: Appl. Phys.* **2011**, *44*, 453001.
- (38) Wang, S.; Zi, Y.; Zhou, Y. S.; Li, S.; Fan, F.; Lin, L.; Wang, Z. L. Molecular surface functionalization to enhance the power output of triboelectric nanogenerators. *J. Mater. Chem. A* **2016**, *4*, 3728-3734.
- (39) Xu, C.; Wang, A. C.; Zou, H.; Zhang, B.; Zhang, C.; Zi, Y.; Pan, L.; Wang, P.; Feng, P.; Lin, Z.; Wang, Z. L. Raising the Working Temperature of a Triboelectric Nanogenerator by Quenching Down Electron Thermionic Emission in Contact-Electrification. *Adv. Mater.* **2018**, *30*, e1803968.
- (40) Xu, C.; Zhang, B.; Wang, A. C.; Zou, H.; Liu, G.; Ding, W.; Wu, C.; Ma, M.; Feng, P.; Lin, Z.; Wang, Z. L. Contact-Electrification between Two Identical Materials: Curvature Effect. *ACS Nano* **2019**, *13*, 2034-2041.
- (41) Dong, K.; Peng, X.; Wang, Z. L., Fiber/Fabric-Based Piezoelectric and Triboelectric Nanogenerators for Flexible/Stretchable and Wearable Electronics and Artificial Intelligence. *Adv. Mater.* **2020**, *32*, e1902549.
- (42) Dong, S.; Xu, F.; Sheng, Y.; Guo, Z.; Pu, X.; Liu, Y. Seamlessly knitted stretchable comfortable textile triboelectric nanogenerators for E-textile power sources. *Nano Energy* **2020**, *78*, 105327.
- (43) He, X.; Zi, Y.; Guo, H.; Zheng, H.; Xi, Y.; Wu, C.; Wang, J.; Zhang, W.; Lu, C.; Wang, Z. L. A Highly Stretchable Fiber-Based Triboelectric Nanogenerator for Self-Powered Wearable Electronics. *Adv. Funct. Mater.* **2017**, *27*, 1604378.
- (44) Chen, J.; Wen, X.; Liu, X.; Cao, J.; Ding, Z.; Du, Z. Flexible hierarchical helical yarn with broad strain range for self-powered motion signal monitoring and human-machine interactive. *Nano Energy* **2021**, *80*, 105446
- (45) Cheng, Y.; Lu, X.; Chan, K. H.; Wang, R.; Cao, Z.; Sun, J.; Ho, G. W. A Stretchable

CHAPTER 2

Fiber Nanogenerator for Versatile Mechanical Energy Harvesting and Self-Powered Full-Range Personal Healthcare Monitoring. *Nano Energy* **2017**, *41*, 511–518.

(46) Kwak, S. S.; Kim, H.; Seung, W.; Kim, J.; Hinchet, R.; Kim, S. W., Fully Stretchable Textile Triboelectric Nanogenerator with Knitted Fabric Structures. *ACS Nano* **2017**, *11*, 10733-10741.

(47) Somkuwar, V. U.; Pragma, A.; Kumar, B., Structurally engineered textile-based triboelectric nanogenerator for energy harvesting application. *J. Mater. Sci.* **2020**, *55*, 5177-5189.

(48) Niu, L.; Miao, X.; Jiang, G.; Wan, A.; Li, Y.; Liu, Q. Biomechanical Energy Harvest Based on Textiles Used in Self Powering Clothing. *J. Eng. Fibers Fabr.* **2020**, *15*, 155892502096735.

(49) Dong, K.; Deng, J.; Ding, W.; Wang, A. C.; Wang, P.; Cheng, C.; Wang, Y.-C.; Jin, L.; Gu, B.; Sun, B.; Wang, Z. L., Versatile Core-Sheath Yarn for Sustainable Biomechanical Energy Harvesting and Real-Time Human-Interactive Sensing. *Adv. Energy Mater.* **2018**, *8*, 1801114.

(50) Xie, L.; Chen, X.; Wen, Z.; Yang, Y.; Shi, J.; Chen, C.; Peng, M.; Liu, Y.; Sun, X. Spiral Steel Wire Based Fiber-Shaped Stretchable and Tailorable Triboelectric Nanogenerator for Wearable Power Source and Active Gesture Sensor. *Nano-Micro Lett.* **2019**, *11*, 1-10.

(51) Chen, J.; Guo, H.; Pu, X.; Wang, X.; Xi, Y.; Hu, C. Traditional weaving craft for one-piece self-charging power textile for wearable electronics. *Nano Energy* **2018**, *50*, 536-543.

(52) Paosangthong, W.; Wagih, M.; Torah, R.; Beeby, S., Textile-based triboelectric nanogenerator with alternating positive and negative freestanding woven structure for harvesting sliding energy in all directions. *Nano Energy* **2022**, *92*, 106739.

(53) Zhou, T.; Zhang, C.; Han, C. B.; Fan, F. R.; Tang, W.; Wang, Z. L. Woven

CHAPTER 2

structured triboelectric nanogenerator for wearable devices. *ACS Appl. Mater. Interfaces* **2014**, *6*, 14695-701.

(54) Ma, L.; Wu, R.; Liu, S.; Patil, A.; Gong, H.; Yi, J.; Sheng, F.; Zhang, Y.; Wang, J.; Wang, J.; Guo, W.; Wang, Z. L. A Machine-Fabricated 3D Honeycomb-Structured Flame-Retardant Triboelectric Fabric for Fire Escape and Rescue. *Adv. Mater.* **2020**, *32*, e2003897.

(55) Dassanayaka, D. G.; Alves, T. M.; Wanasekara, N. D.; Dharmasena, I. G.; Ventura, J. Recent Progresses in Wearable Triboelectric Nanogenerators. *Adv. Funct. Mater.* **2022**, 2205438.

(56) Ma, L.; Zhou, M.; Wu, R.; Patil, A.; Gong, H.; Zhu, S.; Wang, T.; Zhang, Y.; Shen, S.; Dong, K.; Yang, L.; Wang, J.; Guo, W.; Wang, Z. L. Continuous and Scalable Manufacture of Hybridized Nano-Micro Triboelectric Yarns for Energy Harvesting and Signal Sensing. *ACS Nano* **2020**, *14*, 4716-4726.

(57) Zhang, D.; Yang, W.; Gong, W.; Ma, W.; Hou, C.; Li, Y.; Zhang, Q.; Wang, H., Abrasion Resistant/Waterproof Stretchable Triboelectric Yarns Based on Fermat Spirals. *Adv. Mater.* **2021**, *33*, e2100782.

(58) Chen, M.; Wang, Z.; Zhang, Q.; Wang, Z.; Liu, W.; Chen, M.; Wei, L. Self-powered multifunctional sensing based on super-elastic fibers by soluble-core thermal drawing. *Nat. Commun.* **2021**, *12*, 1416.

(59) Chen, Y.; Deng, Z.; Ouyang, R.; Zheng, R.; Jiang, Z.; Bai, H.; Xue, H. 3D printed stretchable smart fibers and textiles for self-powered e-skin. *Nano Energy* **2021**, *84*, 105866.

(60) Jiang, C.; Li, X.; Ying, Y.; Ping, J. A multifunctional TENG yarn integrated into agrotexile for building intelligent agriculture. *Nano Energy* **2020**, *74*, 104863.

(61) Ning, C.; Dong, K.; Cheng, R.; Yi, J.; Ye, C.; Peng, X.; Sheng, F.; Jiang, Y.; Wang, Z. L. Flexible and Stretchable Fiber-Shaped Triboelectric Nanogenerators for

CHAPTER 2

Biomechanical Monitoring and Human-Interactive Sensing. *Adv. Funct. Mater.* **2021**, *31*, 2006679.

(62) Lan, L.; Jiang, C.; Yao, Y.; Ping, J.; Ying, Y. A stretchable and conductive fiber for multifunctional sensing and energy harvesting. *Nano Energy* **2021**, *84*, 105954.

(63) Park, J.; Choi, A. Y.; Lee, C. J.; Kim, D.; Kim, Y. T. Highly stretchable fiber-based single-electrode triboelectric nanogenerator for wearable devices. *RSC Adv.* **2017**, *7*, 54829-54834.

(64) Bai, Z.; He, T.; Zhang, Z.; Xu, Y.; Zhang, Z.; Shi, Q.; Yang, Y.; Zhou, B.; Zhu, M.; Guo, J.; Lee, C. Constructing highly tribopositive elastic yarn through interfacial design and assembly for efficient energy harvesting and human-interactive sensing. *Nano Energy* **2022**, *94*, 106956.

(65) Sim, H. J.; Choi, C.; Kim, S. H.; Kim, K. M.; Lee, C. J.; Kim, Y. T.; Lepro, X.; Baughman, R. H.; Kim, S. J. Stretchable Triboelectric Fiber for Self-powered Kinematic Sensing Textile. *Sci. Rep.* **2016**, *6*, 1-7.

(66) Ning, C.; Cheng, R.; Jiang, Y.; Sheng, F.; Yi, J.; Shen, S.; Zhang, Y.; Peng, X.; Dong, K.; Wang, Z. L. Helical Fiber Strain Sensors Based on Triboelectric Nanogenerators for Self-Powered Human Respiratory Monitoring. *ACS Nano* **2022**, *16*, 2811-2821.

(67) Fu, K.; Zhou, J.; Wu, H.; Su, Z. Fibrous self-powered sensor with high stretchability for physiological information monitoring. *Nano Energy* **2021**, *88*, 106258.

(68) Gong, W.; Hou, C.; Guo, Y.; Zhou, J.; Mu, J.; Li, Y.; Zhang, Q.; Wang, H. A wearable, fibroid, self-powered active kinematic sensor based on stretchable sheath-core structural triboelectric fibers. *Nano Energy* **2017**, *39*, 673-683.

(69) Kim, S.; Cho, W.; Won, D.-J.; Kim, J. Textile-type triboelectric nanogenerator using Teflon wrapping wires as wearable power source. *Micro Nano Syst. Lett.* **2022**, *10*, 1-8.

CHAPTER 2

- (70) He, Q.; Wu, Y.; Feng, Z.; Fan, W.; Lin, Z.; Sun, C.; Zhou, Z.; Meng, K.; Wu, W.; Yang, J. An all-textile triboelectric sensor for wearable teleoperated human-machine interaction. *J. Mater. Chem. A* **2019**, *7*, 26804-26811.
- (71) Guan, X.; Xu, B.; Wu, M.; Jing, T.; Yang, Y.; Gao, Y. Breathable, washable and wearable woven-structured triboelectric nanogenerators utilizing electrospun nanofibers for biomechanical energy harvesting and self-powered sensing. *Nano Energy* **2021**, *80*, 105549.
- (72) Shuai, L.; Guo, Z. H.; Zhang, P.; Wan, J.; Pu, X.; Wang, Z. L. Stretchable, self-healing, conductive hydrogel fibers for strain sensing and triboelectric energy-harvesting smart textiles. *Nano Energy* **2020**, *78*, 105389.
- (73) Zhang, X.; Wang, J.; Xing, Y.; Li, C., Woven Wearable Electronic Textiles as Self-Powered Intelligent Tribo-Sensors for Activity Monitoring. *Glob. Chall.* **2019**, *3*, 1900070.
- (74) Yan, L.; Mi, Y.; Lu, Y.; Qin, Q.; Wang, X.; Meng, J.; Liu, F.; Wang, N.; Cao, X. Weaved piezoresistive triboelectric nanogenerator for human motion monitoring and gesture recognition. *Nano Energy* **2022**, *96*, 107135.
- (75) Lai, Y.-C.; Deng, J.; Zhang, S. L.; Niu, S.; Guo, H.; Wang, Z. L. Single-Thread-Based Wearable and Highly Stretchable Triboelectric Nanogenerators and Their Applications in Cloth-Based Self-Powered Human-Interactive and Biomedical Sensing. *Adv. Funct. Mater.* **2017**, *27*, 1604462.
- (76) Chen, C.; Guo, H.; Chen, L.; Wang, Y. C.; Pu, X.; Yu, W.; Wang, F.; Du, Z.; Wang, Z. L. Direct Current Fabric Triboelectric Nanogenerator for Biomotion Energy Harvesting. *ACS Nano* **2020**, *14*, 4585-4594.
- (77) Dong, K.; Wang, Y. C.; Deng, J.; Dai, Y.; Zhang, S. L.; Zou, H.; Gu, B.; Sun, B.; Wang, Z. L. A Highly Stretchable and Washable All-Yarn-Based Self-Charging Knitting Power Textile Composed of Fiber Triboelectric Nanogenerators and

CHAPTER 2

Supercapacitors. *ACS Nano* **2017**, *11*, 9490-9499.

(78) Gunawardhana, K.; Wanasekara, N. D.; Dharmasena, R. Towards Truly Wearable Systems: Optimizing and Scaling Up Wearable Triboelectric Nanogenerators. *iScience* **2020**, *23*, 101360.

(79) Wu, R.; Ma, L.; Patil, A.; Meng, Z.; Liu, S.; Hou, C.; Zhang, Y.; Yu, W.; Guo, W.; Liu, X. Y. Graphene decorated carbonized cellulose fabric for physiological signal monitoring and energy harvesting. *J. Mater. Chem. A* **2020**, *8*, 12665-12673.

(80) Lin, Z.; Yang, J.; Li, X.; Wu, Y.; Wei, W.; Liu, J.; Chen, J.; Yang, J. Large-Scale and Washable Smart Textiles Based on Triboelectric Nanogenerator Arrays for Self-Powered Sleeping Monitoring. *Adv. Funct. Mater.* **2018**, *28*, 1704112.

(81) Feng, M.; Wu, Y.; Feng, Y.; Dong, Y.; Liu, Y.; Peng, J.; Wang, N.; Xu, S.; Wang, D. Highly wearable, machine-washable, and self-cleaning fabric-based triboelectric nanogenerator for wireless drowning sensors. *Nano Energy* **2022**, *93*, 106835.

(82) Sala de Medeiros, M.; Chanci, D.; Moreno, C.; Goswami, D.; Martinez, R. V. Waterproof, Breathable, and Antibacterial Self-Powered e-Textiles Based on Omniphobic Triboelectric Nanogenerators. *Adv. Funct. Mater.* **2019**, *29*, 1904350.

(83) Arica, T. A.; Isık, T.; Guner, T.; Horzum, N.; Demir, M. M. Advances in Electrospun Fiber-Based Flexible Nanogenerators for Wearable Applications. *Macromol. Mater. Eng.* **2021**, *306*, 2100143.

(84) Sun, N.; Wang, G.-G.; Zhao, H.-X.; Cai, Y.-W.; Li, J.-Z.; Li, G.-Z.; Zhang, X.-N.; Wang, B.-L.; Han, J.-C.; Wang, Y.; Yang, Y. Waterproof, breathable and washable triboelectric nanogenerator based on electrospun nanofiber films for wearable electronics. *Nano Energy* **2021**, *90*, 106639.

(85) Shi, Y.; Wei, X.; Wang, K.; He, D.; Yuan, Z.; Xu, J.; Wu, Z.; Wang, Z. L. Integrated All-Fiber Electronic Skin toward Self-Powered Sensing Sports Systems.

CHAPTER 2

ACS Appl. Mater. Interfaces **2021**, *13*, 50329-50337.

(86) Peng, X.; Dong, K.; Ye, C.; Jiang, Y.; Zhai, S.; Cheng, R.; Liu, D.; Gao, X.; Wang, J.; Wang, Z. L. A Breathable, Biodegradable, Antibacterial, and Self-Powered Electronic Skin Based on All Nanofiber Triboelectric Nanogenerators. *Sci. Adv.* **2020**, *6*, eaba9624.

(87) Gong, W.; Wang, X.; Yang, W.; Zhou, J.; Han, X.; Dickey, M. D.; Su, Y.; Hou, C.; Li, Y.; Zhang, Q.; Wang, H. Wicking-Polarization-Induced Water Cluster Size Effect on Triboelectric Evaporation Textiles. *Adv. Mater.* **2021**, *33*, e2007352.

(88) Yang, W.; Gong, W.; Hou, C.; Su, Y.; Guo, Y.; Zhang, W.; Li, Y.; Zhang, Q.; Wang, H. All-fiber tribo-ferroelectric synergistic electronics with high thermal-moisture stability and comfortability. *Nat. Commun.* **2019**, *10*, 5541.

(89) Yin, Y.; Wang, J.; Zhao, S.; Fan, W.; Zhang, X.; Zhang, C.; Xing, Y.; Li, C. Stretchable and Tailorable Triboelectric Nanogenerator Constructed by Nanofibrous Membrane for Energy Harvesting and Self-Powered Biomechanical Monitoring. *Adv. Mater. Technol.* **2018**, *3*, 1700370.

(90) Zhou, K.; Zhao, Y.; Sun, X.; Yuan, Z.; Zheng, G.; Dai, K.; Mi, L.; Pan, C.; Liu, C.; Shen, C. Ultra-stretchable triboelectric nanogenerator as high-sensitive and self-powered electronic skins for energy harvesting and tactile sensing. *Nano Energy* **2020**, *70*, 104546.

(91) Dong, K.; Peng, X.; Cheng, R.; Ning, C.; Jiang, Y.; Zhang, Y.; Wang, Z. L. Advances in High-Performance Autonomous Energy and Self-Powered Sensing Textiles with Novel 3D Fabric Structures. *Adv. Mater.* **2022**, e2109355.

(92) Chen, C.; Chen, L.; Wu, Z.; Guo, H.; Yu, W.; Du, Z.; Wang, Z. L. 3D double-faced interlock fabric triboelectric nanogenerator for bio-motion energy harvesting and as self-powered stretching and 3D tactile sensors. *Mater. Today* **2020**, *32*, 84-93.

(93) Li, M.; Xu, B.; Li, Z.; Gao, Y.; Yang, Y.; Huang, X., Toward 3D Double-electrode

CHAPTER 2

Textile Triboelectric Nanogenerators for Wearable Biomechanical Energy Harvesting and Sensing. *Chem. Eng. J.* **2022**, *450*, 137491.

(94) Wang, Q.; Peng, X.; Zu, Y.; Jiang, L.; Dong, K. Scalable and washable 3D warp-knitted spacer power fabrics for energy harvesting and pressure sensing. *J. Phys. D: Appl. Phys.* **2021**, *54*, 424006.

(95) Tao, X.; Zhou, Y.; Qi, K.; Guo, C.; Dai, Y.; He, J.; Dai, Z. Wearable textile triboelectric generator based on nanofiber core-spun yarn coupled with electret effect. *J. Colloid Interface Sci.* **2022**, *608*, 2339-2346.

(96) He, E.; Sun, Y.; Wang, X.; Chen, H.; Sun, B.; Gu, B.; Zhang, W. 3D angle-interlock woven structural wearable triboelectric nanogenerator fabricated with silicone rubber coated graphene oxide/cotton composite yarn. *Composites, Part B* **2020**, *200*, 108244.

(97) Dong, K.; Peng, X.; An, J.; Wang, A. C.; Luo, J.; Sun, B.; Wang, J.; Wang, Z. L. Shape adaptable and highly resilient 3D braided triboelectric nanogenerators as e-textiles for power and sensing. *Nat. Commun.* **2020**, *11*, 2868.

(98) Barras, R.; dos Santos, A.; Calmeiro, T.; Fortunato, E.; Martins, R.; Águas, H.; Barquinha, P.; Igreja, R.; Pereira, L. Porous PDMS conformable coating for high power output carbon fibers/ZnO nanorod-based triboelectric energy harvesters. *Nano Energy* **2021**, *90*, 106582.

(99) Bayan, S.; Pal, S.; Ray, S. K., Interface engineered silver nanoparticles decorated g-C₃N₄ nanosheets for textile based triboelectric nanogenerators as wearable power sources. *Nano Energy* **2022**, *94*, 106928.

(100) Choi, D.; Yang, S.; Lee, C.; Kim, W.; Kim, J.; Hong, J., Highly Surface-Embossed Polydimethylsiloxane-Based Triboelectric Nanogenerators with Hierarchically Nanostructured Conductive Ni-Cu Fabrics. *ACS Appl. Mater. Interfaces* **2018**, *10*, 33221-33229.

CHAPTER 2

- (101) Jian, G.; Meng, Q.; Jiao, Y.; Feng, L.; Shao, H.; Wang, F.; Meng, F. Hybrid PDMS-TiO₂-stainless steel textiles for triboelectric nanogenerators. *Chem. Eng. J.* **2021**, *417*, 127974.
- (102) Yu, X.; Pan, J.; Zhang, J.; Sun, H.; He, S.; Qiu, L.; Lou, H.; Sun, X.; Peng, H. A coaxial triboelectric nanogenerator fiber for energy harvesting and sensing under deformation. *J. Mater. Chem. A* **2017**, *5*, 6032-6037.
- (103) Zhang, L.; Su, C.; Cheng, L.; Cui, N.; Gu, L.; Qin, Y.; Yang, R.; Zhou, F. Enhancing the Performance of Textile Triboelectric Nanogenerators with Oblique Microrod Arrays for Wearable Energy Harvesting. *ACS Appl. Mater. Interfaces* **2019**, *11*, 26824-26829.
- (104) Zhang, L.; Su, C.; Cui, X.; Li, P.; Wang, Z.; Gu, L.; Tang, Z. Free-Standing Triboelectric Layer-Based Full Fabric Wearable Nanogenerator for Efficient Mechanical Energy Harvesting. *ACS Appl. Electron. Mater.* **2020**, *2*, 3366-3372.
- (105) Zou, Y.; Xu, J.; Chen, K.; Chen, J. Advances in Nanostructures for High-Performance Triboelectric Nanogenerators. *Adv. Mater. Technol.* **2021**, *6*, 2000916.
- (106) Feng, P. Y.; Xia, Z.; Sun, B.; Jing, X.; Li, H.; Tao, X.; Mi, H. Y.; Liu, Y., Enhancing the Performance of Fabric-Based Triboelectric Nanogenerators by Structural and Chemical Modification. *ACS Appl. Mater. Interfaces* **2021**, *13*, 16916-16927.
- (107) Guo, Y.; Li, K.; Hou, C.; Li, Y.; Zhang, Q.; Wang, H., Fluoroalkylsilane-Modified Textile-Based Personal Energy Management Device for Multifunctional Wearable Applications. *ACS Appl. Mater. Interfaces* **2016**, *8*, 4676-83.
- (108) Huang, J.; Hao, Y.; Zhao, M.; Li, W.; Huang, F.; Wei, Q., All-Fiber-Structured Triboelectric Nanogenerator via One-Pot Electrospinning for Self-Powered Wearable Sensors. *ACS Appl. Mater. Interfaces* **2021**, *13*, 24774-24784.
- (109) Yang, C.-R.; Ko, C.-T.; Chang, S.-F.; Huang, M.-J. Study on fabric-based

CHAPTER 2

triboelectric nanogenerator using graphene oxide/porous PDMS as a compound friction layer. *Nano Energy* **2022**, *92*, 106791.

(110) Zhang, L.; Yu, Y.; Eyer, G. P.; Suo, G.; Kozik, L. A.; Fairbanks, M.; Wang, X.; Andrew, T. L. All-Textile Triboelectric Generator Compatible with Traditional Textile Process. *Adv. Mater. Technol.* **2016**, *1*, 1600147.

(111) Guan, X.; Xu, B.; Huang, J.; Jing, T.; Gao, Y. Fiber-Shaped Stretchable Triboelectric Nanogenerator with a Novel Synergistic Structure of Opposite Poisson's Ratios. *Chem. Eng. J.* **2021**, *427*, 131698.

(112) Huang, T.; Zhang, J.; Yu, B.; Yu, H.; Long, H.; Wang, H.; Zhang, Q.; Zhu, M. Fabric texture design for boosting the performance of a knitted washable textile triboelectric nanogenerator as wearable power. *Nano Energy* **2019**, *58*, 375-383.

(113) Kwon, D.-H.; Kwon, J.-H.; Jeong, J.; Lee, Y.; Biswas, S.; Lee, D.-W.; Lee, S.; Bae, J.-H.; Kim, H. Textile Triboelectric Nanogenerators with Diverse 3D-Spacer Fabrics for Improved Output Voltage. *Electronics* **2021**, *10*, 937.

(114) Pyo, S.; Kim, M.-O.; Kwon, D.-S.; Kim, W.; Yang, J.-H.; Cho, H. S.; Lee, J. H.; Kim, J. All-textile wearable triboelectric nanogenerator using pile-embroidered fibers for enhancing output power. *Smart Mater. Struct.* **2020**, *29*, 055026.

(115) Tian, Z.; He, J.; Chen, X.; Zhang, Z.; Wen, T.; Zhai, C.; Han, J.; Mu, J.; Hou, X.; Chou, X.; Xue, C. Performance-boosted triboelectric textile for harvesting human motion energy. *Nano Energy* **2017**, *39*, 562-570.

(116) Jing, T.; Xu, B.; Xin, J. H.; Guan, X.; Yang, Y., Series to parallel structure of electrode fiber: an effective method to remarkably reduce inner resistance of triboelectric nanogenerator textiles. *J. Mater. Chem. A* **2021**, *9*, 12331-12339.

(117) Cheng, R.; Dong, K.; Chen, P.; Ning, C.; Peng, X.; Zhang, Y.; Liu, D.; Wang, Z. L., High output direct-current power fabrics based on the air breakdown effect. *Energy Environ. Sci.* **2021**, *14*, 2460-2471.

CHAPTER 2

- (118) Wu, C.; Wang, A. C.; Ding, W.; Guo, H.; Wang, Z. L. Triboelectric Nanogenerator: A Foundation of the Energy for the New Era. *Adv. Energy Mater.* **2019**, *9*, 1802906.
- (119) Parida, K.; Xiong, J.; Zhou, X.; Lee, P. S. Progress on triboelectric nanogenerator with stretchability, self-healability and bio-compatibility. *Nano Energy* **2019**, *59*, 237-257.
- (120) Li, H.; Zhao, S.; Du, X.; Wang, J.; Cao, R.; Xing, Y.; Li, C. A Compound Yarn Based Wearable Triboelectric Nanogenerator for Self-Powered Wearable Electronics. *Adv. Mater. Technol.* **2018**, *3*, 1800065.
- (121) Lou, M.; Abdalla, I.; Zhu, M.; Wei, X.; Yu, J.; Li, Z.; Ding, B. Highly Wearable, Breathable, and Washable Sensing Textile for Human Motion and Pulse Monitoring. *ACS Appl. Mater. Interfaces* **2020**, *12*, 19965-19973.
- (122) Ye, C.; Dong, S.; Ren, J.; Ling, S. Ultrastable and High-Performance Silk Energy Harvesting Textiles. *Nano-Micro Lett.* **2019**, *12*, 1-15.
- (123) Gong, J.; Xu, B.; Guan, X.; Chen, Y.; Li, S.; Feng, J. Towards truly wearable energy harvesters with full structural integrity of fiber materials. *Nano Energy* **2019**, *58*, 365-374.
- (124) Choi, A. Y.; Lee, C. J.; Park, J.; Kim, D.; Kim, Y. T. Corrugated Textile based Triboelectric Generator for Wearable Energy Harvesting. *Sci. Rep.* **2017**, *7*, 45583.
- (125) He, T.; Sun, Z.; Shi, Q.; Zhu, M.; Anaya, D. V.; Xu, M.; Chen, T.; Yuce, M. R.; Thean, A. V.-Y.; Lee, C. Self-powered glove-based intuitive interface for diversified control applications in real/cyber space. *Nano Energy* **2019**, *58*, 641-651.
- (126) Rezaei, J.; Nikfarjam, A. Rib Stitch Knitted Extremely Stretchable and Washable Textile Triboelectric Nanogenerator. *Adv. Mater. Technol.* **2021**, *6*, 2000983.
- (127) Wu, H.; Huang, Y.; Xu, F.; Duan, Y.; Yin, Z. Energy Harvesters for Wearable and Stretchable Electronics: From Flexibility to Stretchability. *Adv. Mater.* **2016**, *28*,

CHAPTER 2

9881-9919.

(128) Lai, Y. C.; Lu, H. W.; Wu, H. M.; Zhang, D.; Yang, J.; Ma, J.; Shamsi, M.; Vallem, V.; Dickey, M. D. Elastic Multifunctional Liquid–Metal Fibers for Harvesting Mechanical and Electromagnetic Energy and as Self-Powered Sensors. *Adv. Energy Mater.* **2021**, *11*, 2100411.

(129) Ryu, J.; Kim, J.; Oh, J.; Lim, S.; Sim, J. Y.; Jeon, J. S.; No, K.; Park, S.; Hong, S. Intrinsically stretchable multi-functional fiber with energy harvesting and strain sensing capability. *Nano Energy* **2019**, *55*, 348-353.

(130) Chen, L.; Chen, C.; jin, L.; Guo, H.; Wang, A. C.; Ning, F.; Xu, Q.; Du, Z.; Wang, F.; Wang, Z. L. Stretchable Negative Poisson's Ratio Yarn for Triboelectric Nanogenerator as Environmental Energy Harvesting and Self-powered sensors. *Energy Environ. Sci.* **2021**, *14*, 955-964.

(131) Ye, C.; Xu, Q.; Ren, J.; Ling, S., Violin String Inspired Core-Sheath Silk/Steel Yarns for Wearable Triboelectric Nanogenerator Applications. *Adv. Fiber Mater.* **2020**, *2*, 24-33.

(132) Du, X.; Zhang, K. Recent progress in fibrous high-entropy energy harvesting devices for wearable applications. *Nano Energy* **2022**, *101*, 107600.

(133) Fan, W.; He, Q.; Meng, K.; Tan, X.; Zhou, Z.; Zhang, G.; Yang, J.; Wang, Z. L. Machine-Knitted Washable Sensor Array Textile for Precise Epidermal Physiological Signal Monitoring. *Sci. Adv.* **2020**, *6*, No. eaay2840.

(134) Gunawardhana, K. R. S.; Wanasekara, N. D.; Wijayantha, K. G.; Dharmasena, R. D. I. Scalable Textile Manufacturing Methods for Fabricating Triboelectric Nanogenerators with Balanced Electrical and Wearable Properties. *ACS Appl. Electron. Mater.* **2022**, *4*, 678-688.

(135) Li, Z.; Zhu, M.; Shen, J.; Qiu, Q.; Yu, J.; Ding, B. All-Fiber Structured Electronic Skin with High Elasticity and Breathability. *Adv. Funct. Mater.* **2019**, *30*, 1908411.

CHAPTER 2

(136) Busolo, T.; Szewczyk, P. K.; Nair, M.; Stachewicz, U.; Kar-Narayan, S. Triboelectric Yarns with Electrospun Functional Polymer Coatings for Highly Durable and Washable Smart Textile Applications. *ACS Appl. Mater. Interfaces* **2021**, *13*, 16876-16886.

(137) Zhao, Z.; Huang, Q.; Yan, C.; Liu, Y.; Zeng, X.; Wei, X.; Hu, Y.; Zheng, Z. Machine-washable and breathable pressure sensors based on triboelectric nanogenerators enabled by textile technologies. *Nano Energy* **2020**, *70*, 104528.

(138) Zhao, Z.; Yan, C.; Liu, Z.; Fu, X.; Peng, L. M.; Hu, Y.; Zheng, Z. Machine-Washable Textile Triboelectric Nanogenerators for Effective Human Respiratory Monitoring through Loom Weaving of Metallic Yarns. *Adv. Mater.* **2016**, *28*, 10267-10274.

(139) Shin, Y.-E.; Lee, J.-E.; Park, Y.; Hwang, S.-H.; Chae, H. G.; Ko, H., Sewing machine stitching of polyvinylidene fluoride fibers: programmable textile patterns for wearable triboelectric sensors. *J. Mater. Chem. A* **2018**, *6*, 22879-22888.

(140) Zhang, M.; Zhao, M.; Jian, M.; Wang, C.; Yu, A.; Yin, Z.; Liang, X.; Wang, H.; Xia, K.; Liang, X.; Zhai, J.; Zhang, Y. Printable Smart Pattern for Multifunctional Energy-Management E-Textile. *Matter* **2019**, *1*, 168-179.

(141) Dong, L.; Wang, M.; Wu, J.; Zhu, C.; Shi, J.; Morikawa, H. Deformable Textile-Structured Triboelectric Nanogenerator Knitted with Multifunctional Sensing Fibers for Biomechanical Energy Harvesting. *Adv. Fiber Mater.* **2022**, 1-14.

(142) Jing, T.; Xu, B.; Yang, Y. Organogel electrode based continuous fiber with large-scale production for stretchable triboelectric nanogenerator textiles. *Nano Energy* **2021**, *84*, 105867.

(143) Wu, Y.; Dai, X.; Sun, Z.; Zhu, S.; Xiong, L.; Liang, Q.; Wong, M.-C.; Huang, L.-B.; Qin, Q.; Hao, J. Highly integrated, scalable manufacturing and stretchable conductive core/shell fibers for strain sensing and self-powered smart textiles. *Nano*

CHAPTER 2

Energy **2022**, *98*, 107240.

(144) Li, Y.; Zhang, Y.; Yi, J.; Peng, X.; Cheng, R.; Ning, C.; Sheng, F.; Wang, S.; Dong, K.; Wang, Z. L. Large-scale fabrication of coreshell triboelectric braided fibers and power textiles for energy harvesting and plantar pressure monitoring. *EcoMat* **2022**, *3*, 12191-12203.

(145) Wang, W.; Yu, A.; Liu, X.; Liu, Y.; Zhang, Y.; Zhu, Y.; Lei, Y.; Jia, M.; Zhai, J.; Wang, Z. L. Large-scale fabrication of robust textile triboelectric nanogenerators. *Nano Energy* **2020**, *71*, 104605.

(146) Niu, L.; Peng, X.; Chen, L.; Liu, Q.; Wang, T.; Dong, K.; Pan, H.; Cong, H.; Liu, G.; Jiang, G.; Chen, C.; Ma, P. Industrial production of bionic scales knitting fabric-based triboelectric nanogenerator for outdoor rescue and human protection. *Nano Energy* **2022**, *97*, 107168.

(147) Xu, F.; Dong, S.; Liu, G.; Pan, C.; Guo, Z. H.; Guo, W.; Li, L.; Liu, Y.; Zhang, C.; Pu, X.; Wang, Z. L. Scalable fabrication of stretchable and washable textile triboelectric nanogenerators as constant power sources for wearable electronics. *Nano Energy* **2021**, *88*, 106247.

(148) Feng, Z.; Yang, S.; Jia, S.; Zhang, Y.; Jiang, S.; Yu, L.; Li, R.; Song, G.; Wang, A.; Martin, T.; Zuo, L.; Jia, X. Scalable, Washable and Lightweight Triboelectric-Energy-Generating Fibers by the Thermal Drawing Process for Industrial Loom Weaving. *Nano Energy* **2020**, *74*, 104805.

(149) Dong, C.; Leber, A.; Das Gupta, T.; Chandran, R.; Volpi, M.; Qu, Y.; Nguyen-Dang, T.; Bartolomei, N.; Yan, W.; Sorin, F. High-efficiency super-elastic liquid metal based triboelectric fibers and textiles. *Nat. Commun.* **2020**, *11*, 3537.

(150) Zheng, L.; Zhu, M.; Wu, B.; Li, Z.; Sun, S.; Wu, P. Conductance-stable liquid metal sheath-core microfibers for stretchy smart fabrics and self-powered sensing. *Sci. Adv* **2021**, *7*, No. eabg4041.

CHAPTER 2

(151) Gao, Y.; Li, Z.; Xu, B.; Li, M.; Jiang, C.; Guan, X.; Yang, Y. Scalable core–spun coating yarn-based triboelectric nanogenerators with hierarchical structure for wearable energy harvesting and sensing via continuous manufacturing. *Nano Energy* **2022**, *91*, 106672.

(152) Yang, Y.; Xu, B.; Gao, Y.; Li, M. Conductive Composite Fiber with Customizable Functionalities for Energy Harvesting and Electronic Textiles. *ACS Appl. Mater. Interfaces* **2021**, *13*, 49927-49935.

(153) Gong, W.; Hou, C.; Zhou, J.; Guo, Y.; Zhang, W.; Li, Y.; Zhang, Q.; Wang, H. Continuous and scalable manufacture of amphibious energy yarns and textiles. *Nat. Commun.* **2019**, *10*, 868.

(154) Yang, W.; Gong, W.; Gu, W.; Liu, Z.; Hou, C.; Li, Y.; Zhang, Q.; Wang, H. Self-Powered Interactive Fiber Electronics with Visual-Digital Synergies. *Adv. Mater.* **2021**, *33*, e2104681.

(155) Ye, C.; Yang, S.; Ren, J.; Dong, S.; Cao, L.; Pei, Y.; Ling, S. Electroassisted Core-Spun Triboelectric Nanogenerator Fabrics for IntelliSense and Artificial Intelligence Perception. *ACS Nano* **2022**, *16*, 4415-4425.

(156) He, X.; Zou, H.; Geng, Z.; Wang, X.; Ding, W.; Hu, F.; Zi, Y.; Xu, C.; Zhang, S. L.; Yu, H.; Xu, M.; Zhang, W.; Lu, C.; Wang, Z. L. A Hierarchically Nanostructured Cellulose Fiber-Based Triboelectric Nanogenerator for Self-Powered Healthcare Products. *Adv. Funct. Mater.* **2018**, *28*, 1805540.

(157) He, H.; Liu, J.; Wang, Y.; Zhao, Y.; Qin, Y.; Zhu, Z.; Yu, Z.; Wang, J. An Ultralight Self-Powered Fire Alarm e-Textile Based on Conductive Aerogel Fiber with Repeatable Temperature Monitoring Performance Used in Firefighting Clothing. *ACS Nano* **2022**, *16*, 2953-2967.

(158) Jiang, Y.; Dong, K.; An, J.; Liang, F.; Yi, J.; Peng, X.; Ning, C.; Ye, C.; Wang, Z. L. UV-Protective, Self-Cleaning, and Antibacterial Nanofiber-Based Triboelectric

CHAPTER 2

Nanogenerators for Self-Powered Human Motion Monitoring. *ACS Appl. Mater. Interfaces* **2021**, *13*, 11205-11214.

(159) Lai, Y. C.; Hsiao, Y. C.; Wu, H. M.; Wang, Z. L. Waterproof Fabric-Based Multifunctional Triboelectric Nanogenerator for Universally Harvesting Energy from Raindrops, Wind, and Human Motions and as Self-Powered Sensors. *Adv. Sci.* **2019**, *6*, 1801883.

(160) Xiong, J.; Lin, M.-F.; Wang, J.; Gaw, S. L.; Parida, K.; Lee, P. S. Wearable All-Fabric-Based Triboelectric Generator for Water Energy Harvesting. *Adv. Energy Mater.* **2017**, *7*, 1701243.

(161) Yuan, W.; Zhang, C.; Zhang, B.; Wei, X.; Yang, O.; Liu, Y.; He, L.; Cui, S.; Wang, J.; Wang, Z. L. Wearable, Breathable and Waterproof Triboelectric Nanogenerators for Harvesting Human Motion and Raindrop Energy. *Adv. Mater. Technol.* **2021**, *7*, 2101139.

(162) He, M.; Du, W.; Feng, Y.; Li, S.; Wang, W.; Zhang, X.; Yu, A.; Wan, L.; Zhai, J. Flexible and stretchable triboelectric nanogenerator fabric for biomechanical energy harvesting and self-powered dual-mode human motion monitoring. *Nano Energy* **2021**, *86*, 106058.

(163) Li, L.; Chen, Y.-T.; Hsiao, Y.-C.; Lai, Y.-C. Mycena chlorophos-inspired autoluminescent triboelectric fiber for wearable energy harvesting, self-powered sensing, and as human–device interfaces. *Nano Energy* **2022**, *94*, 106944.

(164) Ma, L.; Wu, R.; Patil, A.; Yi, J.; Liu, D.; Fan, X.; Sheng, F.; Zhang, Y.; Liu, S.; Shen, S.; Wang, J.; Wang, Z. L. Acid and Alkali-Resistant Textile Triboelectric Nanogenerator as a Smart Protective Suit for Liquid Energy Harvesting and Self-Powered Monitoring in High-Risk Environments. *Adv. Funct. Mater.* **2021**, *31*, 2102963.

(165) Zhang, Y.; Li, Y.; Li, K.; Kwon, Y. S.; Tennakoon, T.; Wang, C.; Chan, K. C.;

CHAPTER 2

Fu, S.-C.; Huang, B.; Chao, C. Y. H. A large-area versatile textile for radiative warming and biomechanical energy harvesting. *Nano Energy* **2022**, *95*, 106996.

(166) Si, S.; Sun, C.; Qiu, J.; Liu, J.; Yang, J. Knitting integral conformal all-textile strain sensor with commercial apparel characteristics for smart textiles. *Appl. Mater. Today* **2022**, *27*, 101508.

(167) Wang, Z.; Ruan, Z.; Ng, W. S.; Li, H.; Tang, Z.; Liu, Z.; Wang, Y.; Hu, H.; Zhi, C. Integrating a Triboelectric Nanogenerator and a Zinc-Ion Battery on a Designed Flexible 3D Spacer Fabric. *Small Methods* **2018**, *2*, 1800150.

(168) Han, J.; Xu, C.; Zhang, J.; Xu, N.; Xiong, Y.; Cao, X.; Liang, Y.; Zheng, L.; Sun, J.; Zhai, J.; Sun, Q.; Wang, Z. L. Multifunctional Coaxial Energy Fiber toward Energy Harvesting, Storage, and Utilization. *ACS Nano* **2021**, *15*, 1597-1607.

(169) Mao, Y.; Li, Y.; Xie, J.; Liu, H.; Guo, C.; Hu, W. Triboelectric nanogenerator/supercapacitor in-one self-powered textile based on PTFE yarn wrapped PDMS/MnO₂NW hybrid elastomer. *Nano Energy* **2021**, *84*, 105918.

(170) Ren, X.; Xiang, X.; Yin, H.; Tang, Y.; Yuan, H. All-yarn triboelectric nanogenerator and supercapacitor based self-charging power cloth for wearable applications. *Nanotechnology* **2021**, *32*, 315404.

(171) Yang, Y.; Xie, L.; Wen, Z.; Chen, C.; Chen, X.; Wei, A.; Cheng, P.; Xie, X.; Sun, X. Coaxial Triboelectric Nanogenerator and Supercapacitor Fiber-Based Self-Charging Power Fabric. *ACS Appl. Mater. Interfaces* **2018**, *10*, 42356-42362.

(172) Wang, W.; Yu, A.; Zhai, J.; Wang, Z. L. Recent Progress of Functional Fiber and Textile Triboelectric Nanogenerators: Towards Electricity Power Generation and Intelligent Sensing. *Adv. Fiber Mater.* **2021**, *3*, 394-412.

(173) Hu, Y.; Zhao, Z.; Liu, Z. Textile triboelectric nanogenerator for wearable electronics. *Adv. Mater. Lett.* **2018**, *9*, 199-204.

(174) He, W.; Fu, X.; Zhang, D.; Zhang, Q.; Zhuo, K.; Yuan, Z.; Ma, R. Recent

CHAPTER 2

progress of flexible/wearable self-charging power units based on triboelectric nanogenerators. *Nano Energy* **2021**, *84*, 105880.

(175) Chen, G.; Li, Y.; Bick, M.; Chen, J. Smart Textiles for Electricity Generation. *Chem. Rev.* **2020**, *120*, 3668-3720.

(176) Kim, T.; Jeon, S.; Lone, S.; Doh, S. J.; Shin, D.-M.; Kim, H. K.; Hwang, Y.-H.; Hong, S. W. Versatile nanodot-patterned Gore-Tex fabric for multiple energy harvesting in wearable and aerodynamic nanogenerators. *Nano Energy* **2018**, *54*, 209-217.

(177) Ye, C.; Liu, D.; Peng, X.; Jiang, Y.; Cheng, R.; Ning, C.; Sheng, F.; Zhang, Y.; Dong, K.; Wang, Z. L. A Hydrophobic Self-Repairing Power Textile for Effective Water Droplet Energy Harvesting. *ACS Nano* **2021**, *15*, 18172-18181.

(178) Gang, X.; Guo, Z. H.; Cong, Z.; Wang, J.; Chang, C.; Pan, C.; Pu, X.; Wang, Z. L. Textile Triboelectric Nanogenerators Simultaneously Harvesting Multiple “High-Entropy” Kinetic Energies. *ACS Appl Mater Interfaces* **2021**, *13*, 20145-20152.

(179) Cao, Y.; Shao, H.; Wang, H.; Li, X.; Zhu, M.; Fang, J.; Cheng, T.; Lin, T. A full-textile triboelectric nanogenerator with multisource energy harvesting capability. *Energy Convers. Manage.* **2022**, *267*, 115910.

(180) Seung, W.; Yoon, H. J.; Kim, T. Y.; Kang, M.; Kim, J.; Kim, H.; Kim, S. M.; Kim, S. W. Dual Friction Mode Textile-Based Tire Cord Triboelectric Nanogenerator. *Adv. Funct. Mater.* **2020**, *30*, 2002401.

(181) Zhou, Z.; Weng, L.; Tat, T.; Libanori, A.; Lin, Z.; Ge, L.; Yang, J.; Chen, J. Smart Insole for Robust Wearable Biomechanical Energy Harvesting in Harsh Environments. *ACS Nano* **2020**, *14*, 14126-14133.

(182) Xu, H.; Tao, J.; Liu, Y.; Mo, Y.; Bao, R.; Pan, C. Fully Fibrous Large-Area Tailorable Triboelectric Nanogenerator Based on Solution Blow Spinning Technology for Energy Harvesting and Self-Powered Sensing. *Small* **2022**, *18*, 2202477.

CHAPTER 2

- (183) Fang, Y.; Zou, Y.; Xu, J.; Chen, G.; Zhou, Y.; Deng, W.; Zhao, X.; Roustaei, M.; Hsiai, T. K.; Chen, J. Ambulatory Cardiovascular Monitoring Via a Machine-Learning-Assisted Textile Triboelectric Sensor. *Adv. Mater.* **2021**, *33*, 2104178.
- (184) Chen, G.; Au, C.; Chen, J. Textile Triboelectric Nanogenerators for Wearable Pulse Wave Monitoring. *Trends Biotechnol.* **2021**, *39*, 1078-1092.
- (185) Jiang, C.; Lai, C. L.; Xu, B.; So, M. Y.; Li, Z. Fabric-rebound triboelectric nanogenerators with loops and layered structures for energy harvesting and intelligent wireless monitoring of human motions. *Nano Energy* **2022**, *93*, 106807.
- (186) Li, Z.; Xu, B.; Han, J.; Huang, J.; Fu, H. A Polycation-Modified Nanofillers Tailored Polymer Electrolytes Fiber for Versatile Biomechanical Energy Harvesting and Full-Range Personal Healthcare Sensing. *Adv. Funct. Mater.* **2021**, *32*, 2106731.
- (187) Sahu, M.; Hajra, S.; Panda, S.; Rajaiitha, M.; Panigrahi, B. K.; Rubahn, H.-G.; Mishra, Y. K.; Kim, H. J. Waste textiles as the versatile triboelectric energy-harvesting platform for self-powered applications in sports and athletics. *Nano Energy* **2022**, *97*, 107208.
- (188) Tong, Y.; Feng, Z.; Kim, J.; Robertson, J. L.; Jia, X.; Johnson, B. N. 3D printed stretchable triboelectric nanogenerator fibers and devices. *Nano Energy* **2020**, *75*, 104973.
- (189) Wu, R.; Liu, S.; Lin, Z.; Zhu, S.; Ma, L.; Wang, Z. L. Industrial Fabrication of 3D Braided Stretchable Hierarchical Interlocked Fancy-Yarn Triboelectric Nanogenerator for Self-Powered Smart Fitness System. *Adv. Energy Mater.* **2022**, *12*, 2201288.
- (190) Wang, W.; Yu, A.; Wang, Y.; Jia, M.; Guo, P.; Ren, L.; Guo, D.; Pu, X.; Wang, Z. L.; Zhai, J. Elastic Kernmantle E-Braids for High-Impact Sports Monitoring. *Adv. Sci.* **2022**, *9*, 2202489.
- (191) Wu, F.; Lan, B.; Cheng, Y.; Zhou, Y.; Hossain, G.; Grabher, G.; Shi, L.; Wang,

CHAPTER 2

R.; Sun, J. A stretchable and helically structured fiber nanogenerator for multifunctional electronic textiles. *Nano Energy* **2022**, *101*, 107588.

(192) Fang, H.; Guo, J.; Wu, H. Wearable triboelectric devices for haptic perception and VR/AR applications. *Nano Energy* **2022**, *96*, 107112.

(193) Jiang, Y.; An, J.; Liang, F.; Zuo, G.; Yi, J.; Ning, C.; Zhang, H.; Dong, K.; Wang, Z. L. Knitted self-powered sensing textiles for machine learning-assisted sitting posture monitoring and correction. *Nano Research* **2022**, 1-9.

(194) He, H.; Guo, J.; Illés, B.; Géczy, A.; Istók, B.; Hliva, V.; Török, D.; Kovács, J. G.; Harmati, I.; Molnár, K. Monitoring Multi-respiratory Indices via a Smart Nanofibrous Mask Filter Based on a Triboelectric Nanogenerator. *Nano Energy* **2021**, *89*, 106418.

(195) Ho, D. H.; Han, J.; Huang, J.; Choi, Y. Y.; Cheon, S.; Sun, J.; Lei, Y.; Park, G. S.; Wang, Z. L.; Sun, Q.; Cho, J. H. β -Phase-Preferential blow-spun fabrics for wearable triboelectric nanogenerators and textile interactive interface. *Nano Energy* **2020**, *77*, 105262.

(196) Yi, J.; Dong, K.; Shen, S.; Jiang, Y.; Peng, X.; Ye, C.; Wang, Z. L. Fully Fabric-Based Triboelectric Nanogenerators as Self-Powered Human–Machine Interactive Keyboards. *Nano-Micro Lett.* **2021**, *13*, 1-13.

(197) Lan, B., Wu, F., Cheng, Y., Zhou, Y., Hossain, G., Grabher, G., Shi, L., Wang, R., Sun, J. Scalable, stretchable and washable triboelectric fibers for self-powering human-machine interaction and cardiopulmonary resuscitation training. *Nano Energy* **2022**, *102*, 107737.

(198) Gogurla, N.; Pratap, A.; Um, I. C.; Kim, S. Brush drawing multifunctional electronic textiles for human-machine interfaces. *Curr. Appl. Phys.* **2022**, *41*, 131-138.

(199) Zhang, Q.; Jin, T.; Cai, J.; Xu, L.; He, T.; Wang, T.; Tian, Y.; Li, L.; Peng, Y.; Lee, C. Wearable Triboelectric Sensors Enabled Gait Analysis and Waist Motion

CHAPTER 2

Capture for IoT-Based Smart Healthcare Applications. *Adv. Sci.* **2022**, 9, 2103694.

(200) He, T.; Shi, Q.; Wang, H.; Wen, F.; Chen, T.; Ouyang, J.; Lee, C. Beyond energy harvesting - multi-functional triboelectric nanosensors on a textile. *Nano Energy* **2019**, 57, 338-352.

(201) Hossain, G.; Rahman, M.; Hossain, I. Z.; Khan, A. Wearable socks with single electrode triboelectric textile sensors for monitoring footsteps. *Sens. Actuators, A* **2022**, 333, 113316.

Chapter 3: One-Dimensional PVDF Yarn-Based Textile Triboelectric Nanogenerator Assisted by Wet Spinning and Braiding Engineering

3.1 Introduction

Textile-based TENGs with the advantages of inherent flexibility, lightweight and portability show promising applications in energy harvesting and self-powered sensing. To date, a wide range of textile-based TENGs have been proposed, including fiber-based TENGs,¹⁻⁶ fabric-based TENGs,⁷⁻⁹ and nanofiber-based TENGs.¹⁰⁻¹² Among them, fiber/yarn shaped TENG is considered as an effective method to improve freedom of movement, designability and comfort, especially the compatibility of textiles. The One-dimensional fiber/yarn structures can not only be directly integrated into two-dimensional textiles through textile techniques, but also suitable for the production of miniaturized and integrated electronics.

Poly (vinylidene fluoride) (PVDF) as one of the most promising for wearable TENGs has drawn great interest due to its strong electro-negativity in the triboelectric series,¹³ high resistance to chemicals and flexibility.^{14, 15} For example, Li et al. developed an electronic skin with excellent elasticity and breathability based on TENG by the electrospinning technology, which was fabricated with PVDF nanofibers (NFs), carbon NFs, and polyurethane (PU) NFs.¹⁶ Sun et al. proposed a nanofiber-based triboelectric nanogenerator with polyamide 66 (PA66)/multi-walled carbon nanotubes (MWCNTs), PVDF nanofiber film, conductive fabric and the waterproof and breathable fabric, which exhibited good waterproof, breathable and washable properties.¹⁷ Yin et al. used

CHAPTER 3

electrospinning and ultrasonic welding technologies to prepare a continuous arch structured TENG with good stretchability, which consisted of PVDF supported by conducting fabric and thermoplastic polyurethanes (TPU) supported by Ag elastic fabric.¹⁸ In these works, the majority of research are based on either the form of PVDF films or electro-spun mats (nanofiber), which have great limitations in their practical use as smart textiles due to weak mechanical properties and poor ability to integrate seamlessly with textiles. In contrast, triboelectric yarn provides better opportunities for textile integration.¹⁹⁻²² Yarn-based TENG operating in the single-electrode mode offers one of the soundest solutions owing to its excellent wearability, lightweight and good flexibility as well as easy deployment.²³ Busolo et al. designed a triboelectric yarn with a core-shell structure of conducting carbon nanotube coated electrospun PVDF fibers by a customized electrospinning process.²⁴ Although the triboelectric yarn exhibits good durability and washability, its fabrication is restricted to laboratory scale, resulting in short-length that is not compatible with diverse applications. Meanwhile, the designability of the yarn TENG made by this method is relatively simple. Therefore, yarns with good triboelectric effect and strong mechanical property by a scalable method are required to provide new potential for functional yarns and next-generation t-TENGs.

In this chapter, a 1D braided core-shell structured single-electrode triboelectric yarn (BYTENG) fabricated by a polyamide (PA) conductive yarn and wet-spun PVDF yarn has been developed by scalable wet spinning and braiding technologies. Different from the previous reported PVDF-based t-TENG devices, the wet-spun PVDF yarn was fabricated into the BYTENG, which endowed it with highly negative triboelectrification and good integration capability, further broadening its application scenarios. The BYTENG can deliver a voltage of 35 V, current of 0.35 μ A and excellent

CHAPTER 3

pressure sensing. The feasibility of applying the BYTENG into sports products for exercise detection has been demonstrated, such as household portable pedal puller and boxing reaction ball. With the merits of mechanical robustness, flexibility and washability, the BYTENG can be integrated into fabric by weaving and knitting technologies. The developed knitted and woven triboelectric fabrics possess good air permeability and can be applied into textile products for human motion signals monitoring, such as seat cushion, backrest and carpet, demonstrating a variety of potential applications.

3.2 Experimental Section

3.2.1 Materials

PVDF ($M_w \sim 900000$) powder was purchased from Piezotech (Piezotech S.A.S, France). N,N-dimethylformamide (DMF, $\geq 99.8\%$, ACS reagent) was purchased from DIECKMANN. Conductive Ag yarns (70D and 360D) were bought from Suzhou TEK Silver Fiber Technology Co., Ltd., China.

3.2.2 Fabrication of the BYTENG

A novel BYTENG was designed with braided core-shell structure. A commercial silver-coated nylon yarn was selected as the core conductive electrode, due to its low cost and maturity in industrial production. PVDF was used as triboelectric material, which was served as shell layer considering its high electron affinity, excellent stability and desirable flexibility. Figure 3.1 schematically depicts the fabrication process of the BYTENG. The PVDF yarn was prepared by wet spinning, which was facile for scaled-

CHAPTER 3

up and continuous production. As shown in Figure 3.1, continuous spinning of PVDF yarn was conducted through using a customer-made wet spinning setup. A uniform spinning solution of 14 wt% PVDF in DMF was prepared by stirring in water bath for 8 h at 60 °C, and then transferred to a 10 mL syringe equipped with a metal needle. Wet spinning was conducted using custom-designed fiber spinning unit. The solution was spun, and then introduced to a DI water for coagulation. The as-spun yarns were taken up with a roller. The prepared yarns were kept immersed in DI water at room temperature for a day to remove the residual DMF in the yarn. In order to better wrap the core conductive electrode with PVDF yarns and improve the mechanical properties, a braiding machine was adopted. As illustrated in Figure 3.1, four PVDF yarns together with the Ag yarn were drawn from the bobbins and interwoven with each other. In the process of braiding, the core yarn was straightened under a certain tension control, then PVDF yarns were tightly and uniformly wrapped on the core yarn. Taking advantage of the take-up device, the fabricated BYTENG without length limitations could be continuously wound on the reel. Notably, combining wet spinning and braiding technology provides a facile, efficient, and scalable method to fabricate functional yarns.

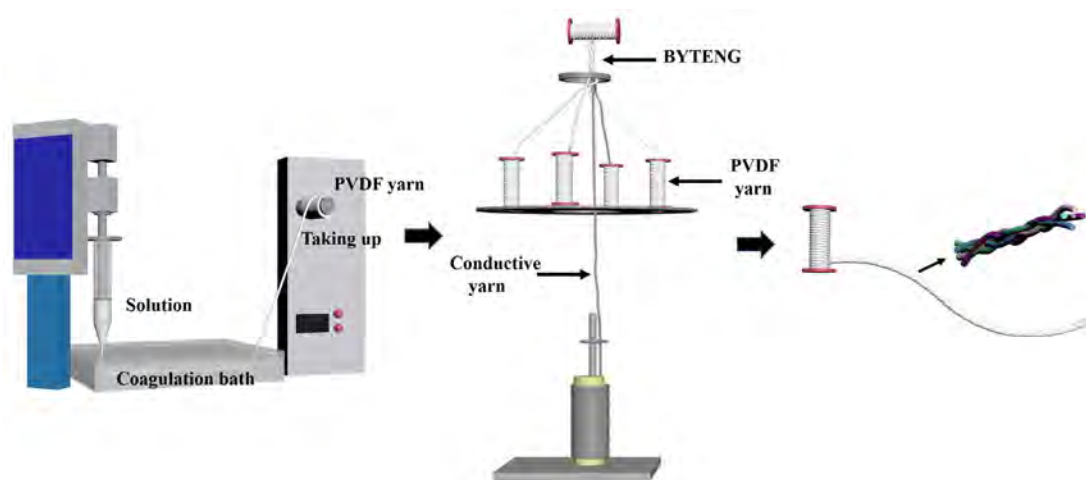


Figure 3.1 Schematic illustration of the fabrication process of the BYTENG.

CHAPTER 3

3.2.3 Fabrication of the woven and knitted FTENGs

The woven and knitted FTENGs were fabricated by using a sample loom (SL8900, CCI TECH INC.) and hand flat knitting machine, respectively.

3.2.4 Characterization and evaluation

The surface morphologies of the BYTENG were characterized by Leica M165C (DFC 290HD, Leica Microsystems Ltd.) and SEM (Hitachi TM-3000). The tensile properties of as-spun PVDF yarns, Ag yarn and BYTENG were determined by using Instron 5566 with a 10 N load cell according to ASTM standard D2256. The BYTENG was washed by a commercial laundering machine (3XWTW5905SW0, Whirlpool) following AATCC Test Method 135. Air permeability measurements of knitted and woven FTENGs were conducted by air permeability tester (KES-F8-API, Kato Tech Co., Ltd). A keyboard life tester (ZX-A03) was used to control the contact and separate motion for the BYTENG. The output voltage and current were measured by a programmable electrometer (Keithley 6514).

3.3 Results and Discussion

3.3.1 Characterization of the PVDF yarn and BYTENG

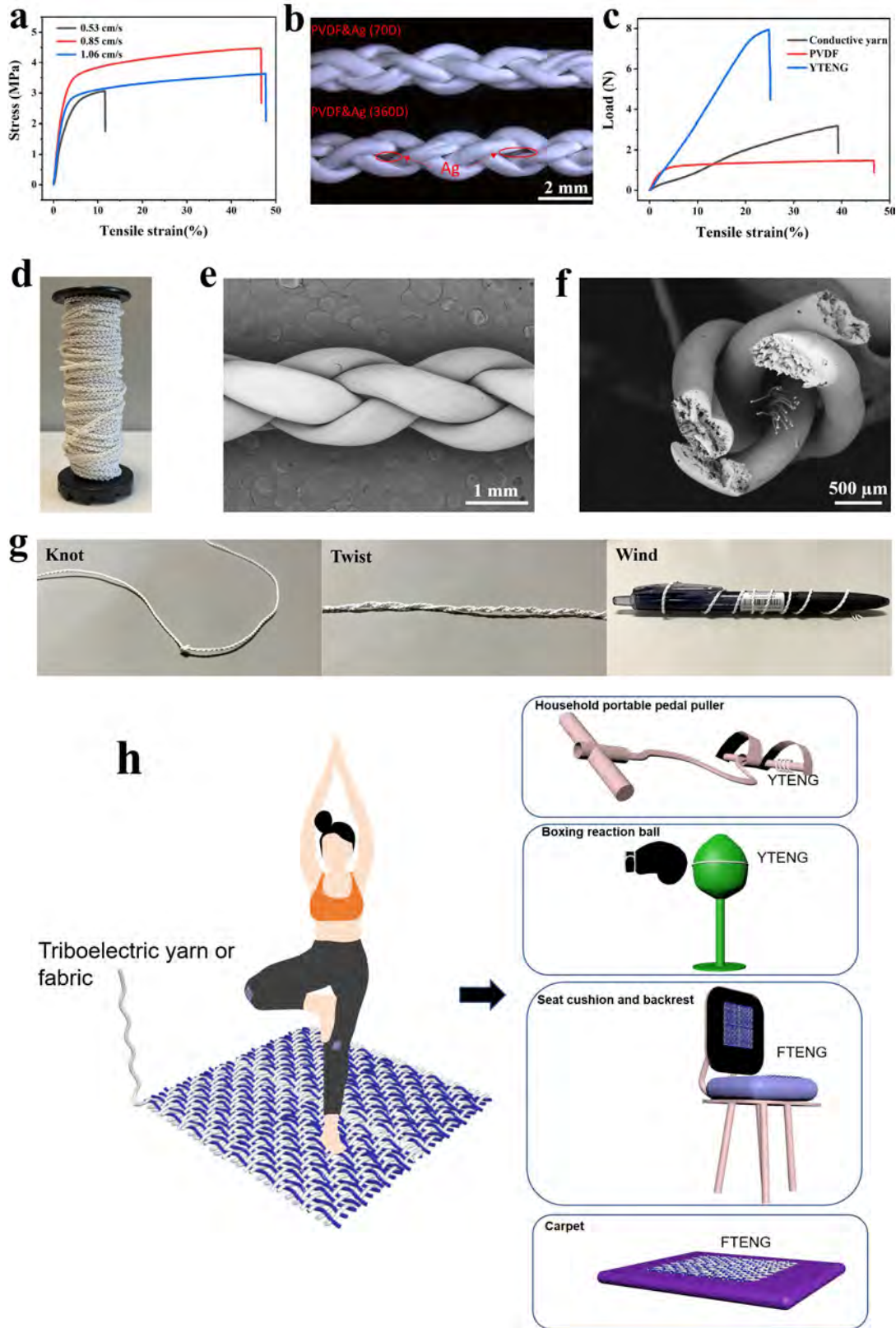
During the process of wet spinning, the take-up speed has a great influence on the diameter and mechanical properties of the spun PVDF yarn. In order to select the suitable diameter, the PVDF yarns were spun by using different take-up speeds (The take-up speeds were 0.53, 0.85, 1.06 cm s⁻¹, respectively). The corresponding diameters

CHAPTER 3

of as-prepared PVDF yarns are 0.835 mm, 0.647 mm and 0.613 mm, respectively. When the take-up speed increases, the yarn diameter decreased due to the decreased cross-sectional area. Figure 3.2a shows the stress-strain of PVDF yarns with various take-up speeds. As exhibited in Figure 3.2a, the PVDF yarn using the take-up speed of 0.85 cm s^{-1} possesses higher stress and strain, which was chosen as the wrapping yarn. Regarding braiding, the number of PVDF yarn and fineness of conductive electrode have a great influence on the wrapping effect. When the conductive electrode was braided with eight PVDF yarns, the resulting triboelectric yarns were too thick and stiff to be compatible with common textile weaving/knitting techniques. Figure 3.2b presents the wrapping effects of four PVDF yarns wrapping 70D conductive yarn and four PVDF yarns wrapping 360D conductive yarn. It can be clearly observed that the conductive yarns of 360D cannot be fully covered by four PVDF yarns, which may lead to leakage of partial charge. After a comprehensive trade-off of wrapping effect and thickness, the four PVDF yarns wrapping 70D conductive yarn were selected to fabricate the BYTENG. In addition, the tensile properties of the PVDF yarn, conductive yarn and BYTENG were measured and evaluated. As exhibited in Figure 3.2c, the BYTENG has showed an enhanced strength compared with the PVDF and conductive yarn. Figure 3.2d shows the fabricated BYTENG without length limitation, which indicates the large-scale production potential. As demonstrated in Figure 3.2e and f, the four PVDF yarns were closely wrapped along the conductive yarn with a total diameter of 1.469 mm. Figure 3.2g shows the fabricated BYTENG, which can withstand multiple mechanical deformations such as knotting, twisting and winding. Also, Table 3.1 shows the price of raw materials. The material cost of the BYTENG is only 1.38 RMB/m. High softness, great scalability, productivity, and low cost will contribute to the widespread application of the BYTENG. Meanwhile, it could be woven/knitted into breathable triboelectric fabrics (FTENGs). As indicated in Figure 3.2h, the BYTENG

CHAPTER 3

and FTENGs show great application potential in sports and human motion energy harvesting and monitoring due to their good integration capabilities.



CHAPTER 3

Figure 3.2 Mechanical property, photographs and potential application scenarios of the BYTENG. (a) Strain-stress curves of wet-spun PVDF yarns using different take-up speeds. (b) Optical microscope images of the wrapping effects of four PVDF yarns wrapping 70D conductive yarn and four PVDF yarns wrapping 360D conductive yarn. (c) Strain-tension curves of the conductive yarn, PVDF yarn and BYTENG. (d) Photograph of the BYTENG. (e) Surface morphology of the BYTENG. (f) SEM image of the cross section of the BYTENG. (g) Photographs of the BYTENG in various deformable states including knotting, twisting and winding. (h) Schematic diagram of application scenarios of triboelectric yarn/fabrics for daily motion sensing.

Table 3.1 The price of the raw materials of the BYTENG.

Item	Price
PA conductive yarn (70D)	710 RMB/500g
PVDF	140 RMB/100g
DMF	390 HKD/4L
BYTENG	1.38 RMB/m

Note: D: Grams per 9,000 metres of yarn.

3.3.2 Working mechanism

Taking nylon fabric as external fabric, when the BYTENG is contact with nylon fabric, in the original stage, there is no electrical potential on the surface of the PVDF and nylon. Through pressing nylon fabric onto the BYTENG, the same amount of opposite charges are generated on the surfaces of the PVDF yarn and nylon fabric (Figure 3.3I). The BYTENG is negatively charged due to the ability of the PVDF to attract more electrons than the nylon. As they move away from each other, negative charges of the PVDF will induce positive charge of conductive yarn, yielding electrons that flow from

CHAPTER 3

the electrode to the ground (Figure 3.3II). When the nylon and the BYTENG are completely separated, a new electrical equilibrium is achieved. Therefore, the electrons stop transferring (Figure 3.3III). When the nylon approaches the BYTENG again, electrons flow inversely from the ground to electrode to realize the balanced state (Figure 3.3IV). As the nylon has intimate contact with the BYTENG, the charge neutralization occurs again. Thus, repeated contact-separation of the nylon and the BYTENG can continuously bring alternating electricity.

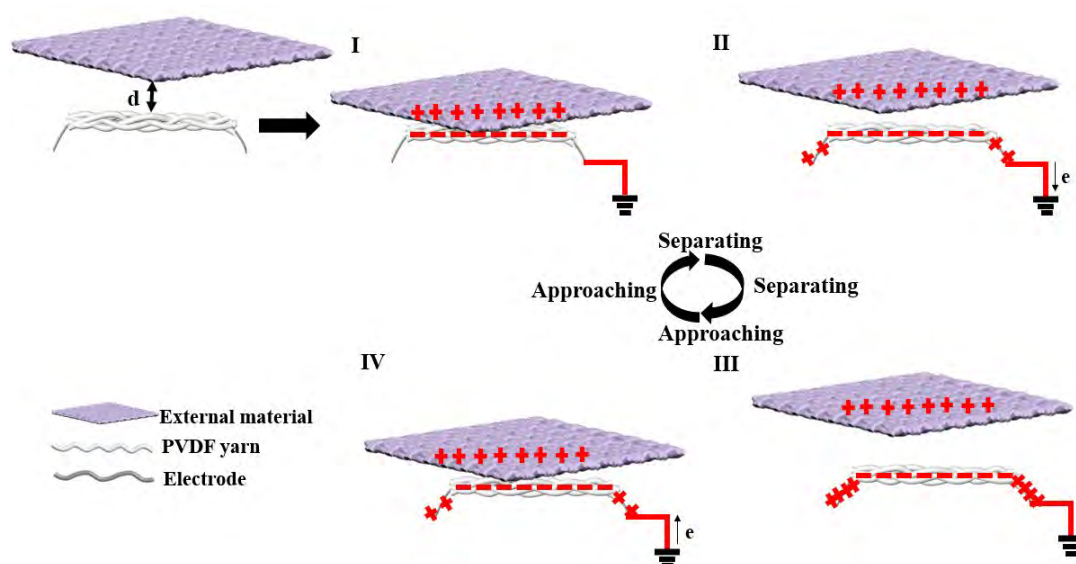


Figure 3.3 Schematic diagram of the BYTENG working mechanism.

3.3.3 Electrical output performance of the BYTENG

To study the electrical properties of the BYTENG under different forces, frequencies and friction materials, the BYTENG of 15 cm² was wound on cardboard, which was contacted and separated with nylon fabric. The mechanical force was about 130 N and the frequency was 3 Hz unless otherwise specified. As depicted in Figure 3.4a and b, when the force is increased from 10 N to 190 N, the output voltage and current go up from 10 V and 0.08 μ A to 35 V and 0.35 μ A. This increase is due to the fact that greater

CHAPTER 3

force results in a larger contact area, and subsequently, stronger triboelectric electrification. Meanwhile, good linear correlations can be observed in the linear fit of voltage and current with pressure from 7 kPa to 127 kPa (Figure 3.4c). The corresponding fitting equations are shown as follows:

$$V = 0.2195P + 7.936 \quad (1)$$

$$I = 0.0022P + 0.068 \quad (2)$$

where V , I and P represent the voltage, current and pressure, respectively. Consequently, it could be employed as a pressure or weight sensor in a wide pressure/weight range.

The frequency response of the BYTENG was further analyzed. As presented in Figure 3.4d, the output of voltage is approximately stable, showing that equal triboelectric charges are transferred by the BYTENG and the same static charges are created on both ends of the electrode. Therefore, the equal potential difference is maintained between the two electrodes. While the current exhibits an increasing trend from 0.08 to 0.27 μA as the increasing frequency from 1 to 3 Hz (Figure 3.4e). Based on the formula,

$$I = N \times e \times s \times v \quad (3)$$

where I is the current, N is the quantity of transferred electrons, e is electron charge, s is electron transport area, v is the rate of electron transport. When the frequency increases, electron transfer rate will also increase accordingly, which leads to the rising trend of current.

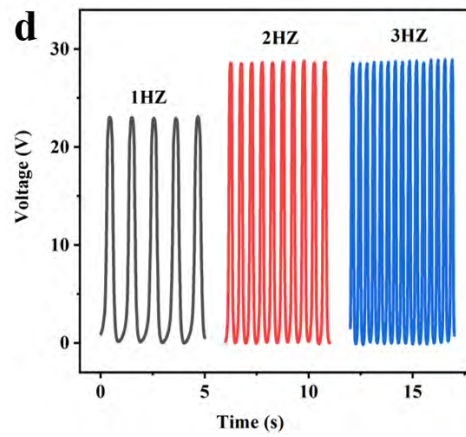
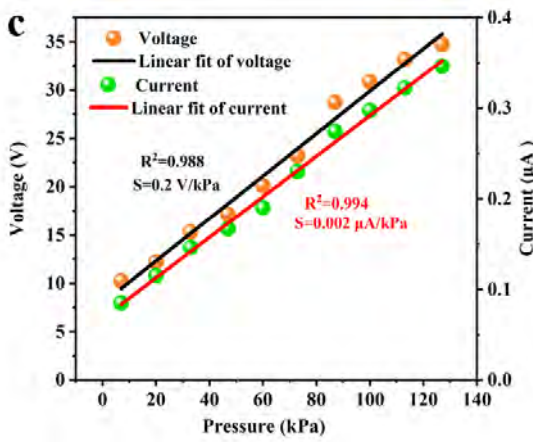
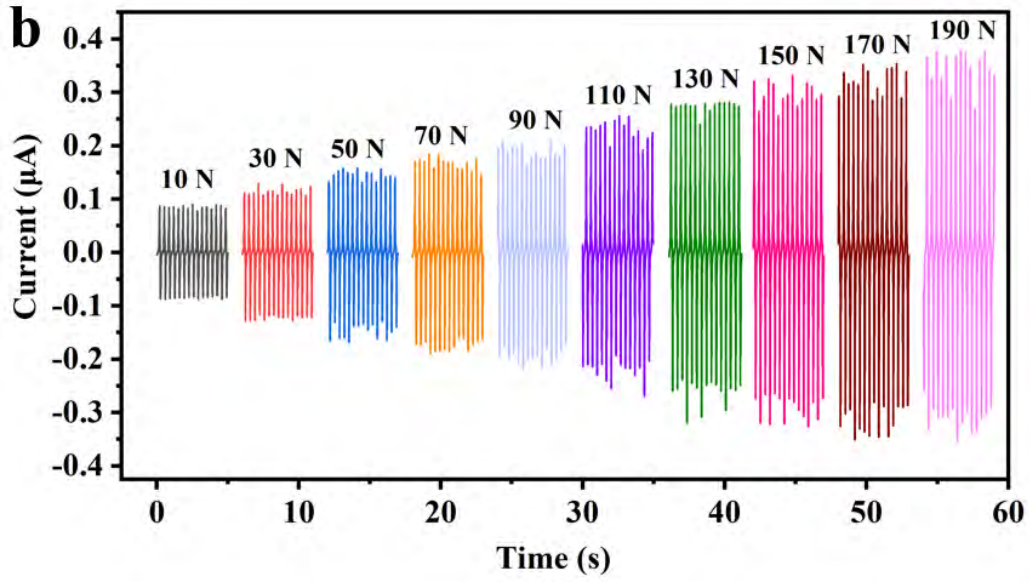
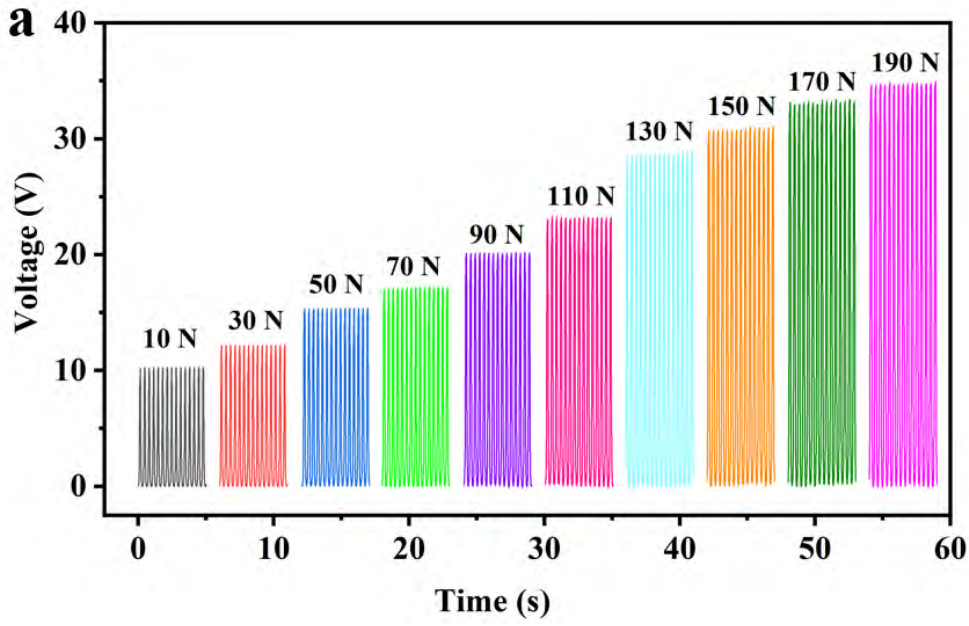
Since one of the principal goals of this study is to fabricate self-powered sensor suitable for various types of textile material, further studies were carried out on nylon fabric, cotton fabric, polyester fabric, acetate fabric, acrylic fabric, rubber film as shown in Figure 3.4f and g. All five common and available fabrics with various structures

CHAPTER 3

(knitted or woven) and compositions were used as the external contact material. The results of electrical output show that the six materials are found to be effective for generating triboelectric as contacting with the BYTENG. It suggests that our BYTENG can be applied to different versatile clothes. Meanwhile, compared with other materials, polyester fabric exhibits the largest output voltage (34 V) and current (0.3 μ A) under the impacting force of 130 N and frequency of 3 Hz. However, this trend is inconsistent with the triboelectric sequence, which may be attributed to different effective contact areas due to differences in fabric density, thickness and structure.

Figure 3.4h presents the output power of the BYTENG with various external resistances. The current and power density were measured by connecting with external resistances from 1 k Ω to 1 G Ω . It shows that output current decreases with the increase of load resistance. At a load resistance of 400 M Ω , the power density can reach 6.478 mW/ m². The electricity produced by the BYTENG could be further stored in commercial capacitors. The charging capacity of the BYTENG for various capacitors was studied (1, 3.3, 4.7, 10 and 22 μ F), as shown in Figure 3.4i. The charge rate decreases as the capacitance increases. With reference to standard AATCC 135, the machine washability of the BYTENG was evaluated. The BYTENG and 1.8 kg ballast together with sixty-six grams AATCC standard reference detergent were put into the laundering machine. The quick washing mode was performed. The entire washing procedure included soaking, rinsing and spinning stages, which was lasted for 40 min per wash cycle. After finishing the whole washing process, the BYTENG and ballast were taken out and dried by using an automatic tumble dryer. Then, the dried BYTENG was used for evaluation. As illustrated in Figure 3.4j, the BYTENG can maintain its output voltage after machine washing for three times.

CHAPTER 3



CHAPTER 3

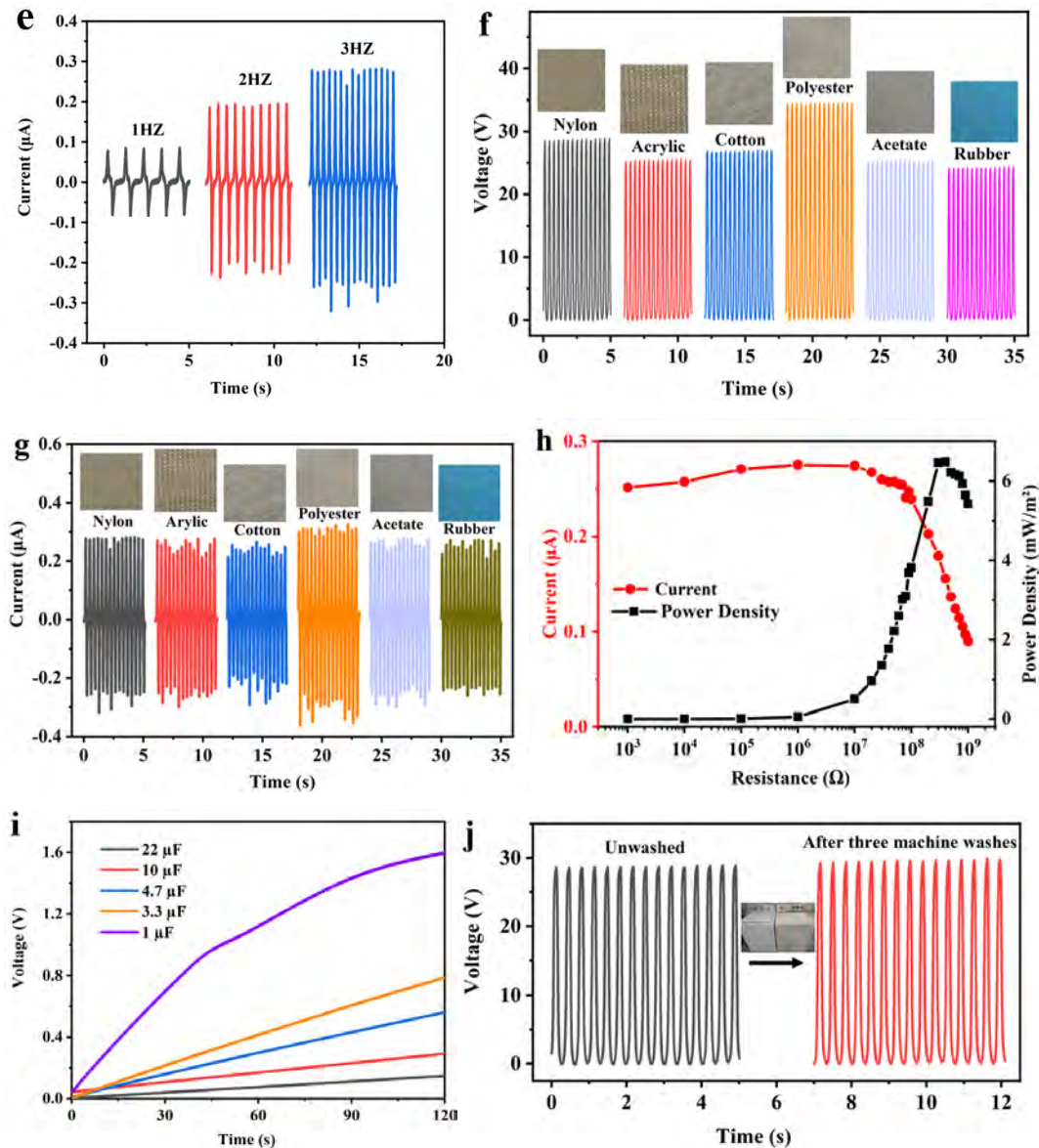
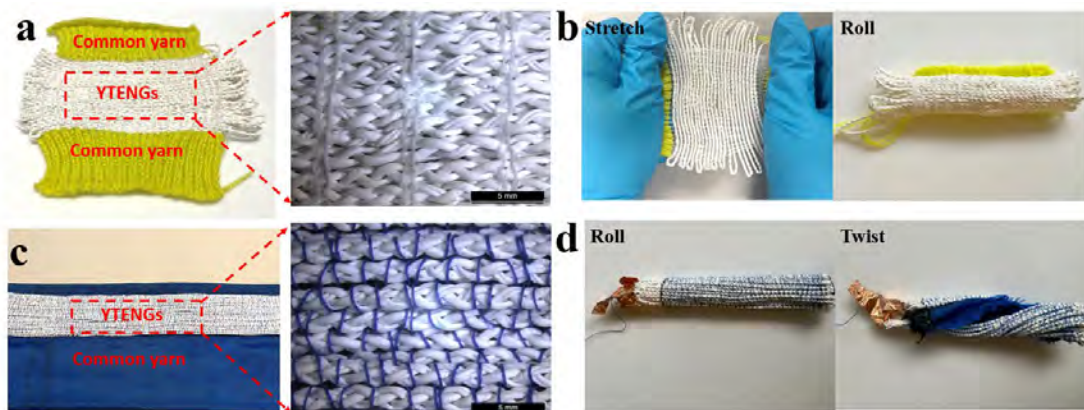


Figure 3.4 The electrical performance of the BYTENG. (a) Output voltage and (b) current of the BYTENG under various impacting forces. (c) The linear fit of the voltage and current of the BYTENG with increasing pressure from 7 kPa to 127 kPa. (d) Output voltage and (e) current of the BYTENG at various frequencies. (f) Output voltage and (g) current of the BYTENG with various friction materials. (h) The current and power density of the BYTENG at a series of external loads. (i) Measured voltages of different capacitors charged by the BYTENG. (j) Output voltage of the BYTENG before and after three machine washes.

3.3.4 Integration diversity of the BYTENG

CHAPTER 3

Compared with methods of directly attaching the BYTENG into commercial textiles, weaving and knitting of one-dimensional functional fibers have the merits of fabricating relatively diverse structures. Based on the obtained BYTENG, it could be further woven and knitted into the FTENGs. The photos of the as-prepared knitted FTENG and woven FTENG are demonstrated in Figure 3.5a-d. As shown in Figure 3.5a, the knitted FTENG was fabricated by the common yarns and BYTENGs. Meanwhile, the woven FTENG was produced by using cotton yarns as warp yarn, common yarns and the BYTENGs as weft yarns (Figure 3.5c). Figure 3.5b and d demonstrate the flexibility of two FTENGs, such as being twisted, rolled, and bended. Compared with the woven FTENG, the knitted FTENG exhibits better stretchability. The air permeability of the knitted FTENG and woven FTENG was tested by using a KES-F8-API air permeability tester. Different commercial fabrics with various materials, thickness, structures were also measured for comparison. In the test, the tested fabric was mounted a plate, and airflow was pumped through the fabric sample. The air resistance value ($\text{kPa}\cdot\text{s}/\text{m}$) was obtained by measuring and converting the pressure drop caused by the resistance of the fabric sample. As shown in Figure 3.5e, the woven FTENG and knitted FTENG exhibit very low air resistance values ($0.03 \text{ kPa}\cdot\text{s}/\text{m}$ and $0.06 \text{ kPa}\cdot\text{s}/\text{m}$) compared to those of commercial fabrics ($0.26\text{-}1.21 \text{ kPa}\cdot\text{s}/\text{m}$), demonstrating excellent breathability.



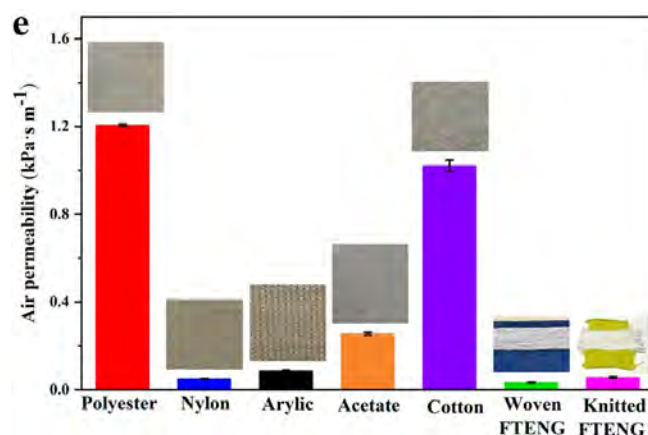


Figure 3.5 Digital photographs, flexibility, and air permeability of the BYTENG-based knitted and woven FTENGs. (a) Photographic images of the BYTENG-based knitted FTENG. (b) Knitted FTENG under stretched and rolled state. (c) Digital photographs of the BYTENG-based woven FTENG. (d) Woven FTENG under rolled and twisted state. (e) Air permeability of knitted FTENG, woven FTENG and various commercial fabrics.

3.3.5 Application as self-powered wearable sensors

Real-time detection and monitoring of the human motion is an upcoming research area. Textile-based wearable sensors have received particular attention recently because they can be woven into clothing to monitor movement and physiological signals in real time. With the merits of good electrical output and softness, the BYTENG can be used for harvesting mechanical energy as well as self-powered pressing sensor in the fields of sports, such as smart household portable pedal puller for multifunctional exercise. As shown in Figure 3.6a, the BYTENG can be wrapped around pedals for exercise frequency statistical analysis and real-time exercise detection. Figure 3.6b illustrates the output current of the BYTENG when the pedal puller is stretched by hand and foot, respectively. Every stretching of the pedal puller by hand leads to a friction between the foot and the BYTENG, therefore an electrical signal is generated. The magnitude of the stretching amplitude by hand has an effect on the contact force between the foot

CHAPTER 3

and the BYTENG, which will further influence the output current. Also, the difference of the hand stretching speed will lead to the different output current curves of the BYTENG as shown by the grey line (time interval of 2.833s) and red line (time interval of 1.696 s) in Figure 3.6b. Similarly, when the pedal puller is stretched by foot, the output current of the BYTENG depends on the contact force between the foot and the BYTENG. As the force exerted by the foot decreases, the output also decreases, as demonstrated by the blue line and green line in the Figure 3.6b. Meanwhile, the number of stretching can be obtained by calculating the electrical signal peaks, since every exercise motion produces an electrical signal. In addition, to demonstrate diverse applicability of the BYTENG, the BYTENG was wrapped to a boxing reaction ball, as shown in Figure 3.6c. When a person uses boxing gloves to hit the BYTENG of the boxing reaction ball, the BYTENG can generate current output due to the contact-separation between the box glove and BYTENG. The results show that the BYTENG can produce different output current curves when the reaction ball is hit with medium (grey line), high (red line) and low speeds (blue line) respectively. Therefore, it can be observed that compared with bulky and rigid TENG sensors, the BYTENG as a self-powered sensor to detect exercise has natural advantages, such as light weight, softness, low cost and strong adaptability to different home sports products.

A sedentary lifestyle is prevalent around the world, which brings some health risks and increases the risk of various diseases, such as cardiovascular disease, diabetes, obesity etc. Portable and convenient woven and knitted FTENGs with self-powered function could be applied into seat cushions for tracking sitting posture. When people are sitting for a long time, such as sitting for a long time at work or playing games, this sensor will sense and issue a warning. As shown in Figure 3.6d, when the monitored person stands up from the chair, a positive current is generated because of the separation of the cloth

CHAPTER 3

and the FTENG. Then, as the person sits down, a negative current signal is detected. Sitting times of ~6 and ~13 s are observed by the interval between two opposite current peaks generated by knitted FTENG, respectively. Similarly, for the woven FTENG, sitting times of ~9 and ~14 s are observed. Besides, the application of knitted and woven FTENGs on the backrest is demonstrated, as indicated in the Figure 3.6e. It can be seen clearly that a positive current signal is produced when a person moves away from the backrest. On the contrary, as the person leans back, a negative current is generated. Correspondingly, the backrest time (8s, 7s, 11s) can be obtained by the knitted FTENG. With regards to woven FTENG, the backrest time of 7s, 7s, 15s is measured. Consequently, the fabricated knitted FTENG and woven FTENG could be employed for detecting sitting state according to the variation of the output current signal. Further, with the advantages of its soft, comfortable and washable as well as easy-to-trigger properties, the knitted and woven FTENGs can also be applied into carpet (Figure 3.6f). For demonstration, they were placed on the carpet for human motion detection. When a person steps on the carpet, the sock contacts and separates from the FTENG to generate an electrical output signal. In the two states of walking and jumping, the knitted TENG can reach peak-to-peak currents of ~0.06 μA and ~0.18 μA , respectively. At the same time, the woven TENG can obtain peak-to-peak currents of ~0.1 μA and ~0.63 μA , respectively. The above results demonstrate that the FTENGs woven/knitted by the BYTENGs can be used as sensing fabrics for real-time motion monitoring.

CHAPTER 3

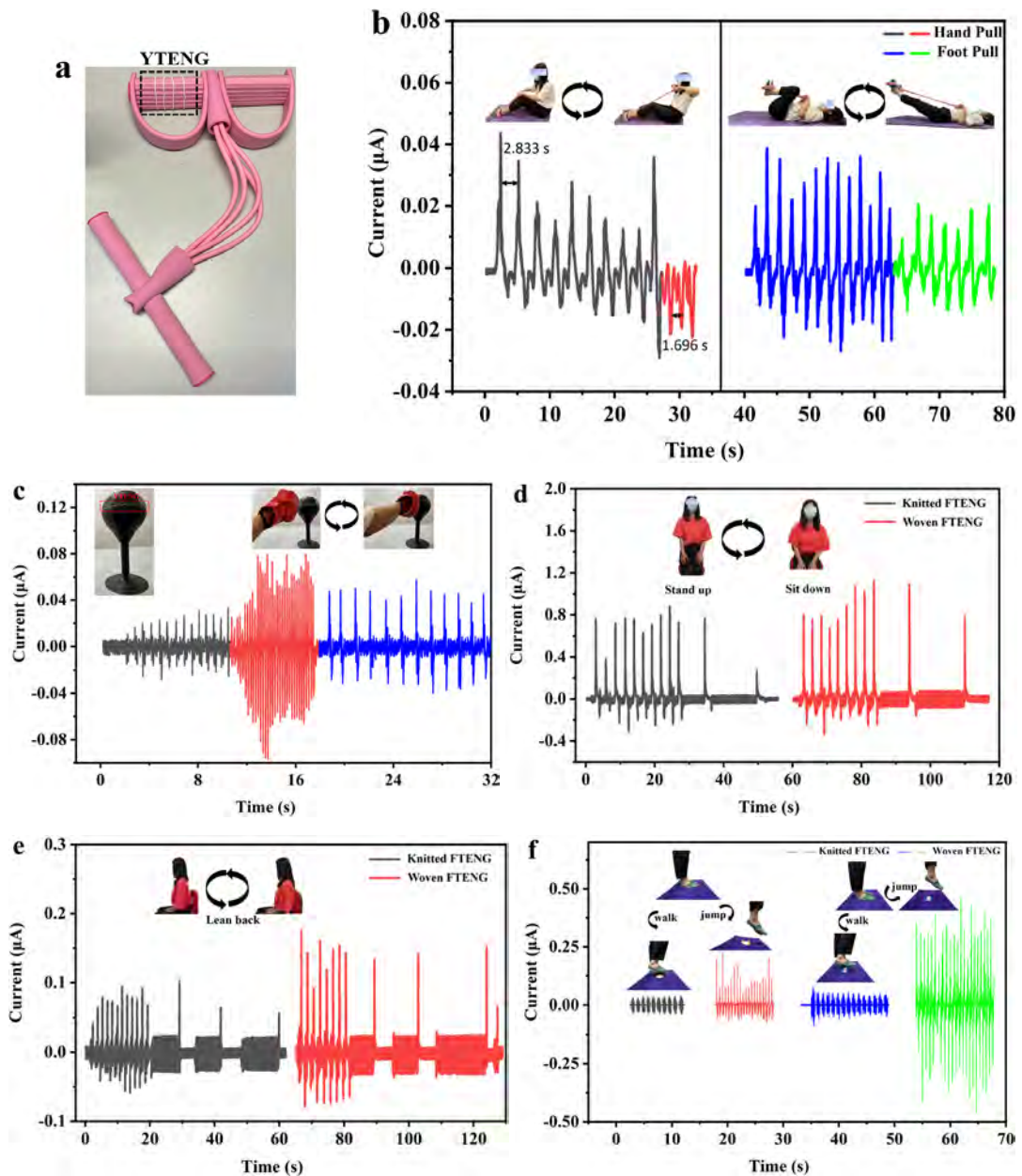


Figure 3.6 Application of the BYTENG and FTENGs. (a) The photograph of the BYTENG applied into household portable pedal puller. (b) Output current of the BYTENG during the hand pull and foot pull. (c) Output current of the BYTENG during hitting boxing reaction ball. Output current of knitted FTENG and woven FTENG applied into (d) seat cushion, (e) backrest and (f) carpet.

3.4 Conclusion

In summary, we developed a 1D braided core-shell structured single-electrode

CHAPTER 3

triboelectric yarn with PVDF triboelectric material and PA conductive yarn by using simple, continuous wet spinning and braiding technologies. The obtained BYTENG exhibits good flexibility, electrical output and machine washability. Owing to the good adaptability and pressure sensitivity of the BYTENG, it can be employed as self-powered multifunctional sensor for real-time exercise detection, such as household portable pedal puller, boxing reaction ball and other sports products. As a demonstration of good integration capability, the BYTENG can be further fabricated into knitted FTENG and woven FTENG through the different weaving methods of textiles. The as-prepared FTENGs have good softness and breathability, which can be applied into seat cushions, backrest and carpet for human motion monitoring. Furthermore, the fabrication process (from wet spinning, braiding to knitting and weaving) of the FTENG presented in this work possesses promising potential in highly integrated and continuous manufacturing triboelectric yarns and fabrics, which will advance the field of smart textiles.

CHAPTER 3

References

- (1) Xie, L.; Chen, X.; Wen, Z.; Yang, Y.; Shi, J.; Chen, C.; Peng, M.; Liu, Y.; Sun, X. Spiral Steel Wire Based Fiber-Shaped Stretchable and Tailorable Triboelectric Nanogenerator for Wearable Power Source and Active Gesture Sensor. *Nano-Micro Lett.* **2019**, *11*, 1-10.
- (2) Park, J.; Choi, A. Y.; Lee, C. J.; Kim, D.; Kim, Y. T. Highly stretchable fiber-based single-electrode triboelectric nanogenerator for wearable devices. *RSC Adv.* **2017**, *7*, 54829-54834.
- (3) Ning, C.; Dong, K.; Cheng, R.; Yi, J.; Ye, C.; Peng, X.; Sheng, F.; Jiang, Y.; Wang, Z. L. Flexible and Stretchable Fiber-Shaped Triboelectric Nanogenerators for Biomechanical Monitoring and Human-Interactive Sensing. *Adv. Funct. Mater.* **2020**, *31*, 2006679.
- (4) Lai, Y. C.; Lu, H. W.; Wu, H. M.; Zhang, D.; Yang, J.; Ma, J.; Shamsi, M.; Vallem, V.; Dickey, M. D. Elastic Multifunctional Liquid-Metal Fibers for Harvesting Mechanical and Electromagnetic Energy and as Self-Powered Sensors. *Adv. Energy Mater.* **2021**, *11*, 2100411.
- (5) Cheng, Y.; Lu, X.; Chan, K. H.; Wang, R.; Cao, Z.; Sun, J.; Ho, G. W. A stretchable fiber nanogenerator for versatile mechanical energy harvesting and self-powered full-range personal healthcare monitoring. *Nano Energy* **2017**, *41*, 511-518.
- (6) Gong, W.; Hou, C.; Guo, Y.; Zhou, J.; Mu, J.; Li, Y.; Zhang, Q.; Wang, H. A wearable, fibroid, self-powered active kinematic sensor based on stretchable sheath-core structural triboelectric fibers. *Nano Energy* **2017**, *39*, 673-683.
- (7) Chen, J.; Guo, H.; Pu, X.; Wang, X.; Xi, Y.; Hu, C. Traditional weaving craft for one-piece self-charging power textile for wearable electronics. *Nano Energy* **2018**, *50*, 536-543.

CHAPTER 3

- (8) Cheng, R.; Dong, K.; Liu, L.; Ning, C.; Chen, P.; Peng, X.; Liu, D.; Wang, Z. L. Flame-Retardant Textile-Based Triboelectric Nanogenerators for Fire Protection Applications. *ACS Nano* **2020**, *14*, 15853-15863.
- (9) Pu, X.; Song, W.; Liu, M.; Sun, C.; Du, C.; Jiang, C.; Huang, X.; Zou, D.; Hu, W.; Wang, Z. L. Wearable Power-Textiles by Integrating Fabric Triboelectric Nanogenerators and Fiber-Shaped Dye-Sensitized Solar Cells. *Adv. Energy Mater.* **2016**, *6*, 1601048.
- (10) Shi, Y.; Wei, X.; Wang, K.; He, D.; Yuan, Z.; Xu, J.; Wu, Z.; Wang, Z. L. Integrated All-Fiber Electronic Skin toward Self-Powered Sensing Sports Systems. *ACS Appl. Mater. Interfaces* **2021**, *13*, 50329-50337.
- (11) Gong, W.; Wang, X.; Yang, W.; Zhou, J.; Han, X.; Dickey, M. D.; Su, Y.; Hou, C.; Li, Y.; Zhang, Q.; Wang, H. Wicking-Polarization-Induced Water Cluster Size Effect on Triboelectric Evaporation Textiles. *Adv. Mater.* **2021**, *33*, 2007352.
- (12) Peng, X.; Dong, K.; Ye, C.; Jiang, Y.; Zhai, S.; Cheng, R.; Liu, D.; Gao, X.; Wang, J.; Wang, Z. L. A Breathable, Biodegradable, Antibacterial, and Self-Powered Electronic Skin Based on All Nanofiber Triboelectric Nanogenerators. *Sci. Adv.* **2020**, *6*, eaba9624.
- (13) Shin, Y.-E.; Lee, J.-E.; Park, Y.; Hwang, S.-H.; Chae, H. G.; Ko, H. Sewing machine stitching of polyvinylidene fluoride fibers: programmable textile patterns for wearable triboelectric sensors. *J. Mater. Chem. A* **2018**, *6*, 22879-22888.
- (14) Lee, J.-E.; Shin, Y.-E.; Lee, G.-H.; Kim, J.; Ko, H.; Chae, H. G. Polyvinylidene fluoride (PVDF)/cellulose nanocrystal (CNC) nanocomposite fiber and triboelectric textile sensors. *Composites, Part B* **2021**, *223*, 109098.
- (15) Mokhtari, F.; Spinks, G. M.; Sayyar, S.; Cheng, Z.; Ruhparwar, A.; Foroughi, J. Highly Stretchable Self-Powered Wearable Electrical Energy Generator and Sensors. *Adv. Mater. Technol.* **2020**, *6*, 2000841.

CHAPTER 3

- (16) Li, Z.; Zhu, M.; Shen, J.; Qiu, Q.; Yu, J.; Ding, B. All-Fiber Structured Electronic Skin with High Elasticity and Breathability. *Adv. Funct. Mater.* **2019**, *30*, 1908411.
- (17) Sun, N.; Wang, G.-G.; Zhao, H.-X.; Cai, Y.-W.; Li, J.-Z.; Li, G.-Z.; Zhang, X.-N.; Wang, B.-L.; Han, J.-C.; Wang, Y.; Yang, Y. Waterproof, breathable and washable triboelectric nanogenerator based on electrospun nanofiber films for wearable electronics. *Nano Energy* **2021**, *90*, 106639.
- (18) Yin, Y.; Wang, J.; Zhao, S.; Fan, W.; Zhang, X.; Zhang, C.; Xing, Y.; Li, C. Stretchable and Tailorable Triboelectric Nanogenerator Constructed by Nanofibrous Membrane for Energy Harvesting and Self-Powered Biomechanical Monitoring. *Adv. Mater. Technol.* **2018**, *3*, 1700370.
- (19) Ma, L.; Wu, R.; Liu, S.; Patil, A.; Gong, H.; Yi, J.; Sheng, F.; Zhang, Y.; Wang, J.; Wang, J.; Guo, W.; Wang, Z. L. A Machine-Fabricated 3D Honeycomb-Structured Flame-Retardant Triboelectric Fabric for Fire Escape and Rescue. *Adv. Mater.* **2020**, *32*, 2003897.
- (20) Ma, L.; Wu, R.; Patil, A.; Yi, J.; Liu, D.; Fan, X.; Sheng, F.; Zhang, Y.; Liu, S.; Shen, S.; Wang, J.; Wang, Z. L. Acid and Alkali-Resistant Textile Triboelectric Nanogenerator as a Smart Protective Suit for Liquid Energy Harvesting and Self-Powered Monitoring in High-Risk Environments. *Adv. Funct. Mater.* **2021**, *31*, 2102963.
- (21) Ma, L.; Zhou, M.; Wu, R.; Patil, A.; Gong, H.; Zhu, S.; Wang, T.; Zhang, Y.; Shen, S.; Dong, K.; Yang, L.; Wang, J.; Guo, W.; Wang, Z. L. Continuous and Scalable Manufacture of Hybridized Nano-Micro Triboelectric Yarns for Energy Harvesting and Signal Sensing. *ACS Nano* **2020**, *14*, 4716-4726.
- (22) Ye, C.; Yang, S.; Ren, J.; Dong, S.; Cao, L.; Pei, Y.; Ling, S. Electroassisted Core-Spun Triboelectric Nanogenerator Fabrics for IntelliSense and Artificial Intelligence Perception. *ACS Nano* **2022**, *16*, 4415-4425.

CHAPTER 3

(23) Zhang, D.; Yang, W.; Gong, W.; Ma, W.; Hou, C.; Li, Y.; Zhang, Q.; Wang, H. Abrasion Resistant/Waterproof Stretchable Triboelectric Yarns Based on Fermat Spirals. *Adv. Mater.* **2021**, *33*, 2100782.

(24) Busolo, T.; Szewczyk, P. K.; Nair, M.; Stachewicz, U.; Kar-Narayan, S. Triboelectric Yarns with Electrospun Functional Polymer Coatings for Highly Durable and Washable Smart Textile Applications. *ACS Appl. Mater. Interfaces* **2021**, *13*, 16876-16886.

Chapter 4: One-Dimensional Core-Spun Yarn Structured Triboelectric Nanogenerator Based on Chitosan/Tencel Fibers for Improving the Scalability and Functionality

4.1 Introduction

With the growing global energy consumption and environmental problems, sustainable energy harvesting technologies have received extensive attention. Due to the advantages of high output performance and diverse material selection as well as easy fabrication, triboelectric nanogenerator (TENG) as biomechanical energy harvester and self-powered sensor have been widely investigated. TENG is based on the triboelectrification effect of materials with different electron affinities and electrostatic induction. Consequently, the tribomaterials selection and structure design of TENGs are crucial. However, a majority of tribomaterials utilized in TENGs are synthetic polymers or metallic materials, which are generally non-renewable and non-biodegradable, thus limiting the potential development of cost-effective and eco-friendly TENGs and causing severe electronic waste.¹ Despite some studies have realized the fabrication of biodegradable and environmentally friendly TENG by using suitable natural materials, such as wood,^{2,3} paper,^{4,5} feather,⁶ etc., the preparation approaches are relatively complicated, time-consuming and expensive. In addition, the fabricated eco-friendly TENGs are usually planar structured, which greatly restrict the wearability, comfort and compatibility with textile technology. In comparison with other forms of wearable TENGs, the advantage of fiber/yarn based TENG is its small size, which can be arbitrarily incorporated into textiles. Therefore, an eco-friendly fiber/yarn-based TENG is highly desirable.

CHAPTER 4

Nonetheless, the development of fiber/yarn based TENG still faces some big challenges. First, the large-scale production technology of fiber/yarn based TENGs is not yet mature because the widely used processing methods are restricted by complicated process, low speed and limited fiber length as well as small yield.⁷ Existing fiber/yarn based TENGs usually have large diameters and uneven fineness, which greatly affect the weavability.⁸⁻¹⁰ Besides, the softness is sacrificed in some fiber/yarn based TENGs due to the utilization of rigid metal strands, which has great impact on the mechanical and tactile properties.¹¹ It directly influences the durability, wearability, comfort of the clothing. Apart from these issues, many t-TENGs improve the contact area by introducing nanomaterials, which are easily damaged after long-term wearing and washing, leading to unstable output. In this regard, there is still a great need to fabricate eco-friendly fiber/yarn based TENG with small diameter, good mechanical strength, excellent wearability using green materials by simple, cost-effective and sustainable manufacturing methods.

In this chapter, we have designed and developed an extremely durable and eco-friendly single-electrode triboelectric yarn (CYTENG) as a composite yarn which was made of polyamide (PA) conductive yarn (core yarn) and Tencel-chitosan blended yarn (wrapping yarn) by a scalable fancy spinning twister technology. Owing to small diameter, large scalability and high production, the weaveability of the CYTENG has been significantly improved. Under the working principle of single-electrode mode, a voltage with value of 14.2 V and a current of 0.8 μ A can be obtained from the CYTENG with the length of 45 cm under impacting frequency of 3 HZ and force of 100 N. Also, the as-prepared CYTENG possesses high sensitivity to impact force, which demonstrates their potential application as self-powered wearable sensor to monitor human motion.

CHAPTER 4

4.2 Experimental Section

4.2.1 Materials

Tencel fiber and chitosan fiber with a length of about 38 mm and a fineness of about 1.5 dtex were bought from Tianjin Zhongsheng Biological Engineering Co. Ltd., China. The degree of deacetylation of chitosan fiber is 88%. Ag-plated nylon6 multifilament (yarn number is 70D) was purchased from Suzhou TEk Silver Fiber Technology Co. Ltd., China.

4.2.2 Fabrication of the CYTENG

First, the 24 Ne Tencel/chitosan (85/15) blended yarns were developed by opening and blowing, carding, drawing, combing, roving, spinning, and winding. Second, the blended yarns obtained were transferred to the two hollow bobbins from the large bobbin. Third, the core yarn and two hollow bobbins were placed in corresponding positions of the machine (SFM32-04, Multifunctional fancy twisting machine, Kunshan Shunfeng Textile Co., Ltd.). The CYTENG was continuously fabricated after setting reasonable parameters.

4.2.3 Characterization and evaluation

The surface morphologies of the conductive yarn, Tencel/chitosan blended yarn and CYTENG were characterized by Leica M165C (DFC 290HD, Leica Microsystems Ltd.). The yarn blending ratio test was conducted according to GB/T 35257-2017 standard. The molecular information of chitosan fiber, Tencel fiber and Tencel/chitosan

CHAPTER 4

blended yarn was investigated by Fourier-transform infrared spectrometer (FTIR, PerkinElmer, USA). The tensile tests of conductive yarn, Tencel/chitosan blended yarn and CYTENG were implemented with an INSTRON tensile tester (INSTRON 5566) equipped with a 10 N load cell according to ASTM D2256. The gauge length and tensile rate used were 25 cm and 300 mm/min, respectively. An electrometer (Keithley 6514) and oscilloscope (DS1000Z) were used to measure the electrical output of the CYTENG. The compressing motions were applied via a Keyboard Life Tester (ZX-A03).

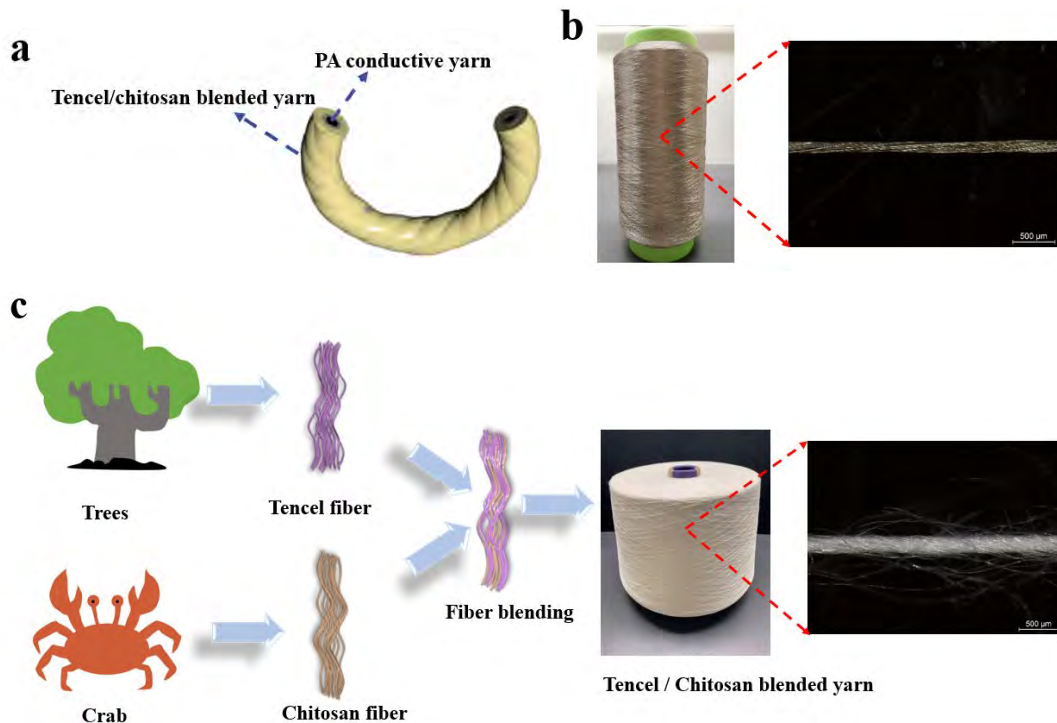
4.3 Results and Discussion

4.3.1 Design and fabrication of the CYTENG

A new-type CYTENG was designed, as schematically illustrated in Figure 4.1a. This CYTENG is characterized by a core-shell structure, where the polyamide (PA) yarn coated with Ag was selected as the core yarn and conductive electrode, and a Tencel/chitosan blended yarn was chosen as the wrapping yarn. The outer dielectric layer tightly twines around the core conductive fiber as a building block. Figure 4.1b shows the morphologies of the conductive yarn. The PA conductive yarn showed a very low resistance of 12 Ω /cm, which demonstrated good electrical conductivity. As presented in Figure 4.1c, Tencel fiber as an environmentally friendly green fiber is obtained from sustainably grown wood. In the production process of Tencel fiber, no derivatives and chemical action will be generated, which reduces the impact of production on the environment. According to the triboelectric series, Tencel, which belongs to cellulose, sits at the slightly positive position. The previous study indicated the lyocell fabric exhibited higher values of positive charge density compared with the

CHAPTER 4

tribo-charge densities of fabrics made from natural fibers like cotton, ramie and wool.¹² Therefore, the Tencel fiber adopted in the CYTENG can guarantee its comfortability and good electrical output. Chitosan is a widely used biopolymer material which can be extracted from the exoskeleton of crustaceans in nature, namely crabs and shrimps, indicated in Figure 4.1c. Due to its non-toxicity, biodegradability and non-allergenicity, it has received more and more attention. The excellent antibacterial effect can be achieved by blending a small proportion of chitosan fiber into Tencel fiber. The material also opens up new material engineering directions for the development of TENG using eco-friendly and recyclable materials. To achieve the above structure, the fabrication process selected should be properly designed. Figure 4.1d schematically depicts the details of the fabrication process. A fancy yarn machine was employed, as displayed in Figure 4.1e.



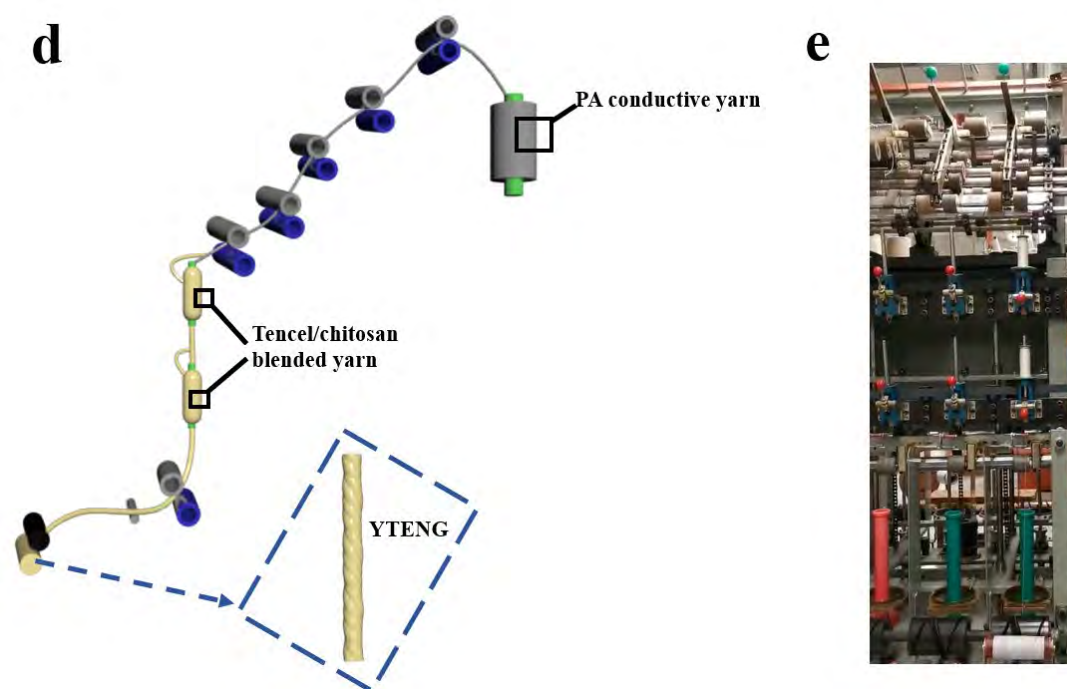


Figure 4.1 (a) Schematic illustration of structure of the CYTENG. (b) Images showing the morphologies of conductive yarn. (c) Images showing the morphologies of Tencel/chitosan yarn. (d) Schematic illustration of the CYTENG fabrication processing. (e) Photograph of fancy yarn machine.

4.3.2 Morphology, structure and mechanical property of the CYTENG

The chitosan in the blended yarn can also be verified by the Fourier transform infrared spectroscopy (FTIR) result. As shown in Figure 4.2, it can be seen that the absorption peaks of chitosan include 1646 cm^{-1} (C=O in amide groups which is amide I band) and 1593 cm^{-1} (NH_2 bending vibration in amino group). The results support the presence of chitosan fibers in the blended yarn.^{13,14} In order to examine the actual blending ratio, the blending ratio test was conducted according to GB/T 35257-2017 standard. The result shows that the actual blended ratio (84.2/15.8) of the Tencel/Chitosan yarn is close to the design ratio (85/15). The use of green fiber as the outer shell fiber is conducive to improving the comfort of the human body. Because there is no chemical fiber that directly contacts the skin causing discomfort.

CHAPTER 4

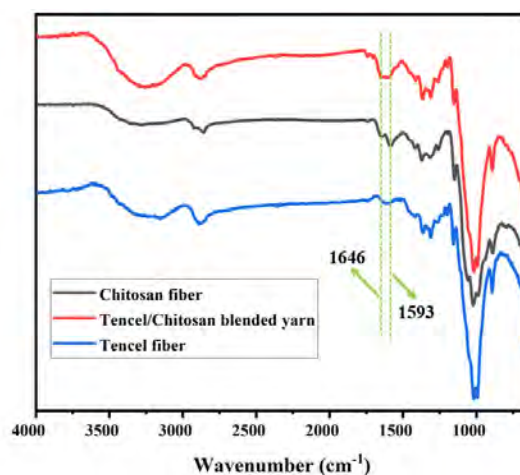


Figure 4.2 FTIR spectra of chitosan fiber, Tencel fiber and Tencel/Chitosan blended yarn.

The photograph of as-fabricated CYTENG with unlimited length and good flexibility is shown in Figure 4.3a, which can meet the requirements of continuous yarn production. The image (Figure 4.3b) presents that the CYTENG has a small diameter, which is comparable to the yarns commonly employed on industrial looms. The weight per unit length of the CYTENG is only 0.08 g/m. Figure 4.3c further presents the mechanical properties of conductive yarn, Tencel/chitosan blended yarn and as-made CYTENG. The CYTENG exhibits tensile strength of 10.98 cN/tex at a strain of 25.4%, showing the excellent mechanical properties. It guarantees that CYTENG can endure various, complex, and durable deformations. The inner conductive yarn along with outer Tencel/chitosan yarn constructed the CYTENG with a core-shell structure as confirmed by Figure 4.3d and e. Tencel/chitosan blended yarns are tightly twined around conductive yarns, which is further observed in Figure 4.3f. The resistance variation of the CYTENG under bending and straightening is presented in Figure 4.3g. As observed, the CYTENG can maintain its conductivity in the bending and straightening state. The price of raw material is illustrated in Table 4.1. For 100 meters of the CYTENG, the material cost is only RMB 2.31. The production cost is greatly reduced which

CHAPTER 4

contributes to the widespread application of t-TENG. High flexibility, small diameter and light weight, great scalability as well as productivity promote the excellent weaveability of the CYTENG, which is compatible with existing textile technology.

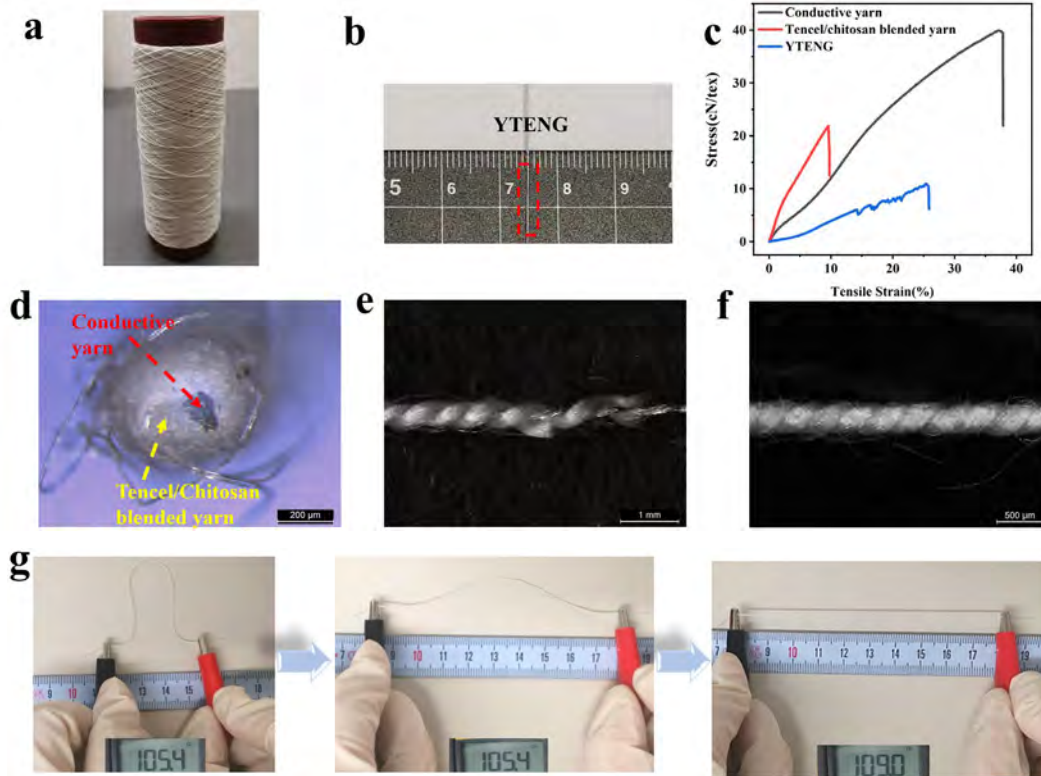


Figure 4.3 (a) Photograph of the fabricated CYTENG. (b) Visual fineness of the CYTENG. (c) Tensile stress versus strain curve of the conductive yarn, Tencel/chitosan blended yarn and the CYTENG. (d) Cross section of the CYTENG. (e-f) Optical microscope images of the CYTENG. (g) Resistance variation of the CYTENG under bending and straightening.

Table 4.1 The price of raw materials.

Item	Price
PA conductive yarn (70D)	1.11 RMB/100m
Chitosan/Tencel blended yarn (25tex)	0.6 RMB/100m
CYTENG	2.31 RMB/100m

CHAPTER 4

4.3.3 Working mechanism

Taking Polydimethylsiloxane (PDMS) as external contact material, the mechanism of the CYTENG working in the single electrode mode is schematically illustrated in Figure 4.4. When the Tencel/chitosan blended yarn is contacted with PDMS under an external mechanical force, contact electrification occurs at the material interface owing to their different electron affinities (Figure 4.4I). Because the surface electron affinity of the Tencel/chitosan blended yarn is lower than PDMS, negative triboelectric charges will be transferred from the Tencel/chitosan blended yarn to PDMS. Once relative separation occurs, the positive charges from the exterior of the Tencel/chitosan blended yarn induce negative charges, leading to the flow of instantaneous electrons from ground to the electrode (Figure 4.4II). When the external material and the CYTENG are completely separated, the electron in the CYTENG is in a balanced state, so that there is no electrical signal output (Figure 4.4III). When the PDMS approaches the CYTENG again, the opposite electron flow occurs from the electrode to ground till PDMS has intimate contact with the CYTENG again (Figure 4.4IV). Therefore, the generator continuously produces alternating output through the entire cycle of the contact and separation process.

CHAPTER 4

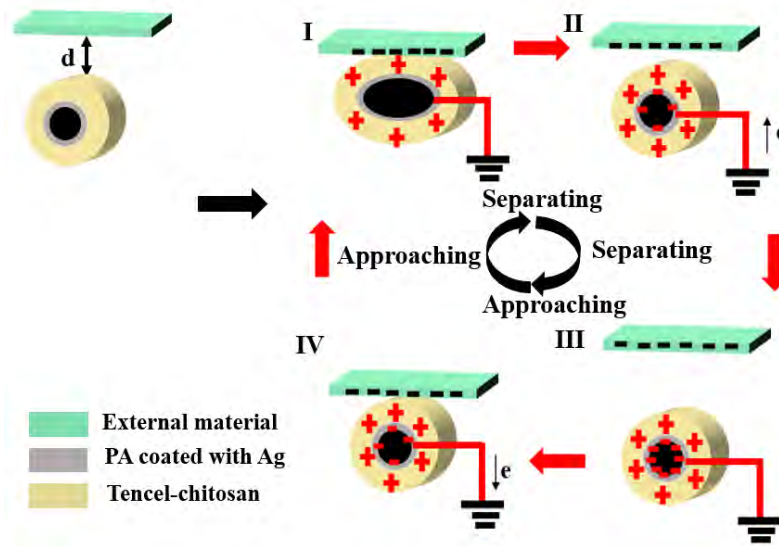


Figure 4.4 Working principle of the CYTENG, contacting (I), separating (II), separated (III) and approaching (IV).

4.3.4 Electrical output performance of the CYTENG

In practical life, various impact forces are often applied to human body. Therefore, it is necessary to investigate the effects of forces on the output performance of the CYTENG. To study the relationship between electrical output and impact force, the output voltage and current of the CYTENG were measured with different vertical contact forces. Figure 4.5a and b show the output voltage and current of the CYTENG (45 cm) with various impacting forces at the fixed mechanical impacting frequency of 3 Hz. The results present that the output voltage and current of the CYTENG continue to rise under increased applied force from 0 to 20 N. Besides, with the rise of applied force from 20 N to 100 N, the increasing of the output voltage and current can still be observed, but the rise rate is slower than that from 0 to 20 N, which indicates that the CYTENG has different response behaviors towards various forces. Values of 14.2 V and 0.8 μ A are acquired at a force of 100 N. The enhancement of the output voltage and

CHAPTER 4

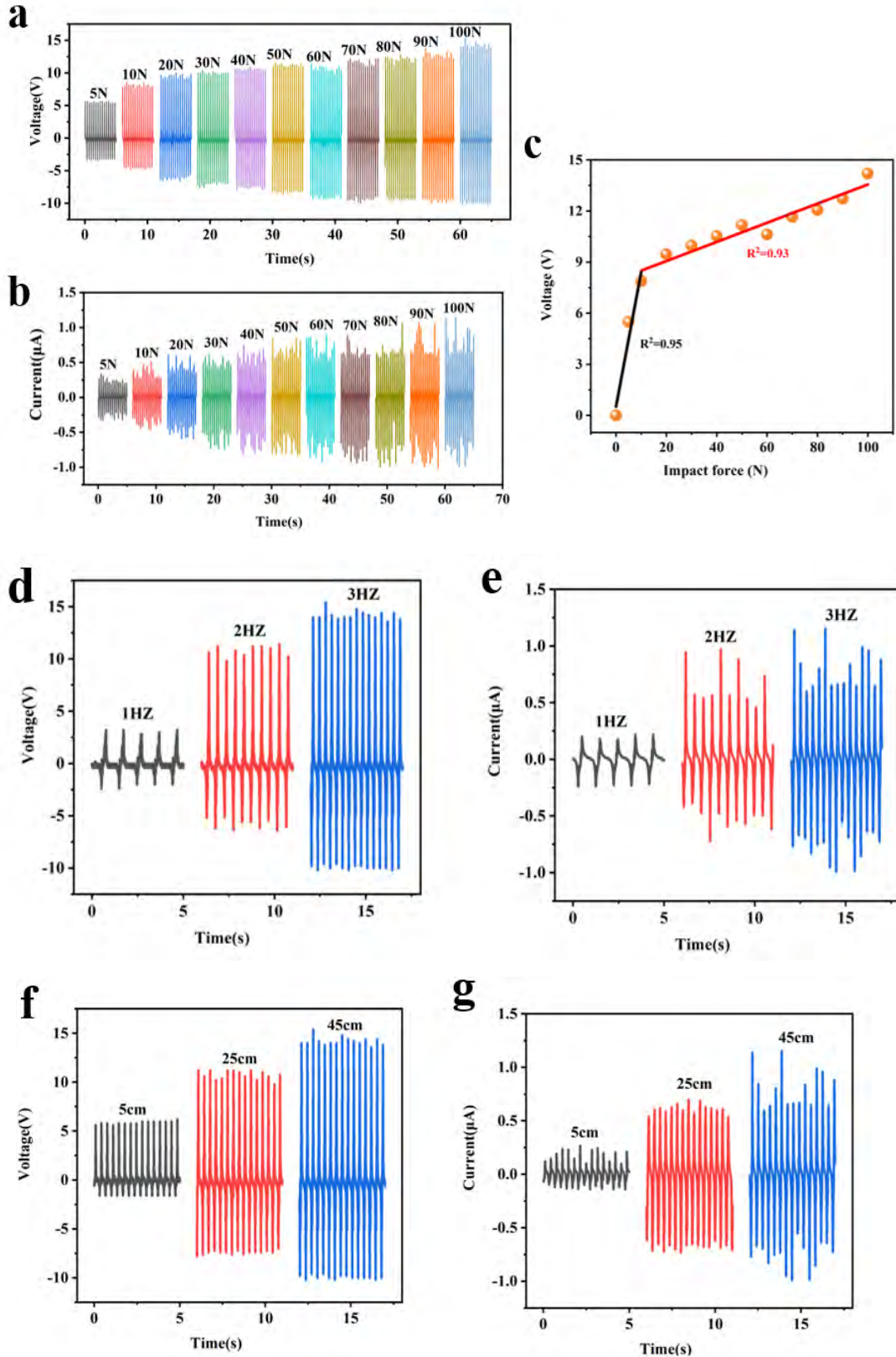
current of the CYTENG can be explained by the more intimate contact between PDMS film and the CYTENG. However, when the applied force is greater than 20 N, the output voltage and current of the CYTENG basically increase slightly. This might be due to the fact that the PDMS film and CYTENG are in full contact, resulting in a slight increase in the output voltage and current. In order to accurately explore the performance of the CYTENG as a self-powered sensor, the voltage towards different impacting forces is plotted as shown in Figure 4.5c. Distinct stages simulations are seen clearly via the linear simulations. In terms of voltage output towards various impact forces, linearities of 0.95 and 0.93 are displayed in 0 N-20 N (black fitting line) and 20 N-100 N (red fitting line), respectively. The fabricated CYTENG shows the sensitivity of $0.47 \text{ V}\cdot\text{N}^{-1}$ and $0.06 \text{ V}\cdot\text{N}^{-1}$ in a wide pressure range of 0 to 20 N and 20 to 100 N, respectively.

In real life, the frequency of the impacting force applied to the TENG will vary depending on the environment. Therefore, the output performance of the CYTENG (45 cm) at different frequencies under a fixed force of 100 N is discussed. As shown in Figure 4.5d and e, the output voltage and current of the CYTENG increase with the increasing of the impact frequency from 1 to 3 Hz, and the output voltage ($\sim 14.2 \text{ V}$) and current ($\sim 0.8 \mu\text{A}$) are obtained at a frequency of 3 Hz. At higher frequencies, the rate of charge transfer increases, resulting in a reduced duration of current peaks and higher current output.

In order to further examine the effect of the CYTENG length on the electrical performance, the output voltage and current of the CYTENG with different lengths under same condition were measured. Figure 4.5f and g display the output voltage and current towards different CYTENG lengths. As the length of the CYTENG increases

CHAPTER 4

from 5 cm to 45 cm, the output voltage and current of obtained CYTENG increase. The reason is that the larger contact area can generate more charge, leading to higher output.



CHAPTER 4

Figure 4.5 The electrical performance of the CYTENG. (a) The output voltage and (b) current of the CYTENG with various impacting forces (the frequency is fixed at 3 Hz). (c) The relationship between voltage and impacting force. The lines correspond to the linear fitting function. (d) The output voltage and (e) current of the CYTENG with different impacting frequencies (the force is fixed at 100 N and testing length of the CYTENG is 45 cm). (f) The output voltage and (g) current of the CYTENG with different lengths (the impacting force and frequency are fixed at 100 N and 3 HZ, respectively).

4.3.5 Self-powered wearable sensors based on the CYTENG

To demonstrate the capability of the CYTENG in sensing finger motions, three CYTENGs with a length of 35 cm were sewn into index finger, middle finger and ring finger knuckle area inside a textile glove respectively, as shown in Figure 4.6a. Figure 4.6b shows that this smart glove can detect and distinguish various gesture signals. When the movements between the two materials by hand gestures were repeated, the smart glove generated a triboelectric output voltage, which could distinguish different gesture signals. This result shows that the smart glove with the CYTENG's triboelectric sensor can distinguish specific gestures in real time. When the output voltage of this self-powered sensor is 2.9 V (I), 1.7 V (II) and 0.9 V (III), the finger gesture can be recognized as index finger, middle finger and ring finger, as shown in Figure 4.6b. In addition, the output voltage of 4.8 V (IV) is detected as making a fist.

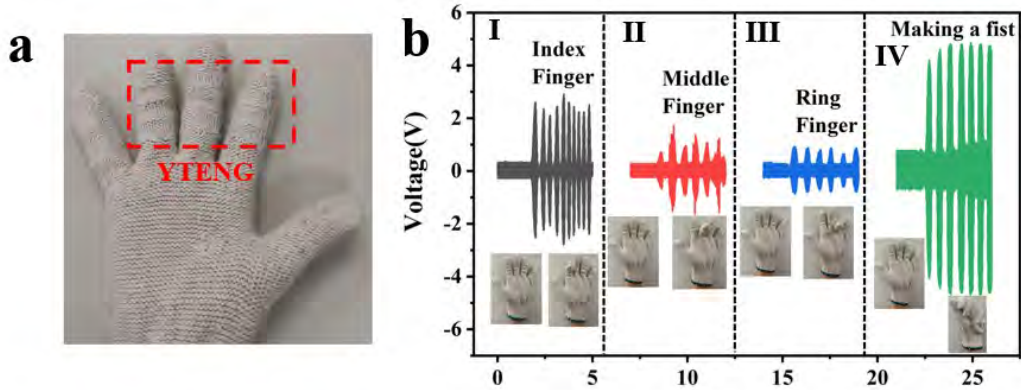


Figure 4.6 (a) Image of a smart glove sewn with the CYTENG. (b) Output voltage of the smart glove during the motion of different fingers, index finger (I), middle finger (II), ring finger (III) and making a fist (IV).

4.4 Conclusion

In this chapter, a new triboelectric yarn was successfully prepared by a scalable fancy yarn spinning technology using Tencel and chitosan fibers, which exhibits high flexibility, small diameter, low weight, high scalability, and productivity as well as low cost. It is well demonstrated that the impact force, frequency, and CYTENG length have a great influence on electrical output. Specifically, under a working principle of single-electrode mode, a voltage with value of 14.2 V and a current of 0.8 μA can be obtained from the CYTENG with the length of 45 cm under an impacting frequency of 3 HZ and force of 100 N. In addition, the CYTENG possesses high sensitivity to impact and can be used as a high-performance self-powered sensor. With the merits of good shape-adaptability, easy deployment, low cost, and eco-friendliness, the CYTENG shows promising potential in wearable use, which can be further woven into breathable fabric t-TENG or integrated with cloth. This continuously scalable manufacturing technology contributes to the commercial production of eco-friendly fiber/yarn based t-TENGs and also provides guidance for the fabrication of functional yarn.

CHAPTER 4

References

- (1) Mule, A. R.; Dudem, B.; Patnam, H.; Graham, S. A.; Yu, J. S. Wearable Single-Electrode-Mode Triboelectric Nanogenerator via Conductive Polymer-Coated Textiles for Self-Power Electronics. *ACS Sustainable Chem. Eng.* **2019**, *7*, 16450-16458.
- (2) Luo, J.; Wang, Z.; Xu, L.; Wang, A. C.; Han, K.; Jiang, T.; Lai, Q.; Bai, Y.; Tang, W.; Fan, F. R.; Wang, Z. L. Flexible and Durable Wood-Based Triboelectric Nanogenerators for Self-Powered Sensing in Athletic Big Data Analytics. *Nat. Commun.* **2019**, *10*, 5147.
- (3) Shi, X.; Luo, J.; Luo, J.; Li, X.; Han, K.; Li, D.; Cao, X.; Wang, Z. L. Flexible Wood-Based Triboelectric Self-Powered Smart Home System. *ACS nano* **2022**, *16*, 3341-3350.
- (4) Zhang, Z.; Jie, Y.; Zhu, J.; Zhu, Z.; Chen, H.; Lu, Q.; Zeng, Y.; Cao, X.; Wang, Z. L. Paper triboelectric nanogenerator designed for continuous reuse and quick construction. *Nano Research* **2022**, *15*, 1109-1114.
- (5) Nie, S.; Guo, H.; Lu, Y.; Zhuo, J.; Mo, J.; Wang, Z. L. Superhydrophobic Cellulose Paper-Based Triboelectric Nanogenerator for Water Drop Energy Harvesting. *Adv. Mater. Technol.* **2020**, *5*, 2000454-2000462.
- (6) Zhu, J.; Cheng, Y.; Hao, S.; Wang, Z. L.; Wang, N.; Cao, X. A self-healing triboelectric nanogenerator based on feathers for sensing and energy harvesting. *Adv. Funct. Mater.* **2021**, *31*, 2100039.
- (7) Ma, L.; Zhou, M.; Wu, R.; Patil, A.; Gong, H.; Zhu, S.; Wang, T.; Zhang, Y.; Shen, S.; Dong, K.; Yang, L.; Wang, J.; Guo, W.; Wang, Z. L. Continuous and Scalable Manufacture of Hybridized Nano-Micro Triboelectric Yarns for Energy Harvesting and Signal Sensing. *ACS Nano* **2020**, *14*, 4716-4726.
- (8) Dong, K.; Deng, J.; Ding, W.; Wang, A. C.; Wang, P.; Cheng, C.; Wang, Y.-C.; Jin, L.; Gu, B.; Sun, B.; Wang, Z. L., Versatile Core-Sheath Yarn for Sustainable

CHAPTER 4

Biomechanical Energy Harvesting and Real-Time Human-Interactive Sensing. *Adv. Energy Mater.* **2018**, *8*, 1801114.

(9) Xie, L.; Chen, X.; Wen, Z.; Yang, Y.; Shi, J.; Chen, C.; Peng, M.; Liu, Y.; Sun, X. Spiral Steel Wire Based Fiber-Shaped Stretchable and Tailorable Triboelectric Nanogenerator for Wearable Power Source and Active Gesture Sensor. *Nano-Micro Lett.* **2019**, *11*, 1-10.

(10) Ning, C.; Cheng, R.; Jiang, Y.; Sheng, F.; Yi, J.; Shen, S.; Zhang, Y.; Peng, X.; Dong, K.; Wang, Z. L. Helical Fiber Strain Sensors Based on Triboelectric Nanogenerators for Self-Powered Human Respiratory Monitoring. *ACS Nano* **2022**, *16*, 2811-2821.

(11) Feng, Z.; Yang, S.; Jia, S.; Zhang, Y.; Jiang, S.; Yu, L.; Li, R.; Song, G.; Wang, A.; Martin, T.; Zuo, L.; Jia, X. Scalable, Washable and Lightweight Triboelectric-Energy-Generating Fibers by the Thermal Drawing Process for Industrial Loom Weaving. *Nano Energy* **2020**, *74*, 104805.

(12) Liu, S.; Zheng, W.; Yang, B.; Tao, X. Triboelectric charge density of porous and deformable fabrics made from polymer fibers. *Nano Energy* **2018**, *53*, 383-390.

(13) Pawlak, A., Mucha, M. Thermogravimetric and FTIR studies of chitosan blends. *Thermochim. Acta* **2013**, *396*, 153-166.

(14) López, F. A., Mercê, A. L. R., Alguacil, F. J., López-Delgado, A. A kinetic study on the thermal behaviour of chitosan. *J. Therm. Anal. Calorim* **2008**, *91*, 633-639.

Chapter 5: Two-Dimensional Fabric Triboelectric Nanogenerator by Integrating One-Dimensional Core-Spun Triboelectric Yarn

5.1 Introduction

To improve electrical output performance and broaden its application, flexible TENGs with fabric forms were highly desired, which promote the development of fabric-based TENG (FTENG) as energy-harvesting device and self-powered sensor. Consequently, a variety of fabric-structured TENGs have been developed.¹⁻⁵ One approach is to weave modified yarns or wires into TENG fibers/yarns for fabricating FTENG.⁶⁻¹⁴ For the electrodes of TENGs, carbonaceous material coating, metal wires, yarn or fabric with conductive metal, and conductive polymers have been commonly used.¹⁵⁻²¹ Moreover, dielectric polymer films such as polydimethylsiloxane (PDMS) and silicone rubber have been typically coated on conductive yarn or metal wires as triboelectrification layers.²²⁻³³ Another method of fabric-structured TENGs is to utilize conductive and dielectric coating on fabrics.³⁴⁻³⁶ In addition to these techniques, screen-printing, electrospinning and electrospray method, reactive ion etching and metal-mask plasma etching have also been explored.³⁷⁻⁴²

Although these developed FTENGs have demonstrated the effectiveness of power supply, there are still some challenges ahead that need to address. A majority of FTENGs are fabricated by using the fabric as the substrate and then attaching functional materials with good triboelectric properties to the substrate, which greatly affects the comfort.⁴³ In addition, t-TENGs as wearable self-powered sensors are in constant

CHAPTER 5

contact, bacteria are also easy to multiply, which will pose a huge threat to human health. In this case, antibacterial property is an important performance optimization for the tactile sensor to prevent bacterial infections. Furthermore, in terms of the extension of their applications, most t-TENGs are incompatible with current textile manufacturing process.⁴⁴ The methods that have been reported are complex, time-consuming and expensive.

In this chapter, to address the above-mentioned challenges, a novel FTENG based on woven structure was successfully fabricated by using the CYTENG developed in chapter 4, which overcomes the complex manufacturing process, high cost, poor comfort and small-scale production. The prepared FTENG with the size of $5 \times 5 \text{ cm}^2$ presents a desirable open-circuit voltage of 31.3 V, a short-circuit current of 1.8 μA and instantaneous power density of 15.8 mW/m^2 under a load resistance of 70 $\text{M}\Omega$. In addition, the FTENG exhibits excellent wearability and comfort, such as high flexibility, desirable breathability and good machine washability. The FTENG performs excellent antibacterial property. The inhibition rates against *Staphylococcus aureus* (*S. aureus*), *Escherichia coli* (*E. coli*) and *Candida albicans* (*C. albicans*) can reach up to 99%. Furthermore, it can work as a self-powered sensor, wherein the developed FTENG can be attached under the arm and foot to demonstrate the ability to detect different body movements. Therefore, the FTENG showed in this work can be integrated into multifunctional textiles and clothing. This platform will pave a way for the widespread application of the Internet of Things.

5.2 Experimental Section

5.2.1 Materials

CHAPTER 5

Cotton yarn as warp yarn was provided from the lab. The CYTENGs prepared in chapter 4 were used as weft yarns.

5.2.2 Fabrication of the FTENG

An automatic rapier sample loom (SL8900, CCI TECH INC.) was employed to weave an FTENG. Cotton yarns were prepared as warp yarns, and as-prepared CYTENGs in chapter 4 were employed as weft yarns. After entering the fabric structure details and appropriate weft density in the loom machine, the weaving process started.

5.2.3 Characterizations

The air permeability of the FTENG was evaluated by air Permeability Tester (SDL International M021S) according to standard (ASTM D737). The water vapor transmission (WVT) rate ($\text{g}/\text{m}^2\cdot\text{day}$) of the obtained FTENG was characterized according to the standard (GB/T 12704.1-2009). An electrometer (Keithley 6514) and oscilloscope (DS1000Z) were used to measure the electrical output of the FTENG. The compressing motions were applied via a Keyboard Life Tester (ZX-A03). The machine washability of the as-made FTENG was tested according to the standard (AATCC 135), and the antibacterial property of the FTENG was measured following GB/T 20944.3 (Shake flake method).

5.3 Results and Discussion

5.3.1 Design and fabrication of the FTENG

CHAPTER 5

Figure 5.1a shows the weave structure of the FTENG. The blank represents the weft yarn (CYTENG) exposed on the surface, and the black dot represents the warp yarn (cotton) presented on the surface. A woven structured FTENG is illustrated, as displayed in Figure 5.1b. All the electrodes of weft yarns of the FTENG are connected in parallel, which are connected to a ground via an external load. Figure 5.1c shows the fabrication process of the FTENG. Industrial sample weaving loom was used for automatic weaving. The optical image of the FTENG is shown in Figure 5.1c, presenting surface morphology of the FTENG. The FTENG has a larger weft float length, and almost all surface of the fabric is covered by the CYTENG as the weft yarns. Compared with plain weave and twill weave, the interlacing points in sateen structure are the least, so the hand feel is softer. Figure 5.1d shows a typical cross section of the FTENG where the weft and warp yarns interweave up and down with each another. In one unit, seven weft yarns (CYTENGs) are above the warp yarns (cotton), and one weft yarn is below the warp yarns. Like common cotton fabrics, Figure 5.1e proves the FTENG being kneaded (I), scrolled (I) and folded (III), obviously displaying the flexibility feature of the FTENG.

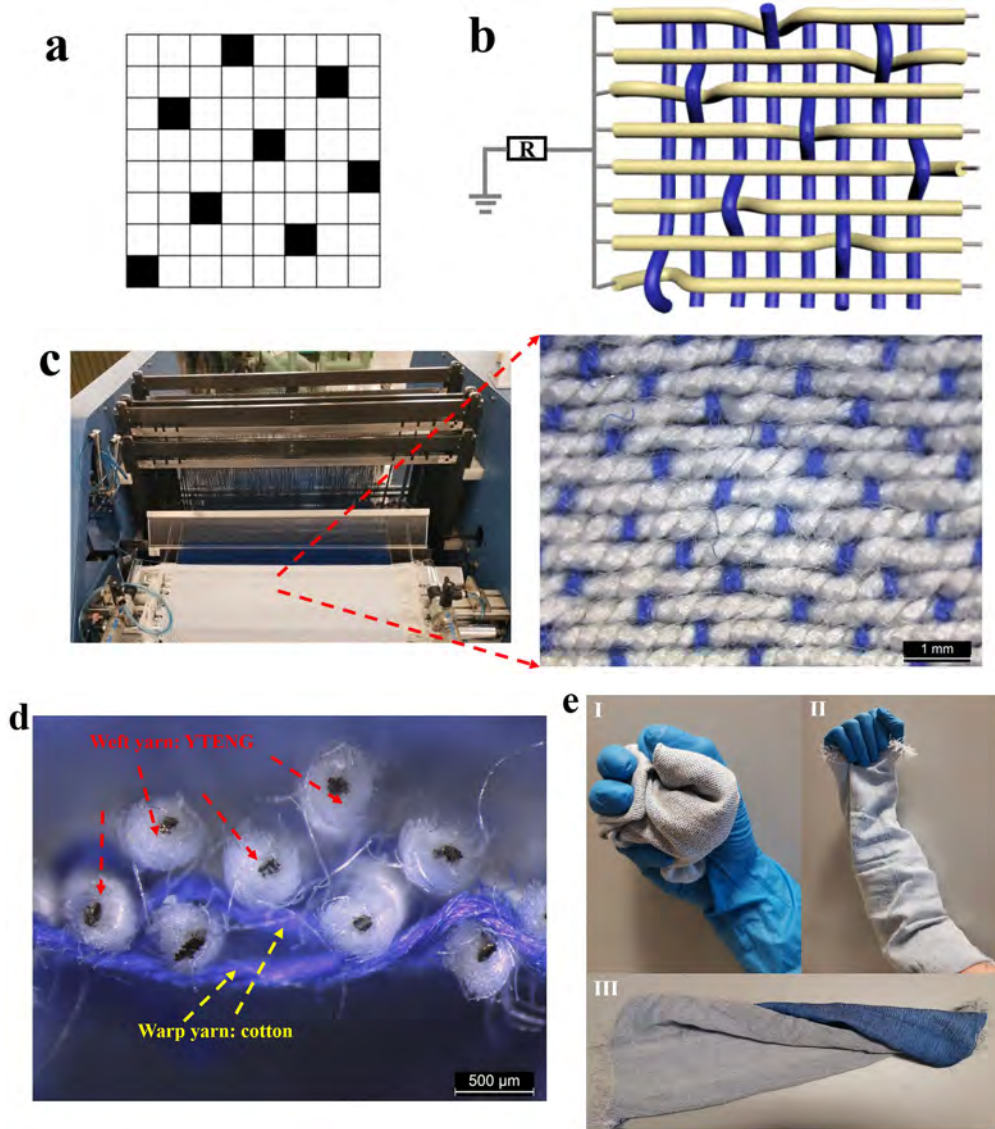


Figure 5.1 (a) Weave structure of the FTENG. (b) Schematic illustration of the FTENG. (c) Photograph of the fabricated FTENG. (d) Cross section of the fabricated FTENG. (e) Photographs of the FTENG under different deformations, such as kneaded (I), scrolled (II), and folded (III).

5.3.2 Working mechanism

Figure 5.2 illustrates the working mechanism of the FTENG, which is similar with that of the CYTENG.

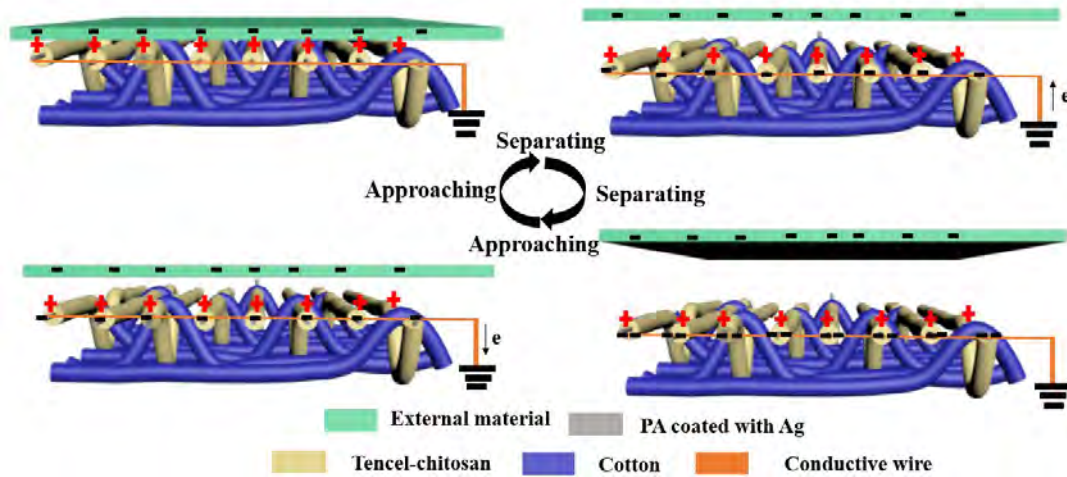


Figure 5.2 Working principle of the FTENG.

5.3.3 Breathability

Breathability is a significant factor for the FTENG with cloth/skin for wearable applications. The air permeability of the FTENG can reach 49 ml/s/cm^2 , which is the rate of air flow passing perpendicularly via the fabric. The higher rate indicates better air permeability. For comparison, three types of chitosan blended woven fabrics were also tested which were fabricated with polyester/cotton/chitosan, cotton/chitosan and Tencel/ polyester /chitosan yarns, respectively. As illustrated in Figure 5.3, the results show that the FTENG is comparable to three chitosan blended woven fabrics, which can meet the requirements of human skin for air permeability. Additionally, benefiting from the material and structure of the FTENG, it exhibits good permeability of water vapor. As shown in Figure 5.3, the water vapor transmission (WVT) of obtained FTENG is $656.12 \text{ g/m}^2 \cdot 24 \text{ h}$. The comparison with three other woven fabrics confirms its excellent breathability.

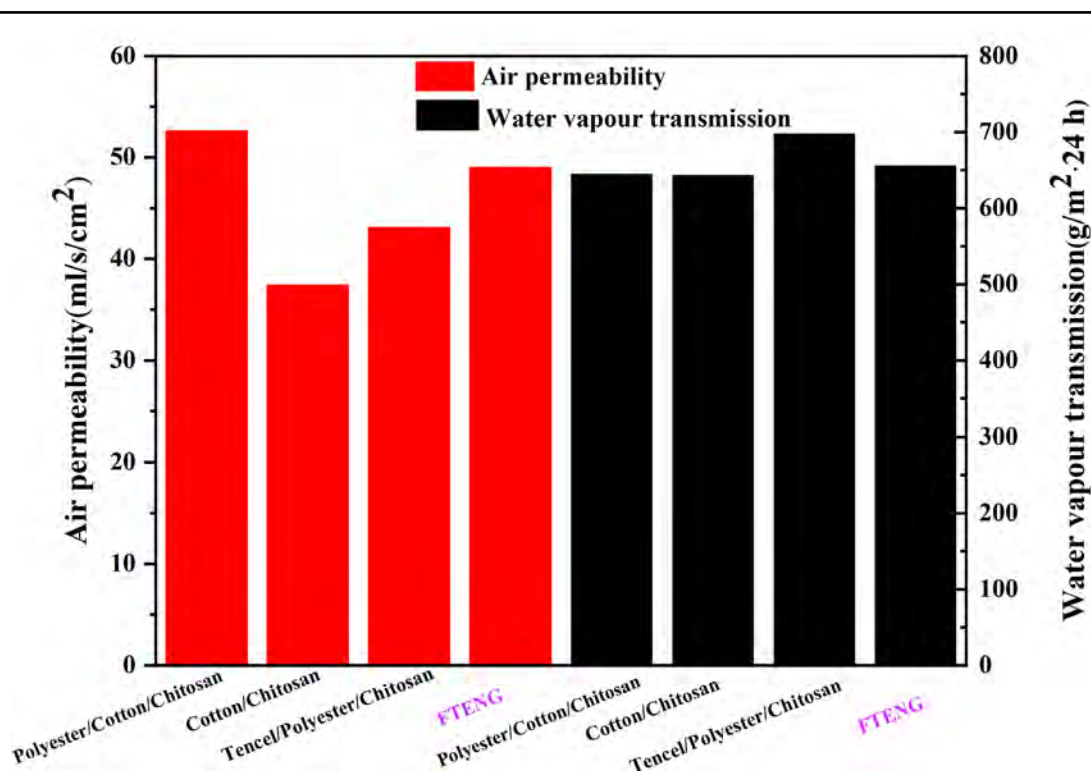


Figure 5.3 Air permeability and water vapor permeability of the as-prepared FTENG and different fabrics.

5.3.4 Electrical output performance of the FTENG

The electrical output performance of the FTENG was quantitatively tested. A PDMS film was driven by a Keyboard Life Tester to apply forces on the FTENG cyclically. Detailed study of the factors affecting the output performance of the FTENG were also investigated, including the impact force, test area and frequency.

In practical life, various impact forces are often applied to human body. Therefore, it is necessary to investigate the effect of force on the output performance of the FTENG. Figure 5.4a and b show the voltage and current of the FTENG (5 cm*5 cm) with different impact forces ranging from 0 to 200 N at the fixed mechanical impacting frequency of 3 Hz. The results clearly reveal that the voltage and current of the FTENG

CHAPTER 5

are gradually enhanced by increasing the applied impact force. The increase of the effective friction area between the PDMS film and FTENG can explain the increase in output voltage and current of the FTENG. However, as the applied force continues to rise, the output voltage and current of the FTENG basically increase slightly. This may be due to the fact that the PDMS film and FTENG are in complete contact, resulting in saturation of the effective friction area. Output voltage of 31.3 V and current of 1.8 μ A can be achieved by applying a force of 100 N on the FTENG. To further understand the relation between the pressure and output performance, the output voltage and current with respect to increased pressure are plotted in Figure 5.4c and d. As observed, the plot of relationship between output voltage and pressure is composed of three stages, pressure region under 8 kPa, pressure from 8 kPa to 32 kPa and pressure from 32 kPa to 40 kPa. Under the low-pressure stage (less than 8 kPa), the FTENG presents a well-behaved response. A very high linearity of 0.980 and sensitivity of 1.940 V/kPa are displayed (black fitting line) due to a relatively large change of the effective friction area. As the pressure grows further, a decreased sensitivity can be clearly seen (red fitting line), which is attributed to small variation of effective friction area. The fitting line suggests that the pressure and voltage exhibit a linear relationship with a correlation of 0.997 in the range of 8-32 kPa. When the pressure exceeds 32 kPa, the change in output voltage becomes very small, or the device enters an approximate saturation state (blue fitting line) owing to saturation of the effective friction area. Meanwhile, a similar trend can be observed in the output current. The detailed reason of three pressure stages is illustrated. The output voltage can be expressed as ⁴⁵

$$V(t) = R \frac{dQ}{dt} = -\frac{Q}{S\varepsilon_0} \left(\frac{d_1}{\varepsilon_{r1}} + \frac{d_2}{\varepsilon_{r2}} + x(t) \right) + \frac{\sigma x(t)}{\varepsilon_0} \quad (1)$$

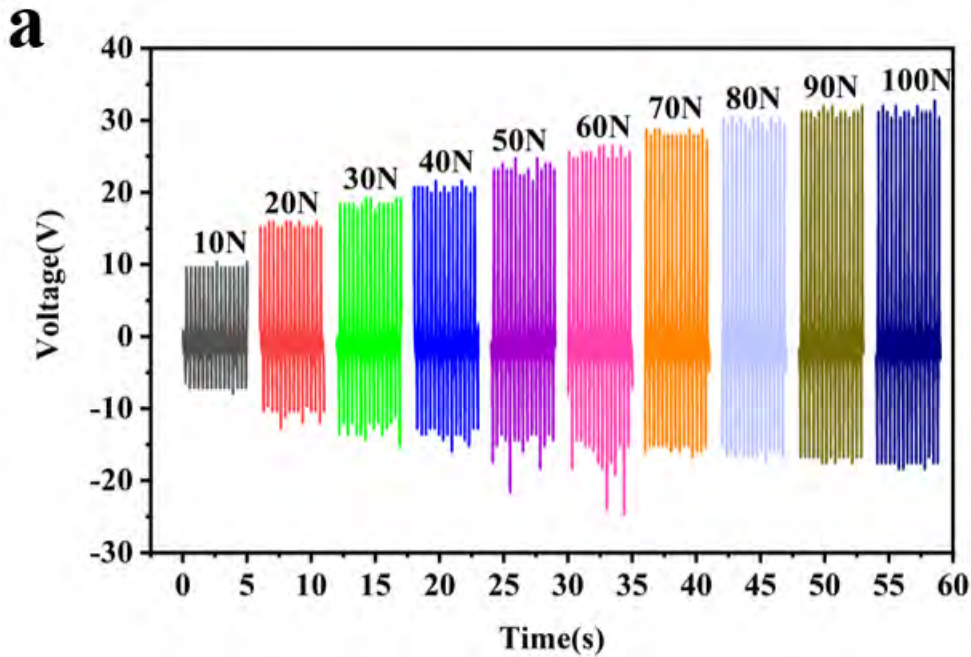
where V is the output voltage, Q is the transferred charge amount between electrodes, S is the contact area during working, ε_0 is the vacuum permittivity, ε_r is the relative

CHAPTER 5

permittivity of dielectric layers, d_1 and d_2 are the effective thickness of two dielectric materials. x is the separation distance between the two triboelectric charged layers, σ means the charge density. It can be observed that a large change in the effective friction area ΔS results in a large change in the output voltage ΔV . The pressure sensitivity can be expressed as

$$S = \frac{\Delta V}{\Delta P} \quad (2)$$

where ΔP is the change of pressure. So a large change of the effective friction area will contribute to high pressure sensitivity. Because of the interweaving of warp and weft yarns, the FTENG shows three deformation stages with various pressures, as presented in Figure 5.4e. From stage 1 to stage 2 under low pressure region (< 8 kPa), a relative large change of the effective friction area ΔS can be seen. However, there is small variation of effective friction area ΔS from the stage 2 to stage 3 (8 kPa-32 kPa). In the stage 3 (32 kPa-40 kPa), the effective contact area ΔS is basically saturated.



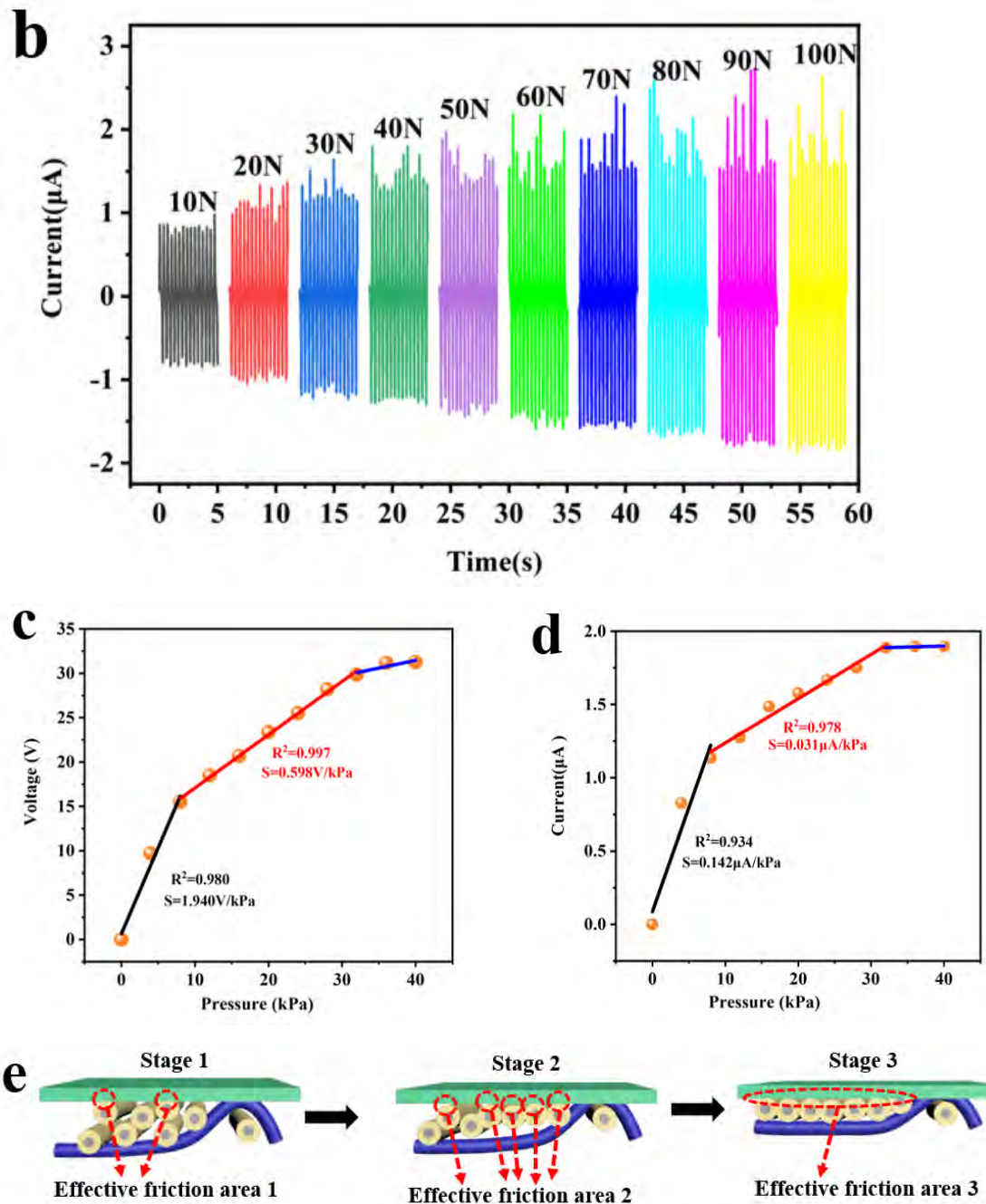


Figure 5.4 (a) The output voltage and (b) current of the FTENG with various impacting forces (the frequency is fixed at 3 Hz and area is 5 cm*5 cm). (c) The relationship between voltage of the FTENG and pressure. (d) The relationship between current of the FTENG and pressure. The lines correspond to the linear fitting function. (e) Different deformation stages of the FTENG under different pressures.

The output performance of the FTENG with different areas is also explored in this work. It is obvious that the output performance of the voltage and current can be gradually

CHAPTER 5

enhanced as the contact area of the FTENG increases. When the area of the FTENG varies from 3 cm*3 cm to 5 cm*5 cm, the voltage and current increase from about 14.6 V, 1.1 μ A to about 31.3 V, 1.8 μ A, respectively, as demonstrated in Figure 5.5a and b. The enhanced output performance can be attributed to the following reason. The larger area of the FTENG increases the contact area of friction layer, which can generate higher outputs.

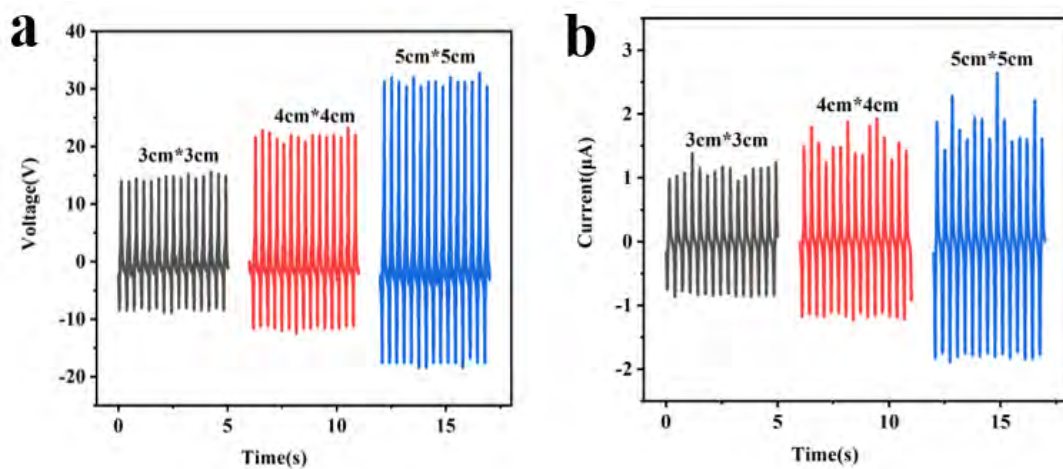


Figure 5.5 (a) The output voltage and (b) current of the FTENG with different testing areas (the force and frequency are fixed at 100 N and 3 HZ, respectively).

Additionally, the electrical output performance is also evaluated at different impact frequencies via maintaining the external impact force at 100 N and area of 5 cm*5 cm. When the impact frequency rises from 1 Hz to 3 Hz, an increase of voltage from 11.3 V to 31.3 V can be observed, as presented in Figure 5.6a. Under the increasing frequency, the surface charge of the friction layer will not be completely neutralized, which may boost the voltage. Meanwhile, as shown in Figure 5.6b, the current of FTENG increases from 0.6 μ A to 1.8 μ A. The enhancement can be attributed to a higher impact frequency that can increase the number of pressure per unit time. This improves the rate of charge transfer and reduces the sustained period of current peak, thus

inducing higher current.

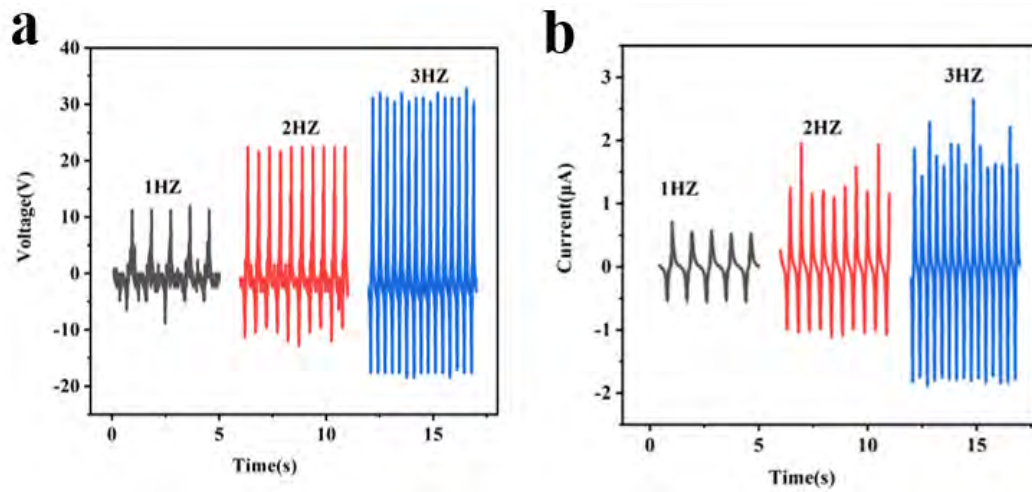


Figure 5.6 (a) The output voltage and (b) current of the FTENG with different frequencies (the force and area are fixed at 100 N and 5 cm*5 cm, respectively).

In order to make wearable electronics, the main requirement is to withstand washing procedures. In this regard, the as-made FTENG was washed and dried by using a commercial washing machine and dryer. The electrical output performance of the FTENG before and after being washed was tested and analyzed comprehensively. Figure 5.7a shows the output voltage of the FTENG under the identical external condition after machine washing. The voltage of the FTENG under the first machine washing exhibits very minor degradation. After the 2nd, 3rd, and 5th washes, the output voltage remains stable without obvious declining. It can be ascribed to the slight yarn shrinkage which is a common phenomenon of yarns after their first wash, leading to the change of relative position of yarns and effective contact area. These observed experimental results prove that the FTENG has good machine-washability for daily use. As presented in Figure 5.7b, it can be observed that the output voltage of the FTENG does not change obviously under 100 cyclic times of folding and twisting owing to the flexibility of the FTENG.

CHAPTER 5

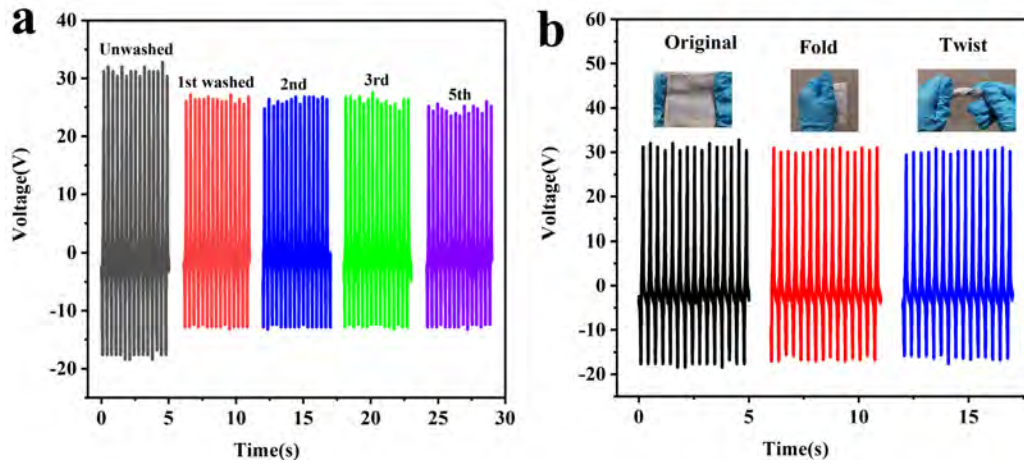


Figure 5.7 (a) The output voltage of the FTENG before and after machine washing. (b) The output voltage of the FTENG after suffering various deformations (100 cyclic times of folding and twisting).

The dependence of output current of the FTENG on the external loading resistance was investigated by connecting with external resistors. As exhibited in Figure 5.8, it is found that the output current is basically maintained at a value with the increment of load resistance from $10^3 \Omega$ to $10^6 \Omega$, and subsequently decreases when the resistance is further increased to $10^8 \Omega$. The average power density can be expressed as:

$$W = \frac{I^2 R}{A} \quad (3)$$

where W represents the power density, I is the corresponding current, R is the resistance value, and A is the effective area. The power density of 15.8 mW/m^2 under a load resistance of $70 \text{ M}\Omega$ is achieved.

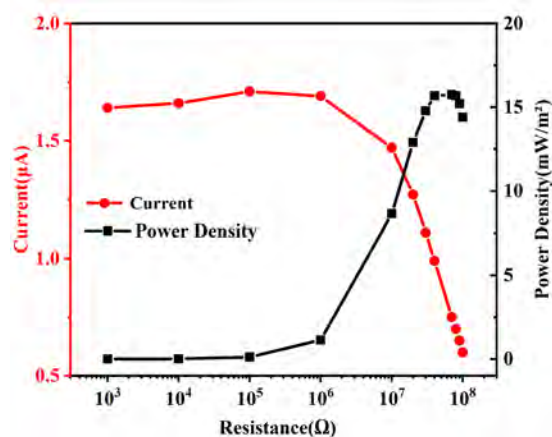


Figure 5.8 The current and peak power of the FTENG measured with various external load resistances with frequency of 3 HZ and impacting force of 100 N.

5.3.5 Antibacterial property of the FTENG

The antibacterial property of as-fabricated FTENG was evaluated following GB/T 20944.3 (Shake flake method). The concentration of bacteria and inhibition rate of FTENG are summarized in Table 5.1. For *S. aureus*, the number of bacteria in the blank sample increased significantly from 2.0×10^4 CFU mL⁻¹ in 0 h to 8.7×10^5 CFU mL⁻¹ in 18 h while the number of bacteria in the FTENG decreased significantly to 1.0×10^2 CFU mL⁻¹ after 18 h. The inhibition rate of 99% against *S. aureus* can be observed. The same inhibition rate against *E. coli* is presented. With regard to *C. albicans*, the inhibition rate of the FTENG can reach up to 99%. The excellent antibacterial property of the FTENG is mainly attributed to the chitosan material blended in yarns and Ag coated on the PA yarn, which possess the ability to inhibit and kill bacteria. The results demonstrate that the antibacterial activity of the FTENG is excellent and our FTENG exhibits great potential in antibacterial wearable electronics.

Table 5.1 Antibacterial efficiency after inoculation with *S. aureus*, *E. coli* and *C. albicans* suspensions incubated with the FTENG for 18 h.

CHAPTER 5

Bacteria	<i>S. aureus</i>		<i>E. coli</i>		<i>C. albicans</i>	
	Blank	FTENG	Blank	FTENG	Blank	FTENG
The number of bacteria at 0 h contact time (CFU mL ⁻¹)		2.0 × 10 ⁴		2.2 × 10 ⁴		1.8 × 10 ⁴
The number of bacteria at 18 h contact time (CFU mL ⁻¹)	8.7 × 10 ⁵	1.0 × 10 ²	3.1 × 10 ⁶	3.1 × 10 ³	4.6 × 10 ⁵	2.6 × 10 ³
Inhibition (%)		> 99		> 99		> 99

5.3.6 Application of the FTENG

In order to prove the ability of the FTENG as a power source for electronics, fifteen commercial light-emitting diodes (LEDs) were connected to the electrodes of the FTENG. When impacting on the FTENG with an active area of 5 cm × 5 cm, 15 LEDs were lit up, as displayed in Figure 5.9a. In addition to powering electronic devices, the electrical energy generated by the FTENG could also be stored in several capacitors through a bridge circuit. The effect of capacitance capacity (1 μF, 4.7 μF, 10 μF) on the charging ability of the FTENG was also investigated. Figure 5.9b presents the voltage-charging curve of different capacitors, which was measured under impacting and releasing the FTENG. As the capacitance capacity increases, a slower charging velocity can be seen. The electricity stored in capacitor could power wearable electronics. A circuit was designed for driving electronic watch. The screen of watch indicates the watch works normally, as exhibited in Figure 5.9c.

CHAPTER 5

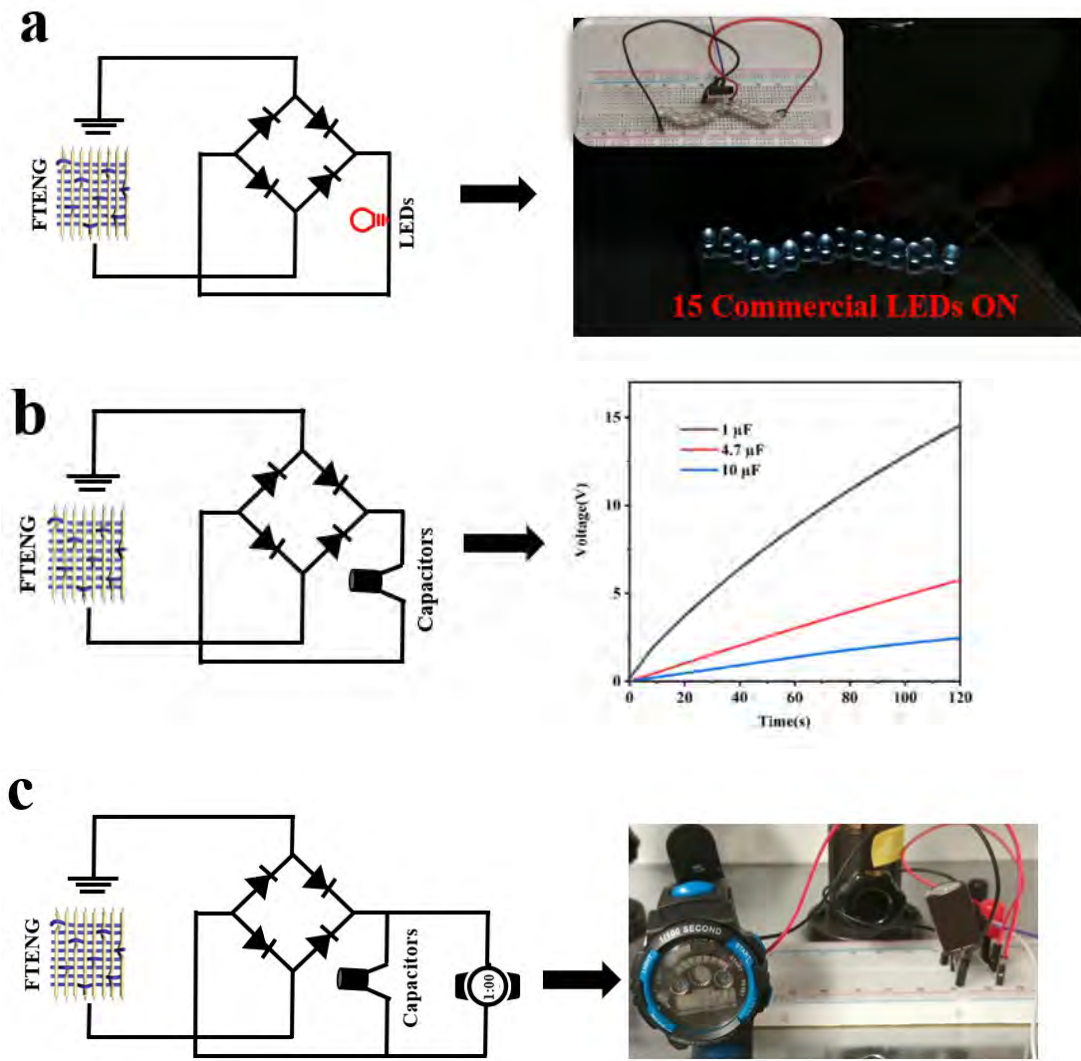


Figure 5.9 (a) A series of LEDs powered by the FTENG. (b) The capacitor charging ability of the FTENG with 5 cm*5 cm area under impacting frequency of 3 Hz and impacting force of 100 N. (c) Circuit diagram for powering electronic watch.

In gait and posture analysis, monitoring the foot motion is very significant for footwear design, sports biomechanics and wearable medical systems. Figure 5.10a presents a schematic illustration of the FTENG for the foot monitoring. The FTENG was put under the heel and forefoot, respectively. For example, as illustrated in Figure 5.10a, the human foot served as the friction layer to contact the FTENG. Slow motion and fast motion were applied to the foot heel. The corresponding output value can reach about

CHAPTER 5

2.3 V (I) and 2.5 V (II). However, the output voltage of 1.2 V(III) can be obtained when using forefoot to contact the FTENG. Moreover, for comparison, the heel and forefoot wearing cotton socks were employed to contact the FTENG. The output voltages obtained are obviously different, about 1.8 V (IV) and 0.8 V(V) respectively. This foot pressure monitoring function of the FTENG can be utilized for posture correction and rehabilitation in sports industries and personal health monitoring.

In addition, the FTENG was integrated on different positions of the human body to obtain energy and monitor human movements. A FTENG (5 cm*5 cm) was pasted on the waist of cloth. Figure 5.10b shows the output voltage of the FTENG by this arm swinging. Meanwhile, the voltage of the FTENG at different speeds of human motion was recorded. Peak voltages about 1.2 V (I) and 5.1 V (II) were obtained from arm swinging in slow speed and fast speed, respectively. In comparison, the voltage generated by arm flapping is relatively higher with 7.3 V (III) for the slow motion and 17.8 V (IV) for the fast motion. According to the above discussions, the FTENG served as a self-powered sensor is successfully demonstrated, which is flexible, portable and has promising potential for future smart healthcare sensor.

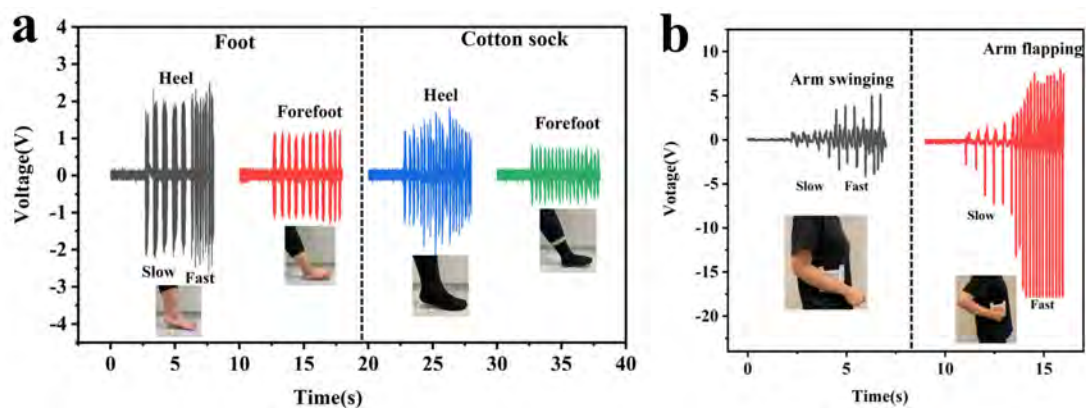


Figure 5.10 (a) Output voltage of the FTENG fixed under the foot, slow motion of heel (I), fast motion of heel (II), forefoot motion (III), heel motion wearing a cotton

CHAPTER 5

sock (IV) and forefoot motion wearing a cotton sock (V). (b) Output voltage of the FTENG fixed under the arm, slow motion of arm swinging (I), fast motion of arm swinging (II), slow motion of arm flapping (III) and fast motion of arm flapping (IV).

5.4 Conclusion

In this chapter, we have successfully developed eco-friendly and antibacterial 2D FTENG through the employment of green fibers based on existing spinning and weaving technology. The electrical performance of the FTENG operating at a single-electrode mode is desirable, which can reach 31.3 V, 1.8 μA , 15.8 mW/m^2 by applying a 3 Hz mechanical drive of 100 N with the size of $5 \times 5 \text{ cm}^2$. Besides, the FTENG has achieved the outstanding wearability including the unique advantages of safety, lightness, comfort, breathability and washability. Moreover, The FTENG performs excellent antibacterial property, wherein the inhibition rates against *S. aureus*, *E. coli* and *C. albicans* can reach up to 99%. Furthermore, the output voltage and current exhibit excellent sensitivity towards impact force. The FTENG can sense the intensity of mechanical stimulation in real time in a self-powered manner. The above compelling features of the proposed FTENG by employing eco-friendly material and scalable manufacturing process demonstrate its promising potential for multifunctional applications in wearable electronics.

CHAPTER 5

References

- (1) Kwak, S. S.; Kim, H.; Seung, W.; Kim, J.; Hinchet, R.; Kim, S. W. Fully stretchable textile triboelectric nanogenerator with knitted fabric structures. *ACS Nano* **2017**, *11*, 10733-10741.
- (2) Zhou, T.; Zhang, C.; Han, C. B.; Fan, F. R.; Tang, W.; Wang, Z. L. Woven structured triboelectric nanogenerator for wearable devices. *ACS Appl. Mater. Interfaces* **2014**, *6*, 14695-14701.
- (3) Pyo, S.; Kim, M.O.; Kwon, D.S.; Kim, W.; Yang, J.H.; Cho, H. S.; Lee, J. H.; Kim, J. All-textile wearable triboelectric nanogenerator using pile-embroidered fibers for enhancing output power. *Smart Mater. Struct.* **2020**, *29*, 055026.
- (4) Dong, S.; Xu, F.; Sheng, Y.; Guo, Z.; Pu, X.; Liu, Y. Seamlessly knitted stretchable comfortable textile triboelectric nanogenerators for E-textile power sources. *Nano Energy* **2020**, *78*, 105327.
- (5) Fan, W.; He, Q.; Meng, K.; Tan, X.; Zhou, Z.; Zhang, G.; Yang, J.; Wang, Z. L. Machine-knitted washable sensor array textile for precise epidermal physiological signal monitoring. *Sci. Adv.* **2020**, *6*, 2840.
- (6) Feng, Z.; Yang, S.; Jia, S.; Zhang, Y.; Jiang, S.; Yu, L.; Li, R.; Song, G.; Wang, A.; Martin, T.; Zuo, L.; Jia, X. Scalable, washable and lightweight triboelectric-energy-generating fibers by the thermal drawing process for industrial loom weaving. *Nano Energy* **2020**, *74*, 104805.
- (7) Yu, A.; Pu, X.; Wen, R.; Liu, M.; Zhou, T.; Zhang, K.; Zhang, Y.; Zhai, J.; Hu, W.; Wang, Z.L. Core-shell-yarn-based triboelectric nanogenerator textiles as power cloths. *ACS Nano* **2017**, *11*, 12764-12771.
- (8) Zhao, Z.; Huang, Q.; Yan, C.; Liu, Y.; Zeng, X.; Wei, X.; Hu, Y.; Zheng, Z. Machine-washable and breathable pressure sensors based on triboelectric nanogenerators

CHAPTER 5

enabled by textile technologies. *Nano Energy* **2020**, *70*, 104528.

(9) Jiang, C.; Li, X.; Ying, Y.; Ping, J. A multifunctional TENG yarn integrated into agrotextile for building intelligent agriculture. *Nano Energy* **2020**, *74*, 104863.

(10) Ma, L.; Wu, R.; Liu, S.; Patil, A.; Gong, H.; Yi, J.; Sheng, F.; Zhang, Y.; Wang, J.; Wang, J.; Guo, W.; Wang, Z.L. A machine-fabricated 3D honeycomb-structured flame-retardant triboelectric fabric for fire escape and rescue. *Adv. Mater.* **2020**, *32*, 2003897.

(11) Ma, L.; Zhou, M.; Wu, R.; Patil, A.; Gong, H.; Zhu, S.; Wang, T.; Zhang, Y.; Shen, S.; Dong, K.; Yang, L.; Wang, J.; Guo, W.; Wang, Z.L. Continuous and scalable manufacture of hybridized nano-micro triboelectric yarns for energy harvesting and signal sensing. *ACS Nano* **2020**, *14*, 4716-4726.

(12) Park, J.; Kim, D.; Choi, A.Y.; Kim, Y.T. Flexible single-strand fiber-based woven-structured triboelectric nanogenerator for self-powered electronics. *APL Mater.* **2018**, *6*, 101106.

(13) Zhu, J.; Zhu, P.; Yang, Q.; Chen, T.; Wang, J.; Li, J. A fully stretchable textile-based triboelectric nanogenerator for human motion monitoring. *Mater. Lett.* **2020**, *280*, 128568.

(14) Shuai, L.; Guo, Z.H.; Zhang, P.; Wan, J.; Pu, X.; Wang, Z. L. Stretchable, self-healing, conductive hydrogel fibers for strain sensing and triboelectric energy-harvesting smart textiles. *Nano Energy* **2020**, *78*, 105389.

(15) He, X.; Zi, Y.; Guo, H.; Zheng, H.; Xi, Y.; Wu, C.; Wang, J.; Zhang, W.; Lu, C.; Wang, Z.L. A highly stretchable fiber-based triboelectric nanogenerator for self-powered wearable electronics. *Adv. Funct. Mater.* **2016**, *27*, 1604378.

(16) He, E.; Sun, Y.; Wang, X.; Chen, H.; Sun, B.; Gu, B.; Zhang, W. 3D angle-interlock woven structural wearable triboelectric nanogenerator fabricated with silicone rubber coated graphene oxide/cotton composite yarn. *Composites, Part B* **2020**, *200*, 108244.

CHAPTER 5

- (17) Zhu, M.; Huang, Y.; Ng, W.S.; Liu, J.; Wang, Z.; Wang, Z.; Hu, H.; Zhi, C. 3D spacer fabric based multifunctional triboelectric nanogenerator with great feasibility for mechanized large-scale production. *Nano Energy* **2016**, *27*, 439-446.
- (18) Chen, J.; Wen, X.; Liu, X.; Cao, J.; Ding, Z.; Du, Z. Flexible hierarchical helical yarn with broad strain range for self-powered motion signal monitoring and human-machine interactive. *Nano Energy* **2021**, *80*, 105446.
- (19) Huang, T.; Zhang, J.; Yu, B.; Yu, H.; Long, H.; Wang, H.; Zhang, Q.; Zhu, M. Fabric texture design for boosting the performance of a knitted washable textile triboelectric nanogenerator as wearable power. *Nano Energy* **2019**, *58*, 375-383.
- (20) Zhang, X.; Wang, J.; Xing, Y.; Li, C. Woven Wearable Electronic Textiles as Self-Powered Intelligent Tribo-Sensors for Activity Monitoring. *Global Challenges* **2019**, *3*, 1900070.
- (21) Zhu, M.; Shi, Q.; He, T.; Yi, Z.; Ma, Y.; Yang, B.; Chen, T.; Lee, C. Self-powered and self-functional cotton sock using piezoelectric and triboelectric hybrid mechanism for healthcare and sports monitoring. *ACS Nano* **2019**, *13*, 1940-1952.
- (22) Dong, K.; Deng, J.; Zi, Y.; Wang, Y.C.; Xu, C.; Zou, H.; Ding, W.; Dai, Y.; Gu, B.; Sun, B.; Wang, Z.L. 3D orthogonal woven triboelectric nanogenerator for effective biomechanical energy harvesting and as self-powered active motion sensors. *Adv. Mater.* **2017**, *29*, 1702648.
- (23) Dong, K.; Peng, X.; An, J.; Wang, A. C.; Luo, J.; Sun, B.; Wang, J.; Wang, Z.L. Shape adaptable and highly resilient 3D braided triboelectric nanogenerators as e-textiles for power and sensing. *Nat. Commun.* **2020**, *11*, 1-11.
- (24) Ning, C.; Dong, K.; Cheng, R.; Yi, J.; Ye, C.; Peng, X.; Sheng, F.; Jiang, Y.; Wang, Z.L. Flexible and stretchable fiber-shaped triboelectric nanogenerators for biomechanical monitoring and human-interactive sensing. *Adv. Funct. Mater.* **2021**, *31*, 2006679.

CHAPTER 5

(25) Seung, W.; Yoon, H.J.; Kim, T.Y.; Kang, M.; Kim, J.; Kim, H.; Kim, S. M.; Kim, S.W. Dual Friction Mode Textile-Based Tire Cord Triboelectric Nanogenerator. *Adv. Funct. Mater.* **2020**, *30*, 2002401.

(26) Dong, K.; Wang, Y.C.; Deng, J.; Dai, Y.; Zhang, S. L.; Zou, H.; Gu, B.; Sun, B.; Wang, Z.L. A highly stretchable and washable all-yarn-based self-charging knitting power textile composed of fiber triboelectric nanogenerators and supercapacitors. *ACS Nano* **2017**, *11*, 9490-9499.

(27) Lai, Y.C.; Deng, J.; Zhang, S. L.; Niu, S.; Guo, H.; Wang, Z. L. Single-thread-based wearable and highly stretchable triboelectric nanogenerators and their applications in cloth-based self-powered human-interactive and biomedical sensing. *Adv. Funct. Mater.* **2016**, *27*, 1604462.

(28) Xie, L.; Chen, X.; Wen, Z.; Yang, Y.; Shi, J.; Chen, C.; Peng, M.; Liu, Y.; Sun, X. Spiral steel wire based fiber-shaped stretchable and tailorable triboelectric nanogenerator for wearable power source and active gesture sensor. *Nano-Micro Lett.* **2019**, *11*, 39.

(29) Chen, C.; Chen, L.; Wu, Z.; Guo, H.; Yu, W.; Du, Z.; Wang, Z. L. 3D double-faced interlock fabric triboelectric nanogenerator for bio-motion energy harvesting and as self-powered stretching and 3D tactile sensors. *Mater. Today* **2020**, *32*, 84-93.

(30) Kim, D.; Park, J.; Kim, Y.T. Core-shell and helical-structured cylindrical triboelectric nanogenerator for wearable energy harvesting. *ACS Appl. Energy Mater.* **2019**, *2*, 1357-1362.

(31) Tian, Z.; He, J.; Chen, X.; Wen, T.; Zhai, C.; Zhang, Z.; Cho, J.; Chou, X.; Xue, C. Core-shell coaxially structured triboelectric nanogenerator for energy harvesting and motion sensing. *RSC Adv.* **2018**, *8*, 2950-2957.

(32) Dong, K.; Wu, Z.; Deng, J.; Wang, A.C.; Zou, H.; Chen, C.; Hu, D.; Gu, B.; Sun, B.; Wang, Z.L. A stretchable yarn embedded triboelectric nanogenerator as electronic

CHAPTER 5

skin for biomechanical energy harvesting and multifunctional pressure sensing. *Adv. Mater.* **2018**, *30*, 1804944.

(33) Park, J.; Choi, A. Y.; Lee, C. J.; Kim, Y. T. Highly stretchable fiber-based single-electrode triboelectric nanogenerator for wearable devices. *RSC Adv.* **2017**, *7*, 54829-54834.

(34) Pu, X.; Song, W.; Liu, M.; Sun, C.; Du, C.; Jiang, C.; Huang, X.; Zou, D.; Hu, W.; Wang, Z. L. Wearable power-textiles by integrating fabric triboelectric nanogenerators and fiber-shaped dye-sensitized solar cells. *Adv. Energy Mater.* **2016**, *6*, 1601048.

(35) Zhang, Z.; Chen, Y.; Debeli, D.K.; Guo, J. S. Facile method and novel dielectric material using a nanoparticle-doped thermoplastic elastomer composite fabric for triboelectric nanogenerator applications. *ACS Appl. Mater. Interfaces* **2018**, *10*, 13082-13091.

(36) Yuan, F.; Liu, S.; Zhou, J.; Fan, X.; Wang, S.; Gong, X. A smart Kevlar-based triboelectric nanogenerator with enhanced anti-impact and self-powered sensing properties. *Smart Mater. Struct.* **2020**, *29*, 125007.

(37) Cao, R.; Pu, X.; Du, X.; Yang, W.; Wang, J.; Guo, H.; Zhao, S.; Yuan, Z.; Zhang, C.; Li, C.; Wang, Z.L. Screen-printed washable electronic textiles as self-powered touch/gesture tribo-sensors for intelligent human-machine interaction. *ACS Nano* **2018**, *12*, 5190-5196.

(38) Guan, X.; Xu, B.; Wu, M.; Jing, T.; Yang, Y.; Gao, Y. Breathable, washable and wearable woven-structured triboelectric nanogenerators utilizing electrospun nanofibers for biomechanical energy harvesting and self-powered sensing. *Nano Energy* **2021**, *80*, 105549.

(39) Qiu, Q.; Zhu, M.; Li, Z.; Qiu, K.; Liu, X.; Yu, J.; Ding, B. Highly flexible, breathable, tailorable and washable power generation fabrics for wearable electronics. *Nano Energy* **2019**, *58*, 750-758.

CHAPTER 5

- (40) Zhang, L.; Su, C.; Cui, X.; Li, P.; Wang, Z.; Gu, L.; Tang, Z. Free-Standing Triboelectric Layer-Based Full Fabric Wearable Nanogenerator for Efficient Mechanical Energy Harvesting. *ACS Appl. Electron. Mater.* **2020**, *2*, 3366-3372.
- (41) Kim, T.; Jeon, S.; Lone, S.; Doh, S.J.; Shin, D.M.; Kim, H.K.; Hwang, Y.H.; Hong, S.W. Versatile nanodot-patterned Gore-Tex fabric for multiple energy harvesting in wearable and aerodynamic nanogenerators. *Nano Energy* **2018**, *54*, 209-217.
- (42) Peng, X., Dong, K., Ye, C., Jiang, Y., Zhai, S., Cheng, R., Liu, D.; Gao, X.; Wang, J.; Wang, Z. L. A breathable, biodegradable, antibacterial, and self-powered electronic skin based on all-nanofiber triboelectric nanogenerators. *Sci. Adv.* **2020**, *6*, eaba9624.
- (43) Cheng, R.; Dong, K.; Liu, L.; Ning, C.; Chen, P.; Peng, X.; Liu, D.; Wang, Z.L. Flame-retardant textile-based triboelectric nanogenerators for fire protection applications. *ACS Nano* **2020**, *14*, 15853-15863.
- (44) Dong, K., Hu, Y., Yang, J., Kim, S. W., Hu, W., Wang, Z. L. Smart textile triboelectric nanogenerators: Current status and perspectives. *MRS Bull.* **2021**, *46*, 512-521.
- (45) Niu, S., Wang, S., Lin, L., Liu, Y., Zhou, Y. S., Hu, Y., Wang, Z. L. Theoretical study of contact-mode triboelectric nanogenerators as an effective power source. *Energy Environ. Sci.* **2013**, *6*, 3576-3583.

Chapter 6: Three-Dimensional Woven Structured Triboelectric Nanogenerator with Enhanced Wearability and Durability

6.1 Introduction

The rapid development of wearable electronics has brought tremendous convenience to our daily life, and has gradually applied into various fields, such as health management, smart sports, and entertainment.¹⁻³ However, the flexible power source suitable for these wearable electronics is still an urgent mission. The triboelectric nanogenerator (TENG) is a newly developed energy harvesting technology that can effectively convert biomechanical energy into electrical energy, based on the coupling effect of contact electrification and electrostatic induction.⁴⁻⁷ Considering its inherent characteristics such as low cost, extensive material source, high efficiency and versatility, TENG has promising applications in harvesting energy.⁸⁻¹⁰ As one of common and sustainable energy, human motion can be harvested by wearable textile-based triboelectric nanogenerators (t-TENGs).¹¹ The cloth made of t-TENG not only meets the comfort of wearing, but also can collect human movement energy for power supply at anywhere and anytime. In view of this, textiles can be chosen as the best medium for TENG owing to its lightness, breathability and flexibility. The emerging TENG combined with traditional textile technology provides a broad application for self-powered textiles.¹²

Up to now, some t-TENGs with numerous materials, various structures and fabrication techniques have been reported.¹³⁻²³ However, the further development of t-TENGs still faces several dilemmas. Firstly, some woven structured t-TENGs consist of one

CHAPTER 6

material, which greatly limits the functionality of TENGs. For example, the water transport in some t-TENGs with prevention of water penetration fabricated by hydrophobic fibers is bidirectional,²⁴⁻²⁷ which means that the inner face of t-TENGs will still be cling to the body in the process of moisture transfer.²⁸ Moreover, multilayer fabric-based TENGs realized by directly stacking functional fabrics/films together have been extensively studied and reported, including stacking of nanofiber films,^{29, 30} stacking of fabrics,³¹ stacking of films and fabrics,³²⁻³⁵ and so on. Some directional water transport textiles were also fabricated through stacking of nanofibers.³⁶ But the biggest problem with this structure is that the interface is easily delaminated. Furthermore, most t-TENGs were fabricated by coating, electrospinning, electrospraying and other techniques, which attached some conductive and frictional materials to the yarn and fabric.³⁷⁻⁴³ Due to the variable bending structure and uneven surface characteristics of textiles, the coating on t-TENG is easy cracking/delamination, leading to low abrasion resistance and poor durability.⁴⁴⁻⁴⁹ Because the complex and time-consuming chemical preparation process is neither economical nor environmentally friendly, it is difficult to mass-produce with existing textile manufacturing technology.⁵⁰⁻⁵⁵ Some directional water transport textiles created through chemical finishing may have the above problems and cause environmental pollution and health issues.⁵⁶

In this chapter, a 3D triboelectric nanogenerator fabric (SP-FTENG) was designed and fabricated with support zone and functional zone which was composed of three layers, including the inner polypropylene (PP)-cotton fabric layer close to skin for moisture transfer and absorption, the middle Ag-cotton fabric layer for conducting electrode and antibacterial agent, and the outer polytetrafluoroethylene (PTFE)-cotton fabric layer for tribo-negative layer and repelling water, respectively. Based on structural design and

CHAPTER 6

rational materials configuration, versatility of woven-structured t-TENG is realized, including excellent electrical performance, wearability (directional water transport and breathability) and antibacterial property. Compared with t-TENGs with multilayer nanofiber film/fabric stacking structures, the fabric interface of this new structure fabricated by weaving the support area and the functional area together is not easily delaminated. In addition, fabric geometric models have been proposed to calculate the effective area of each yarn on each side for explaining the mechanism of water transport and the difference in output performance of various 3D FTENGs. This work addresses issues of wearing comfort and scalable manufacturing of versatile t-TENG with low-cost, and eco-friendly materials, while providing new insights into human motion monitoring from time to time, resulting in a promising research direction for sustainable smart and functional textiles.

6.2 Experimental Section

6.2.1 Materials

Polypropylene yarns of about 250 D and 900 D were bought from Alibaba where D (Denier) is a measurement of linear density of yarn: Grams per 9,000 metres of yarn. A Ag-plated nylon6 multifilament (yarn number 360 D) was purchased from Suzhou TEK Silver Fiber Technology Co., Ltd., China. Polytetrafluoroethylene yarn of 500 D was purchased from Shandong Senrong New Materials Co., Ltd, China. Polydimethylsiloxane (PDMS) was bought from Dow Corning.

6.2.2 Fabrication of the 3D FTENGs

CHAPTER 6

Cotton yarns were used as warp yarns, and the PTFE, Ag, PP yarns were prepared as weft yarns, which were set in corresponding positions according to the design of fabric weave. The 3D machine woven FTENGs were fabricated through an automatic rapier sample loom (SL8900, CCI TECH INC.).

6.2.3 Fabrication of the 3D SCP-FTENG

The 3D SP-FTENG with desired area was employed as flexible substrate for the construction of the SCP-FTENG. Firstly, PDMS (sylgard 184 silicone elastomer, Dow Corning) was prepared by mixing the two components with the weight ratio of 1:10. After mixing, the PDMS was degassed in vacuum for about 5 min to remove the air bubbles. Next, the PDMS was uniformly coated on the outer layer of functional zone with a brush. Finally, it was dried in an oven at 60 °C until the PDMS was dry and the 3D SCP-FTENG was formed. The conductive tapes were attached on the Ag layer.

6.2.4 Characterization and evaluation

The sample morphologies were investigated by the scanning electron microscope (SEM) of VEGA3, Tescan. The air permeability was characterized by an air permeability tester (SDL International M021S) following the standard (ASTM D737). Referring to ASTM E96-Option B, the water vapor transmission was investigated. The water contact angle (CA) of the 3D FTENGs was evaluated by using an optical contact angle measuring device (SDC-350, Sindin, China). By using a moisture management tester (MMT, SDL ATLAS, Ltd., China), the moisture management behavior of the 3D FTENGs was characterized. The electrical output performance of the 3D FTENGs was measured by an electrometer (Keithley 6514) and oscilloscope (DS1054Z). A keyboard life tester

CHAPTER 6

(ZX-A03) was employed to provide the compressing motion. The SP-FTENG was washed according to the standard method (AATCC 135). Abrasion resistance was investigated using the SDL Atlas Martindale Abrasion Tester. The antibacterial activities of the SP-FTENG were evaluated referring to GB/T 20944.3.

6.3 Results and Discussion

6.3.1 Design and fabrication of the 3D SP-FTENG

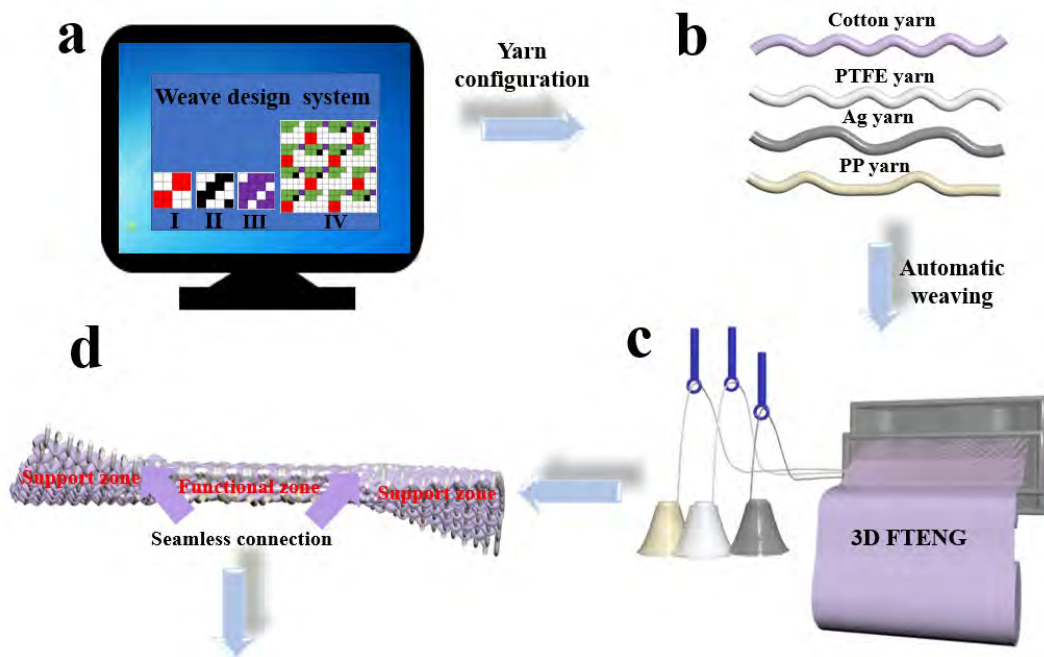
The fabrication procedures of the 3D SP-FTENG by traditional weaving technology are schematically described in Figure 6.1a-e. Figure 6.1a presents the weaving design system on which the 3D SP-FTENG was designed in professional weaving language. In the functional zone design of the SP-FTENG, the fabric structure has three levels from the inner layer to outer layer. As shown in Figure 6.1a, a matt weave structure (I) was designed for the outer layer owing to its greater compactness. Meanwhile, the arrangement ratio of the warp yarn density was designed as 1:1:2 from the inner, middle to the outer layers. The middle layer adopts a 2/2 right twill weave (II), and the inner layer used a 3/1 right twill weave (III). The red, black and purple dots represent warp interlacing points of the outer, middle, and inner layers, respectively. The combination of three-layer organization and green warp interlacing points constitutes the on-machine diagram of the SP-FTENG (IV). In Figure 6.1b, four types of yarns were selected to fabricate the SP-FTENG. PTFE yarn is hydrophobic and chosen as the negative dielectric material. Sliver (Ag) yarn was used as the antibacterial material and conductive material. By taking advantage of their inherent characteristics, cotton yarn and PP yarn were employed as hygroscopic and moisture conducting materials, respectively. The 3D SP-FTENG was woven by using an automatic rapier sample loom

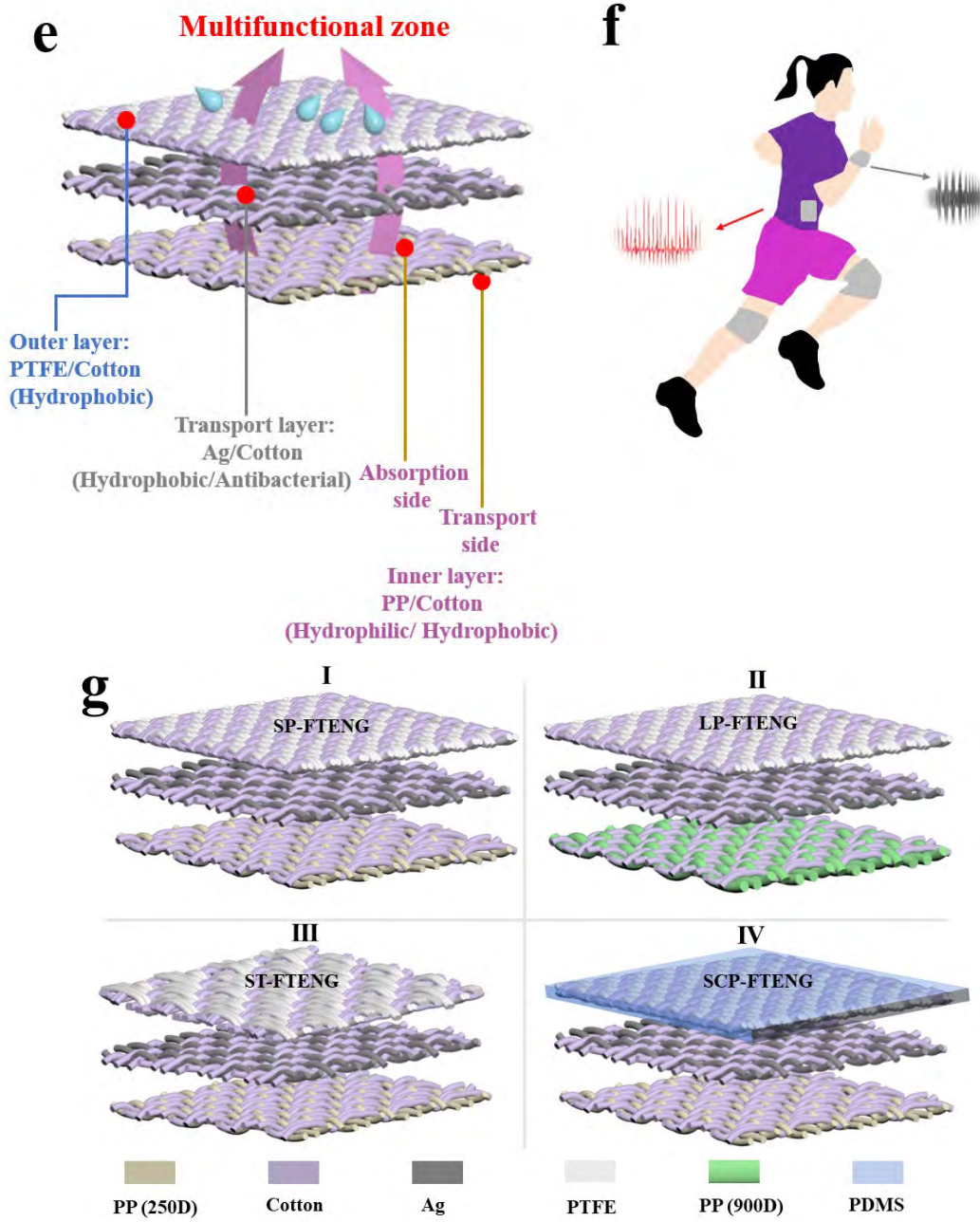
CHAPTER 6

(Figure 6.1c). Figure 6.1d presents the schematic illustration of the 3D SP-FTENG, which is divided into three various zones with both the functional zone for providing various functions and the support zones for targeting on mechanical support. This weaving technology makes the functional and support zones seamlessly connected to ensure the versatility and mechanical stability of the 3D SP-FTENG. Figure 6.1e schematically illustrates the design of the functional zone of the 3D SP-FTENG, which consists of three fabric layers from the inner to the outer layers, including the inner layer for moisture transfer and skin contact, the middle layer for conducting electrode and antibacterial agent, and the outer layer for contact electrification and repelling water. The inner layer mainly uses PP fibers as the skin-friendly layer, which have typical water-absorbing and hydrophobic characteristics. Therefore, it can quickly drain body surface sweat to the outer surface without a wet and sticky feeling. The cotton fiber was employed to fabricate the inner, middle and outer layers because it is a natural hydrophilic material that easily absorbs a large amount of water. Three layers with different cotton fiber content can quickly transfer the moisture from the inner layer to the middle and outer layer while storing excessive moisture. Regarding the materials of the outer layer, the PTFE as hydrophobic fiber can be utilized to achieve the hydrophobic function. Moreover, the strong ability of PTFE to attract electrons can ensure good electrical output. Due to the soft nature of the yarn, the fabric is endowed with wearability, which promotes their application as wearable devices. As shown in Figure 6.1f, the 3D SP-FTENG can be used for sportswear, which can harvest energy during exercise. To investigate the effect of yarn arrangement and PDMS coating on the electrical output and wearability, four types of 3D FTENGs with different functional zones were designed and compared, named SP-FTENG (I), LP-FTENG (II), ST-FTENG (III) and SCP-FTENG (IV) as follows in Figure 6.1g. Firstly, the difference between SP-FTENG (I) and LP-FTENG (II) is that the PP yarns used in the inner layer.

CHAPTER 6

Secondly, SP-FTENG (I) and ST-FTENG (III) adopt various outer layer structure. Thirdly, to explore the effect of PDMS coating on the electrical performance and wearability, the outer layer of functional zone of the SP-FTENG (I) was coated with PDMS, abbreviated as SCP-FTENG (IV), as presented in Figure 6.1g. The cross section of functional zone of the SP-FTENG and SEM images of the yarns used are illustrated in Figure 6.1h. The structures of the outer layer, middle layer and inner layer are the same as the designed structure. Owing to the soft and flexible characteristics of the SP-FTENG, it can be easily folded and rolled, just like the clothes we usually wear (Figure 6.1i).





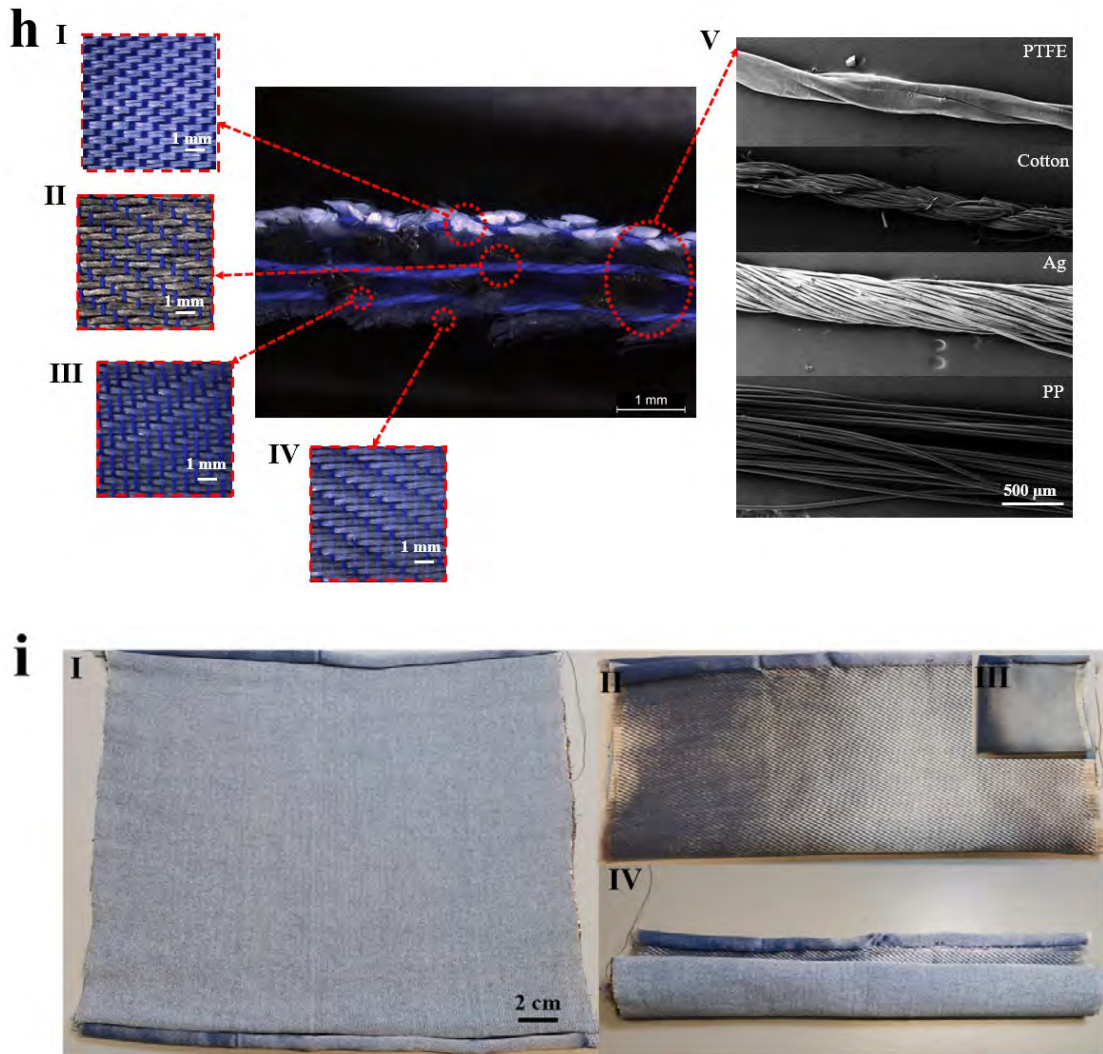


Figure 6.1 Structural design, schematic illustration and fabrication process of a 3D SP-FTENG. (a) Design system and weave structure of functional zone of the 3D SP-FTENG, outer layer (I), middle layer (II), inner layer (III), on-machine diagram (IV). (b) Schematic of weaving yarns. (c) Schematic diagram of fabrication process of the 3D SP-FTENG. (d) Schematic illustration of the 3D SP-FTENG. (e) Schematic diagram of the multifunctional zone structure of the 3D SP-FTENG. (f) Application scenarios of the 3D SP-FTENG. (g) Schematic diagrams of different functional zones of 3D FTENGs: (I) SP-FTENG; (II) LP-FTENG; (III) ST-FTENG; (IV) SCP-FTENG. (h) The photographs of functional zone of the 3D SP-FTENG, outer layer consisting of PTFE yarn and cotton yarn (I), middle layer consisting of Ag yarn and cotton yarn (II),

CHAPTER 6

inner layer consisting of PP yarn and cotton yarn (III and IV), SEM images of PTFE yarn, cotton yarn, Ag yarn and PP yarn (V). (i) Photographic images of the fabricated 3D SP-FTENG (I) with different deformations, such as folded (II and III) and scrolled (IV).

6.3.2 Working mechanism of the SP-FTENG

As shown in Figure 6.2, the SP-FTENG operates in the typical single-electrode mode. Taking rubber film as the external contact material, under a vertical impacting force, the rubber film periodically contacts and separates from the SP-FTENG. Since the rubber film and PTFE have different electron affinities, the PTFE that contacts with the rubber film is endowed with negative charges, and the surface of rubber film is positively charged due to the triboelectrification effect (Figure 6.2I). When the rubber film and the SP-FTENG are separated from each other, electrons flow from the electrode to the ground for the purpose of equilibrating the triboelectric potential (Figure 6.2II). When the rubber film and the SP-FTENG are completely separated, the electrostatic equilibrium is reached (Figure 6.2III). Subsequently, as the rubber film is driven to contact with the SP-FTENG again, the opposite electron flow appears from the ground to the electrode (Figure 6.2IV). When the rubber film has intimate contact with the SP-FTENG again, all induced charges are neutralized again (Figure 6.2I). As a consequence, a periodical alternating current generates with cyclic contact and separation.

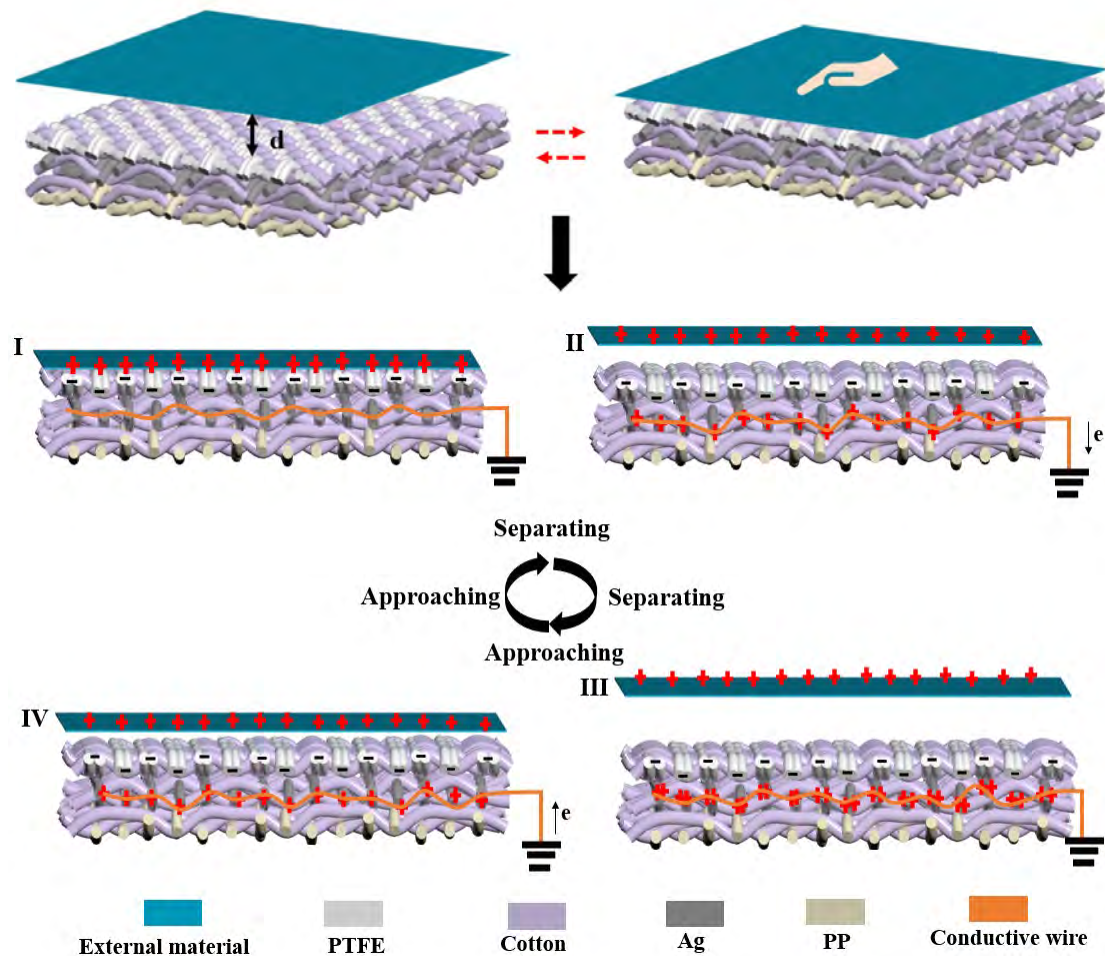


Figure 6.2 Schematic illustration of the operation principle of the SP-FTENG.

6.3.3 Geometric models of the functional zones of the 3D FTENGs

The yarn area presented in each layer not only affects the electrical output of the TENGs but also has a significant impact on the wearability of the TENGs. Due to the different yarn organization structures and fineness of three layers including the outer, middle, and inner layers, the percentage of yarn area presented on each side of every layer is different. Therefore, it is necessary to establish related geometric models of the functional zones of the 3D FTENGs to calculate yarn area. As shown in Figure 6.3a, there are six sides in the three layers, which are abbreviated as O1 and O2 for outer layer, M3 and M4 for middle layer, I5 and I6 for inner layer.

CHAPTER 6

Figure 6.3b shows the diagrams of outer layer structure of the SP-FTENG. In this structure, one repeating unit includes eight warp and weft yarns, respectively. Regarding the weave repeat unit, six geometrical parameters are proposed for calculating the cotton and PTFE yarns area percentage of outer layer. In order to obtain the values of geometric parameters, a Leica M165 C microscope was used to capture the microscopic image of the fabric. Based on these images, these parameters were measured. The area of PTFE and cotton yarns presented on the outer surface of the SP-FTENG could be calculated by the following equations:

$$\text{cotton area percentage in one unit} = \frac{16f_1d_0}{L_0W_0} = \frac{16f_1d_0}{(2f_1+4d_1)(2f_0+4d_0)} \quad (1)$$

$$\text{PTFE area percentage in one unit} = \frac{16f_0d_1}{L_0W_0} = \frac{16f_0d_1}{(2f_1+4d_1)(2f_0+4d_0)} \quad (2)$$

where d_0 and d_1 are the warp and weft yarn diameters of outer layer, respectively. W_0 is the width of one repeating unit. L_0 is the length of one repeating unit. f_0 and f_1 are the yarn floats as given by the presented geometric model.

Meanwhile, the related parameters of cotton, Ag and PP yarns in the middle and inner layers of the SP-FTENG were acquired using the same method, as presented in Figure 6.3c-e. The area of cotton and Ag yarns presented on the middle surface of the SP-FTENG could be calculated by the following equations:

$$\text{cotton area percentage in one unit} = \frac{4f_4d_2}{L_1W_1} = \frac{4f_4d_2}{(f_4+f_5+2d_3)(f_2+f_3+2d_2)} \quad (3)$$

$$\text{Ag area percentage in one unit} = \frac{(f_2+f_3)*d_3*4}{L_1W_1} = \frac{(f_2+f_3)*d_3*4}{(f_4+f_5+2d_3)(f_2+f_3+2d_2)} \quad (4)$$

where d_2 and d_3 are the warp and weft yarn diameters of middle layer, respectively. W_1 is the width of one repeating unit. L_1 is the length of one repeating unit. f_2, f_3, f_4, f_5 are the yarn floats, as given by the shown geometric model (Figure 6.3c).

CHAPTER 6

The area of cotton and PP yarns presented on the inner surface (I5 side) of the SP-FTENG could be calculated by the following equations:

$$\text{cotton area percentage in one unit} = \frac{4f_8d_4}{L_2W_2} = \frac{4f_8d_4}{(f_8+d_5)(f_6+2f_7+3d_4)} \quad (5)$$

$$\text{PP area percentage in one unit} = \frac{(f_6+2f_7)*4d_5}{L_2W_2} = \frac{(f_6+2f_7)*4d_5}{(f_8+d_5)(f_6+2f_7+3d_4)} \quad (6)$$

where d_4 and d_5 are the warp and weft yarn diameters of inner layer, respectively. W_2 is the width of one repeating unit. L_2 is the length of one repeating unit. f_6, f_7, f_8 are given by the shown geometric model (Figure 6.3d).

The area of cotton and PP yarns presented on the inner surface (I6 side) of the SP-FTENG could be calculated by the following equations:

$$\text{cotton area percentage in one unit} = \frac{4f_{10}d_6}{L_3W_3} = \frac{4f_{10}d_6}{(f_{10}+2f_{11}+3d_7)(f_9+d_6)} \quad (7)$$

$$\text{PP area percentage in one unit} = \frac{4f_9d_7}{L_3W_3} = \frac{4f_9d_7}{(f_{10}+2f_{11}+3d_7)(f_9+d_6)} \quad (8)$$

where d_6 and d_7 are the warp and weft yarn diameters of inner layer, respectively. W_3 is the width of one repeating unit. L_3 is the length of one repeating unit. f_9, f_{10}, f_{11} are given by the shown geometric model (Figure 6.3e).

The area of cotton and PTFE yarns presented on the outer surface (O1 side) of the ST-FTENG could be calculated by the following equations:

$$\text{cotton area percentage in one unit} = \frac{8f_{13}d_8}{L_4W_4} = \frac{8f_{13}d_8}{(f_{14}+f_{13})(f_{12}+2d_8)} \quad (9)$$

$$\text{PTFE area percentage in one unit} = \frac{(f_{14}+f_{13})f_{12}}{L_4W_4} = \frac{(f_{14}+f_{13})f_{12}}{(f_{14}+f_{13})(f_{12}+2d_8)} \quad (10)$$

where d_8 is the warp yarn diameter of outer layer. W_4 is the width of one repeating unit.

CHAPTER 6

L_4 is the length of one repeating unit. f_{12}, f_{13}, f_{14} are given by the shown geometric model (Figure 6.3f).

The area of cotton and PTFE yarns presented on the outer surface (O2 side) of the ST-FTENG could be calculated by the following equations:

$$\text{cotton area percentage in one unit} = \frac{8f_{17}d_9}{L_5W_5} = \frac{8f_{17}d_9}{(f_{17}+2d_{10})(f_{15}+2f_{16}+6d_9)} \quad (11)$$

$$\text{PTFE area percentage in one unit} = \frac{(f_{15}+2f_{16}) \cdot 8d_{10}}{L_5W_5} = \frac{(f_{15}+2f_{16}) \cdot 8d_{10}}{(f_{17}+2d_{10})(f_{15}+2f_{16}+6d_9)} \quad (12)$$

where d_9 and d_{10} are the warp and weft yarn diameters of outer layer. W_5 is the width of one repeating unit. L_5 is the length of one repeating unit. f_{15}, f_{16}, f_{17} are given by the shown geometric model (Figure 6.3g).

The area of cotton and PP yarns presented on the inner surface (I5 side) of the LP-FTENG could be calculated by the following equations:

$$\text{cotton area percentage in one unit} = \frac{4f_{20}d_{11}}{L_6W_6} = \frac{4f_{20}d_{11}}{(f_{20}+d_{12})(f_{18}+2f_{19}+3d_{11})} \quad (13)$$

$$\text{PP area percentage in one unit} = \frac{(f_{20}+d_{12})(f_{18}+2f_{19})}{L_6W_6} = \frac{(f_{20}+d_{12})(f_{18}+2f_{19})}{(f_{20}+d_{12})(f_{18}+2f_{19}+3d_{11})} \quad (14)$$

where d_{11} and d_{12} are the warp and weft yarn diameters of inner layer, respectively. W_6 is the width of one repeating unit. L_6 is the length of one repeating unit. f_{18}, f_{19}, f_{20} are given by the shown geometric model (Figure 6.3h).

The area of cotton and PP yarns presented on the inner surface (I6 side) of the LP-FTENG could be calculated by the following equations:

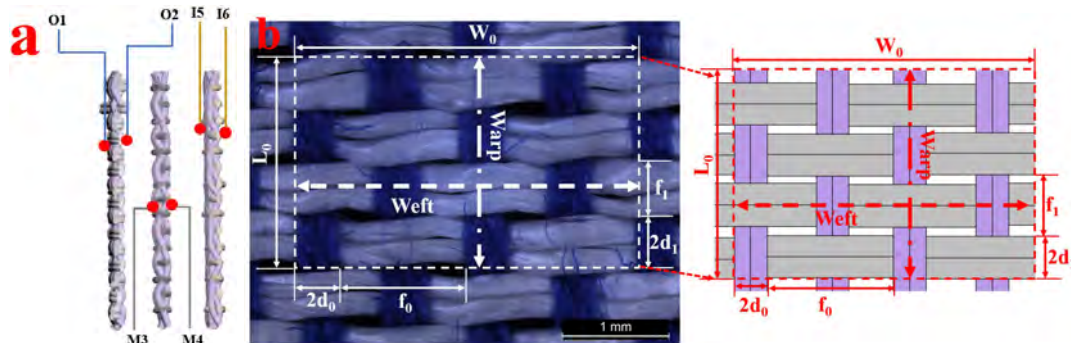
$$\text{cotton area percentage in one unit} = \frac{4d_{14}d_{13}}{L_7W_7} = \frac{4d_{14}d_{13}}{(f_{23}+f_{22})(f_{21}+d_{13})} \quad (15)$$

CHAPTER 6

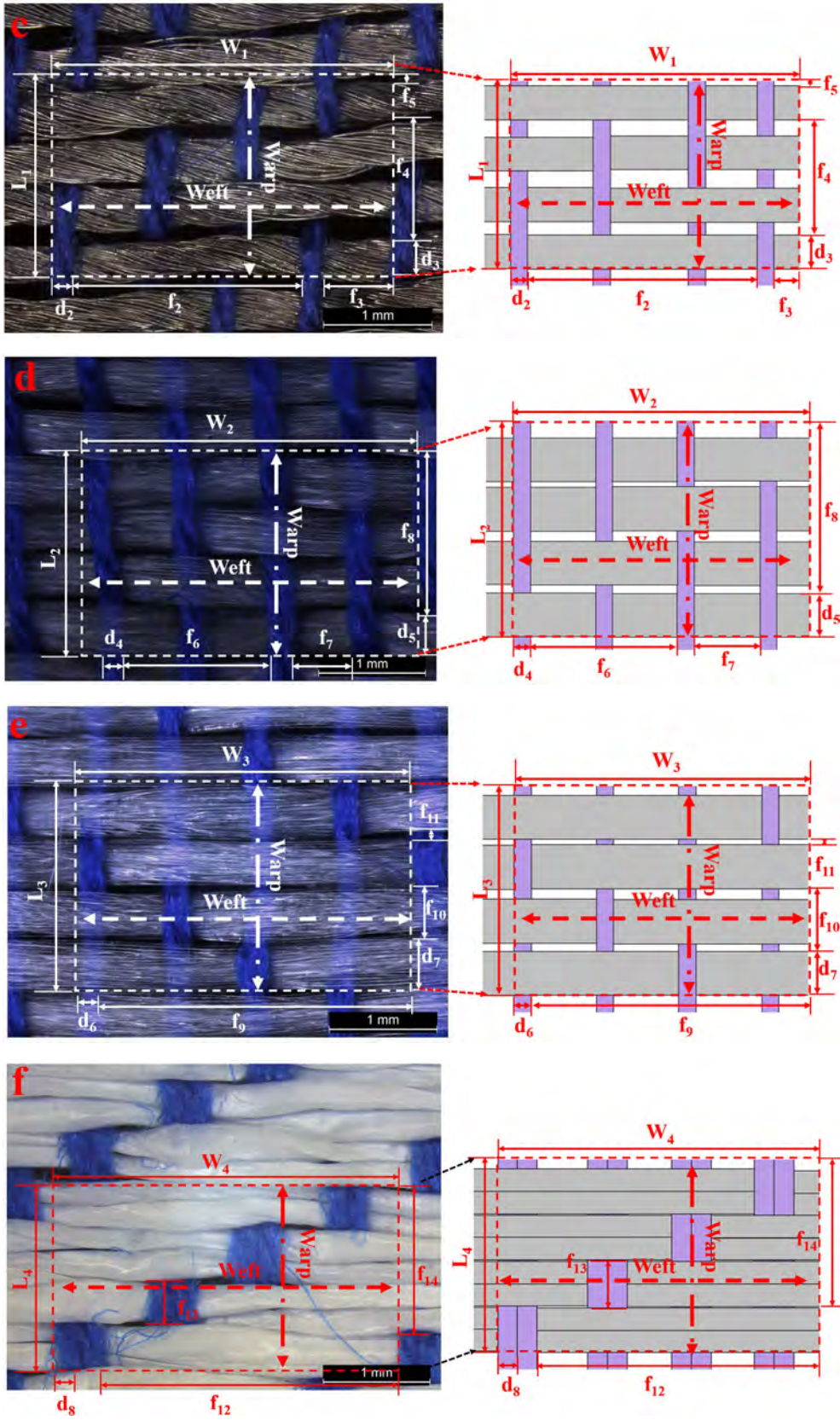
$$PP \text{ area percentage in one unit} = \frac{(f_{23}+f_{22})f_{21}}{L_7W_7} = \frac{(f_{23}+f_{22})f_{21}}{(f_{23}+f_{22})(f_{21}+d_{13})} \quad (16)$$

where d_{13} and d_{14} are the warp and weft yarn diameters of inner layer, respectively. W_7 is the width of one repeating unit. L_7 is the length of one repeating unit. f_{21} , f_{22} , f_{23} are given by the shown geometric model (Figure 6.3i).

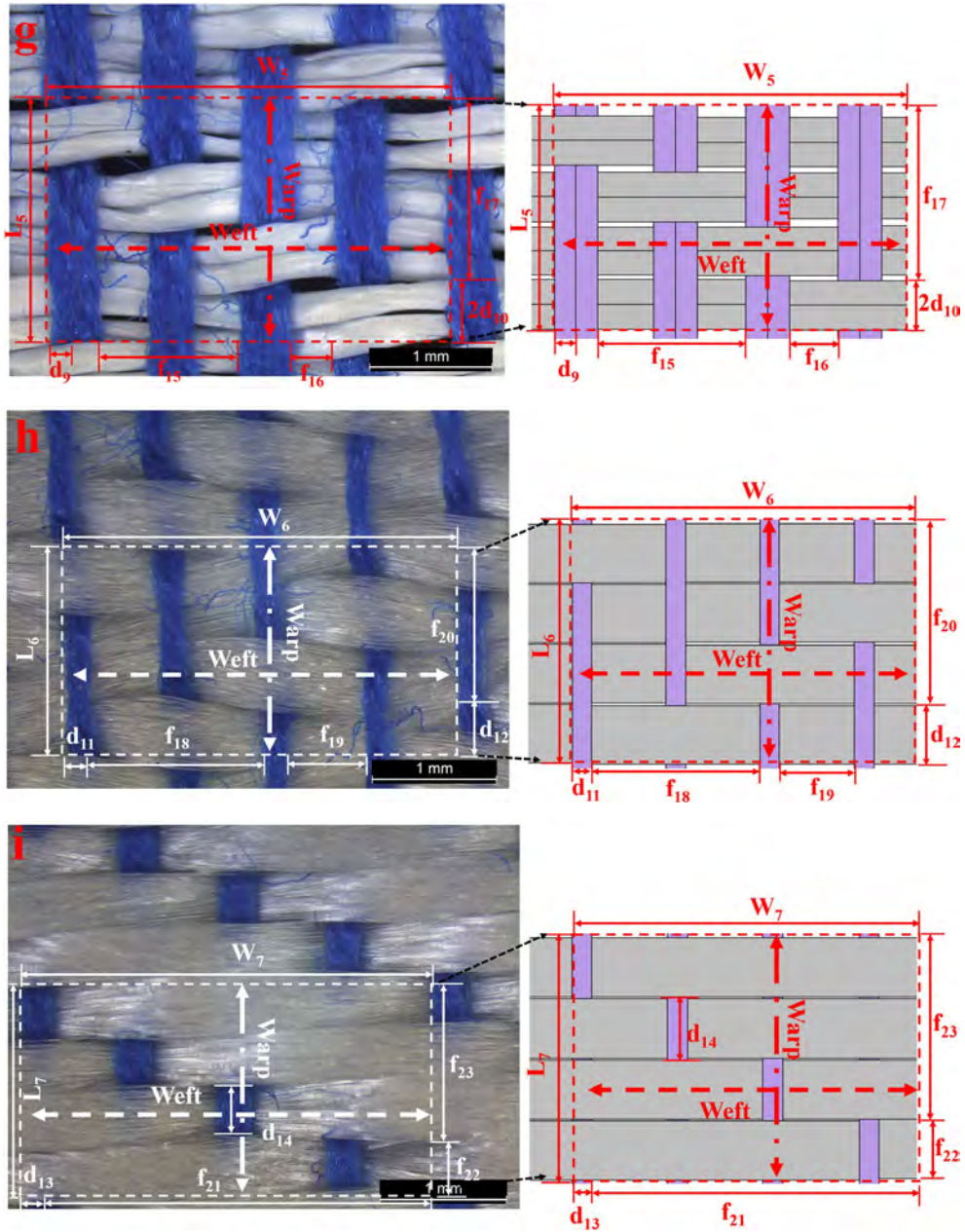
Based on the geometric models, the yarn area percentage of various 3D FTENGs is calculated, as indicated in Figure 6.3j. For the SP-FTENG, it can be observed that PTFE, Ag and PP yarns are the main yarns constituting the outer, middle and inner layers, respectively. The difference between the SP-FTENG and LP-FTENG is the fineness of PP yarn in the inner layer. It is found that there is little difference in the surface area percentages of the cotton and PP yarns presented on inner layer (I5 and I6 sides) of the SP-FTENG and LP-FTENG. The area percentages of PTFE and cotton yarns on the O1 side of the SP-FTENG are 70% and 26%, respectively. Since the SP-FTENG and ST-FTENG adopt different outer structures, namely matt and derivation twill weave, the area percentages of PTFE and cotton yarns on the O1 side of the ST-FTENG are 87% and 15%, respectively. After the outer layer of the SP-FTENG was coated with PDMS, the PDMS film covered the O1 and O2 sides of the SCP-FTENG.



CHAPTER 6



CHAPTER 6



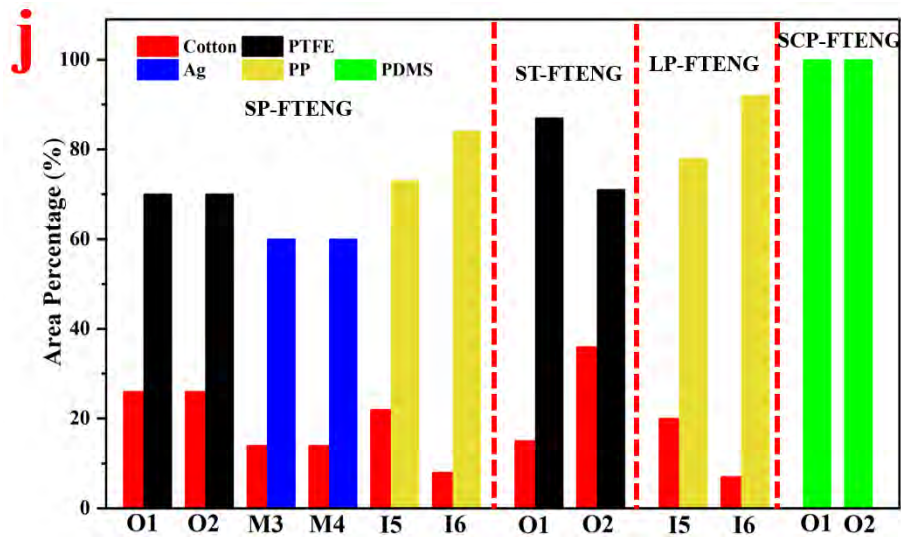


Figure 6.3 (a) Description of different sides of the functional zone. Characterization of geometry of functional zone in the SP-FTENG, outer layer (b), middle layer (c), inner layer (I5 side: (d), I6 side: (e)). Characterization of geometry of the ST-FTENG outer layer (O1 side: (f), O2 side: (g)). Characterization of geometry of the LP-FTENG inner layer (I5 side: (h), I6 side: (i)). (j) Yarn area percentage on different sides of functional zone in various 3D FTENGs.

6.3.4 Electrical output performance

The output performance of four 3D FTENGs was systematically studied. As indicated in Figure 6.4, the peak voltage values for the SP-FTENG, LP-FTENG, ST-FTENG and SCP-FTENG are 27.47 V, 24.03 V, 32.08 V and 47.63 V, respectively. Such difference in output could be attributed to the effective contact area and materials. For the electrical output of the SP-FTENG and LP-FTENG, the voltage only varies up and down in a small range. However, the output voltage of the ST-FTENG is higher than that of the SP-FTENG. Because the polarity difference of the PTFE and rubber is higher than that of the rubber and cotton, the PTFE yarn area percentage of the O1 side contacting with rubber film is a pivotal geometric parameter that determines the

CHAPTER 6

electrical output performance. The area percentages of PTFE yarns in O1 sides of the SP-FTENG and the ST-FTENG are 70% and 87%, respectively. Therefore, the difference of the electrical output voltage can be ascribed to more PTFE yarns exposed on the surface, thereby having more contact area with the rubber film. When the outer layer of the SP-FTENG is coated with PDMS, the output voltage of the SCP-FTENG is increased by 1.7 times compared with the untreated SP-FTENG. The remarkable enhancement can be attributed to the larger effective contact area of the film. The effective contacting area percentage of film is 100%, which is higher than that of the untreated SP-FTENG.

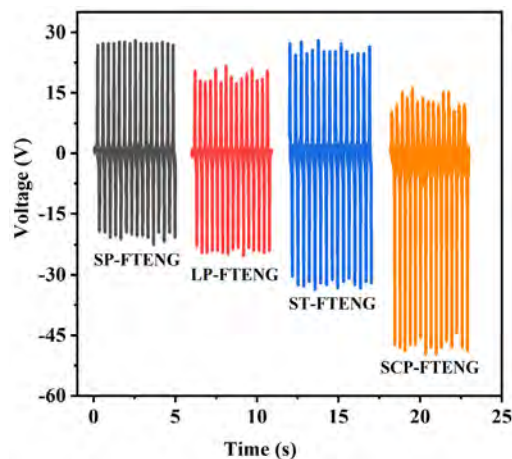


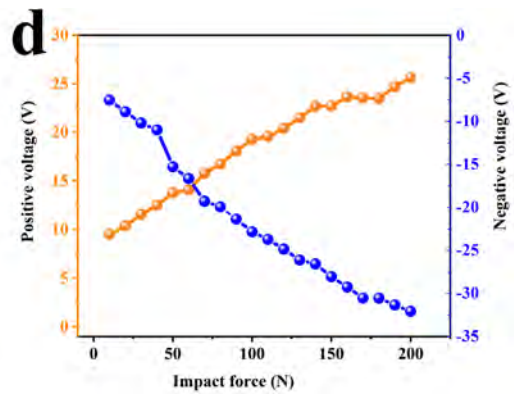
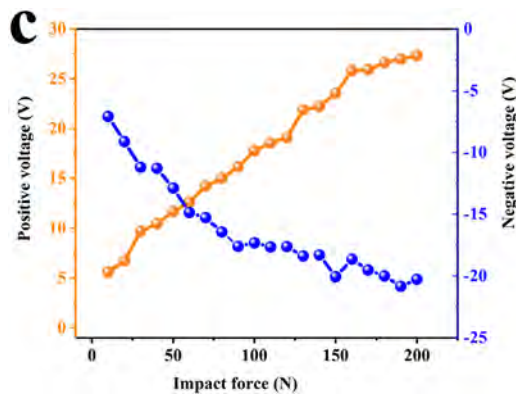
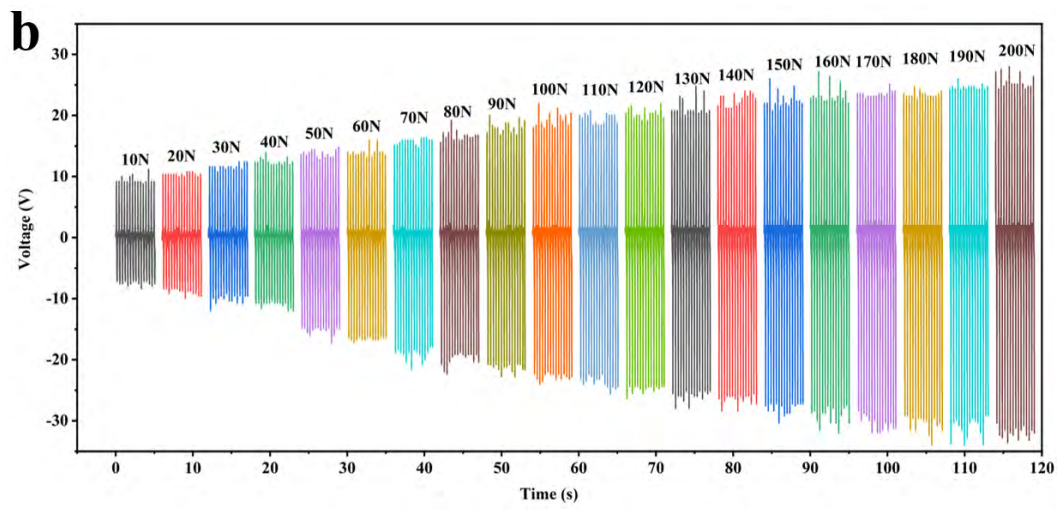
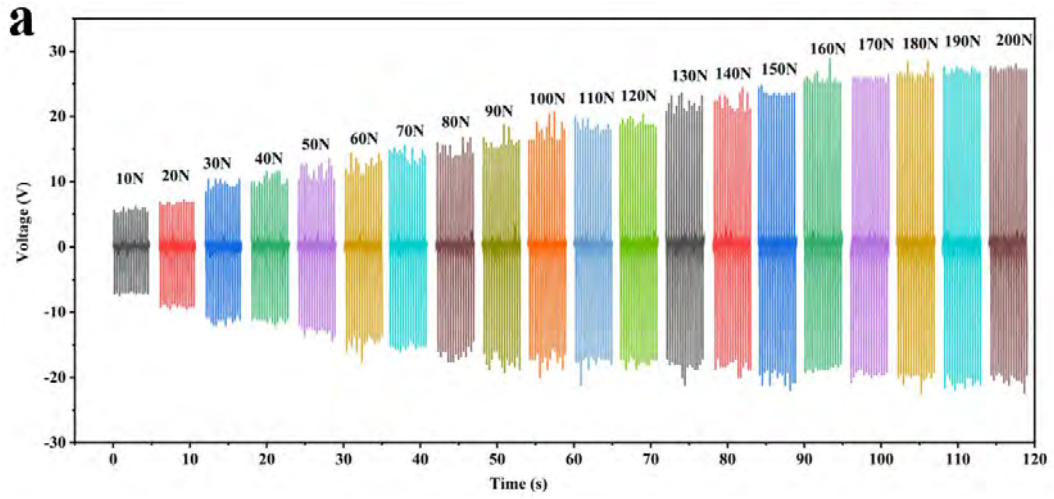
Figure 6.4 The output voltage of the 3D FTENGs with different structures and materials.

In order to further study the sensing performance of the SP-FTENG and ST-FTENG, the effect of impact force on the output voltage was evaluated. The output voltages of the SP-FTENG and ST-FTENG under a mechanical force from 10 N to 200 N are shown in Figure 6.5a and b. The results reveal that the voltages of the 3D FTENGs are gradually enhanced with the increasing force. Additionally, there is a phenomenon of asymmetric positive and negative peaks. As indicated in Figure 6.5c and d, it can also be observed that there exists a difference between the positive peak and negative peak

CHAPTER 6

voltage during contact and separation stage. Initially, with the increase of impact force, the negative peak output voltage of SP-FTENG increases quickly. But as the impact force exceeds 150 N, the negative voltage shows little fluctuation and enters a plateau. It can eventually reach -20.27 V. However, the peak value of the positive voltage presents a sustained and rapid increase. The maximum of 27.33 V can be achieved. Regarding the ST-FTENG, as the impacting force increases from 10 N to 200 N, the positive and negative peak output voltages increase quickly, respectively. The maximum voltage of 25.63 V and -32.90 V can be obtained. The phenomenon should be primarily relevant to the inherent adhesion of the triboelectric surfaces, which leads to the 3D FTENGs layers to separate sporadically with an applied motion, thus inducing impulsive separation.⁵⁷ When the impact force is small, the contact of the triboelectric surface is relatively smooth. So the corresponding voltage peak is uniform. Under the very large impact force, the air of the impact interface is significantly squeezed out owing to the strong compression of the 3D FTENGs. Therefore, the 3D FTENGs are flattened and temporarily adsorbed on impact plate together with the rubber film. The 3D FTENGs are driven by the impact board for a certain distance at the initial stage of separation. As a result, the effective increase of the vertical separation area and velocity means that more charge transfer occurs per unit time. This results in the asymmetry between the positive and negative peak. Furthermore, the relationships between the pressure and peak-to-peak voltage were plotted, as presented in Figure 6.5e. The linear fit indicates a good linear correction with pressure from 4 kPa to 80 kPa. Therefore, the 3D FTENGs can be used as pressure sensors.

CHAPTER 6



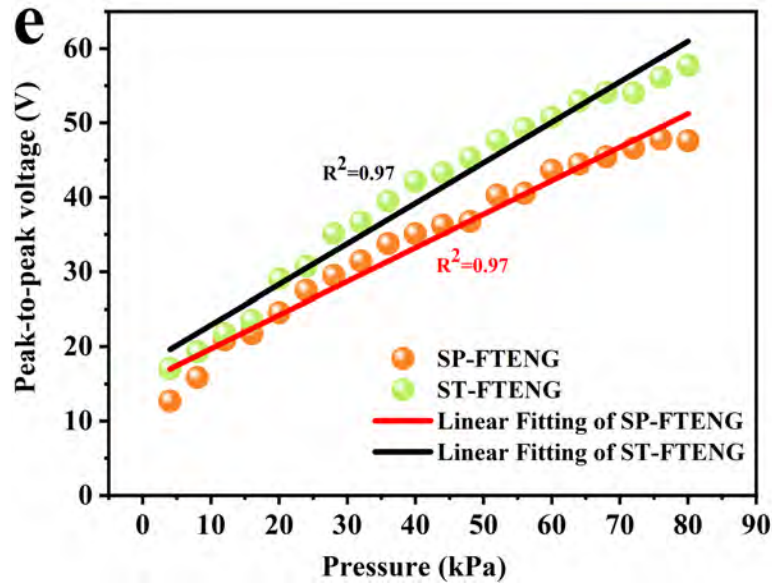


Figure 6.5 Output voltage of the 3D SP-FTEENG (a) and 3D ST-FTEENG (b) at different impact forces from 10 N to 200 N. The positive and negative voltage of the SP-FTEENG (c) and ST-FTEENG (d) at different impact forces from 10 N to 200 N. (e) The linear fit of the peak to peak voltages of the 3D FTENGs with increasing pressure from 4 kPa to 80 kPa.

The output performance by varying the contact/separation frequency under the impact force of 200 N is presented in Figure 6.6a and b. It is obvious that the output current increases from 0.76 μA to 1.76 μA because a larger impact frequency causes the increase of the number of pressures per unit time, which enhances the rate of charge transfer, thus leading to a higher current. In this study, the output voltage was measured by the device (oscilloscope) which is based on the measurement of flowing current through oscilloscope.⁵⁸ Therefore, the output voltage increases from 8.24 V to 27.33 V when the impacting frequency varies from 1 to 3 Hz.

CHAPTER 6

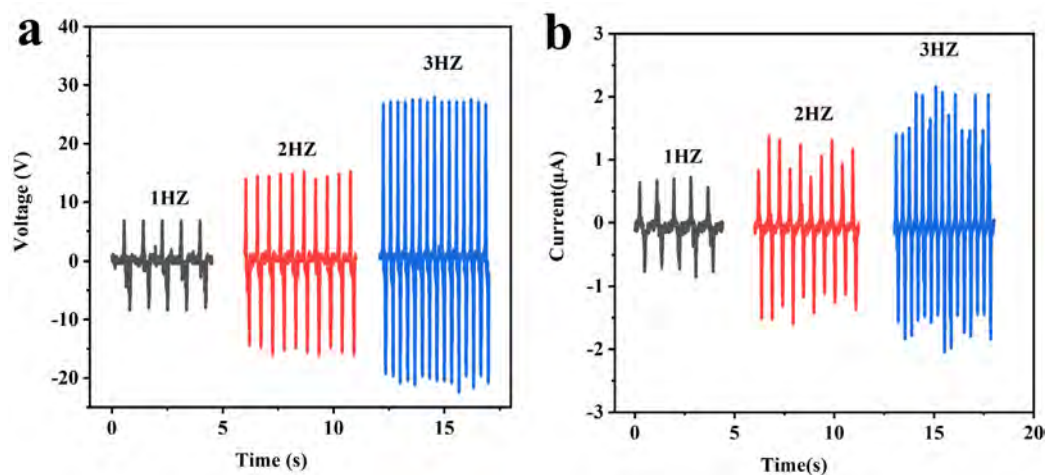


Figure 6.6 Output voltage (a) and current (b) of the SP-FTENG at different frequencies from 1 to 3 Hz.

In addition, the friction material is not limited to rubber film. Four common fabrics including acetate, cotton, nylon and acrylic fabrics in contact with the SP-FTENG were evaluated. Figure 6.7a and b present the output voltage and current of the SP-FTENG contacted with rubber film, acetate, cotton, nylon and acrylic fabrics. The output voltages achieve 27.33 V, 16.99 V, 8.6 V, 8 V and 6.03 V, respectively. The corresponding currents are 1.76 μA , 1.17 μA , 0.62 μA , 0.52 μA and 0.33 μA , respectively. The previous study indicated that structural characteristics of the textile fabrics, especially the effective surface area under densification pressure, had great influence on the effective charge density.⁵⁹ In this regard, the rubber film possesses higher output performance than that of common fabrics due to larger effective contact area induced by the rubber film. When the SP-FTENG is paired with acetate fabric, the output performance is also good which is superior to that of cotton fabric, due to its stronger electron losing ability. Meanwhile, cotton and nylon fabrics exhibit similar output performance, because the cotton fabric is tighter than nylon fabric, resulting in a larger effective contact area with the SP-FTENG, even nylon possesses a stronger electron losing ability. Since acrylic and PTFE have similar positions in the friction

CHAPTER 6

sequence, the output performance of the SP-FTENG is small when the acrylic fabric is used as the friction material.

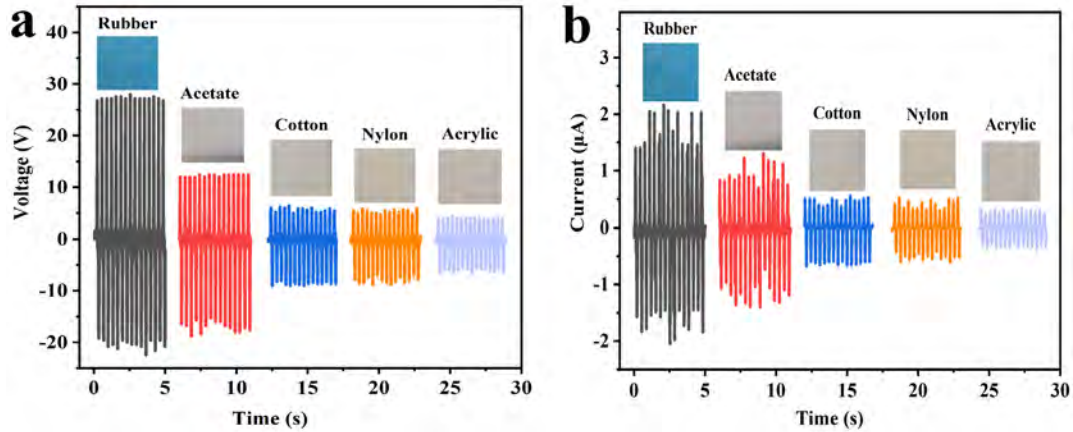
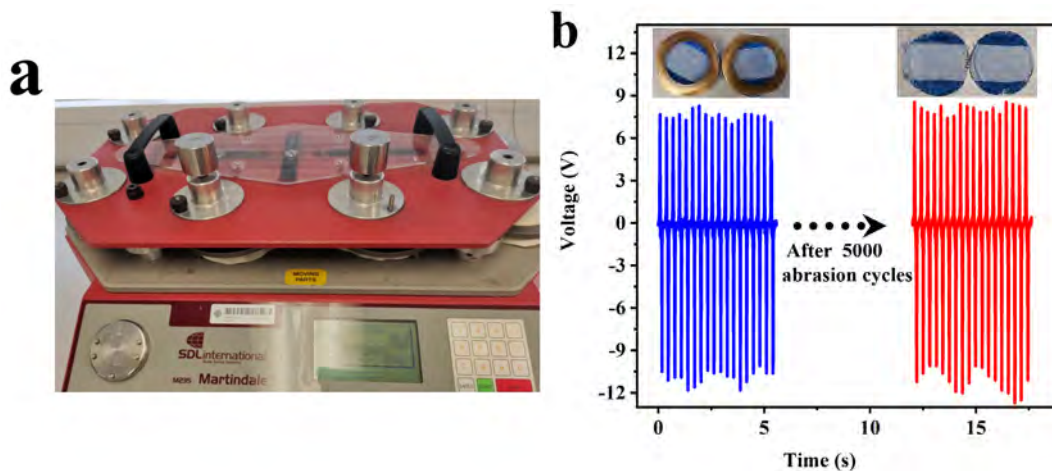


Figure 6.7 Output voltage (a) and current (b) of the SP-FTENG with various friction materials.

In practical application, the fabric may be affected by different external factors, especially frequent friction with surrounding objects, resulting in different degrees of wear and even damage, further affecting its electrical properties. Therefore, the abrasion resistance of the SP-FTENG was evaluated using a martindale standard abrasion test (Figure 6.8a). After 5000 cycles of abrasion, no significant degradation is observed in the electrical performance of the SP-FTENG, as presented in Figure 6.8b. Furthermore, the results indicate that the output current has no decline during 8000 cycles of contact-separation motions (Figure 6.8c), illustrating that the SP-FTENG possesses good mechanical robustness and long-term durability. In terms of machine washing ability, the SP-FTENG was directly washed and dried without packaging by a commercial washing machine and dryer according to rigorous washing tests. The results present that the voltage of the SP-FTENG exhibits a very slight drop during the first machine wash (Figure 6.8d). After the 2nd and 3rd washes, the output voltage remains stable. This change can be attributed to a slight shrinkage of the yarns after the first wash cycle of

CHAPTER 6

textiles, resulting in changes of the effective contact area. The good abrasion resistance, machine washability and durability are due to the fact that the electrode and electrification yarns of the SP-FTENG are not simply attached, but woven together. Besides, no chemical is coated on the surface of the insulating yarn, therefore, the stability of electrical performance is not affected. It is worth noting that the power signal of the FTENG is determined by the matching between the internal resistance of the power source and the external load resistance.⁵⁰ As presented in Figure 6.8e, the current basically remains at a value when the load resistance increases from $10^3 \Omega$ to $10^7 \Omega$ and subsequently decreases as the resistance is further increased to $120 \text{ M}\Omega$. When the load resistance arrives $10^8 \Omega$, the value of maximum power density reaches 61.6 mW/m^2 .



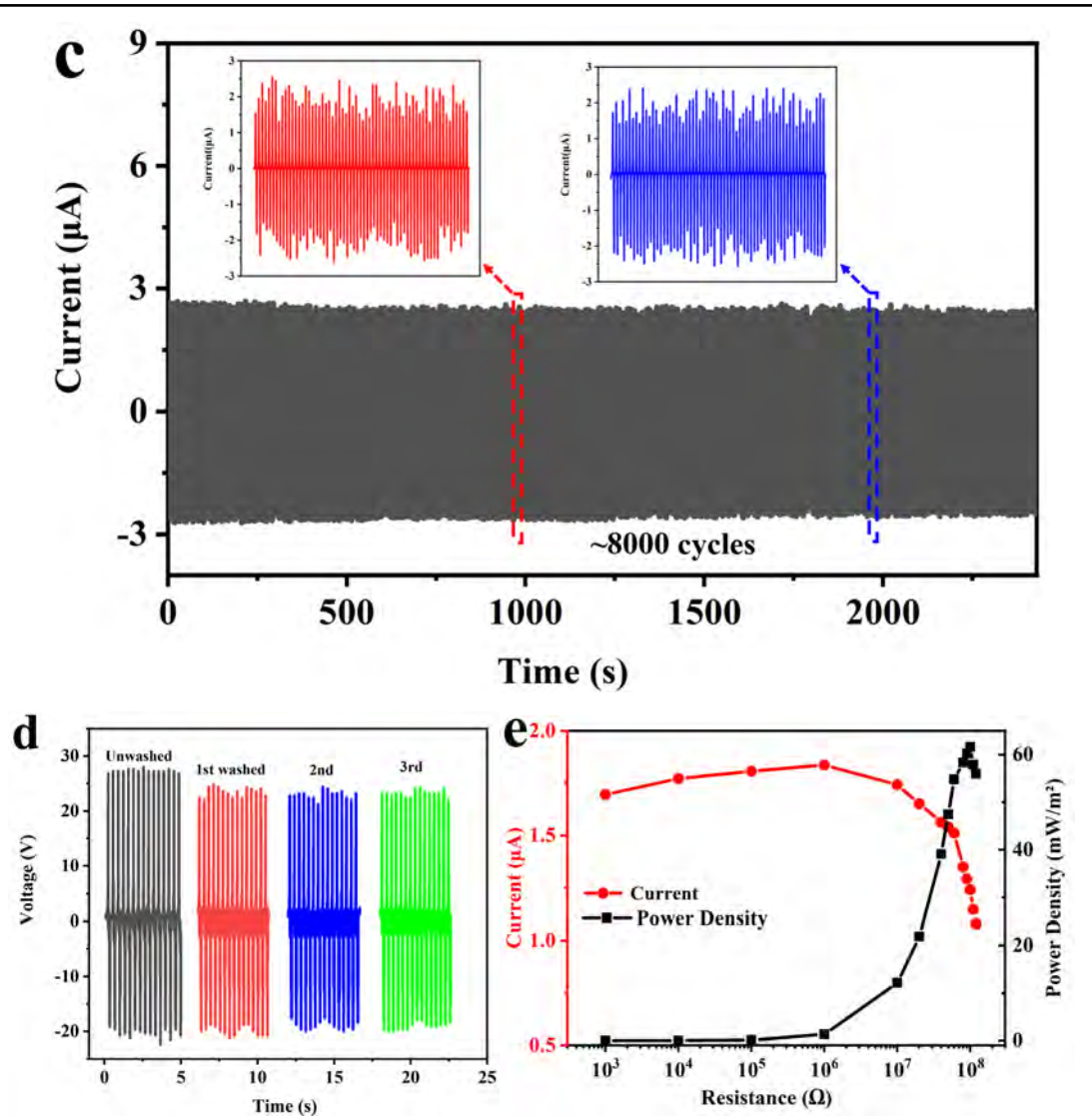


Figure 6.8 (a) Digital photograph of martindale abrasion tester. (b) The electrical output performance of the SP-FTENG after 5000 cycles of abrasion. (c) Stability test of the SP-FTENG under ~ 8000 cycles at a frequency of 3.3 Hz and 200 N mechanical force. Inset: the current waveform of the SP-FTENG at 1000 s and 2000 s, respectively. (d) Output voltage of the SP-FTENG after standard machine wash tests. (e) Current and power density curve of the SP-FTENG at various load resistances. The mechanical force is about 200 N and the frequency is 3 Hz unless otherwise specified.

6.3.5 Mechanism, characterization and optimization of directional water transport

For the purpose of understanding the water transport process through the SP-FTENG,

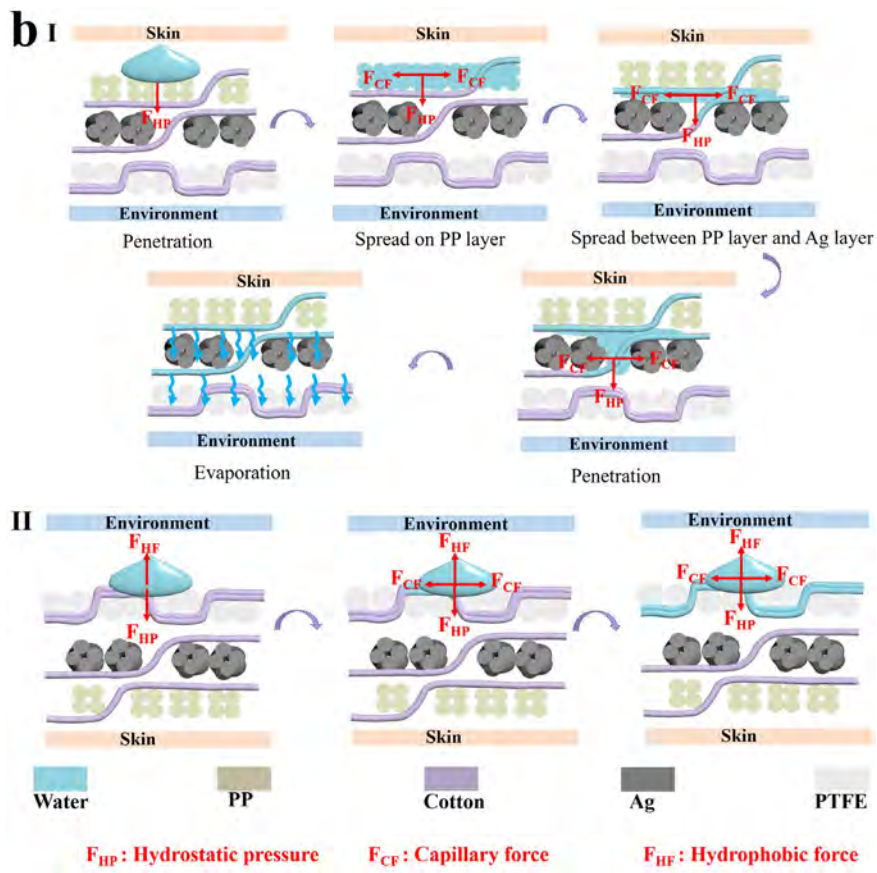
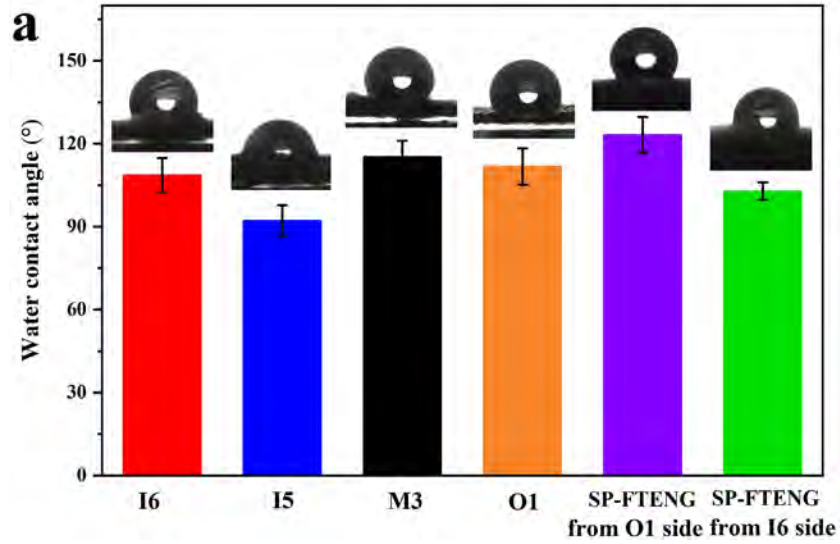
CHAPTER 6

the contribution of every yarn at each layer needs to be taken into account. Because the area percentage of cotton, PTFE, Ag and PP yarns on each side is different, a wettability gradient is created. Owing to the characteristics of yarn configuration, cotton yarns and PTFE yarns present the same area on the O1 and O2 sides. The area of Ag and cotton yarns on the M3 side and M4 side is the same. However, cotton and PP yarns show different areas on the I5 and I6 sides. On the outer layer, the percentages of the surface area occupied by cotton and PTFE yarns are 26% and 70%, respectively. For the middle layer, the percentages of the surface area of cotton and Ag yarns are 14% and 60%, respectively. Owing to the hydrophobic properties of PTFE and Ag yarns, the surface is not easily wetted by water. However, cotton yarns composed of cellulose have an inherent affinity for water. Therefore, for the woven fabric consisting of cotton, PTFE and Ag yarns, the surface wettability is determined by the percentage of cotton, PTFE and Ag yarns. The outer and middle layers with a small cotton yarn percentage are regarded as the hydrophobic layers. The cotton fibers in each layer of the SP-FTENG can be seen as a “bridge” that guides water transmission. With regards to the inner layer, the area percentages of cotton and PP yarns on the I5 side are 22% and 73%, respectively. However, the area of cotton and PP yarns presented on the I6 side occupies 8% and 84%, respectively. Therefore, a wettability gradient between I5 and I6 side of inner layer is created, which improves the water penetration properties. Figure 6.9a presents the contact angles of the single layers, including outer, middle and inner layers of the SP-FTENG. It can be seen that the water contact angles of the outer (O1) and middle layer (M3) are 112° and 115° , respectively. Due to the different yarn area percentages on the two sides of the inner layer, the contact angles of the two sides are different. Compared with 109° contact angle of the I6 side, the I5 possesses a lower water contact angle with 92° owing to a higher cotton content. For the contact angle of the SP-FTENG from O1 and I6 side, it can reach 123° and 103° , respectively.

CHAPTER 6

Based on the investigation, the water transport process of the SP-FTENG can be illustrated in Figure 6.9b. When the water droplet contacts with the inner layer (I), downward hydrostatic pressure (F_{HP}) acts, which depends on the size of water drop. Liquid moisture is quickly absorbed and diffused along the horizontal direction due to the high capillary force (F_{CF}) of PP yarns. Meanwhile, the inner layer is made of PP yarns and cotton yarns interlaced with each other. Due to the excellent moisture conductivity of PP yarns and different yarn area arrangement of two sides in the inner layer, the moisture is transferred to the cotton yarn on the other side of the inner layer, then diffuses and evaporates between the inner layer and the middle layer. The middle layer is made of Ag and cotton yarns. When the other part of the moisture reaches the second layer through the gaps formed between the yarns, it is mainly absorbed by cotton yarns. At the same time, it is transferred to the PTFE layer through the gaps, and then evaporates. This kind of yarn configuration is beneficial to quick draining of the sweat produced by the human body, thus keeping the skin dry and comfortable. On the contrary, when water is dropped on the outer layer (II), the water droplet is subjected to two opposing forces, the hydrostatic pressure (F_{HP}) and the hydrophobic force (F_{HF}). Owing to the F_{CF} , a small amount of water is absorbed by the cotton fibers of outer surface. However, the water penetration could be further blocked due to good hydrophobicity and tight fabric structure of outer layer. As depicted in Figure 6.9c, the water droplet is absorbed within 60 s when the water is dropped on the surface of inner layer (I). However, the water drop maintains its spherical shape and does not spread out within 210 s (II), which illustrates the excellent water resistance of the SP-FTENG.

CHAPTER 6



CHAPTER 6

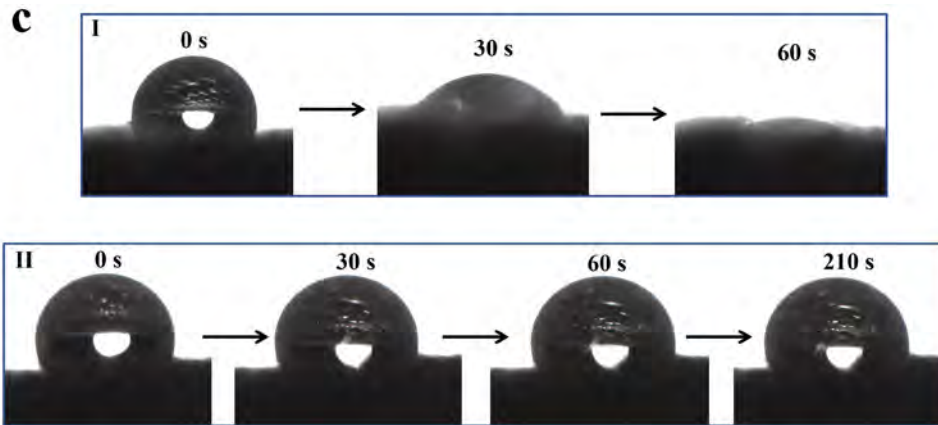


Figure 6.9 (a) Contact angles of different sides of the SP-FTENG. (b) Schematic illustration explaining directional water transport mechanism of the SP-FTENG, water (I) from skin and (II) from environment. (c) Changes of water droplet behavior when water is dropped on inner layer (I) and outer layer (II) of the SP-FTENG, respectively.

Figure 6.10a-h present MMT results of the top and bottom surfaces of four 3D FTENGs, when the inner and outer layer are facing up, respectively. As presented in Figure 6.10a,c,e,g, during dropping water on the inner layer of four 3D FTENGs, the water content of surface increases to the maximum (SP-FTENG: 1170%, LP-FTENG: 570%, ST-FTENG: 620%, SCP-FTENG: 800%). Afterwards, the water content value on the inner layer decreases significantly (SP-FTENG: 400%, LP-FTENG: 170%, ST-FTENG: 270%, SCP-FTENG: 500%) as water supply stopped. Meanwhile, the water content on the outer layer remains at around 0% after 120 s owing to the hydrophobic surface of outer layer. When water is dropped onto the outer layer of the SP-FTENG, the water content is initially rising and then keeps at around the maximum after 120 s, while it keeps about 0% on the inner layer surface, as shown in Figure 6.10b, d, f and h. To further characterize the moisture wicking of four FTENGs from inner layer to outer layer, the key parameters, such as wetting time, absorption rate, max wetted radius and spreading speed, are compared, as presented in Table 3.1. It can be observed that SP-FTENG possesses greater absorption rate (55%/s) than that of other 3D FTENGs while

CHAPTER 6

other parameter values are similar. The possible reason is that different yarn fineness, fabric structure and PDMS treatment lead to different void size and connectivity between voids, thereby affecting water transport performance. This hydrophobicity of the 3D FTENGs is supported by water contact angle test (Figure 6.10i). The contact angles of four different 3D FTENGs are slightly different (SP-FTENG: 123.21°, LP-FTENG: 116.14°, ST-FTENG: 119.12°, SCP-FTENG: 106.11°) due to various yarn arrangements.

Figure 6.10j presents the air permeability of the as-prepared 3D FTENGs and different fabrics. It can be observed that the air permeability of fabrics increases as the pressure difference increases. In comparison with the air permeability of commercial cotton, polyester and acetate fabrics, SP-FTENG (45.3 ml/s/cm²), LP-FTENG (14.3 ml/s/cm²) and ST-FTENG (45.3 ml/s/cm²) still maintain good air permeability, but SCP-FTENG exhibits much lower air permeability (0.16 ml/s/cm²). For the air permeability of fabric, the macro porosity among the threads is more important. One of the significant characteristics of the macro porosity is also the open area of the woven fabric, which is calculated based on the cover factor of the woven fabric. The cover factor (E) is defined as the ratio of surface area covered by yarns to the whole fabric surface area. It can describe the fabric tightness, which could be calculated as follows:

$$E = (P_j d_j + P_w d_w - P_j d_j P_w d_w) * 100 \quad (17)$$

where E is the cover factor of the fabric in %, P_j is the warp density in threads/cm; P_w is the weft density in threads/cm; d_j and d_w are the diameters of the warp and weft yarn (cm), respectively. Open area (O_a) of every layer of the 3D FTENG is calculated using the following equation:

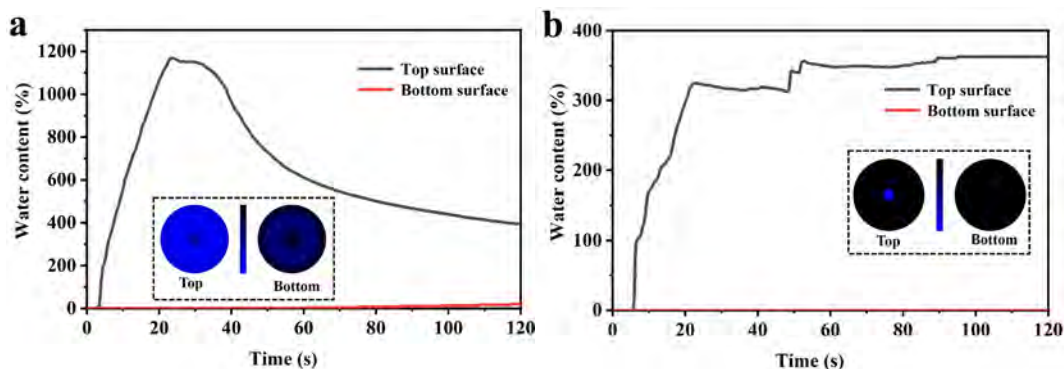
$$O_a = 100 - E \quad (18)$$

where O_a is the open area in %. For the SP-FTENG, the cover factors of the outer layer,

CHAPTER 6

middle layer and inner layer are calculated to be about 94.4%, 84.2% and 95.3%. The corresponding open areas of the outer layer, middle layer and inner layer are 5.6%, 15.8% and 4.7%, respectively. Regarding the ST-FTENG, its cover factor and open area are same as the values of the SP-FTENG. However, the cover factor of the inner layer of the LP-FTENG reaches 110.8%. It illustrates that there is extrusion deformation or overlap between the yarns in the fabric, so it is considered that the yarns are completely covered. The cover factor and open area of the inner layer of the LP-FTENG can be considered to be 100% and 0%, respectively. Although the open area of the inner layer of the LP-FTENG is 0%, the micropores existed in PP fibers endow the layer with good air permeability. Meanwhile, because the open areas of the SP-FTENG and ST-FTENG are higher than that of the LP-FTENG, the air permeability of the SP-FTENG and ST-FTENG is larger than that of the LP-FTENG.

In addition, the SP-FTENG possesses good water vapor transmission ($681.91\text{g}/\text{m}^2\cdot 24\text{h}$), which indicates the water/sweat vapor can be easily transferred from the inner skin to the outer environment through the SP-FTENG. The value is higher than that of commercial cotton and PET fabrics reported by previous work.⁵⁵



CHAPTER 6

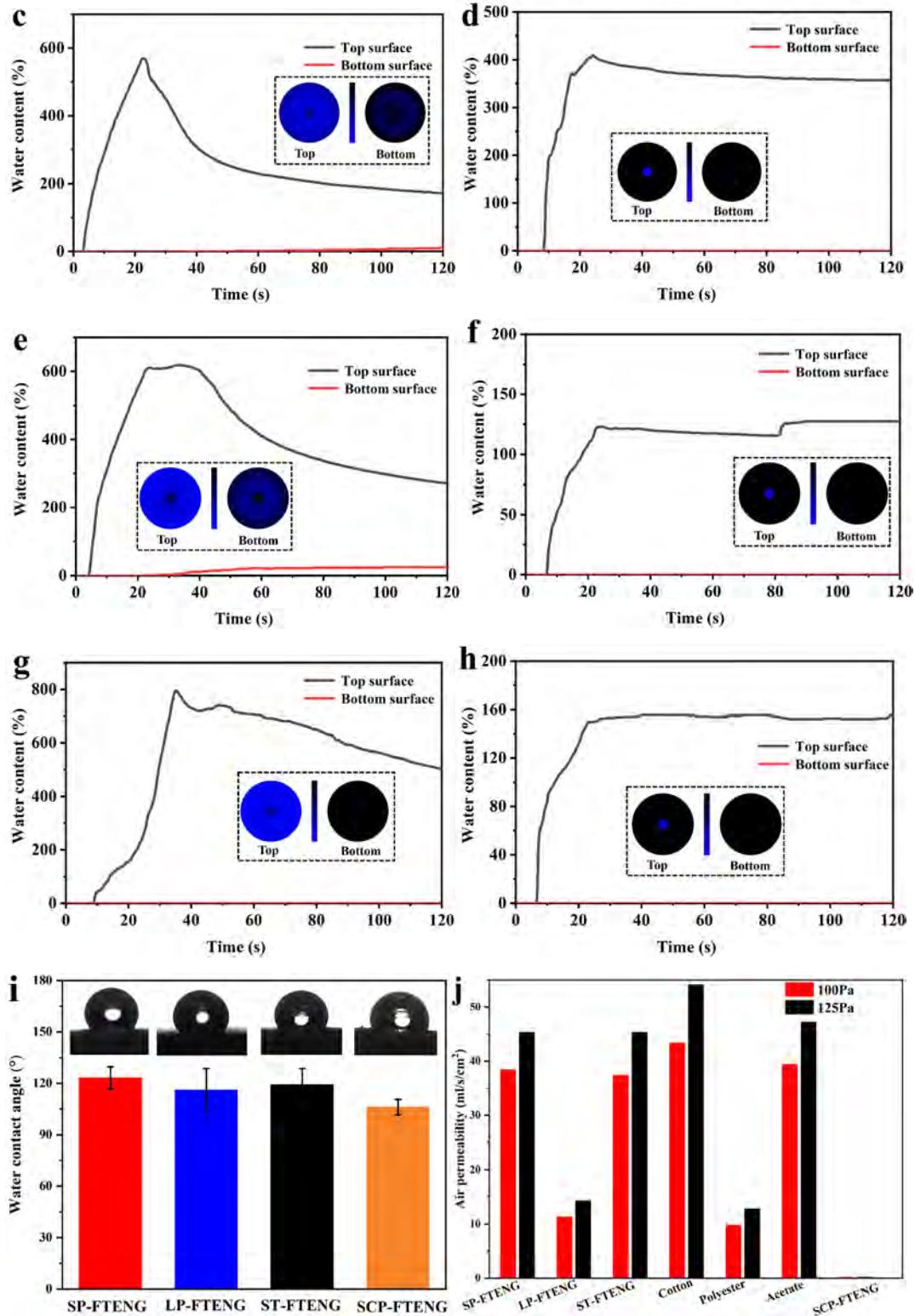


Figure 6.10 MMT results of the top and bottom surfaces of 3D FTENGs when the inner and outer layer are facing up, respectively: (a-b) SP-FTENG, (c-d) LP-FTENG, (e-f) ST-FTENG, (g-h) SCP-FTENG. (i) Contact angles of different 3D FTENGs. (j) Air permeability of the as-prepared 3D FTENGs and different fabrics.

CHAPTER 6

Table 6.1 Wetting time, absorption rate, max wetted radius and spreading speed of functional zones of four 3D FTENGs when water is dropped on inner layer.

3D FTENG code	Wetting time (s)	Absorption rate (%/s)	Max wetted radius (mm)	Spreading speed (mm/s)
SP-FTENG	2.355	54.878	30	11.295
LP-FTENG	2.434	28.170	30	10.594
ST-FTENG	3.074	30.038	30	11.289
SCP-FTENG	8.205	29.401	30	3.414

6.3.6 Antibacterial property of the SP-FTENG

A standard method was adopted referring to GB/T 20944.3 (Shake flake method) to confirm the antibacterial feature of the SP-FTENG. Live bacteria concentration of standard and inhibition rate of the SP-FTENG are shown in Table 6.2. Regarding *S. aureus*, it can be observed that the live bacteria concentration of blank sample increases significantly from 2.0×10^4 CFU/mL in 0 h to 1.0×10^6 CFU/mL in 18 h. However, the live bacteria concentration of the SP-FTENG reduces to 1.1×10^3 CFU/mL after 18 h. The SP-FTENG has presented a very good inhibition rate of *S. aureus* (>99%). Moreover, the inhibition rates of 99% against *E. coli* and 99% against *C. albicans* are observed. The excellent antibacterial activity of the SP-FTENG is primarily ascribed to the Ag layer in the middle layer of the 3D SP-FTENG, which has the ability to inhibit and kill bacteria. It shows great potential to advance the development of antibacterial wearable electronics.

CHAPTER 6

Table 6.2 Antibacterial activity results of the SP-FTENG against *S. aureus*, *E. coli* and *C. albicans*.

Bacteria	<i>S. aureus</i>		<i>E. coli</i>		<i>C. albicans</i>	
	Blank	SP-FTENG	Blank	SP-FTENG	Blank	SP-FTENG
At 0 h contact (CFU/mL)	2.0×10^4		2.1×10^4		1.8×10^4	
After 18 h oscillation (CFU/mL)	1.0×10^6	1.1×10^3	2.7×10^6	7.7×10^3	4.8×10^5	5.3×10^3
Inhibition (%)	> 99		> 99		99	

6.3.7 Performance comparison of the SP-FTENG

Compared with fabric-based t-TENGs reported in previous studies, the fabricated 3D SP-FTENG not only shows good electrical output performance, but also exhibits excellent comfort and durability. These properties can meet the requirements for long-term wearable use in practical applications. Additionally, compared with other fabrication methods, such as coating, electrospinning and electroless deposition, the weaving technology for t-TENGs fabrication offers great advantages in terms of scalable production and low consumption.

CHAPTER 6

Table 6.3 Performance comparison to fabric-based t-TENGs in previous reports.

Ref	Fabrication method	Triboelectric materials	Power	Comfort			Mass production	Durability		
				Air permeability	Water vapor permeability	Moisture management		Abrasion resistance	Wash ability	Cyclical stability
(60)	Conjugated electrospinning and weaving	PU/Si ₃ N ₄ -PVDF	56 $\mu\text{W}/\text{cm}^2$	-	-	-	Medium	-	Machine wash	~150,000 cycles
(50)	Electrospinning	PA66-MWCNTs/PVDF films	1.30 W/m^2	11.5 mm/s	Appreciable	-	Medium	-	Simulated washing	~10,000 cycles
(61)	Doctor-blading and weaving	PTFE/Nylon fabric	5.43 mW/m^2	-	-	-	Medium	-	Machine wash	~40,000 cycles

CHAPTER 6

		Silicone								
(40)	Heat sealing	rubber/Ni-fabric	1.3 μW	-	-	-	Medium	-	Dipping in the water	~5000 cycles
(18)	Twisting and weaving	PTFE/Nylon woven fabric	9.9 $\mu\text{W}/\text{m}^2$	Have	-	-	High	-	Simulated machine wash	~4200 cycles
		Rubber								
(55)	Electrospinning and weaving	film/P(VDF-TrFE)/PA66	93 mW/m^2	164 mm/s	712 \pm 16 $\text{g}/\text{m}^2 \cdot 24\text{h}$	-	Medium	-	Simulated machine wash	~20,000 cycles
		Aluminum								
(62)	Wet-spinning, coating and weaving	foil/Dopamine-MXene-TPU fiber and PTFE yarn	0.16 mW/m^2	Have	Have	-	Medium	-	-	~10,000 cycles
(63)	Knitting	PTFE/Polyester terry fabric	7.7 mW/m^2	Have	-	-	High	-	-	~10,000 cycles

CHAPTER 6

3D		Rubber						~		
SP-		film/PTFE	61.60	45.3	681.91			5000	Machine	
FTE	Weaving	yarn-cotton	mW/m²	ml/s	g/m²·24h	Good	High	cycles of	wash	~8000 cycles
NG		yarn		/cm²				abrasion		

- means the mentioned device does not have relevant properties or that the device has relevant properties but no relevant data is available.

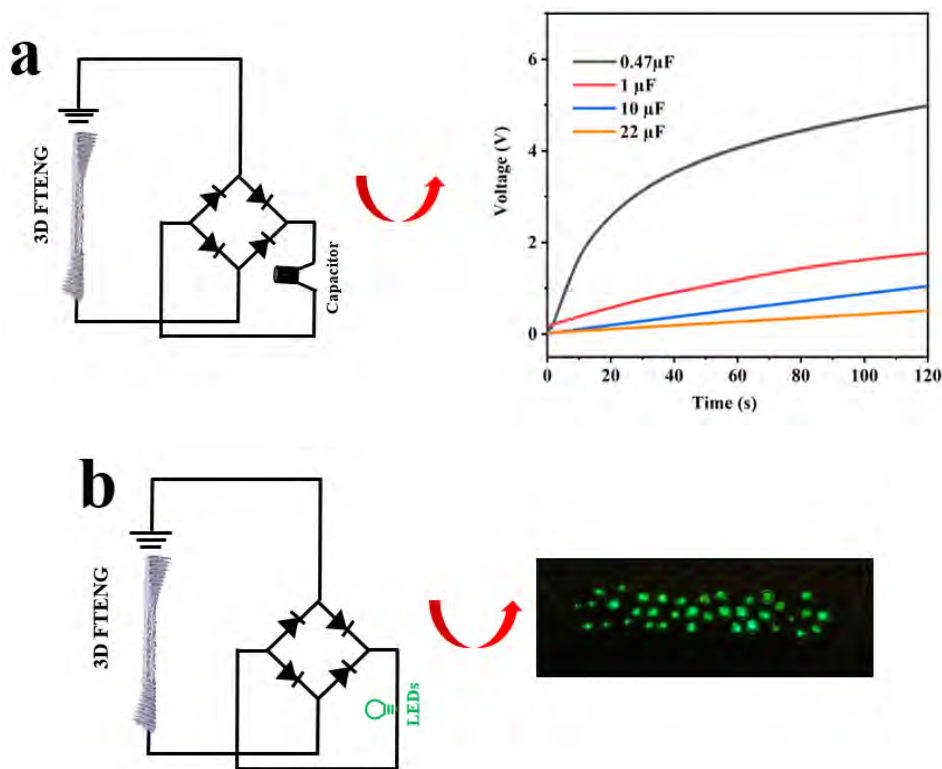
CHAPTER 6

6.3.8 Application of the SP-FTENG

By integrating this wearable SP-FTENG with clothes, energy from human movement can be easily obtained, thus continuing to power lights and electronic products. The charging capacity of the SP-FTENG was investigated by using various capacitors. Figure 6.11a indicates the voltage-charging curve. It is clearly presented that the capacitors can be charged by the SP-FTENG and the charging rate decreases as the capacitance capacity increases. The electricity stored in the capacitor could be used as a power source to drive an electronic watch. Figure 6.11b presents that the SP-FTENG can sufficiently light up 35 green LEDs in series by rubber film tapping. Additionally, the SP-FTENG is connected to a rectifier for current conversion. As indicated in Figure 6.11c, the screen of watch demonstrates that the watch works successfully. With regard to wearable applications, the SP-FTENG can be sewed on clothes for energy harvesting and sensing. As presented in Figure 6.11d, the SP-FTENG was integrated into clothes in order to obtain the human motion energy from arm flapping and swinging. Under the continuous contact and separation between SP-FTENG and arm, the alternating triboelectric signals were generated. The results show that the peak-to-peak voltages obtained by arm flapping and arm swinging are ~ 11.48 V and ~ 12.48 V, respectively. According to above experimental results, the waveforms of the output voltage are slightly different during the movement of various parts of the human body. Consequently, the human motion may be deduced based on the corresponding waveform. Besides, the SP-FTENG could be designed and constructed as an energy harvesting and sensing carpet. Figure 6.11e presents that the SP-FTENG is put under the foot and cotton sock, respectively. Its peak to peak voltage is ~ 16.64 V as the skin repeatedly contacts and separates from the SP-FTENG. The peak to peak voltage produced by the corresponding cotton sock is only ~ 6 V. In addition, owing to the

CHAPTER 6

flexibility of the SP-FTENG, it could be used to fabricate the sports bandage capable of harvesting energy obtained from the bending of the arm. As displayed in Figure 6.11f, the peak to peak voltage can reach ~ 3.98 V. Furthermore, the applicability of the SP-FTENG in detecting the sitting time was demonstrated through placing a SP-FTENG on the chair. As shown in Figure 6.11g, a positive voltage peak (~ 4.4 V) is observed when one sits on a chair. A negative voltage peak (~ -8.18 V) is detected as the person stands up. The sitting time (~ 0.8 s) is indicated by the interval between the two opposite peaks. Owing to low energy consumption of the SP-FTENG, it is a better option to monitor the sitting time of workers. Consequently, the SP-FTENG has enormous potential applications in self-powered smart sensing owing to the unique advantages of material selection and structure configuration.



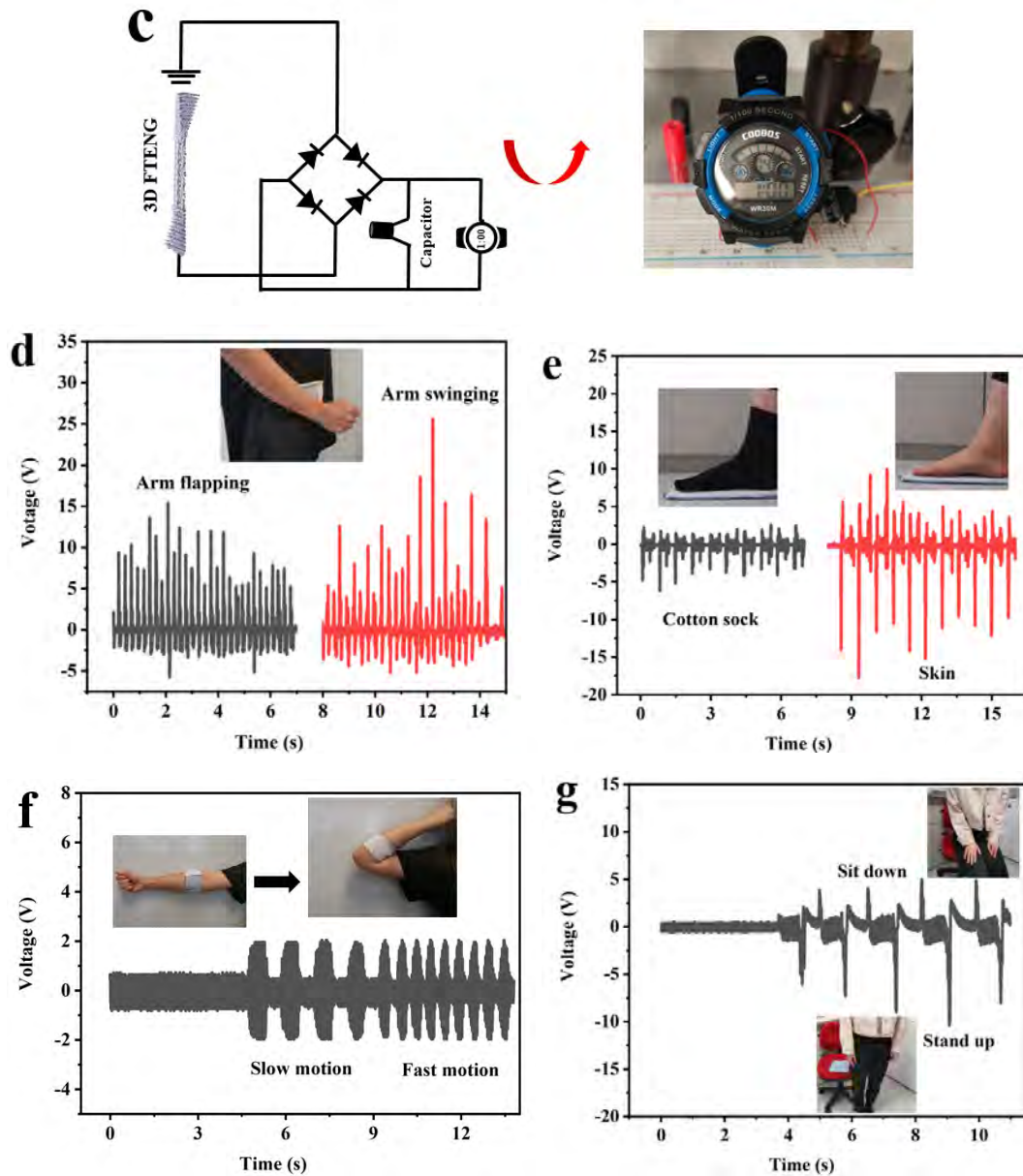


Figure 6.11 Application of the SP-FTENG. (a) Charging performance of the SP-FTENG to different capacitors. (b) Photograph of the SP-FTENG lighting up 36 LEDs. (c) The electrical circuit diagram of powering an electronic watch. (d) A SP-FTENG attached under the arm to detect arm swinging and flapping. (e) Output voltage of the SP-FTENG placed under the foot and cotton sock. (f) Monitoring arm bending by mounting a SP-FTENG on the arm. (g) Detecting sitting behavior of people using a SP-FTENG placed on a chair.

CHAPTER 6

6.4 Conclusion

In this chapter, we have developed a sustainable FTENG based on commercial eco-friendly fiber materials and novel 3D structure with supporting area and functional area. The 3D SP-FTENG can obtain good electrical output (27.33 V, 1.76 μA and 61.6 mW/m^2) owing to the rational configuration of materials and structures. Apart from the output, the 3D SP-FTENG in this work also performs versatility, including wearability (directional water transport and breathability), antibacterial property and durability, which are achieved by the textile engineering strategy without involving any chemical processing. In addition, the SP-FTENG can be employed as sustainable power source for low-energy electronics and self-powered sensor for monitoring the signals of different human behavior. This work proposes a new design concept of 3D FTENG structure, which may pave the way for future daily wearable electronic textiles.

CHAPTER 6

References

- (1) Yi, J.; Dong, K.; Shen, S.; Jiang, Y.; Peng, X.; Ye, C.; Wang, Z. L. Fully Fabric-Based Triboelectric Nanogenerators as Self-Powered Human–Machine Interactive Keyboards. *Nano-Micro Lett.* **2021**, *13*, 1-13.
- (2) Wu, R.; Ma, L.; Hou, C.; Meng, Z.; Guo, W.; Yu, W.; Yu, R.; Hu, F.; Liu, X. Y. Silk Composite Electronic Textile Sensor for High Space Precision 2D Combo Temperature-Pressure Sensing. *Small* **2019**, *15*, 1901558.
- (3) Tian, X.; Chan, K.; Hua, T.; Niu, B.; Chen, S. Wearable strain sensors enabled by integrating one-dimensional polydopamine-enhanced graphene/polyurethane sensing fibers into textile structures. *J. Mater. Sci.* **2020**, *55*, 17266-17283.
- (4) Sala de Medeiros, M.; Chanci, D.; Moreno, C.; Goswami, D.; Martinez, R. V. Waterproof, Breathable, and Antibacterial Self-Powered e-Textiles Based on Omniphobic Triboelectric Nanogenerators. *Adv. Funct. Mater.* **2019**, *29*, 1970294.
- (5) Shi, Y.; Wei, X.; Wang, K.; He, D.; Yuan, Z.; Xu, J.; Wu, Z.; Wang, Z. L. Integrated all-fiber electronic skin toward self-powered sensing sports systems. *ACS Appl. Mater. Interfaces* **2021**, *13*, 50329-50337.
- (6) Wang, Z.; Luan, C.; Zhu, Y.; Liao, G.; Liu, J.; Li, X.; Yao, X.; Fu, J. Integrated and shape-adaptable multifunctional flexible triboelectric nanogenerators using coaxial direct ink writing 3D printing. *Nano Energy* **2021**, *90*, 106534.
- (7) Feng, P. Y.; Xia, Z.; Sun, B.; Jing, X.; Li, H.; Tao, X.; Mi, H. Y.; Liu, Y. Enhancing the performance of fabric-based triboelectric nanogenerators by structural and chemical modification. *ACS Appl. Mater. Interfaces* **2021**, *13*, 16916-16927.
- (8) Guo, Y.; Li, K.; Hou, C.; Li, Y.; Zhang, Q.; Wang, H. Fluoroalkylsilane-modified textile-based personal energy management device for multifunctional wearable applications. *ACS Appl. Mater. Interfaces* **2016**, *8*, 4676-4683.

CHAPTER 6

- (9) Yang, M.; Hua, T. Scalable fabrication of black Cu-embedded polydimethylsiloxane for enhancing triboelectric nanogenerator performance in energy harvesting and self-powered sensing. *Adv. Energy Sustain. Res.* **2021**, *2*, 2100116.
- (10) Yang, M.; Tian, X.; Hua, T. Green and recyclable cellulose based TENG for sustainable energy and human-machine interactive system. *Chem. Eng. J.* **2022**, *442*, 136150.
- (11) Cheng, R.; Dong, K.; Liu, L.; Ning, C.; Chen, P.; Peng, X.; Liu, D.; Wang, Z. L. Flame-retardant textile-Based triboelectric nanogenerators for fire protection applications. *ACS Nano* **2020**, *14*, 15853-15863.
- (12) Dong, K.; Peng, X.; Wang, Z. L. Fiber/fabric-based piezoelectric and triboelectric nanogenerators for flexible/stretchable and wearable electronics and artificial intelligence. *Adv. Mater.* **2020**, *32*, e1902549.
- (13) Dong, C.; Leber, A.; Das Gupta, T.; Chandran, R.; Volpi, M.; Qu, Y.; Nguyen-Dang, T.; Bartolomei, N.; Yan, W.; Sorin, F. High-efficiency super-elastic liquid metal based triboelectric fibers and textiles. *Nat. Commun.* **2020**, *11*, 3537.
- (14) Cao, R.; Pu, X.; Du, X.; Yang, W.; Wang, J.; Guo, H.; Zhao, S.; Yuan, Z.; Zhang, C.; Li, C.; Wang, Z. L. Screen-printed washable electronic textiles as self-powered touch/gesture tribo-sensors for intelligent human-machine interaction. *ACS Nano* **2018**, *12*, 5190-5196.
- (15) Pu, X.; Li, L.; Song, H.; Du, C.; Zhao, Z.; Jiang, C.; Cao, G.; Hu, W.; Wang, Z. L. A self-charging power unit by integration of a textile triboelectric nanogenerator and a flexible lithium-ion battery for wearable electronics. *Adv. Mater.* **2015**, *27*, 2472-2478.
- (16) Shuai, L.; Guo, Z. H.; Zhang, P.; Wan, J.; Pu, X.; Wang, Z. L. Stretchable, self-healing, conductive hydrogel fibers for strain sensing and triboelectric energy-harvesting smart textiles. *Nano Energy* **2020**, *78*, 105389.

CHAPTER 6

- (17) Huang, T.; Zhang, J.; Yu, B.; Yu, H.; Long, H.; Wang, H.; Zhang, Q.; Zhu, M. Fabric texture design for boosting the performance of a knitted washable textile triboelectric nanogenerator as wearable power. *Nano Energy* **2019**, *58*, 375-383.
- (18) Lou, M.; Abdalla, I.; Zhu, M.; Wei, X.; Yu, J.; Li, Z.; Ding, B. Highly wearable, breathable, and washable sensing textile for human motion and pulse monitoring. *ACS Appl. Mater. Interfaces* **2020**, *12*, 19965-19973.
- (19) Zhou, T.; Zhang, C.; Han, C. B.; Fan, F. R.; Tang, W.; Wang, Z. L. Woven structured triboelectric nanogenerator for wearable devices. *ACS Appl. Mater. Interfaces* **2014**, *6*, 14695-14701.
- (20) Wang, W.; Yu, A.; Liu, X.; Liu, Y.; Zhang, Y.; Zhu, Y.; Lei, Y.; Jia, M.; Zhai, J.; Wang, Z. L. Large-scale fabrication of robust textile triboelectric nanogenerators. *Nano Energy* **2020**, *71*, 104605.
- (21) Ma, L.; Zhou, M.; Wu, R.; Patil, A.; Gong, H.; Zhu, S.; Wang, T.; Zhang, Y.; Shen, S.; Dong, K.; Yang, L.; Wang, J.; Guo, W.; Wang, Z. L. Continuous and scalable manufacture of hybridized nano-micro triboelectric yarns for energy harvesting and signal sensing. *ACS Nano* **2020**, *14*, 4716-4726.
- (22) Xu, H.; Tao, J.; Liu, Y.; Mo, Y.; Bao, R.; Pan, C. Fully Fibrous Large-Area Tailorable Triboelectric Nanogenerator Based on Solution Blow Spinning Technology for Energy Harvesting and Self-Powered Sensing. *Small* **2022**, *18*, 2202477.
- (23) Dong, S.; Xu, F.; Sheng, Y.; Guo, Z.; Pu, X.; Liu, Y. Seamlessly knitted stretchable comfortable textile triboelectric nanogenerators for E-textile power source. *Nano Energy* **2020**, *78*, 105327.
- (24) Chen, C.; Chen, L.; Wu, Z.; Guo, H.; Yu, W.; Du, Z.; Wang, Z. L. 3D double-faced interlock fabric triboelectric nanogenerator for bio-motion energy harvesting and as self-powered stretching and 3D tactile sensors. *Mater. Today* **2020**, *32*, 84-93.
- (25) Zhang, D.; Yang, W.; Gong, W.; Ma, W.; Hou, C.; Li, Y.; Zhang, Q.; Wang, H.,

CHAPTER 6

Abrasion Resistant/Waterproof Stretchable Triboelectric Yarns Based on Fermat Spirals.

Adv. Mater. **2021**, *33*, e2100782.

(26) Ma, L.; Wu, R.; Patil, A.; Yi, J.; Liu, D.; Fan, X.; Sheng, F.; Zhang, Y.; Liu, S.; Shen, S.; Wang, J.; Wang, Z. L. Acid and Alkali-Resistant Textile Triboelectric Nanogenerator as a Smart Protective Suit for Liquid Energy Harvesting and Self-Powered Monitoring in High-Risk Environments. *Adv. Funct. Mater.* **2021**, *31*, 2102963.

(27) Dong, K.; Deng, J.; Zi, Y.; Wang, Y. C.; Xu, C.; Zou, H.; Ding, W.; Dai, Y.; Gu, B.; Sun, B.; Wang, Z. L. 3D Orthogonal Woven Triboelectric Nanogenerator for Effective Biomechanical Energy Harvesting and as Self-Powered Active Motion Sensors. *Adv. Mater.* **2017**, *29*, 1702648.

(28) Miao, D.; Huang, Z.; Wang, X.; Yu, J.; Ding, B. Continuous, Spontaneous, and Directional Water Transport in the Trilayered Fibrous Membranes for Functional Moisture Wicking Textiles. *Small* **2018**, *14*, 1801527.

(29) Jiang, Y.; Dong, K.; An, J.; Liang, F.; Yi, J.; Peng, X.; Ning, C.; Ye, C.; Wang, Z. L. UV-Protective, Self-Cleaning, and Antibacterial Nanofiber-Based Triboelectric Nanogenerators for Self-Powered Human Motion Monitoring. *ACS Appl. Mater. Interfaces* **2021**, *13*, 11205-11214.

(30) Li, Z.; Zhu, M.; Shen, J.; Qiu, Q.; Yu, J.; Ding, B. All-Fiber Structured Electronic Skin with High Elasticity and Breathability. *Adv. Funct. Mater.* **2019**, *30*, 1908411.

(31) Kim, T.; Jeon, S.; Lone, S.; Doh, S. J.; Shin, D.-M.; Kim, H. K.; Hwang, Y.-H.; Hong, S. W. Versatile nanodot-patterned Gore-Tex fabric for multiple energy harvesting in wearable and aerodynamic nanogenerators. *Nano Energy* **2018**, *54*, 209-217.

(32) Fang, Y.; Zou, Y.; Xu, J.; Chen, G.; Zhou, Y.; Deng, W.; Zhao, X.; Roustaei, M.; Hsiai, T. K.; Chen, J. Ambulatory Cardiovascular Monitoring Via a Machine-Learning-Assisted Textile Triboelectric Sensor. *Adv. Mater.* **2021**, *33*, 2104178.

CHAPTER 6

- (33) He, H.; Liu, J.; Wang, Y.; Zhao, Y.; Qin, Y.; Zhu, Z.; Yu, Z.; Wang, J. An Ultralight Self-Powered Fire Alarm e-Textile Based on Conductive Aerogel Fiber with Repeatable Temperature Monitoring Performance Used in Firefighting Clothing. *ACS Nano* **2022**, *16*, 2953-2967.
- (34) Lai, Y. C.; Hsiao, Y. C.; Wu, H. M.; Wang, Z. L. Waterproof Fabric-Based Multifunctional Triboelectric Nanogenerator for Universally Harvesting Energy from Raindrops, Wind, and Human Motions and as Self-Powered Sensors. *Adv. Sci.* **2019**, *6*, 1801883.
- (35) Gong, W.; Wang, X.; Yang, W.; Zhou, J.; Han, X.; Dickey, M. D.; Su, Y.; Hou, C.; Li, Y.; Zhang, Q.; Wang, H. Wicking-Polarization-Induced Water Cluster Size Effect on Triboelectric Evaporation Textiles. *Adv. Mater.* **2021**, *33*, e2007352.
- (36) Wang, X.; Huang, Z.; Miao, D.; Zhao, J.; Yu, J.; Ding, B. Biomimetic Fibrous Murray Membranes with Ultrafast Water Transport and Evaporation for Smart Moisture-Wicking Fabrics. *ACS Nano* **2018**, *13*, 1060-1070.
- (37) Barras, R.; dos Santos, A.; Calmeiro, T.; Fortunato, E.; Martins, R.; Águas, H.; Barquinha, P.; Igreja, R.; Pereira, L. Porous PDMS conformable coating for high power output carbon fibers/ZnO nanorod-based triboelectric energy harvesters. *Nano Energy* **2021**, *90*, 106582.
- (38) Choi, D.; Yang, S.; Lee, C.; Kim, W.; Kim, J.; Hong, J., Highly Surface-Embossed Polydimethylsiloxane-Based Triboelectric Nanogenerators with Hierarchically Nanostructured Conductive Ni-Cu Fabrics. *ACS Appl. Mater. Interfaces* **2018**, *10*, 33221-33229.
- (39) Yang, C.-R.; Ko, C.-T.; Chang, S.-F.; Huang, M.-J. Study on fabric-based triboelectric nanogenerator using graphene oxide/porous PDMS as a compound friction layer. *Nano Energy* **2022**, *92*, 106791.
- (40) Zhang, Q.; Jin, T.; Cai, J.; Xu, L.; He, T.; Wang, T.; Tian, Y.; Li, L.; Peng, Y.;

CHAPTER 6

Lee, C. Wearable Triboelectric Sensors Enabled Gait Analysis and Waist Motion Capture for IoT-Based Smart Healthcare Applications. *Adv. Sci.* **2022**, *9*, 2103694.

(41) Li, Y.; Xiong, J.; Lv, J.; Chen, J.; Gao, D.; Zhang, X.; Lee, P. S. Mechanically Interlocked Stretchable Nanofibers for Multifunctional Wearable Triboelectric Nanogenerator. *Nano Energy* **2020**, *78*, 105358.

(42) Qiu, Q.; Zhu, M.; Li, Z.; Qiu, K.; Liu, X.; Yu, J.; Ding, B. Highly flexible, breathable, tailorable and washable power generation fabrics for wearable electronics. *Nano Energy* **2019**, *58*, 750-758.

(43) Jiang, C.; Li, X.; Ying, Y.; Ping, J. A multifunctional TENG yarn integrated into agrotexile for building intelligent agriculture. *Nano Energy* **2020**, *74*, 104863.

(44) Zhu, M.; Huang, Y.; Ng, W. S.; Liu, J.; Wang, Z.; Wang, Z.; Hu, H.; Zhi, C. 3D spacer fabric based multifunctional triboelectric nanogenerator with great feasibility for mechanized large-scale production. *Nano Energy* **2016**, *27*, 439-446.

(45) Xu, F.; Dong, S.; Liu, G.; Pan, C.; Guo, Z. H.; Guo, W.; Li, L.; Liu, Y.; Zhang, C.; Pu, X.; Wang, Z. L. Scalable fabrication of stretchable and washable textile triboelectric nanogenerators as constant power sources for wearable electronics. *Nano Energy* **2021**, *88*, 106247.

(46) Ning, C.; Dong, K.; Cheng, R.; Yi, J.; Ye, C.; Peng, X.; Sheng, F.; Jiang, Y.; Wang, Z. L. Flexible and Stretchable Fiber-Shaped Triboelectric Nanogenerators for Biomechanical Monitoring and Human-Interactive Sensing. *Adv. Funct. Mater.* **2021**, *31*, 2006679.

(47) Paosangthong, W.; Torah, R.; Beeby, S. Recent progress on textile-based triboelectric nanogenerators. *Nano Energy* **2019**, *55*, 401-423.

(48) Ye, C.; Dong, S.; Ren, J.; Ling, S. Ultrastable and High-Performance Silk Energy Harvesting Textiles. *Nano-Micro Lett.* **2019**, *12*, 1-15.

(49) Yu, A.; Pu, X.; Wen, R.; Liu, M.; Zhou, T.; Zhang, K.; Zhang, Y.; Zhai, J.; Hu,

CHAPTER 6

W.; Wang, Z. L. Core-Shell-Yarn-Based Triboelectric Nanogenerator Textiles as Power Cloths. *ACS Nano* **2017**, *11*, 12764-12771.

(50) Sun, N.; Wang, G.-G.; Zhao, H.-X.; Cai, Y.-W.; Li, J.-Z.; Li, G.-Z.; Zhang, X.-N.; Wang, B.-L.; Han, J.-C.; Wang, Y.; Yang, Y. Waterproof, breathable and washable triboelectric nanogenerator based on electrospun nanofiber films for wearable electronics. *Nano Energy* **2021**, *90*, 106639.

(51) He, E.; Sun, Y.; Wang, X.; Chen, H.; Sun, B.; Gu, B.; Zhang, W. 3D angle-interlock woven structural wearable triboelectric nanogenerator fabricated with silicone rubber coated graphene oxide/cotton composite yarn. *Composites, Part B* **2020**, *200*, 108244.

(52) Busolo, T.; Szewczyk, P. K.; Nair, M.; Stachewicz, U.; Kar-Narayan, S. Triboelectric Yarns with Electrospun Functional Polymer Coatings for Highly Durable and Washable Smart Textile Applications. *ACS Appl. Mater. Interfaces* **2021**, *13*, 16876-16886.

(53) Dong, K.; Wang, Y. C.; Deng, J.; Dai, Y.; Zhang, S. L.; Zou, H.; Gu, B.; Sun, B.; Wang, Z. L. A Highly Stretchable and Washable All-Yarn-Based Self-Charging Knitting Power Textile Composed of Fiber Triboelectric Nanogenerators and Supercapacitors. *ACS Nano* **2017**, *11*, 9490-9499.

(54) Xie, L.; Chen, X.; Wen, Z.; Yang, Y.; Shi, J.; Chen, C.; Peng, M.; Liu, Y.; Sun, X. Spiral Steel Wire Based Fiber-Shaped Stretchable and Tailorable Triboelectric Nanogenerator for Wearable Power Source and Active Gesture Sensor. *Nano-Micro Lett.* **2019**, *11*, 1-10.

(55) Guan, X.; Xu, B.; Wu, M.; Jing, T.; Yang, Y.; Gao, Y. Breathable, washable and wearable woven-structured triboelectric nanogenerators utilizing electrospun nanofibers for biomechanical energy harvesting and self-powered sensing. *Nano Energy* **2021**, *80*, 105549.

CHAPTER 6

- (56) Guan, X.; Wang, X.; Huang, Y.; Zhao, L.; Sun, X.; Owens, H.; Lu, J. R.; Liu, X. Smart Textiles with Janus Wetting and Wicking Properties Fabricated by Graphene Oxide Coatings. *Adv. Mater. Interfaces* **2021**, *8*, 2001427.
- (57) Dharmasena, R. D. I. G. Inherent Asymmetry of the Current Output in a Triboelectric Nanogenerator. *Nano Energy* **2020**, *76*, 105045.
- (58) Ra, Y.; You, I.; Kim, M.; Jang, S.; Cho, S.; Kam, D.; Lee, S.-J.; Choi, D. Toward smart net zero energy structures: Development of cement-based structural energy material for contact electrification driven energy harvesting and storage. *Nano Energy* **2021**, *89*, 106389
- (59) Liu, S.; Zheng, W.; Yang, B.; Tao, X. Triboelectric charge density of porous and deformable fabrics made from polymer fibers. *Nano Energy* **2018**, *53*, 383-390.
- (60) Tao, X.; Zhou, Y.; Qi, K.; Guo, C.; Dai, Y.; He, J.; Dai, Z. Wearable textile triboelectric generator based on nanofiber core-spun yarn coupled with electret effect. *J. Colloid Interface Sci.* **2022**, *608*, 2339-2346.
- (61) Paosangthong, W.; Wagih, M.; Torah, R.; Beeby, S. Textile-based triboelectric nanogenerator with alternating positive and negative freestanding woven structure for harvesting sliding energy in all directions. *Nano Energy* **2022**, *92*, 106739.
- (62) Hao, Y., Zhang, Y., Mensah, A., Liao, S., Lv, P., Wei, Q. Scalable, ultra-high stretchable and conductive fiber triboelectric nanogenerator for biomechanical sensing. *Nano Energy* **2023**, *109*, 108291.
- (63) Wang, T., Shen, Y., Chen, L., Wang, K., Niu, L., Liu, G., He, H., Cong, H., Jiang, G., Zhang, Q., Ma, P., Chen, C. Large-scale production of the 3D warp knitted terry fabric triboelectric nanogenerators for motion monitoring and energy harvesting. *Nano Energy* **2023**, *109*, 108309.

Chapter 7: Conclusions and Suggestions for Future

Research

7.1 Conclusions

By summarizing the latest research progress of t-TENGs, the existing issues and challenges in this field are proposed. In order to address these challenges, new types of t-TENGs with different structures were designed and fabricated by using scalable approaches in this thesis. The electrical performance and wearability of as-prepared t-TENGs were characterized. Major conclusions are summarized as follows:

(1) With the merits of simple structure, light weight and easy integration, 1D fiber/yarn based TENG is more suitable for wearable use in a wide range. A 1D braided core-shell structured single-electrode triboelectric yarn with PVDF triboelectric material and PA conductive yarn by using simple, continuous wet spinning and braiding technologies was developed. The good flexibility, mechanical property and adaptability of the as-made BYTENG are demonstrated. Benefitting from the strong electro-negativity of PVDF, the BYTENG is endowed with good pressure sensitivity, which has been successfully employed as self-powered multifunctional sensor for real-time exercise monitoring.

(2) In order to further improve the softness, wearability, weaveability and biodegradability of the t-TENG, 1D core spun yarn structured TENG based on Tencel-chitosan blended yarn and PA conductive yarn was fabricated by using a scalable fancy spinning twister technology. By selecting the Tencel-chitosan blended yarn as

CHAPTER 7

triboelectric functional material, the CYTENG shows excellent tactile comfort and realizes the environmental protection of the TENG. Meanwhile, the high flexibility, small diameter, low weight, high productivity of the CYTENG are obtained, which can meet the requirement of continuous production. This continuously scalable manufacturing technology promotes the commercial production of eco-friendly fiber/yarn based t-TENGs.

(3) The continuously spun CYTENG was further fabricated into 2D woven structured FTENG, which overcomes the complex manufacturing process, high cost, poor comfort and small-scale production. As expected, the FTENG presents a desirable output (31.3 V, 1.8 μA and 15.8 mW/m^2). With the advantage of the materials and structure, the FTENG not only shows outstanding wearability and comfort, such as high flexibility, desirable breathability and good machine washability, but also displays excellent antibacterial property. As for wearable applications, it can work as self-powered sensor to detect different body movements.

(4) To improve the wearability, durability and seamless integration, advanced textile technique is explored to fabricate t-TENG. A triboelectric nanogenerator fabric with 3D woven structure using PTFE, cotton, PA conductive and PP yarns through a cost efficient, eco-friendly, scalable weaving technology is proposed. Owing to structural design and rational materials configuration, versatility of the obtained SP-FTENG is achieved, including good electrical output (27.33 V, 1.76 μA and 61.6 mW/m^2), directional water transport and breathability as well as excellent outstanding durability (machine washability and ultrahigh abrasion resistance). As a demonstration, the fabricated SP-FTENG can drive wearable electronics and be used as a self-powered sensor to constantly detect the movement signals of human body.

CHAPTER 7

In summary, four types of new t-TENGs have been successfully designed and fabricated by exploring the synergistic effect of fiber materials, structures and textile engineering. These t-TENGs demonstrate the feasibility of developing t-TENGs from the textile materials, structures and processing technologies. Firstly, it shows the textile materials can be successfully employed for the fabrication of t-TENGs, which endow the t-TENGs with good electrical performance, flexibility and wearability. Secondly, employing textile processing techniques such as wet-spinning, braiding, yarn spinning, weaving and knitting to fabricate t-TENGs not only achieves large-scale production but also realizes seamless integration of t-TENGs. Thirdly, various structures designed and developed in this research, including 1D braided yarn structured t-TENG, 1D core spun yarn structured t-TENG, 2D woven and knitted structured t-TENG, 3D woven structured t-TENG, can endow the t-TENGs with excellent wearability and multifunctionality.

7.2 Suggestions

In this research, although flexible and wearable t-TENGs have been successfully fabricated, the gap between research and practical commercialization is still widening. Some limitations are still needed to be improved in the future work, which are summarized as below:

1. Enhancement of output performance

In practical applications, providing efficient power output is essential for t-TENGs to power electronic devices because electronic devices need to work continuously for long periods. Although the electrical output performance of t-TENGs has been enhanced, the power output and sensing performance of t-TENGs are relatively lower than those

CHAPTER 7

of conventional nontextile TENGs. The low output of the t-TENG is likely related to the deformable and porous structure of the fabric, which results in a small effective contact area. Numerous approaches relating to materials and structure modification have been proposed to enhance the output performance of t-TENGs. However, their viability is relatively poor due to their complex fabrication process. Further investigation of other potential methods is necessary to improve the output of t-TENGs, such as modifying the operation modes, exploring new triboelectric materials and structures. Further research should focus on exploring the detailed mechanism of output improvement, which can contribute to the development of t-TENGs with good performance.

2. Output stability

In real-life scenarios, the output stability of t-TENGs under machine washing, mechanical abrasion and harsh environmental conditions is critical. Since t-TENGs work through frictional contact between two materials, the output performance and lifetime of t-TENGs may decrease after high-frequency mechanical abrasion. The temperature and sweat on human skin, as well as the ambient temperature and relative humidity, can negatively affect the efficiency and stability of t-TENGs. To deal with this issue, innovative materials and special structure as well as mechanical operation mode should be explored.

3. Integration strategy

As an important link connecting TENGs and electric devices, power management system is an integral part of high-energy transmission. Structural and functional integration of t-TENGs, power management, and back-end functional devices need to be achieved. The intarsia technique seems to be a promising integration strategy for

CHAPTER 7

knitted t-TENGs. However, diverse applications require other applicable seamless integration methods. The wearable intelligent system includes modules such as sensors, management circuits, and wireless transmission. The connection between each functional module and the overall integration with the wearable substrate are unsolved problems that require researchers in various fields to work together to solve.

4. Mass production and low cost

Complex and sophisticated manufacturing techniques are usually not suitable for mass production, which also increases production costs. To realize large-scale industrialized production and lower the cost, economically available materials and efficient structural designs suitable for mass production of t-TENGs need to be explored. Some studies involving the modification of fabric surfaces require expensive equipment, the sample sizes are relatively small, and the fabrication processes are complex. Several studies have developed fiber-based TENGs that are compatible with current textile manufacturing technology. Then, the fiber-based TENGs are woven or knitted into fabric, which provides a possible mass production solution. This method can reduce the time and effort involved in t-TENG fabrication. Although mass production is in the initial stage, the commercialization of t-TENGs shows great potential. Scalability and cost remain key issues that need to be addressed.